Photophysics and mechanism of photoinduced antiviral action of the natural products, hypericin and hypocrellin A

by

Michael James Fehr

A Dissertation Submitted to the

Graduate Faculty in Partial Fulfillment of the

Requirements for the Degree of

DOCTOR OF PHILOSOPHY

Department: Chemistry
Major: Physical Chemistry

Approved:

Signature was redacted for privacy.

In Charge of Major Work

Signature was redacted for privacy.

For the Major Department

Signature was redacted for privacy.

For the Graduate College

Iowa State University
Ames, Iowa

1995

To my parents

TABLE OF CONTENTS

CHAPTER 1. GENERAL INTRODUCTION

Hypericin

Hypericin (Figure 1a) is a polycyclic quinone which occurs naturally in the plant, St. John's Wort [1]. Hypericin possesses diverse biological activity and has achieved interest because it has been shown to inactivate the human immunodeficiency virus (HIV) [2-5]. The antiviral activity of hypericin has been shown to require light by Carpenter and Kraus[6]. The mechanism of this antiviral activity is still unclear but has been suggested to occur via a mechanism involving singlet oxygen since hypericin is known to produce singlet oxygen in high yields (Q.Y. = 0.71) [7].

Hypericin has been used as an antidepressant and has been used in folk-medicine against a variety of ailments [8]. Ingestion of hypericin causes a condition known

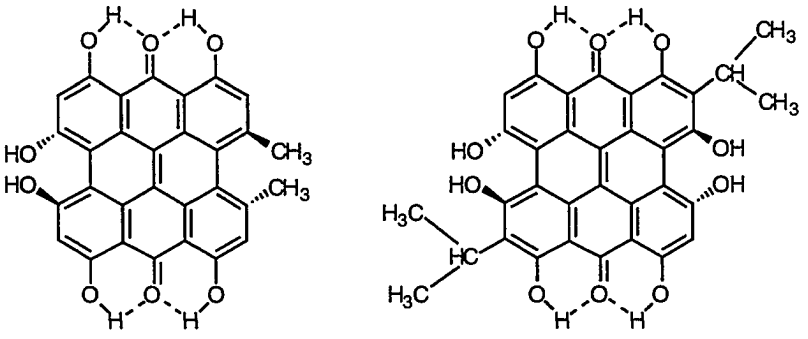

a) b)

Figure 1. a) hypericin b) stentorin

as hypericism, which is characterized by a hypersensitivity to sun light [9]. This condition was first discovered in grazing animals who after ingesting St. John's Wort developed lesions, fevers, and eventually death if left in the sun [9].

Hypericin is an extremely hydrophobic molecule, which is slightly soluble in polar protic and aprotic solvents. In the body, hypericin is thought to accumulate in glycoproteins, cell membranes and other hydrophobic environments including the endoplasmic reticulum and the Golgi apparatus [10]. In water hypericin is thought to form chain like aggregates from pH 2 to pH 10 [11].

Prior to our work little was known about the primary events that occurred after hypericin absorbed a photon of light. Hypericin's fluorescence lifetime has been determined to be between 5.5 and 6.5 ns depending on solvent [12]. Its fluorescence quantum yield and intersystem quantum yield have been determined to be 0.29 and 0.71 respectively in ethanol [12]. Yamazaki et al. performed time-correlated single photon counting and steady-state measurements in an effort to determine if inter- or intramolecular proton transfer was favored [13]. They concluded that no proton transfer takes place, although as we have noted the time scale they used was quite long [13, Chapters 3 and 4].

Cotton et al. have performed surface enhanced resonance raman spectroscopy (SERRS) to attempt to elucidate the vibrational modes in hypericin [14].

While the singlet state of hypericin has received little attention the triplet state of hypericin has been well studied. Jardon and coworkers have performed numerous studies in which they have determinined hypericin's triplet-triplet absorption spectrum, the quantum yield of intersystem crossing (ϕ_{isc} = 0.71 in ethanol), the quantum yield of singlet oxygen production in micelles (ϕ_{Δ} = 0.72), the quantum yield of singlet oxygen production in vesicles (ϕ_{Δ} = 0.35), the effects on the triplet state and on ground state

absorption of hypericin-metal complexes, and the rate of diffusion of hypericin between vesicles [15].

In addition to Jardon's work on the triplet state, Angerhofer et al. have observed phosphorescence from hypericin at 1.2 K in ethanol [16]. They observed a single exponential decay time of 2.79 ms and a triplet-triplet energy level of 13190 cm^{-1} in good agreement with Jardon [15,16]. Malkin and Mazur have also measured triplet transient absorption spectra and the triplet lifetime of hypericin [17]. They report it to be single exponential (τ = 4.3 μs) at room temperature [17]. Their data suggest that in the absence of oxygen hypericin can abstract a hydrogen atom, after undergoing excitation and intersystem crossing to the triplet state, resulting in the formation of a semiquinone species [17].

Weiner and Mazur also observed by EPR the formation of a semiquinone-like radical in the absence of oxygen [18]. Interestingly, the amplitude of the semiquinone-like radical increased approximately 20 fold when hypericin was illuminated with light corresponding to its absorption spectrum [18]. In the presence of oxygen they were also able to observe the formation of superoxide radical by spin trapping techniques [18]. Diwu and Lown report similar results [19]. Redepenning and Tao report that hypericin is both a good reducing agent and a good oxidizing agent in the excited state [20].

Stentorin

Hypericin is structurally similar to the chromophore stentorin. The only difference is that stentorin has two isopropyl groups(Figure 1b) [21]. The chromophore stentorin is thought to confer upon *stentor coeruleus* its photophobic and phototactic response

[22]. Song has observed that *stentor coeruleus*, a small ciliate, uses stentorin embedded in a protein to act as the ciliate's light sensing system [22]. He also observed a pH decrease of the surrounding solution upon illumination of solutions of stentorin embedded in its protein and of the stentorin chromophore imbedded in vesicles [23]. The ultrafast photochemical events of stentorin have been studied by Savikhan et al. and are similar to those that they obseved for hypericin [24].

What is most interesting about stentorin is that under low light flux stentorin is not toxic to *stentor coeruleus* , however under sufficiently high light flux stentorin can induce photodynamic effects [25].

Hypocrellin

Hypocrellin A (Figure 2) is a naturally occurring perylene quinone found in the parasitic fungus, *H. Bambuase,* in parts of the Peoples' Republic of China (PRC) and Sri Lanka [26]. Similarly to hypericin it is known to inactivate the HIV virus and this inactivation is light dependent [27]. Hypocrellin A has been used for many years in folk medicine in the PRC particularly against skin lesions [26].

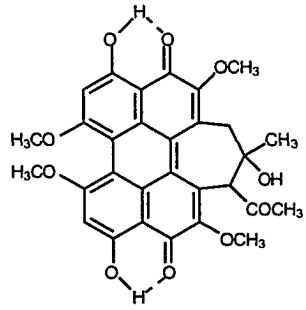

Figure 2. Structure of hypocrellin A.

Because hypocrellin A has been difficult to obtain in the west until recently, little has been known about its physical characteristics and photophysics. Hypocrellin A, similar to hypericin, is soluble in both polar protic and aprotic solvents but unlike hypericin it is also soluble in nonpolar solvents such as cyclohexane and benzene [28]. Diwu et al. have measured the fluorescence quantum yield and fluorescence lifetime in benzene (ϕ_f = 0.14 and τ_f = 1.4 ns), the intersystem crossing quantum yield (ϕ_{ISC} = 0.86), and the quantum yield of singlet oxygen production (ϕ_Δ = 0.83) [29]. They also suggest, by the use of structural analogs, that intramolecular proton transfer plays an important role in the shape of the fluorescence and absorbance spectra [28].

Hu et al. report the triplet transient absorption spectrum of hypocrellin A in cyclohexane [30] They observe that the triplet state of hypocrellin A decays monoexponentially with a decay time constant of 4-6 μs at room temperature [30]. They also determine, by quenching with azulene and perylene, that the triplet energy level of hypocrellin A is 42.5 kcal [30]. It has also been reported that hypocrellin A produces superoxide, hydroxy radical and hydrogen peroxide [26].

Photochemotherapy

Photochemotherapy has emerged as a promising tool to combat various types of cancerous tumors and viruses such as herpes simplex and human immunodeficiency virus (HIV) [2-6,31]. Photochemotherapy occurs when a molecule, known as the photosensitizer, absorbs a photon of light and then interacts, either directly or indirectly, with a biologically important moiety on the tumor or virus, eventually killing it or rendering it useless to further damage against the host system.

Two general types of photochemotherapy mechanisms are recognized in the

literature [32-35]. These are demonstrated graphically in Figure 3. In a Type I photosensitization the photosensitizer interacts initially with the substrate disabling it via hydrogen abstraction or a redox reaction [32-35]. The substrate may then form radical species which in turn may undergo further reaction with molecular oxygen or other substrates [32-35]. Some photosensitizers, such as acridines are known to intercalate in DNA and undergo addition reactions [36].

In a Type II photosensitization the photosensitizer interacts first with the ground state of molecular oxygen ($^3\Sigma_g$-) forming singlet oxygen ($^1\Delta_g$) a highly reactive species [32]. Singlet oxygen then in turn becomes the toxic factor which goes on to disable the tumor or virus [32-35]. When oxygen is involved as a toxic factor, photochemotherapy is generally referred to as photodynamic therapy.

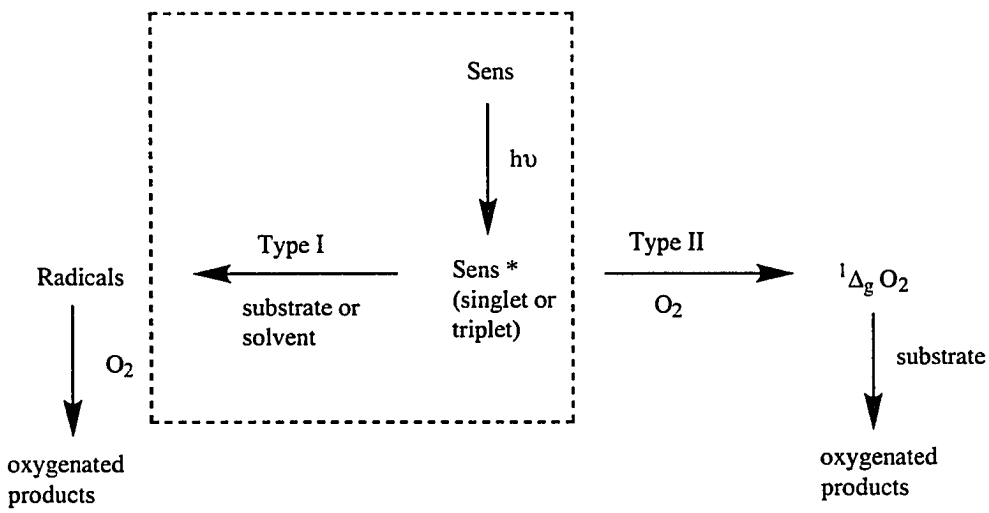

Figure 3. Type I and Type II photosensitization processes.

Although there are some examples of photosensitizers that demonstrate only one type of photosensitization, most photosensitizers can undergo both Type I and Type II processes [33,35]. Generally Type I photosensitization is favored by low light flux, low oxygen tensions, large photosensitizer concentration, and close association of photosensitizer and the substrate [33,35] Type II photosensitization is favored by high light flux and high oxygen tensions [33,35].

Some common photosensitizers that have been developed include photofrin II, furocoumarins, acridines, methylene blue (thiazines), and a host of porphyrins [36,37]. Photosensitizers can be delivered orally, injected, or applied topically [31]. An advantage of photosensitizers is that they are generally ineffective without light so that, if light is selectively applied and if the photosensitizer shows a much greater affinity for the diseased cells over healthy cells, then relatively few side effects result [31]. Some photosensitizers do, however, cause side effects if significant concentrations accumulate in parts of the body accessible to light, such as those close to the skin. This is known as photosensitization [9].

Paradoxically, the disadvantage generally is that light is necessary for the photosensitizer's toxicity which generally means some sort of incision must be made to allow the use of an external light source such as a fiber optic attached to a laser. Other disadvantages are that tumors have a tendency to be hypoxic, that is they lack a significant oxygen tension. This inactivates the Type II process [38].

Photochemotherapy and the development of better photosensitizers are active areas of research and some desirable properties of photosensitizers have been outlined. These are [31-38]:

1. The photosensitizer should have a much higher affinity to the tumor or virus particle over healthy cells. Advantage is taken of the hydrophobic or hydrophilic nature

of the virus or tumor in designing photosensitizers which prefer these environments.

2. Photosensitizers that absorb towards the red end of the visible spectrum are preferred to those which absorb in the blue. Human tissue is most transparent to light between 600-900 nm (it transmits approximately 90% in this wavelength region) [39]. Red light penetrates tissue much deeper than blue light. This is particularly important in treatment of skin cancers.

3. Photosensitizers are desired that undergo efficient intersystem crossing to the triplet state. The triplet state of photosensitizers has been implicated in most photochemotherapy because of its relatively long life time as compared to the singlet state. This allows diffusional quenching by molecular oxygen or time for the photosensitizer to interact with the substrate.

4. Low tendency for aggregation at high concentration of the photosensitizer. Aggregation can markedly change the photophysics of the photosensitizer and it has been observed that this can substantially reduce the amount of triplet state and subsequently the amount of singlet oxygen produced.

Photochemotherapy can cause widespread damage to biological entities. These include, but are not limited to [31-38]:

1. Nuclear damage. Some photosensitizers, such as acridines, have an affinity for DNA and may intercalate or adhere to it. Once bound they can cause serious damage such as single-strand breaks and the formation of alkali-labile bonds. From a singlet oxygen point of view guanine is the favored target, it oxidizes much easier than cytosine, thymine and uracil. Psoralens can add across the 5,6- carbon-carbon bond of pyrimidines in DNA to form cycloadducts.

2. Amino acids and proteins. Five of the twenty amino acids are susceptible to degradation in photosensitized reactions. These are cysteine, histidine, methionine,

tryptophan, and tyrosine. The mechanisms vary with amino acid but involve both Type I and Type II reactions. Degradation of the amino acids can cause inactivation of the protein, particularly when it involves the active site. A large pH dependence has been observed on protein inactivation presumably because of the large conformational change that can result in the three-dimensional structure of the protein with pH. This can alternately hide or expose important, photodegradable moieties. In addition to degradation, cross-linking of proteins also occurs upon photosensitization.

3. Membranes and lipids. Major damage can occur from the oxidation, either by a Type I or Type II process, of the cell membrane. Generally oxidation of lipids in the cell membrane allows the unabated influx of small ions which cause swelling and eventual bursting of the cell.

It is often difficult to differentiate between Type I and Type II photosensitization [32-38]. There are a number of indirect tests which are applied to test whether photosensitization is occurring via a Type I or Type II mechanism. Most of these are designed either to enhance or quench singlet oxygen. In some cases it is possible to tell by the reaction products what type of mechanism is dominant. Cholesterol for example gives distinct products upon reaction with singlet oxygen as compared to hydroxy radical or hydrogen peroxide [34]. However this is usually only feasible in cases where the only constituents are the photosensitizer and the substrate or efficient means of separation are available.

Singlet Oxygen

Since singlet oxygen is often cited as the toxic factor in so many photodynamic compounds it is useful to review some of its physical characteristics and its chemistry.

The ground state of molecular oxygen is a triplet state, $^3\Sigma_g$-. Its lowest excited state is $^1\Delta_g$, which is 22 kcal above the ground state [32]. This relatively low energy level is below the level of many dyes' singlet and triplet excited states which allows energy transfer to take place.

Evidence of singlet oxygen reactions are often difficult to identify as the products of its reactions are often difficult to isolate and are similar to those produced by hydroxide radical and hydrogen peroxide, two possible by-products of Type I photosensitization and of further reaction of two singlet oxygen molecules with water [31-38]. The most unambiguous test for singlet oxygen is the observation of phosphorescence as $^1\Delta_g$ relaxes to $^3\Sigma_g$-. This weak phosphorescence occurs at 1270 nm and detection methods have been developed to separate this from infrared phosphorescence of the photosensitizer [34,38]. This, however, only indicates that singlet oxygen is present and not that it is a toxic factor.

Indirect evidence is often used to obviate singlet oxygen as a possible toxic factor. Singlet oxygen reacts with several visibly colored furans such as 1,3 diphenylisobenzofuran and 2,5 diphenylfuran to form colorless products [31-38]. The reaction can be monitored via a decrease in absorption of the colored furan versus time to deduce the kinetics of singlet oxygen production and reactivity. Firefly luciferase (*photinus pyralis)* has also been used as an assay for detection of singlet oxygen production [40]. Firefly luciferase is efficiently inactivated by singlet oxygen, presumably because of the oxygen binding site it possesses for oxidation of the luciferin substrate [40]. Decreases in luminescence as a function of photosensitization time can be used to deduce the kinetics of singlet oxygen production.

Quenchers, which show specificity towards singlet oxygen such as ß-carotene, sodium azide or DABCO are often used when singlet oxygen mechanisms are thought

to predominate [31-38]. A decrease in toxicity with increased quencher concentration is taken as evidence of a singlet oxygen mechanism. These quenchers however sometimes do not work well in biological systems because of their compartmentalized nature [31-38]. That is, it is often difficult to insure that the quencher will be able to diffuse to the same places as the photosensitizer. An additional problem with quenchers is that they can quench the triplet state of the photosensitizer [31-38]. This will result in a decrease of both Type I and Type II mechanisms but can be incorrectly interpreted as proof of a Type II mechanism.

The lifetime of singlet oxygen in H_2O has been measured at 2-4 μs [31-38]. However singlet oxygen shows a marked increase of lifetime in D_2O to 20-40 μs [31-38]. Hence, running reactions in D_2O and seeing a marked increase in inactivation has also been used as indirect evidence for singlet oxygen. This increase in inactivation is attributed to the increase in singlet oxygen's lifetime which allows it to be able to travel farther and increases the probability it can successfully oxidize a biological moiety. The best test, however, of whether singlet oxygen and hence a Type II mechanism is the toxic factor is to remove oxygen from the system

Equine Infectious Anemia Virus (EIAV) and Human Immunodeficiency Virus (HIV)

The virus used for determining the efficacy of photosensitizers in this dissertation was EIAV, a virus belonging to the family *Retroviridae* and the sub-family *Lentivirinea* [41, 42]. Other retroviruses which are similar in morphology and structure are simian immunodeficiency virus (SIV), feline immunodeficiency virus (FIV) and human immunodeficiency virus (HIV) [41, 42]. The majority of the following discussion on

retroviruses and EIAV will center on HIV as the basis because of the vast amount of information, which has been accumulated recently given HIV's significance.

One of the characteristics of retroviruses is their use of an RNA template for the synthesis of DNA [41, 42]. This is accomplished using reverse transcriptase (RT) [41]. The DNA synthesized by the RNA strands is then incorporated into the host cells' DNA genome where it is known as the provirus [41]. It is this feature that makes retroviruses so difficult to kill once they have infected a host. Retroviruses, as illustrated above, are not limited to human beings but infect large portions of the animal world.

The viruses inflict a wide variety of damage. Some strains of retroviruses result in persistent infection that do not threaten the host system while other retroviruses (such as HIV) eventually weaken the immune system of the host leaving the host vulnerable to other opportunistic viruses and foreign bacteria which left unchecked can eventually overwhelm the host [41,42].

Retroviruses are among the most complicated of viruses. They contain up to 9 genes, parts of which are translated into a variety of enzymes necessary for the life cycle of the retrovirus once it infects the host cell. Some of the more important parts of the RNA are [41, 42]:

Long terminal repeats (LTR) The LTR contains non-coding sequences of DNA. The LTR is important because it contains material important to reverse transcriptase and integration. It can be thought of as a type of "instruction manual" on how to put together the two strands of RNA.

gag gene The gag gene is transcribed as a full length RNA and is used to translate information necessary in producing a polyprotein that finally is used to make 3 to 5 capsid proteins, a matrix protein, a capsid protein and a nucleic acid binding protein.

pol gene The pol gene is used to produce the reverse transcriptase and integrase proteins.

env gene The env gene is used to make the proteins which are inserted into the viral envelope, most notably gp120 and gp41 in HIV, which are used to bind to the host cell.

These are the three genes have been best characterized. There are six other genes which have not been as well characterized but play equally important parts in the virus life cycle.

The retrovirus life cycle can be broken down into the following and is shown graphically in Figure 4 [41-43]:

1. Binding (or attachment) to host cell. Binding occurs through the gp120 of the virus to the CD4 domain of the T-lymphocytes (helper cells). CD4 is a cell surface glycoprotein of 55 kDa molecular weight. Binding of the virus gp120 to CD4 is thought to occur in the D1 domain of CD4.

2. Viral fusion of the retrovirus particle into the host cell. The binding of gp120 to CD4 causes a conformational change in the envelope glycoproteins. This conformational change exposes gp41 (gp45 in EIAV) which is where the major fusion peptide is thought to occur. This fusion peptide most likely provides a hydrophobic interface across which membrane lipids might flow thus fusing the virus particle to the cell membrane. An important side point is that for fusion to occur it is thought that gp120 (gp90 in EIAV) (and CD4) must be cleared from the membrane space, this is also a large conformational movement.

3. Now that the cell and the virus have "fused" the reverse transcriptase can begin to synthesize DNA from the genomic RNA of the virus. It is still unclear where in the cell this occurs. There is some evidence that it occurs within a capsid of

the original virus in the cytoplasm of the cell. The synthesis of viral DNA from the genomic RNA of the virus is a complicated, but well understood process. Readers are referred to the sources listed above for complete details.

4. Once the DNA has been completed it is inserted into the DNA of the host cell. Insertion is not as well understood. Again the reader is referred to the sources above for available details.

5. After insertion of the DNA into the host cell genome (where it is now called the provirus) the production of viral enzymes necessary for continued production of virus particles occurs along with other normal cell functions.

6. mRNA which is created from the host cell genome and includes the provirus is transported out to the cytoplasm where it has two fates. The first is to be packaged into new virus particles and the second is to encode for the production of the surface proteins necessary for the virus particles.

7. Virus particles then are thought to simultaneously assemble and bud through the cell membrane. The membrane of the virus is that of the host cell.

It is possible to evaluate virus infectivity by observing syncytia formation. Syncytia formation (multinucleation of cells) occurs because cells are expressing the viral binding and fusion proteins on their plasma membranes. When these cells are mixed with uninfected cells with the proper binding site the binding proteins which are expressed on the infected cells will bind to the uninfected cells and cause multinucleation.

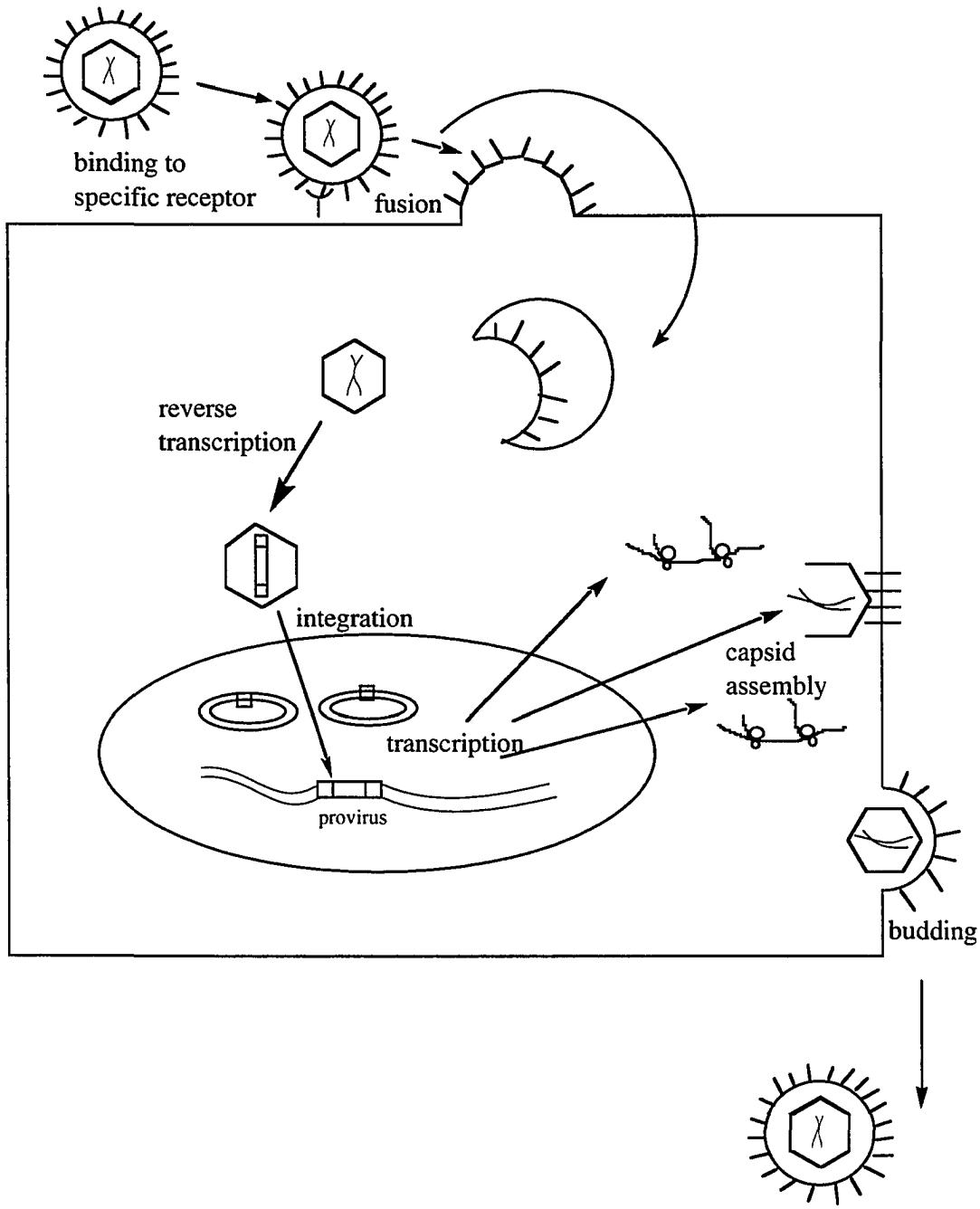

Figure 4. Life cycle of retrovirus.

Previous Work on the Mechanism of Hypericin's Antiviral Activity

Hypericin's ability to inactivate HIV and related viruses was discovered by Meruelo and co-workers who also observed that mice, which were treated simultaneously with hypericin and friend leukemia virus, could have a 100% survival rate [2]. Unfortunately, this result could not be repeated and eventually was determined to be due to the mixing of hypericin and virus in light before administration to the mice [44]. Carpenter and Kraus discovered that hypericin's antiviral activity was dependent on light [6]. Of major importance to the direction of mechanistic studies was that hypericin did not directly inactivate purified reverse transcriptase [2-6].

Meruelo and co-workers attempted the first mechanistic studies of hypericin and pseudo-hypericin's antiviral properties [2,45]. Unfortunately, at the time of their studies, they were unaware of the role of light in hypericin's antiviral activity so there is no mention of light flux or how long the samples were in a position to be illuminated. They did however make two important observations [45]:

1. In cells which had been infected with murine RADLV, treatment with hypericin resulted in a substantial decrease in the release of mature viral particles. This would indicate some type of disruption of viral assembly, possibly with the proper assembly of the virus core or proteins associated with viral core assembly.

2. When hypericin was introduced to mature virus particles it was able to inactivate the virus particle.

Later work by Merulo et al. and Degar et al. showed that a loss of reverse transcriptase activity accompanied the inactivation by hypericin although the loss of RT activity was not due to direct inactivation of reverse transcriptase [3,5]. They observed, by Western Blot analysis, that the mobility of the major capsid proteins, p24 and the p24

precursor p55, was altered [3,5]. A band appeared with a molecular weight of 48 kilodaltons which suggests a cross-linking of p24 and perhaps the inhibition of release of reverse transcriptase [3,5].

Lenard et al. attempted to compare the photodynamic effects of hypericin with rose bengal which also produces singlet oxygen in high yield and is known to associate with enveloped viruses [4]. They observed the following [4]:

1. Hypericin and rose bengal both inhibited syncytia formation in CD4 cells when illuminated in the presence of HIV.

2. Both rose bengal and hypericin appeared to inhibit viral fusion but not viral binding as they found evidence of hemagglutination. Lack of syncytia formation was taken as evidence for non-fusion.

3. There was evidence of cross-linking of viral proteins. gp120 and gp41 were most easily cross-linked while p24, the protein associated with the genomic RNA was not as easily cross-linked.

These results, while certainly evidence for some type of photodynamic inactivation are difficult to interpret because relatively high light flux and relatively long illumination times (1 hour) were used. This can, as mentioned in the previous section, favor a Type II mechanism because of the high steady-state triplet concentration which can be made under high light flux. It is also curious that hypericin was better able to inactivate the virus than rose bengal even though rose bengal has a higher singlet oxygen quantum yield. In addition we have observed that rose bengal may possess significant Type I ability to inactivate viruses.

Further information on the type of viruses that hypericin was effective against was provided by Tang et al. who observed that hypericin's antiviral activity was limited to enveloped viruses [46]. That is, hypericin seemed to be unable to activate viruses

that did not contain lipid membranes. Presumably this is due to hypericin being unable to associate with the virus before it forms aggregates in the aqueous solution because of hypericin's hydrophobicity [46].

Several groups attempted to determine what, if any, effect the polycyclic backbone structure of hypericin has on antiviral activity [47,48]. Schinazi et al. found that anthraquinones with hydroxyl groups and sulfoxy groups adjacent to the carbonyl possessed some antiviral activity [48]. However, no data was given about the use, if any, of illumination. Kraus et al. attempted a similar study, breaking hypericin into "pieces" with analogues such as emodin, mesonaphthobianthrone, and 4,9 dihydroxy 3,10 perylenequinone [47]. They observed no antiviral activity by any of the analogues although again no data is given about illumination of samples [47].

Weber et al. used fluorescence microscopy to follow the uptake of hypericin by cells [10]. They observed that hypericin initially concentrates in cytoplasmic membranes and over the course of time moves to intercellular membranous regions such as the Golgi apparatus and the endoplasmic reticulum [10].

Since hypericinism was first identified in grazing animals, a study by Senthil et al. was undertaken to examine hypericin's photodynamic effects in aqueous model systems [49]. They found that hypericin could inactivate lysozyme when bound to human serum albumin, that is that singlet oxygen or superoxide could travel to inactivate an enzyme [49]. In addition they found that hypericin embedded itself in the cell walls of red blood cell ghosts could cause photohemolysis and lipid peroxidation [49].

Andreoni et al. showed that when hypericin is irradiated with a dye laser it can kill epithelial cells derived from Fisher rat thyroid [50], thus showing that hypericin's photochemotheraputic effects can be extended to whole cells. Thomas and Pardini proved that that oxygen was necessary for hypericin to kill EMT6 mouse mammary

carcinoma cells [51].

Molecular Flashlight

Photochemotherapy is limited, as mentioned previously, by the lack of significant levels of the proper wavelength light within the body and to a lack of specificity. Nature, however, has developed methods of light generation which have been utilized by insects, plants, and sea life [52,53]. Bioluminescence involves the enzymatic generation of an excited state of a molecule, which can then decay radiatively, generally with a large quantum yield. Our model system is that of the north american firefly (*photinus pyralis*) because it has been extensively studied and it is relatively standard practice to incorporate the firefly gene into a variety of cells as an alternative to radioisotopic labelling[52,53].

Generation of light in the firefly is highly efficient and occurs with a quantum yield of approximately unity [54]. Figure 5 illustrates the emission spectrum of the firefly overlapped on the absorption spectrum of hypericin. The region of overlap extends for ~100 nm indicating that firefly luciferase is an ideal emitter to use with hypericin.

Figure 6 shows the important steps in production of light in the firefly system [52]. The first step is the binding of luciferase to luciferin, the unoxidized precursor to the emitter. The second step in the reaction is the addition of a single molecule of ATP to luciferin. It is important to note that ATP is not added as an energy source but as a good leaving group; It has been demonstrated that the reaction is not specific for ATP but that other leaving groups work as well [52.53]. The addition of the ATP causes the loss of two inorganic pyrophosphates to form a luciferyl adenylate. The third step is the addition of molecular oxygen which becomes energetically favorable because of the

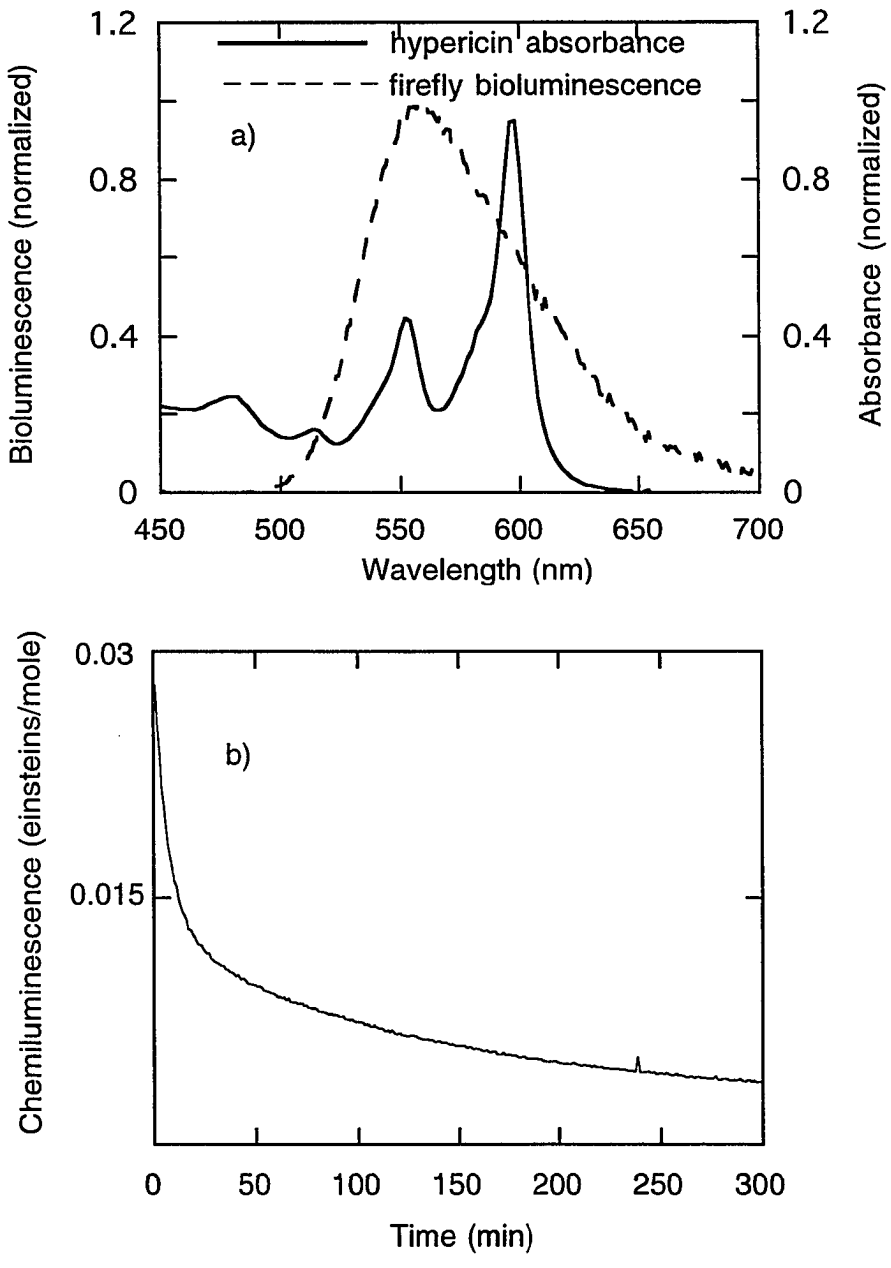

Figure 5 a) Overlap of emission spectra of North American firefly (*photinus pyralis*) with the absorption spectra of hypericin in DMSO. b)Time dependence of firefly emission.

loss of AMP. This results in the formation of a high energy unstable peroxide. The fourth step is the decomposition of the peroxide (by loss of CO_2) to leave the oxyluciferin in an excited state. The oxyluciferin then decays radiatively from the singlet state via a CIEEL mechanism [55].

The wavelength of the firefly emission is pH dependent [56]. As the pH becomes more acidic the firefly emission becomes redder indicating one or more ionizable groups on the oxyluciferin emitter [56]. Gandelman et al. have studied both the steady-state and time-resolved emission of oxyluciferin and have identified which oxyluciferin emitter corresponds to the change in emission wavelength (Figure. 7a) [56].

The production of oxyluciferin from luciferin is an irreversible process; as noted above, one photon of light is produced for every molecule of luciferin oxidized [52,54]. When a solution of luciferase, luciferin, Mg^{2+}, and ATP are mixed the firefly luminescence results in a decay curve of light intensity an example of which is given in Figure 5b. Its shape has been ascribed to inhibition by the oxyluciferin product and the kinetics of this have been variously described by competitive, uncompetitive and noncompetitive inhibition. Most recently a study by Lemasters and Hackenbrock concluded that oxyluciferin was a noncompetitive inhibitor with respect to luciferin and ATP [57-59]. The oxyluciferin product is not the only competitor for the firefly reaction, dehydroluciferin (Figure 7b), a nonemitting product of the decomposition of luciferin in air is known to be a competitive inhibitor [57-59]. Finally, White et al. and Branchini, et al. have both shown that derivatives of luciferin are also catalyzed by luciferase and result in the production of visible light, albeit of different wavelengths [60,61].

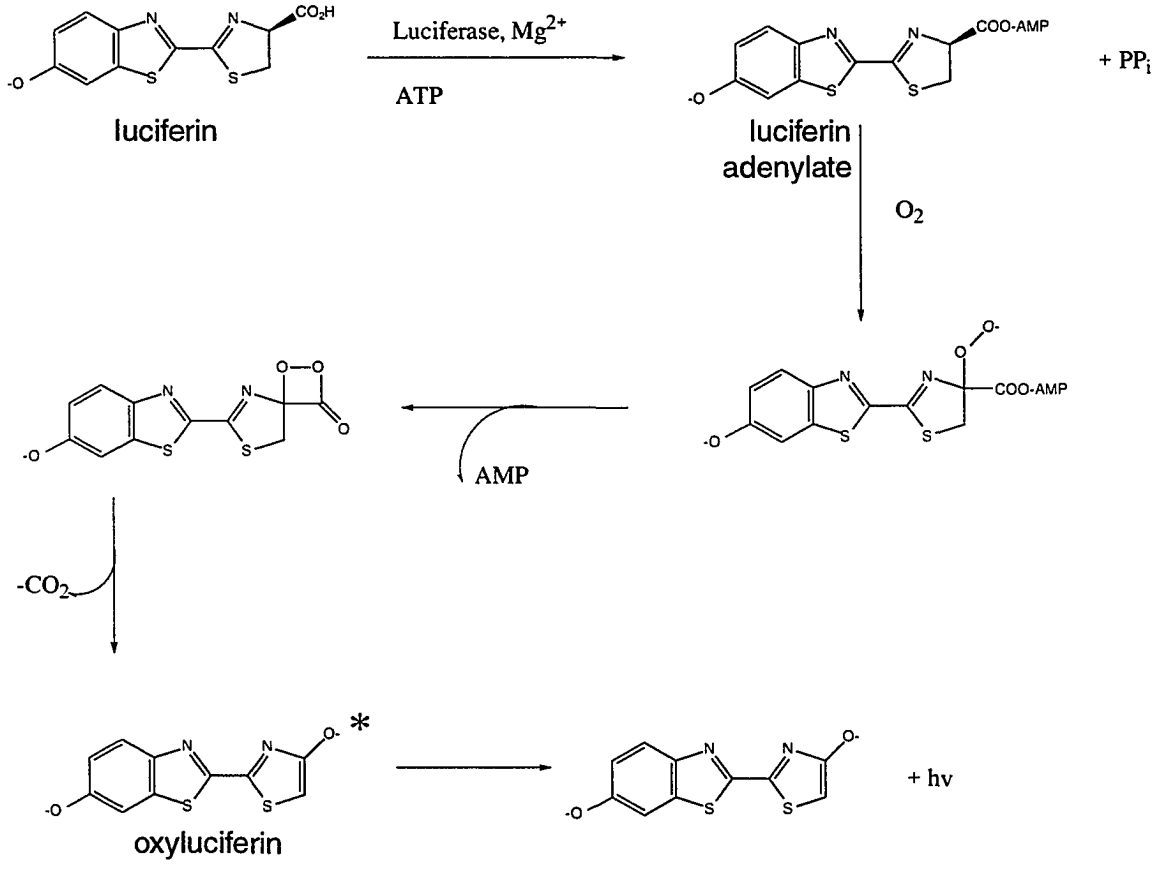

Figure 6. Important steps in the bioluminescent oxidation of luciferin to oxyluciferin.

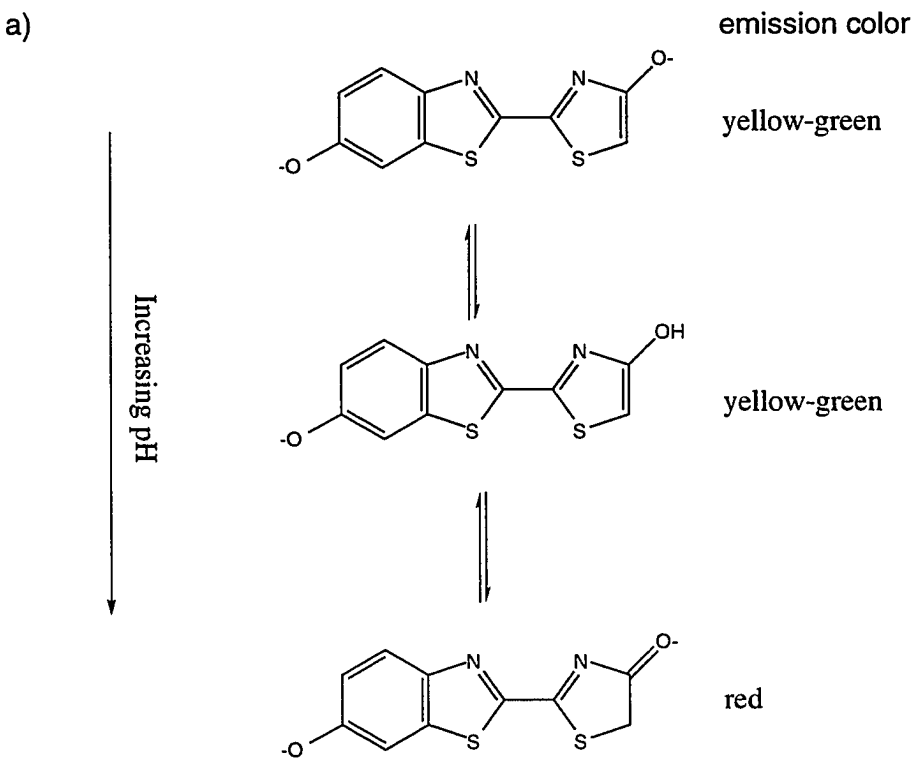

Figure 7. a) Structures of pH dependent oxyluciferin emitters. b) Structure of the competitive inhibitor dehydroluciferin.

Dissertation Organization

The dissertation is organized as follows. Chapter 2 describes in detail the operation and maintenance of the 30 Hz transient absorbance spectrometer with which the measurements in Chapters 3 and 4 were performed. Chapters 3 and 4 discuss the primary photophysical events of hypericin and related analogs and raises questions about what was the dogma concerning hypericin's antiviral mechanism prior to our work. Chapter 5 discusses the role of oxygen in hypericin's antiviral activity against EIAV. Chapter 6 presents a means of incorporating a light source within the body as a way of selectively targeting virally infected cells. Chapter 7 shows that hypericin can acidify its environment upon optical excitation and discusses how this might be related to hypericin's antiviral properties. Chapter 8 compares the oxygen dependence of the antiviral activity of hypocrellin A, a natural product which is structurally similar to hypericin, with hypericin and finds that oxygen is absolutely required for hypocrelllin's antiviral acitivity. In addition, Chapter 8 finds that hypocrellin is unable to acidify its environment under the same conditions as hypericin. Chapter 9 is a general summary of our results and future projects related to this dissertation.

References

1. Durán, N.; Song, P.-S. *Photochem. Photobiol.* 1986, **43**, 677-680. Hypericin and its photodynamic action.
2. Meruelo, D.; Lavie, G.; Lavie, D. *Proc. Natl. Acad. Sci. USA* 1988, **85**, 5230-5234. Therapeutic agents with dramatic antiretroviral activity and little toxicity at effective doses: Aromatic polycyclic diones hypericin and pseudohypericin.

3. Degar, S.; Prince, A. M.; Pascual, D.; Lavie, G.; Levin, B.; Mazur, Y.; Lavie, D.; Ehrlich, L. S.; Carter, C.; Meruelo, D. *AIDS Res. Hum. Retroviruses* 1992, **8**, 1929-1936. Inactivation of the human immunodeficiency virus by hypericin: evidence for photochemical alterations of p24 and a block in uncoating.

4. Lenard, J.; Rabson, A.; Vanderoef, R. *Proc. Natl. Acad. Sci. USA* 1993, **90**, 158-162. Photodynamic inactivation of infectivity of human immunodeficiency virus and other enveloped viruses using hypericin and rose bengal: inhibition of fusion and syncytia formation.

5. Meruelo, D., Degar, S., Nuria, A., Mazur, Y., Lavie, D., Levin B., and Lavie, G. (1992) in Natural Products as Antiviral Agents C. K. Chu and H. G. Cutler, Eds. Plenum Press, New York. pp. 91-119 (and references therein). Inactivation of HIV by Hypericin.

6. Carpenter, S.; Kraus, G. A. *Photochem. Photobiol.* 1991, **53**, 169-174. Photosensitization is required for inactivation of equine infectious anemia virus by hypericin.

7. Racinet, H.; Jardon, P.; Gautron, R. *J. Chim. Phys.* 1988, **85**, 971-977. Formation d'oxygène sigulet photosensibilisée par l'hypericine étude cinétique en milieu micillaire non ionique.

8. Kreitmair, H. *Pharmazie* 1950, **5**, 556-557. Hypericum perforatum—das Johanniskraut.

9. Giese, A. C. in Photochemical and Photobiological Reviews, Volume 5. Smith, K. C., Ed. Plenum; New York; 1980. p. 229. Hypericism.

10. Weber N. D., Murray, B. K., North, J. A. Wood, S. G., *Anti. Chem. Chemotherapy* 1994, **5** 83-90. The antiviral agent hypericin has in vitro activity against HSV-1 through non-specific association with viral and cellular membranes.

11. Sevenants, M. R., *J. Protozool.* 1965, **12**, 240-245. Pigments of *blepharisma undulans* compared with hypericin.

12. Jardon, P. Lazorchak, N. Gautron, R. *J. Chim. Phys.* 1986, **83**, 311-315. Proprietes, du premier etat triplet de L'hypericine etude par spectrocopie laser.

13. Yamazaki, T.; Ohta, N.; Yamazaki, I.; Song, P.-S. *J. Phys. Chem.* 1993, **97**, 7870-7875. Excited-state properties of hypericin: Electronic spectra and fluorescence decay kinetics.

14. Raser, L. N.; Kolaczkowski, S. V.; Cotton, T. M. *Photochem. Photobiol.* 1992, **56**, 157-162. Resonance raman and surface-enhanced resonance raman spectroscopy of hypericin; Wynn, J. L.; Cotton, T. M. *J. Phys. Chem.* 1995, **99**, 4317-4323. Spectroscopic properties of hypericin in solution and surfaces.

15. Nafis, M., Jardon, P., *J. Chim. Phys.* 1994, 91, **9**, 99-112. Proprietes spectroscopiques et photophysiques de complexes metalliques de l'hypericine en relation avec leur activite photodynamique; Bouirig, H., Eloy, D., Jardon, P., *J. Chim. Phys.* 1992, 89, 1391-1411. Formation et reactivite de l'oxygene singulet photosensibilise par l'hypericine dans des liposomes de dipalmitoylphosphatidylcholine. Mise en evidence d'une photooxydation retardee; Bouirig, H., Eloy, D., Jardon, P., *J. Chim. Phys.* 1993, **90**, 2021-2038. Autoextinction de la fluorescence et de l'absorption triplet-triplet de l'hypericine dans des liposomes de dipalmitoylphosphatidylcholine.

16. Angerhofer, A., Falk, H., Meyer, J. Schoppel, G., *J. Photochem. Photobiol. B: Biol.* 1993, **20**, 133-137. Lowest excited triplet states of hypericin and isohypericin.

17. Malkin, J.; Mazur, Y. *Photochem. Photobiol.* 1993, **57**, 929-933. Hypericin derived triplet states and transients in alcohols and water.

18. Weiner, L.; Mazur, Y. *J. Chem. Soc. Perkin Trans. 2* 1992, 1439-1442. EPR studies of hypericin. Photogeneration of free radicals and superoxide.

19. Diwu, Z.; Lowen, J. W. *Free Radical Biology and Medicine* 1993, **14**, 209-215. Photosensitization with anticancer agents 17. EPR studies of photodynamic action of hypericin: Formation of semiquinone radical and activated oxygen species on illumination.

20. Redepenning, J.; Tao, N. *Photochem. Photobiol.* 1993, **58**, 532-535. Measure ment of formal potentials for hypericin in dimethyl sulfoxide.

21. Tao, N.; Orlando, M.; Hyon, J.-S.; Gross, M.; Song, P.-S. *J. Am. Chem. Soc.* 1993, **115**, 2526-2528. A new photoreceptor molecule from *Stentor Coeruleus.*

22. Song, P.-S. *Biochim. Biophys. Acta* 1981, **639**, 1-29. Photosensory transduction in *Stentor coerulus* and related organism; Walker, E. B.; Lee, T. Y.; Song, P.-S. *Biochim. Biophys. Acta* 1979, **587**, 129-144. Spectroscopic characterization of the *Stentor* photoreceptors.

23. Song, P.-S.; Walker, E. B.; Auerbach, R. A.; Robinson, G. W. *Biophys. J.* 1981, **35**, 551-555. Proton release from *Stentor* photoreceptors in the excited states.

24. Tao, N.; Song, P.-S.; Savikhin, S.; Struve, W. S. *J. Phys. Chem.* 1993, **97**, 12379-12386. Ultrafast pump-probe spectroscopy of the photoreceptor stentorins from the ciliate *Stentor coeruleus.*

25. Yang, K.-C.; Prusti, R. K.; Walker, E. B.; Song, P.-S.; Watanabe, M.; Furuya, M. *Photochem. Photobiol.* 1986, **43**, 305-310. Photodynamic action in *Sentor coerulus* sensitized by endogeneous pigment stentorin.

26. Diwu, Z., Lown, J.W. *Photochem. Photobiol.* 1990, 52, 609-616. Hypocrellins and their use in photosensitization.

27. Hudson, J.B., Zhou, J., Chen, J., Harris, L, Yip, L., Towers, G.H.N. *Photochem. Photobiol.* 1994, 60,253-255. Hypocrellin, from *Hypocrella Bambuase*, is phototoxic to human immunodeficiency virus.

28. Diwu, Z.J., Jiang, L.J., Zhang, M.H. *Sci. Sin. (B)* 1989, 33, 18-26. Electronic spectra of hypocrellin A, B and their derivatives.

29. Diwu, Z., Lown, J.W. *J. Photochem.. Photobiol. A: Chem.* 1992, 64, 273-287. Photosensitization by anticancer agents 12. Perylene quiononoid pigments, a novel type of singlet oxygen sensitizer.

30. Hu, Y. Z. , An, J. Y., Qin, L., Jiang, L. J., *J. Photochem.. Photobiol. A: Chem.* 1994, **78**, 247-251. Studies of the triplet state properties of hypocrellin A by nanosecond flash photolysis.

31. Moan, J., Berg, K. *Photochem. Photobiol.* 1992, **55**, 931-948. Photochemotherapy of cancer: Experimental research.; Henderson, B. W., Dougherty, T. J., *Photochem. Photobiol.* 1992, **55**, 145-157. How does photodynamic therapy work?

32. Foote, C. S., *Science*, 1968, 162, 963-970. Mechanisms of photosensitized oxidations.

33. Spikes, J. D. *Adv. Photochemotherapy* 1988, **9**, 92-100. Photochemotherapy: molecular and cellular processes involved.

34. Foote, C. S., *Adv. Photochemotherapy* 1988, **9**, 101-104. Oxidative processes in photosensitization.

35. Pooler, J. P., Valenzeno, D. P. *Med. Phys.* 1981, **8**, 614-628. Dye sensitized photodynamic inactivation of cells.

36. Lochman., E. R., Micheler, A., *Photochem. Photobiol.* 1979, **29**, 1199-1204. Molecular and biochemical aspects of photodynamic action.

37. Ito, T., in Photochemical and Photobiological Reviews, Volume 7. Smith, K. C., Ed. Plenum; New York; 1983. 141-186. Photodynamic agents as tools for cell biology.

38. Parker, J. G. *IEEE Cir. Dev.* 1987. 10-21. Optical monitoring of singlet oxygen generation during photodynamic treatment of tumors.; Allan, D., Gorman, A. A., Hamblett, I., Hodgson, B. W., Lambert, C., *Photochem. Photobiol.* 1993, **57**, 893-894. Upconversion of the singlet oxygen 1269 nm emission to the visible.

39. Svaasand, L. O., Morinelli, E., Gomer, C. J., Profio, A. E., Proceedings of Photodynamic Therapy: Mechanisms II. Dougherty, T. J. Ed. SPIE; Washingtion; 1990. pp 2-11. Optical characteristics of intraocular tumors in the visible and near infrared.

40. Thompson, A., Nigro, J., Seliger, H. H., *Biochem. Biophys. Res. Chem.* 1986, **140**, 888-894. Efficient singlet oxygen inactivation of firefly luciferase.

41. Coffin, J. M., in Fundamental Virology. Fields, B. N., and Knipe, D. N., Ed. Raven Press, New York. 1991 p 645-708. Retroviridae and their replication.

42. Tossberg, J. T., 1991, M. S. Thesis, Iowa State University Functional characterization of the long terminal repeat of equine infectious anemia virus.

43. Moore, J. P., Jameson, B. A., Weiss, R. A., Sattentau, Q. J., in Viral Fusion Mechanisms Bentz, J. Ed. CRC Press, Boca Raton; 1993 pp 233-289. The HIV-cell fusion reaction.

44. Stevenson, N. R., Lenard, J., *Antiviral Res.* 1993, **21**, 119-127. Antiretroviral activities of hypericin and rose bengal: photodynamic effects on Friend leukemia virus infection of mice.

45. Lavie, G., Valentine, F., Levin, B., Mazur, Y., Gallo, G., Lavie, D., Weiner, D., Meruelo, D., *Proc. Natl. Acad. Sci. USA* 1989, **86**, 5963-5967. Studies of the mechanisms of action of the antiretroviral agents hypericin and psuedohypericin.

46. Tang. J., Colacino, J. M., Larsen, S. H., Spitzer, W. *Antiviral Res.* 1990, **13**, 313-326. Virucidal activity of hypericin against enveloped and non-enveloped DNA and RNA viruses.

47. Kraus, G. A., Pratt, D., Tossberg, J., Carpenter, S., *Biochem. Biophys. Res. Com.* 1990, **172**, 149-153. Antiretroviral activity of synthetic hypericin and related analogs.

48. Schinazzi, R. F., Chu, C. K., Babu, J. R., Oswald, B. J., Saalmann, V., Cannon, D. L., Eriksson, B. F. H., Nasr, M. *Antiviral Res.* 1990, **13**, 265-272. Anthraquinones as a new class of antiviral agents against human immunodeficiency virus.

49. Senthil, V., Longworth, J. W., Ghiron, C. A., Grossweiner, L. I., *Biochem. Biophys. Acta.* 1992, **1115**, 192-200. Photosensitization of aqueous model systems by hypericin.; Senthil, V., Jones, L. R., Senthil, K., Grossweiner, L. I., *Photochem. Photobiol.* 1994, **59**, 40-47. Hypericin photosensitization in aqueous model systems.

50. Andreoni, A., Colasanti, A., Colasanti, P., Mastrocinique, M., Riccio, P., Roberti, G., *Photochem. Photobiol.* 1994, **59**, 529-533. Laser photosensitization of cells by hypericin.

51. Thomas, C., Pardini, R. S., *Photochem. Photobiol.* 1992, **55**, 831-837. Oxygen dependence of hypericin phototoxicity to EMT6 mouse mammary carcinoma cells.

52. Chemiluminescence and Bioluminescence Cormier, M. J., Hercules, D. M., Lee, J., Ed. Plenum press, New York; 1973; Chemi- and Bioluminescence Burr, J. G., Ed. Marcel Dekker, Inc. New York; 1985.

53. DeWet, J. R., Wood, K. V., DeLuca, M., Helinski, D. R., Subramani, S., *Can. Cell. Biol.* 1987, **7**, 725-737. Firefly luciferase gene: structure and expression in mammalian cells; Badia, E., Duchesne, M. J., Pons, M., Nicolas, J. C., *Anal. Biochem.* 1994, **217**, 333-335. Membrane targeting of firefly luciferase: a new bioluminescent reporter gene.

54. Seliger, H. H., McElroy, W. D., *Arch. Biochem. Biophys.* 1960, **88**, 136-141. Spectral emission and quantum yield of firefly bioluminescence.

55. Koo, J. Y., Schmidt, S. P., Schuster, G. B., *Proc. Natl. Acad. Sci. USA.* 1978, **75**, 30-33. Bioluminescence of the firefly: key steps in the formation of the electronically excited state for model systems.

56. Gandelman, O. A., Brovko, L.Y., Ugarova, N. N., Chikishev, A. Y., Shkurimov, A. P., *J. Photochem. Photobiol. B: Biol.* 1993, **19**. 187-191. Oxyluciferin fluorescence is a model of native bioluminescence in the firefly luciferin-luciferase system.

57. DeLuca, M., McElroy, W. D., *Biochem.* 1974, **13**, 921-925. Kinetics of the firefly luciferase catalyzed reactions.

58. Gates, B. J., DeLuca, M., *Arch. Biochem. Biophys.* 1975, **169**, 616-621. The production of oxyluciferin during the firefly luciferase light reaction.

59. Lemasters, J. J., Hackenbrock, C. R., *Biochem.* 1977, **16**, 445-447. Kinetics of product inhibition during firefly luciferase luminescence.

60. White, E. H., Worther, H., Seliger, H. H., McElroy, W. D., *J. Am. Chem. Soc.* 1966, **88**, 2015-2019. Amino analogs of firefly luciferin and biological activity thereof.

61. Branchini, B. R., Hayward, M. M., Bamford, S., Brennan, P. M., Lajiness, E. J., *Photochem. Photobiol.* 1989, **49**, 689-695. Naphthyl- and quinolylluciferin: green and red light emitting firefly luciferin analogues.

CHAPTER 2. OPERATION OF 30 HZ PUMP-PROBE TRANSIENT ABSORPTION SPECTROMETER

Introduction

Elucidating the primary photophysical events of hypericin and hypocrellin A depends on the generation of extremely short optical pulses. The development of modelocked solid-state and gas lasers has led to a source of stable, relatively short (<100 ps) optical pulses which can then be used to pump synchronously a dye laser [1]. Synchronous pumping refers to a dye laser whose cavity length has been matched to the repetition rate of the pumping laser. This leads to a condition of a "pulsed" population gain in the dye's lasing medium and to modelocking. The advantage of a dye laser over a solid-state laser is the relatively wide emission spectrum (approximately 50 nm) of the organic dye, which allows tunability of the output pulse through the use of a birefringent filter.

The disadvantage of a synchronously pumped dye laser is the relatively low energy per pulse, typically nanojoules. This becomes a disadvantage when it is necessary to take advantage of nonlinear effects such as self-phase modulation to produce a white-light continuum for two color pump-probe experiments and when large population changes need to be induced in a sample in order to observe small signal changes. The production of a white-light continuum results from the nonlinear reponse of the index of refraction in a medium such as water or CS_2. In order to take advantage of this nonlinear reponse, large electric fields and hence large pulse energies are required. It is possible to circumvent this small pulse energy by amplifying the output of a dye laser

with an amplifier pumped by a regenerative amplifier. This can, when aligned properly, result in amplifications on the order of 10^6 of the incoming dye laser pulse which yields millijoules of energy per a picosecond pulse.

The system described in this chapter is based on a design by Perry *et. al.* [2]. The laser system consists of four components (Figures 1 and 2, Tables 1 and 2). The first is the Antares laser, which is used to pump all of the other components. A dye laser is used for generation of tunable ~1 ps pulses. A regenerative amplifier is used as a source of high energy pulses and a dye amplifier is used as a gain medium for the dye laser pulses. Modifications will be discussed as will the basic theory behind the components used and the pump-probe experiment itself.

One of the major advantages of the pump-probe experiment is that the time resolution of the experiment is determined by the pulse width of the laser pulse and not the detection equipment as in time-correlated single-photon counting.

Antares

A Coherent Model 76-s Antares laser system is used as the "mother" laser to pump all other laser systems. The Antares uses a Nd:YAG rod as the lasing medium to produce 25 W of power in TEM_{00} mode at 1064 nm. The Anatares is actively mode-locked by a Coherent model 7600 mode-locker which produces 100 ps pulses at 76 MHz. Mode-locking is achieved by the application of radio frequencies which periodically forces all of the longitudinal modes to oscillate in phase. We have modified the Antares by removing the original KTP doubling crystal and replacing it by a CSK Optronics SPIA-5 temperature controlled LBO doubling crystal. The LBO crystal is a more efficient doubling crystal and coupled with the temperature control is able to produce 5 W

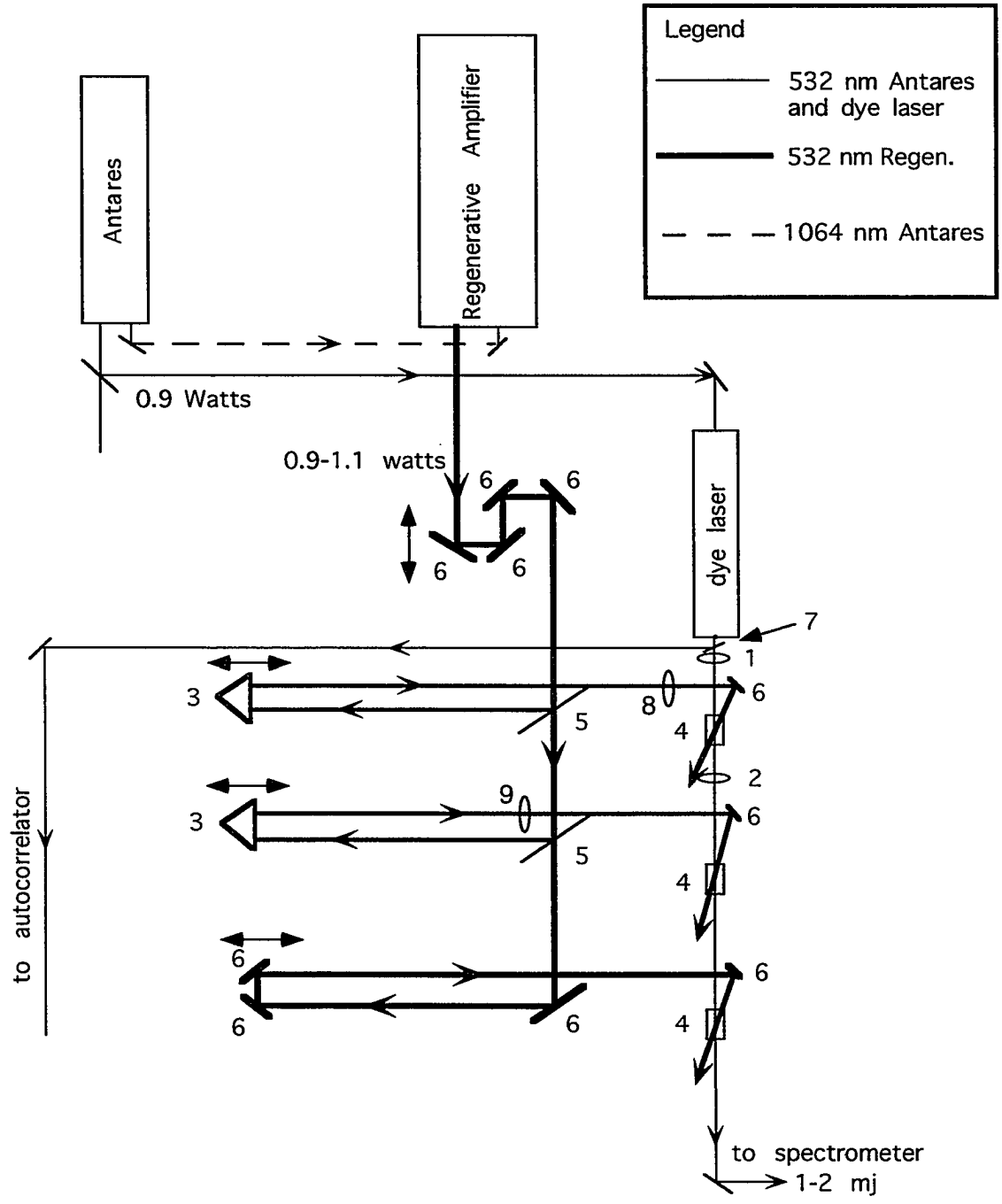

Figure 1. Dye laser amplifier system used to generate ~ 1ps 1-2 mJ pulses for use in the transient absorption spectrometer. Table 1 contains the details on the optics numbered in this figure.

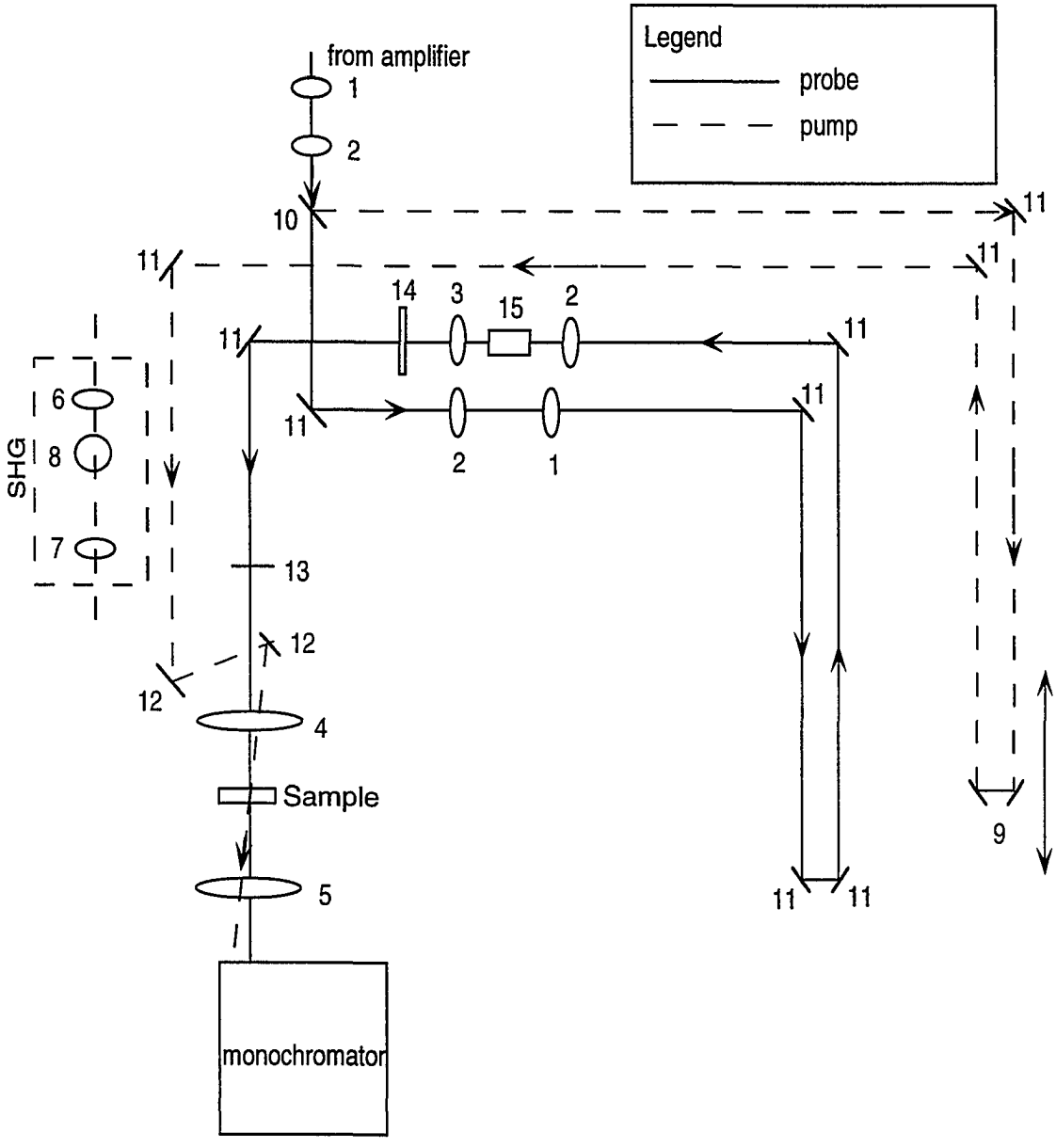

Figure 2. Schematic of transient absorption spectrometer. Table 2 contains details on the optics numbered in this figure.

Table 1. List of optics corresponding to figure 1.

Optic number	Optic	Substrate
1	lens, f = 250 mm	BK-7
2	lens, f = -1000mm	BK-7
3	prism	
4	dye cell	
5	beam splitter, 10%	BK-7
6	mirror, 100%R at 532 nm	high power YAG
7	microscope slide	
8	lens, f = 125 mm	BK-7
9	lens, f = 500 mm	Bk-7

Table 2. List of optics corresponding to figure 2.

Optic number	Optic	Substrate
1	lens, f = 100 mm	BK-7
2	lens, f = 75 mm	BK-7
3	lens, f = 50 mm	BK-7
4	lens, f = 100 mm (2 inch)	fused silica
5	lens, f = 125 mm (2 inch)	BK-7
6	lens, f = 150 mm	BK-7
7	lens, f = 200 mm	fused silica
8	KDP crystal	
9	retroreflector	
10	beam splitter, 20% R, 80% T (vis)	BK-7
	beam splitter, 50% R, 50% T (UV)	BK-7
11	mirror, 95% R (400-800 nm)	
12	mirror, 95% R (250 -800 nm)	
13	microscope slide	
14	cutoff filter	
15	10 cm water cell	

of 532 nm as compared to 2 W produced by KTP. The advantages of increased usable power out of the Antares are that the dye laser output is increased proportionally allowing better frequency doubling from the dye laser output in the time-correlated single photon counting dye laser and it acts as a fourth dye cell in the dye laser amplifier.

Regenerative Amplifier

A Continuum model RGA60 30 Hz regenerative amplifier (regen) is used to pump the dye amplifier system. The regen is seeded by a portion (~ 10%) of the residual fundamental from the Antares; it amplifies a 100 ps 200 nJ pulse to approximately 200 mJ at 1064 nm. Approximately 30 to 40 mJ of energy per pulse at 532 nm is produced via Second Harmonic Generation (SHG) in a KDP crystal.

The regen works as follows: a seed pulse from the Antares is selected via a pockel cell. This seed pulse is switched into an oscillator cavity which acts as a gain medium. The seed pulse oscillates 7 times within the cavity to achieve maximum gain at which time it is switched out of the cavity via another pockel cell. The final gain to the pulse is provided by a single pass amplifier. The advantages of a regenerative amplifier besides the obvious gain in pulse energy is that the output is a stable, repetitive reproduction of the input pulse, i.e. the temporal characteristics are retained.

Dye Laser

A Coherent model 702-1 dye laser is used in conjunction with a saturable absorber to produce 1 nj ~1ps pulses at 76 MHz. In the experiments described within this disertation the lasing medium was Rhodamine 6G in ethylene glycol and the saturable

absorber was DODCI in ethylene glycol. The dye laser is pumped synchronously by the Antares so that the lasing medium is "pulsed". Since the cavity length of the dye laser can be adjusted to match the repitition rate of the antares the stimulated emission collected in the cavity is amplified at intervals corresponding to the arrival of pulses from the Antares (the repitition rate). Shortening of the pulse from 100 ps to ~6 ps occurs because of the rapid depletion of the gain medium by the leading edge of the dye laser pulse [1]. This shortens the pulse by allowing preferential gain of the maximum of the pulse as compared to the pulse wings. Further shortening to an approximately 1 ps pulse is acomplished via a saturable absorber. The saturable absorber absorbs the leading edge of the pulse and leads further to preferential gain of the pulse maximum at the expense of the trailing edge.

Dye Amplifier

The design of the amplifier is based on that of Perry et. al. who realized that previous systems were limited by the long storage times of the dye amplifier medium when pumped by nanosecond regenerative amplifiers [2]. That is to say that when the regen pulse enters the dye amplifier it's energy is stored in the dye. If the regen pulse is long compared to the dye laser pulse then the dye amplifer medium will begin to relax, i.e. lose energy radiatively, and this fluorescence will in turn be amplified. This is known as amplified spontaneous emission (ASE). The resulting output of the dye amplifier is then a short pulse riding on top of a long pulse. Sizer et al., then Wokaun et al. recognized that this problem could be rectified by using a shorter pulse (much shorter than the storage time of the gain medium) to pump the amplifier [3,4]. This allows, when the timing is matched, for high gain (10^6) with low ASE (<1%) because optimum amplifica-

tion is attained when the dye laser pulse enters the gain medium shortly after the maximum of the regen pulse. Since the regen pulse is only 100 ps then only a small fraction of the energy is lost to fluorescence before the gain can be used to amplify the dye laser pulse.

The Pump-Probe Experiment

As mentioned previously the utility of the pump-probe experiment is that the time-resolution is not limited by the detection electronics but is simply determined by the pulse-width of the laser pulse. It should also be noted that the experiments performed on this instrument are known as "two-color" pump-probe experiments. This refers to the fact that the pump pulse and the probe pulse are not the same color. The utility of the two-color pump probe experiment lies in the increased probing range over the one color experiment and the absence of the coherent spike which is indicative of coupling between same colored pump and probe pulses in the one color experiment [1]. The experiment is done as follows; the output from the dye amplifier is split into two separate paths (Figure 2). One path includes a variable translation stage (Compumotor Model LX-L20-P54-AC) which is controlled by a personal computer through an IEEE interface, this path is refered to as the "pump". The other path length is fixed and includes a cuvette of water into which the beam is focused. This produces the aforementioned white-light continuum (self-phase modulation) and is refered to as the "probe". The percentage of light going into each path varies with wether the experiment is pumped in the ultraviolet (50% pump and 50% probe) or the visible (20% pump and 80% probe).

Since the pump and the probe beam travel different paths and the pump beam is on a translation stage it is possible to vary the time between when the pump and the

probe arrive at the sample. When the probe beam is ahead of the pump beam (before "zero time") the probe beam is simply absorbed (if there is a ground state absorbance) or transmitted and no chemistry will be observed except for an attenuation of the probe beam by the normal ground state absorbance of the sample. "Zero time" occurs when the pump and probe beam traverse the same distance and enter the sample at the same time. When the probe beam arrives after the pump beam (after "zero time") the probe beam interrogates the change induced in the sample by the pump beam. These changes can take many forms some of which are:

1. When probing in a region where there is a ground state absorbance the pump beam causes a decrease in the number of molecules in the ground state (which is to say that these molecules have been promoted to an excited state). Because there are fewer molecules in the ground state there will be fewer molecules to absorb the probe beam and there will be an increase in transmission (or decrease in absorbance) of the probe beam as compared to before "zero time". This is commonly refered to as a bleaching of the sample.

2. The molecules that were promoted to the excited-state also have a characteristic absorbance spectrum and it is possible to probe S_1 to S_n absorbances. This is refered to as an excited-state absorbance. As the name implies it involves a decrease in transmission (or increase in absorbance) of the probe beam as compared to before "zero time".

3. If the molecule of interest posesses a sufficiently large radiative rate (fluorescence) it is possible to observe stimulated emission. Stimulated emission is emission which adds in phase to the probe beam. It will appear as an increase in transmission (decrease in absorbance) of the probe beam. Obviously it is difficult to differentiate between the bleaching of the ground-state and stimulated emission in a

signal. It is possible to rule out bleaching if an increase in transmission can be observed in a region where there is no ground-state absorbance.

4. If the molecule makes photoproducts such as electrons, transient species, or tautomers it is possible to observe their excited-state absorbances or ground-state absorbances depending on how they are formed. These absorbances will obviously compete with signals such as are obtained above.

Generally all of these signals are present to some extent in a sample depending on the probe and pump wavelengths. They may, however, not all be observable due to their small amplitude or because of signal cancellation.

Data is collected as a change in probe transmission versus stage delay. Knowing that the speed of light is 2.998×10^{10} cm/s allows calibration of the stage delay directly to time so that a trace of the kinetics can be acquired. It is customary in data handling to convert the change in probe transmission to change in absorbance by the relation:

$$A = \log(I_o / I_t) \qquad 1.$$

Because in this manner the change in absorbance is directly propotional to a change in population of the sample.

Since many of the processes we observe can be on the order of a few picoseconds it is important to know the temporal characteristics of the pumping and probing pulse. The rise time of a kinetic trace is determined by the convolution of the probe and pump pulse (which in our case have identical pulse widths and are modeled by identical pulses) and it has been shown that pulses shortened by a saturable absorber are approximately modeled by a double-sided exponential. Given this information the most accurate method for determining the pulse width for our experiment is to fit a bleach of

a standard molecule such as hypericin in H_2SO_4. We have chosen hypericin in H_2SO_4 because it does not exhibit any transient behavior except a bleach when pumping and probing in areas of ground state absorbance. This bleach is instantaneous on our time scale so the rise time of the bleach allows us to extract temporal information about our pulse. The lifetime of hypericin in H_2SO_4 is 5.5 ns so that for the majority of our experiments the bleach will not decay on the chosen time scale (< 200 ps). Nile blue in ethanol has also been used as a standard, however we have occasionally observed a short decaying component (approximately 5-10 ps) which may result from vibrational relaxation. Because of this short component we use nile blue to maximize the spatial and temporal overlap of the pump and probe beams but use hypericin in H_2SO_4 as a standard for measuring the pulse width.

Typically a guess of the pulse width is made and a double sided exponential pulse is generated via the program expgen.exe (Appendix 1). This pulse is then convoluted with itself using the computer program SPECTRA (Copyright Savikan Software). This convoluted pulse (now refered to as the instrument function) is then used to fit the hypericin in H_2SO_4 curve using the computer program SPECTRA. The pulse width is varied until a satisfactory fit has been achieved which gives a good idea of the pulse width. If the pulse width is acceptable (< 1.5 ps) then the transient absorption spectrometer is ready to perform experiments.

Alignment and Maintenance of 30 Hz System

Antares

As the antares drives both the regenerative amplifier and the dye laser it is of paramount importance that stable pulses are produced. Generally no more than 2-3% deviation in the power of the 532 nm beam can be tolerated. Output into the dye laser can vary between X and Y Watt.

Achieving stable pulses from the antares involves several factors.

1. Stable lamps. Lamps generally last from 200-400 hours. They ultimately determine the stability of the antares.

2. Fine adjustment of cavity length.

3. Fine adjustment of output coupler.

Items 2 and 3 should be done on a daily basis and usually are done several times during the day to account for drift and changes in temperature. In some cases the above adjustments will not result in a suitably stable laser. The following items should be tried one at a time until a stable laser pulse is achieved.

4. Observation of pulse with the fast oscilloscope.

a. Unhook external out from mode locker (the output is hooked to the trigger in of the regenerative amplifier). Hook this into the trigger input of the tektronix 7T11A sampling sweep unit.

b. Place detector at residual IR hole. Adjust detector so that between .1 and .2 mA are displayed on amplifier.

c. Measure pulse width to make sure it is between 70-100 ps. If pulse width is too wide shorten it by adjusting the cavity length.

d. Observe "jitter" of pulse. This should be done immediately after turn-

ing the oscilloscope on because after the oscilloscope has been on for 10 minutes it introduces it's own jitter to the pulse. Jitter should be less than 1%. That is the side to side deviation of the pulse should be small. To observe jitter it is necessary to shorten the time scale down to 100 ps. Jitter can sometimes be corrected by fine adjustment of the cavity length and the output coupler.

Regenerative Amplifier

The regenerative amplifer amplifies a seed pulse from the fundamental of the Antares. The output necessary for achieving good amplification in the dye amplifier is a minimum of .9 Watts (30 mJ) however it is easier to amplify with 1 to 1.1 Watts which the system is quite capable of achieving. Again the power should not deviate by more than 5% for stable amplification. The regen lamps last from 30 million to 70 million shots, with the best indicator of bad lamps being a substantial drop in power.

Several adjustments are typical during a normal day of operation.

1. A 15 minute warm-up period with the residual fromt the Antares going into the regen cavity, shutter open and output shutter closed is recommended before any adjustments are made. If after this warm-up period the system is not up to the desired output the following adjustments can be made.

2. Adjustment of incoming 1064 nm beam from Antares into regen. Generally when the system is running well only minor adjustments of the incoming beam should be necessary. Remember to be extremely carefull of the 1064 nm fundamental from the Antares when adjusting steering mirrors.

3. Adjustment of the crystal angle can be made with the SHG toggle switch.

4. Adjustment of the delay time between arrival of the seed pulse and the

amount of time the pulse oscillates (is amplified) in the cavity can be optimized with the delay screw.

5. We have noticed that occasionally the power will start off in an acceptable range but will degrade after a half to one hour. Sometimes this indicates that part of the beam is being clipped, usually in the final amplifier or the KDP crystal assembly. The beam size and shape should be checked with burn paper and adjustments made accordingly.

Occasionally complete realignment of the regen is necessary. The most important thing to remember is **never** adjust the oscillator cavity within the renerative amplifier! Realignment should involve the two steering mirrors external to the regen itself. Insure that the beam from the Antares is parallel to the table. Direct the beam into the regen using the steering mirror closest to the regen. Using the IR viewer or an IR card direct the beam into the pockel cell and makes sure it is not clipped as it passes. The beam then should be directed onto the final steering mirror which is inside the regen. From here it strikes the half wave plate and goes into the cavity. The beam then needs to be overlapped within the oscillator cavity using the steering mirrors **not** the oscillator cavity mirrors. At this point the regen should be turned on and signs of lasing should be noticed. If it does not lase continue to adjust the steering mirrors until lasing occurs. Note: At all times there should be a weak lasing from the oscillator cavity itself. Remember that you are looking for an increase in this lasing (after it is doubled). If the oscillator cavity is not aligned refer to the regen manual.

Dye laser

The dye medium is usually rhodamine 6G/ethylene glycol which allows lasing in the range of 550 to 610 nm depending on the orientation of the birefringent filter. The

pump probe dye laser differs from the photon counting dye laser in that it does not have a cavity dump driver but instead has a saturable absorber (DODCI/ethylene glycol). The saturable absorber is a dye which absorbs a portion of the light from the dye laser. The purpose of the saturable absorber is to shorten the pulse from ~6 ps to between 0.8 to 1.2 ps. The saturable absorber works by absorbing the leading edge of the pulse, this sharpens the pulse and preferentially amplifies the shortened pulse.

Typical working parameters of the dye laser, with saturable absorber, when pumping with ~1.6 W from the antares are 100 to 130 mW with a .8 to 1.2 ps pulse at 588 nm. If the dye laser is being completely realigned it is best to empty the saturable absorber dye and replace with pure ethylene glycol. Without DODCI, but with the ethylene glycol jet, the power out of the dye laser with the above power from the antares should be 180-200 mW with a 6 ps pulse at 588 nm. It is best to absorb approximately 85% of the incoming Antares beam in the rhodamine dye jet. This can be measured using a power meter and carefully placing a mirror behind the jet and measuring the power of the Antares with the jet on and with the jet off.

Amplifier

The goal of the amplifier is to achieve between 1 to 2 mJ of energy in a .8 to 1.2 ps pulse. The amplifer medium is kiton red in water. The amplifier is pumped by the 30 Hz beam from the regen, so the resultant amplified dye laser beam is amplified at 30 Hz. Temporal and spatial overlap is critical in order to achieve the above energy, so there are means by which to vary both spatial overlap and temporal overlap in the system.

The system consists of three dye cells which contain 2 mM and 1 M of kiton red respectively. Two beam splitters pick off ~10% each of the regen beam for the first two

dye cells with the remaining beam being dumped into the final dye cell. If more than 10% of the regen beam is dumped into the first two dye cells it is much easier to have competing amplified spontaneous emission (ASE) which will have a 100 ps pulse width and degrade the time resolution of the system.

Initial alignment of the system should first include cleaning the optics with methanol and lens cleaning paper. Because of the high peak powers achieved by the regenerative amplifer it is very easy to damage the optics. If the system has not been turned on for some time several basic things should be done.

1. With the input to the regenerative amplifier closed, so only the weak lasing of the oscillator itself is used as the output, check the path of the regen to insure it is not missing any of the optics and to avoid dangerous scattering or stray beams. It is possible at this time to do a rough spatial overlap with the dye laser output in the amplifier cells.

2. With the input still closed check where the optics hit the mirrors, lenses and prisms for any obvious damage to the optics. If the beam is striking a damaged optic, move the position so it does not strike the bad spot.

3. Open the input to the regen so that full power is released to the optics. Check for bright spots which indicate bad spots on the optics. If losing significant power rotate or move the offending optic to bring power up.

4. The regen beam should be level as it traverses the system. Proper adjustments should be made to insure the beam is as level as possible.

5. It is very important that the regen beam and the dye laser beam are as colinear as possible as they enter the dye cell. Adjustments to colinearity should initially be made with the input to the regen closed to avoid possible injury. The dye laser beam and the regen beam should be at the same height and the regen beam should hit

as close to the edge of the steering mirror as possible.

6. Fine adjustment of the dye amplifier system can now be made. Initial amplification is usually best observed on a white piece of paper at the output of the dye amplifier. After amplification is observed place the power meter at the output and tune until maximum power is achieved (20-40 mW).

7. The above adjustments have assumed that temporal overlap has not been lost. If after doing steps 1 to 6 several times without achieving appreciable amplification or if substantial changes were made in the optical path or materials (recall that light moves ~30% slower through glass (i.e. prism)) it is probably wise to check the temporal overlap with an oscilloscope.

8. Using the 400 Mhz scope on the 20 ns time scale with a photodiode attached in front of the first dye cell get both the regen pulse and dye laser pulse on the screen simultaneously. IMPORTANT: make sure suitable neutral density filters are in place so that you don't blow up the photodiode. With the oscilloscope you can tell if you are within 1 ns or so from temporal overlap. It is possible that you will see that the pulses overlap however, they still could be 2 to 3 hundred picoseconds off.

9. Final temporal overlap can only be achieved by trial and error. This is most easily done with two people. The first delay line which should be changed is the initial delay line. The line should be moved in both directions while watching the power meter. IMPORTANT: Moving the delay line over long distances can alter the spatial overlap of the system. Spatial overlap must be re-optimized to tell if significant improvement has been made in the system.

10. After the first delay line is optimized each delay line on the individual turning mirrors must be optimized as above.

The above steps should allow the amplifier to achieve the necessary amplifica-

tion (1-2 mJ/pulse) to proceed with the experiment.

Transient Absorption Spectrometer

Figure 1 shows the optical arrangement for the transient absorption spectrometer. The spectrometer works as follows: The amplified dye laser beam is collimated by lenses 1 and 2. The beam is split by a 50/50 (ultraviolet) or 30/70 (visible) beam splitter. Part of the beam (referred to hereafter as the pump) traverses to a retroreflector on a computer controlled translation stage. The remainder of the beam (referred to hereafter as the probe) traverses a fixed delay line. The probe beam is focused into a 5 cm cell containing water. The purpose of this is to generate a white light continuum. Appropriate cutoff filters are placed to cut out residual laser line (usually around 588 nm). The remaining probe beam is then split with a microscope slide and these two beams (signal and reference) are collimated and directed to the detection system. The signal beam passes through the sample and the reference beam passes below the sample.

The pump beam takes a parallel path to the probe beam so that it can be overlapped spatially within the sample with the probe beam. Because the pump and probe are not perfectly colinear the probe diverges away from the entrance slit of the monochromator however care should be taken to block the beam as completely as possible.to avoid stray reflections into the monochromator.

All beams should pass through (as much as possible) the center of the optics. Slight deviation, from day to day alignment of the dye amplifier, can cause the beams to not pass through the center of the optics and can change the position of "time zero".

The detection system consists of a monochromator (Jarrell Ash Model AZ-410) to select the desired wavelength and two photodiodes, one of which collects the signal and one which collects the reference. Splitting the probe beam into a signal and refer-

ence allows shot-to-shot normalization of the data. This can, if the system is aligned correctly, correct for the noise fluctuation in the dye amplifer pulses. The signal from each diode passes into a preamplifier (EG&G ORTEC model 142) and finally to an amplifier (EG & G ORTEC model 571). The output from the amplifier is split, half is directed to an oscilloscope for real time monitoring of the reference and sample, and half is directed to the data acquistion board. The settings on the amplifier are those found in Table 3. A trigger from the regenerative amplifer is used to trigger the data acquisition board (DT2020) in a personal computer which then collects the signal from each diode. The computer program ASYST (Appendix 2) divides the signal by the reference and displays it on the screen as a function of the translation stage position. The trigger, from the regen, is fed into a delay box (EG & G ORTEC model 416A) prior to the data acquisition board so that the trigger can be delayed properly to insure that the peak of the signal is acquired. Typical settings for the delay box are found in Table 3.

Initial set-up includes insuring that all the optics are clean and that beams are passing fully through the optics. Assure that the signal and the reference are properly entering the monochromator. Signal from the photodiodes should be monitored simultaneously to data collection by an oscilloscope. Appropriate neutral density filters should be placed in front of the entrance slit of the monochromator to prevent saturation of the photodiodes. Signal ranges from .5 to 10 Volts depending on the wavelength being monitored. The reference and the sample beam should be separated by approximately .75 cm at the entrance slit. The sample beam can be moved independently of the reference by using the microscope slide (13 in Figure 2).

If setting up the system from a long down period it may be necessary to take the top off the monochromator and the photodiodes off the exit slit in order to insure the

beams are passing correctly through the system.

Once the sample and reference pulses are observed on the oscilloscope check to insure that there is no bleed through of light into the photodiodes from the reference or the sample beam by blocking each beam and observing the complete dissapearance of signal corresponding to that beam. When this has been achieved observe the pulses to insure that they are "jittering" in sync. If one pulse is jittering wildly the light path through the monochromator is not optimized and the pulses should be moved until they jitter in sync.

Table 3. Normal settings for detection electronics for the 30 Hz pump-probe experiment

Ortec 571 Amplifier

Amplifier Gain	0.5
Coarse Gain	20
Shaping Time	0.5 µsec
BLR	auto

Ortec 416A Gate and Delay Generator

Delay	4.4 µsec
Width	0.5 µsec
Amplitude	5 V
Input	positive

Data collection

As mentioned earlier data is collected by a data translation board connected to a personal computer. The computer program ASYST (ASYST Technologies Incorpo-

rated) handles manipulation of data and screen operations. Use of the ASYST program is described in Appendix 2.

Data collection involves finding "zero-time", insuring the pulse width is acceptable and checking the translation stage for flatness. Nile blue is used as a standard for maximizing overlap because it exhibits a large bleach, however hypericin in H_2SO_4 is used as a standard for checking pulse width and for checking flatness for reasons discussed earlier. Sample concentration should be between 0.3 and 0.7 O.D. units in a 1 mm cell in the pumping region. The structure of nile blue and hypericin are shown in Figure 4 along with their respective absorption and emission spectra in methanol and sulfuric acid.

If the system has been down for long periods of time move the retroreflector as far back as possible on the translation stage to insure that the pump pulse is behind "zero time". Overlap the pump beam and the probe beam in the sample cuvette as best as possible by eye. Block the pump beam with a piece of paper while observing the sample beam on the oscilloscope, there should be no change in the intensity of the sample beam.

If there is an intensity change then the pump beam is ahead of the probe beam. Using ASYST move the translation stage back while observing the sample signal on the oscilloscope. Stop moving the translation stage when the signal diminishes. Restart the program to find "time zero" and maximize the signal.

If there is no intensity change of the probe beam when the pump beam is blocked then set the data collection program to a large step size (5 ps for example) and scan through the region. If a signal can be seen (i.e. an increase in transmission) then stop the program and maximize the signal using the diodes. That is while carefully adjusting the final two mirrors on the pump path watch the probe pulse on the oscilloscope and

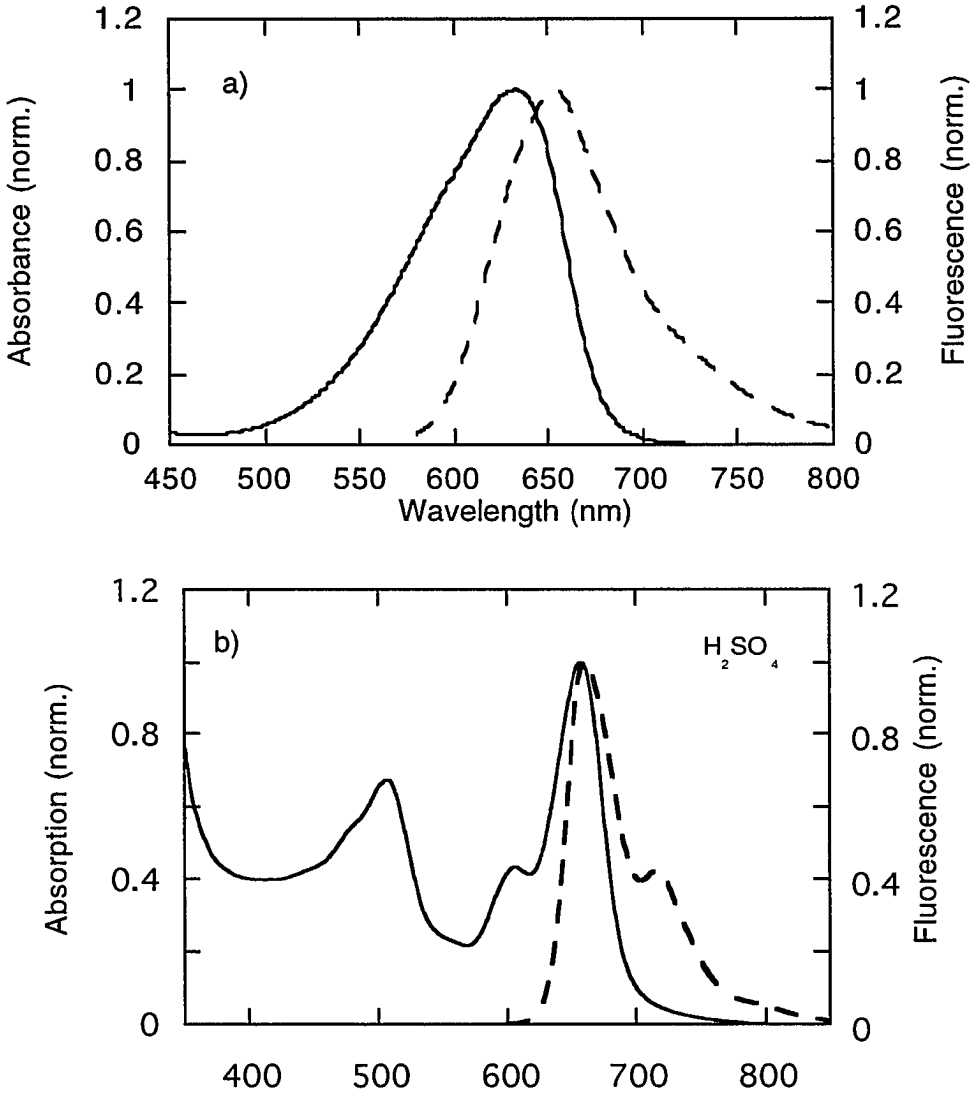

Figure 4. a) Absorption spectrum and emission spectrum of nile blue in methanol.
b) Absorption spectrum and emission spectrum of hypericin in Sulfuric Acid.

try to maximize the signal. Once maximum signal has been achieved exit the program and rerun so "time zero" can be accurately determined.

If no signal is observed stop the program by hitting any key before the translation stage reaches the end of its run. Do not exit the program but allow the translation stage to sit. While observing the probe signal from the diode on the oscilloscope adjust the overlap to obtain maximum signal on the oscilloscope. If a pump dependent signal increase is observed exit the program and rerun the scan to determine "time zero". If no signal is observed then rerun the program with a larger scan step or physically move the translation stage up to move "time zero" into the scan window. Practically speaking it is best to have "time zero" close to the rear of the translation stage to allow maximum scanning range on the translation stage.

Once zero time is located it is possible to close in on it so that it occurs within the first 15 steps of the acquisition window. A time window should be selected (i.e. -20 ps, 40 ps, 100 ps...) and a hypericin in H_2SO_4 scan should be run. Several examples of scans are shown in Figure 5. After a suitable hypericin in H_2SO_4 scan has been obtained several things should be done:

1. The bleach should appear flat on any time scale 200 ps or shorter.
2. The rise time should be 1.5 ps or shorter.
3. The optical density change should be .2 or larger. This number depends on how many neutral density filters are in front of the pump beam.

If the bleach is not flat on the appropiate time scale this means the pump beam is "walking" off the overlap with the probe beam in the sample as the pump beam translates. Fixing this requires making sure the pump beam is level going into the retroreflector and making sure the beam traverses the path level. Checking the walk of the pump beam should be done by projecting the beam across the room (being carefull

of stray beams) onto a white piece of paper. Draw circles around the beam on the paper and then allow the translation stage to go through it's normal distance while observing the spot. Adjust the incoming beam so that the spot remains in the same place for the entire scan.

If the rise time is greater than 1.5 ps shorten the cavity length and/or add more DODCI to the saturable absorber tank. Be carefull of double pulses (wings) by always monitoring the pulse on the autocorrelator. An example of a double pulse in a hypericin/ H_2SO_4 is shown in Figure 5. Note that depending on the cavity length the second pulse can sometimes not be seen on the shorter time scales. Practically speaking it is possible to observe a second pulse by watching the gain through the dye amplifier. Two pulses can be amplified and will give more power because of unused gain in the gain medium. By adjusting the cavity length it is possible to go from a maximum (two pulses) to a minimum (shortest pulse) back to a maximum (long pulse, more energy). This can assist when the second pulse is so small it cannot be seen on the autocorrelator.

Now the following has been accomplished:

1. Acceptable pulse energy
2. Acceptable pulse duration
3. Good overlap between pump and probe in sample
4. Flat translation stage.

At this point it is possible to run a real experiment. Accumulation of a "publishable" hypericin in H_2SO_4 bleach should be obtained in 2 scans. If this is not possible then either the laser system is to noisy or the system is not aligned properly into the diodes. An example of a scan taken with a properly aligned system is shown in Figure 5a. Notice that the line is flat. This is a good measure of laser stability and diode alignment.

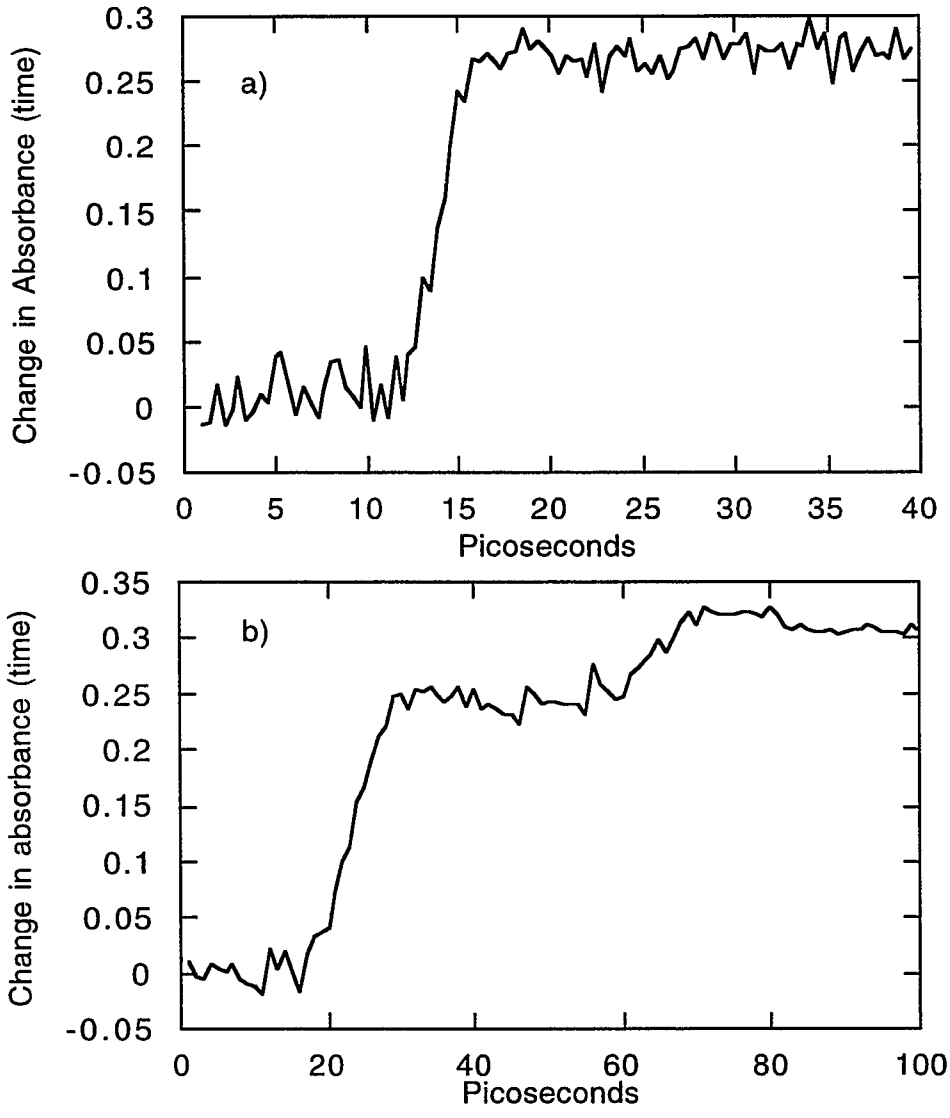

Figure 5.

a) Example of an acceptable bleach of hypericin in sulfuric acid used as a standard for determining pulse width.

b) Example of a second pulse (wings) present in dye laser as observed in bleaching of hypericin in sulfuric acid.

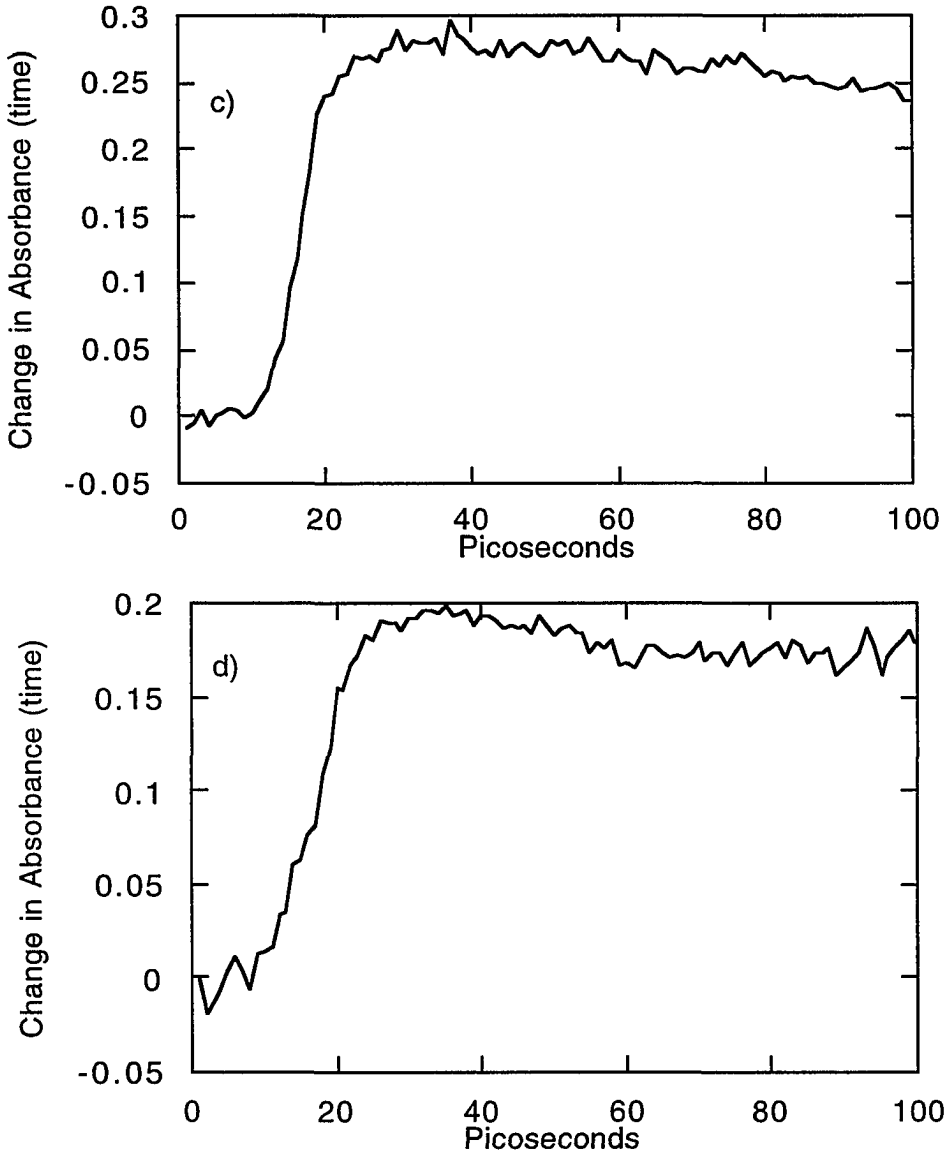

Figure 5 (cont.).

c) Example of translation stage not being flat as shown by bleaching of hypericin in sulfuric acid.

d) Example of problems with using nile blue in methanol as a standard for flatness. It is possible to observe a fast component which precludes testing stage for flatness.

References

1. Fleming, G. R., Chemical Applications of Ultrafast Spectroscopy Oxford University Press, NewYork, 1986.
2. Perry, M. D., Landon, O. L., Weston, J., and Ettlebrick, R., *Opt.Lett.*, **14**, 1989, 42.
3. Sizer II, T., Kafka, J. D., Krisiloff, A., and Mourou, G., *Opt. Commun.*, **39**, 1981, 259.
4. Wokaun, A., Liao, P. F., Freeman, R. R., and Storz, R. H., *Opt. Lett.*, **7**, 1982, 13.

CHAPTER 3. OBSERVATION OF EXCITED-STATE TAUTOMERIZATION IN THE ANTIVIRAL AGENT HYPERICIN AND IDENTIFICATION OF ITS FLUORESCENT SPECIES

A paper published in the *Journal of Physical Chemistry*[1]

F. Gai[2], M. J. Fehr[2], and J. W. Petrich[2,3]

Abstract

The absorption spectra, fluorescence spectra, and fluorescence lifetimes of hypericin, an analog lacking hydroxyl groups, mesonaphthobianthrone, and hexamethylhypericin are obtained in aprotic and protic solvents. In aprotic solvents, mesonaphthobianthrone is nonfluorescent. In strong acids such as sulfuric or triflic acids, it becomes fluorescent. Furthermore, its spectrum is very similar to that of hypericin. Similarly, only in sulfuric acid does hexamethylhypericin afford absorption and emission spectra resembling those of hypericin. We therefore conclude that the fluorescent species of hypericin has one or both of its carbonyl groups protonated. The protonation equilibrium in both the ground- and the excited-state is discussed. The first detailed measurements of the primary processes in the antiviral agent, hypericin, are performed with picosecond resolution and a white-light continuum. Trans-

---

[2]Graduate students and Associate Professor, Department of Chemistry, Iowa State University. Steady-state measurements, synthesis, time-correlated single-photon counting measurements, and CCD measurements performed by M. J. Fehr.

[3] To whom correspondence should be addressed.

ient absorption measurements of hypericin with ~1-ps resolution indicate that upon optical excitation a new species is created that absorbs in the range of roughly 580-640 nm. This species exhibits a 6-12-ps decay, depending on the solvent. It is also observed that the stimulated emission signal, which arises from the fluorescent state, grows in with a time constant of 6-12 ps. Based upon the identification of the fluorescent species as hypericin with one or both carbonyl groups protonated, the rise time for the appearance of the stimulated emission signal is attributed to excited-state tautomerization.

Introduction

The naturally occurring polycyclic quinone, hypericin (Figure 1), possesses important and diverse types of biological activity [1]. It has been shown that hypericin deactivates the human immunodeficiency virus (HIV) [2-4]. Antiviral activity was demonstrated in a lentivirus closely related to HIV, equine infectious anemia virus (EIAV), to require light by Carpenter and Kraus [5]. In addition, hypericin is closely related, both structurally and spectrally, to the photoreceptor (Figure 1) of the protozoan ciliates, *Stentor coerulus* [6] and *Blepharisma japonicum* [7,8]. Although the singlet oxygen produced from hypericin [9,10] is toxic to *S. coerulus* under high light flux (~5000 W/m^2) [11] it is an open question whether the limited exposure to room light in the experiments of Carpenter and Kraus [5] was toxic to EIAV because of photosensitized generation of singlet oxygen by hypericin or because of the presence of additional nonradiative decay processes of the excited states of hypericin. It is of fundamental importance to understand the role of light in the activity of hypericin and hypericin-like molecules.

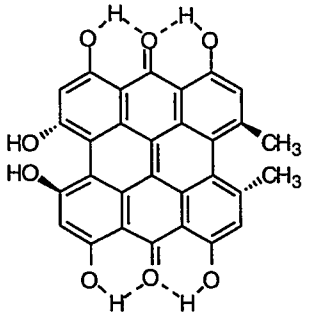

a) hypericin

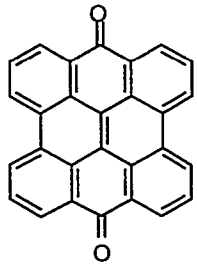

b) mesonaphthobianthrone

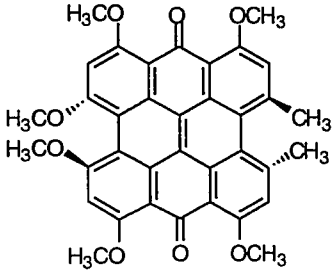

c) hexamethylhypericin

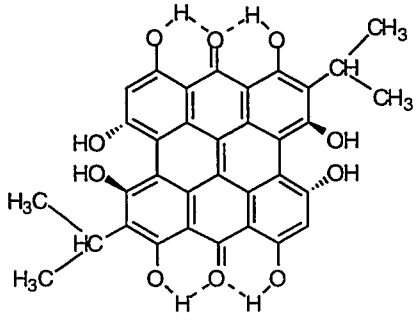

d)

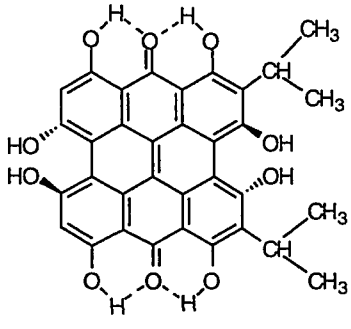

e)

Figure 1. Structures of (a) hypericin, (b) the hypericin deshydroxy analog, mesonaphthobianthrone, (c) hexamethylhypericin, and, (d) and (e), the two possible structures [6] for the stentorin chromophore.

We provide the first detailed investigation that uses both ~1-ps time resolution and a white-light continuum to examine and to unravel the excited-state primary photoprocess of hypericin. In preliminary work, we have observed that hypericin possesses an excited-state absorbance that has a rapid decay component of several picoseconds [12]. The new excited-state absorbance (~580_650 nm, in methanol) is of particular interest due to the earlier observations and suggestions of Song and coworkers [11,13,14] that the excited states of hypericin-like chromophores produce protons upon photoexcitation. We had thus tentatively suggested that a contribution of the excited-state absorption observed in hypericin was due to a species that undergoes excited-state tautomerization [12], and we proposed that deprotonation of the tautomer results in the reported pH decrease.

Because of the attention devoted to the light-dependent properties of hypericin and hypericin-like chromophores by a broad spectrum of investigators, namely those studying antiviral activity [2-5], synthetic pathways [39-43], and the directional responses of microorganisms [6-8], it is imperitive that a detailed picture of the primary photoprocesses of hypericin be established. Such is the aim of this article, whose plan is as follows:

1. Model compounds are investigated that demonstrate that a protonated carbonyl group is required in order to obtain hypericin-like absorption and emission spectra.

2. Time-resolved absorption (stimulated emission) spectra and kinetics are presented that indicate that the hypericin emission spectrum grows in on a 6-12-ps time scale. Based on the model compounds, the rise time for the appearance of the hypericin emission is taken as evidence for an excited-state proton transfer.

3. Our results and conclusions are discussed in the context of previous work on

hypericin and what is currently known about excited-state proton transfer reactions. We consider possible objections to our assignment of the excited-state reaction to proton transfer.

Finally we note that observation of proton transfer on this time scale is of fundamental importance because its measurement is accesible by "standard" ultrafast spectroscopic techniques. Consequently, theories of proton transfer can be tested using hypericin.

Materials and Methods

Hypericin was obtained from Carl Roth GmbH & Co. and used without further purification. Synthetic hypericin was also generously provided by Professor G. A. Kraus. Solvents were obtained from Aldrich. The hypericin analog, mesonaphthobianthrone (Figure 1), was prepared as described by Koch et al. [15].

In order to prepare hexamethylhypericin, hypericin (1 mg) was dissolved in 1 ml of N,N-dimethylformamide (DMF). Two equivalents of NaH were added, and the solution was stirred. Evolution of a gas and a characteristic green color indicated removal of hydroxyl protons from hypericin. Excess CH_3I was then added. This procedure was repeated 3 times No change in color occured upon addition of NaH the fourth time indicating complete removal of labile protons. The resulting solution was orange and its UV/VIS absorption spectrum agreed with that described in the literature [40].

Deuteration of hypericin was effected by two methods. The first was to equilibrate hypericin in a deuterated solvent such as CH_3OD overnight or longer. The second involved dissolving 0.5 mg of hypericin in 0.5 ml of CH_3OD and adding 2 equivalents of $NaOCH_3$ while stirring. A chararcteristic green color indicated removal of hy-

droxyl protons. The solution was diluted up to 1 ml with CH_3OD and consequently changed back to its normal red color indicating deuteration of the hypericin. The solution was then allowed to equilibrate for two days.

Fluorescence spectra were measured with a Spex Fluoromax at room temperature. In certain cases, the spectra were analyzed by fitting to sums of log normal curves (see Figure 5 and Table II). The time-resolved absorption and time-correlated single-photon counting experiments are performed with the apparatus described elsewhere [16-18]. Transient absorption spectra were obtained with a liquid nitrogen cooled charge-coupled device (CCD) (Princeton Instruments LN/CCD-1152UV) mounted on an HR320 (Instruments SA, Inc.) monochromator with a grating (1200g/mm) blazed at 5000 Å. The following protocol was employed. The CCD pixels were binned such as to allow simultaneous collection of both the probe and the reference beams, I and I_0 respectively, of the transient absorption spectrometer. The signal was integrated for 30 seconds. Absorption spectra were constructed from $\log(I/I_0)$. These spectra were corrected by subtraction of background spectra obtained with a probe delay of -20 ps. Five such corrected spectra were then averaged together. Two succesive acquistions at -20 ps and -10 ps yield a flat baseline centered on zero when substracted from each other. Figure 8d compares the absorption spectrum taken at "time zero" of the dye nile blue in ethanol with its steady-state spectrum obtained with a Shimadzu UV-2101PC double-beam spectrometer. The agreement is excellent, especially when it is borne in mind that our laser system operates at 30 Hz and that we generate continuum with ~1-ps pulses. For the absorption and stimulated emission experiments, identical kinetics were observed whether the pump beam was rotated parallel, perpendicular, or at the magic angle (54.7°) to the probe beam. Unless otherwise indicated, experiments were performed at room temperature, 22°C. Sample concentrations for hypericin were ~4 x

10^{-6} M for fluorescence measurements and ~5 x 10^{-5} M for transient absorption measurements.

Results

I. Steady-State Absorption and Fluorescence Measurements

A. Hypericin in Protic and Aprotic Solvents

Figure 2a presents the absorption and fluorescence spectra of hypericin in DMSO. Table I presents absorption and emission maxima for various protic and aprotic solvents. The absorption and emission spectra display mirror symmetry. Figure 2b presents the fluorescence and absorption spectra of hypericin in H_2SO_4. The shape of both fluorescence and absorption spectra are identical to those obtained in methanol and DMSO although red shifted by 60 and 50 nm, respectively.

As will be discussed in more detail below, hypericin in water at pH values between 3 and 11 is barely, if at all, soluble and is nonfluorescent. Figure 2c and Table I indicate, however, that hypericin in a 40 mM solution of ß-cyclodextrin at pH 4.0 gives rise to fluorescence and absorption spectra very similar to those obtained in less polar solvents in which hypericin is soluble. ß-Cyclodextrin is composed of 7 D(+)-glucopyranose units joined by α-(1,4)-linkages. The result is a cyclic molecule with an inner diameter of ~7.0 Å and a depth of ~7.0 Å [19]. While such a cavity is too small to accomodate the entire hypericin molecule, which can be crudely approximated as a rectangle of dimensions 12.8 x 9.2 Å, it is spacious enough to hold at least the corner of the molecule bearing the carbonyl group and the ß-hydroxyl group adjacent to it. There

Table I. Summary of Hypericin Photophysics

solvent	lifetime (ns)	λ^{max}_{abs} (nm)	λ^{max}_{ems} (nm)
DMSO	6.5	598	598
CH_3CN	5.5	594	594
MeOH	5.5	588	588
MeOH/10mM HCl[a]	3.5	580	580
H_2SO_4	5.5	658	661
H_2O, pH 13[b]	4.5	650	693
40mM ß-cyclodextrin[c]	___	~593	593

[a] Song and coworkers [14] reported the fluorescence spectrum of hypericin in a mixture of ethanol and HCl (10 mM). While retaining mirror symmetry, the resultant fluorescence and absorption spectra are blue-shifted 8 and 18 nm from those obtained in methanol and DMSO, respectively. The spectrum in the alcohol/HCl mixture is qualitatively similar to those obtained in protic and aprotic solvents.

[b] In water at pH < 3, hypericin is soluble but nonfluorescent. Above pH 11, hypericin is both soluble and fluorescent.

[c] The fluorescence intensity was too weak to permit an accurate determination of the excited-state lifetime. The solution was at pH 4.0.

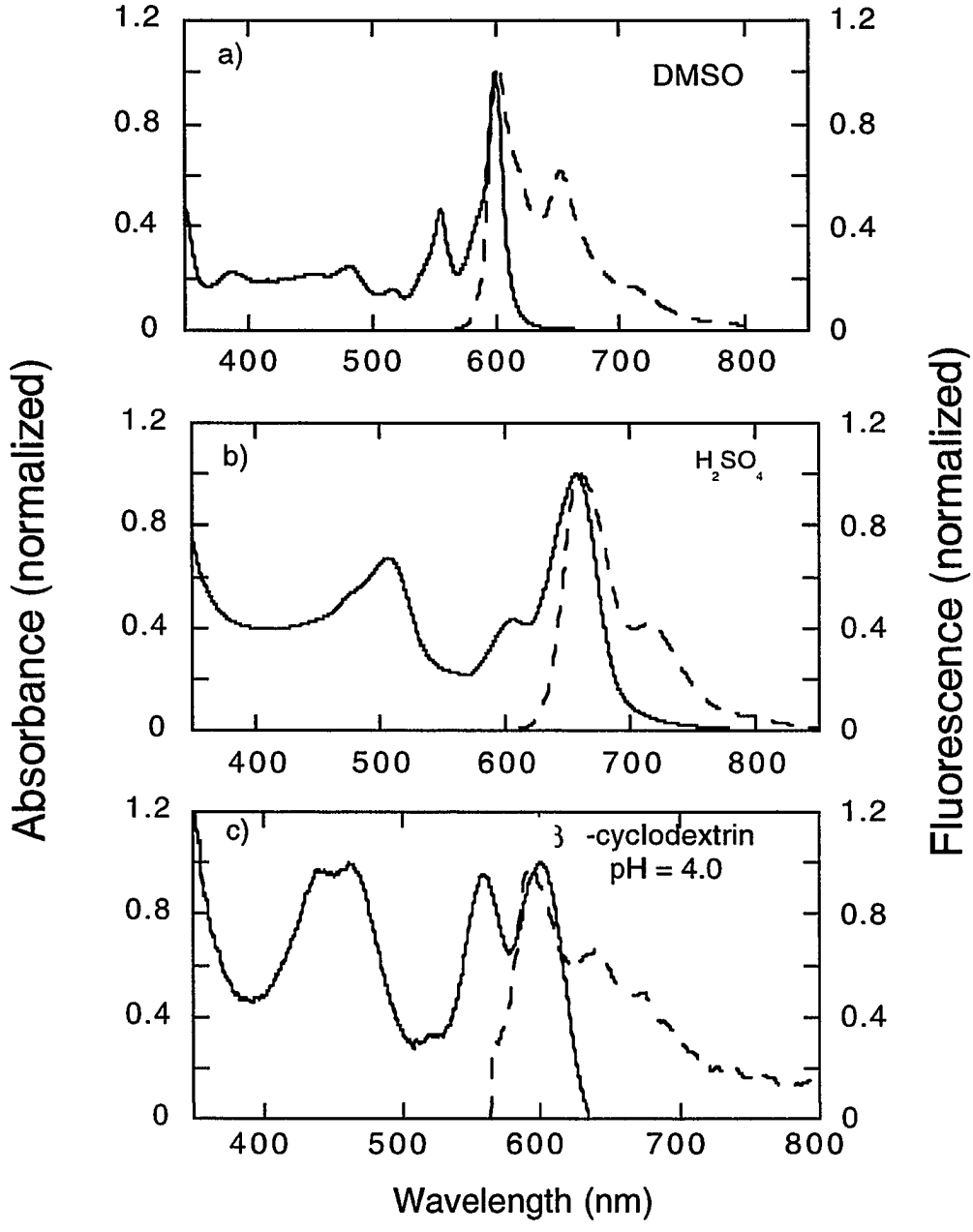

Figure 2. Normalized fluorescence spectra (——) and absorption spectra (____) of hypericin in (a) DMSO, (b) H_2SO_4, and (c) a solution of 40 mM ß-cyclodextrin at pH 4.0.

are examples of ß-cyclodextrin forming complexes with both porphyrins [31] and pyrene [32]. It is likely that hypericin forms an inclusion complex with ß-cyclodextrin under conditions (water at pH 4.0) where it is otherwise insoluble, and that this complex facilitates proton transfer between the hydroxyl and the carbonyl groups, which is responsible for the distinctive visible absorption and fluorescence spectra. This result is significant because it implies that the photoreceptor complex in the protozoan ciliate *S. coerulus*, for which no x-ray structure exists, most likely efficiently shields the stentorin chromophore from an aqueous environment.

B. Mesonapthobianthrone and Hexamethylhypericin in Protic and Aprotic Solvents

In contrast to hypericin, its deshydroxy analog, mesonaphthobianthrone (Figure 1) is nonfluorescent in the aprotic solvents DMSO (Figure 3a) and CH_3CN. When, however, it is dissolved in a protic solvent such as methanol (in which it is only sparingly soluble), a fluorescence band appears with a maximum at 467 nm (Figure 3b). Finally, dissolving it in a strong acid such as sulfuric or triflic acid generates a fluorescence spectrum that has nearly the same shape as that of hypericin in DMSO and that is blue shifted from the hypericin spectrum by about 14 nm. Its emission maximum is 584 nm. These results demonstrate the importance of a protonated carbonyl group for producing a fluorescent hypericin-like molecule. The visible absorption spectrum of mesonaphthobianthrone in H_2SO_4 is curious in that it resembles a blue shifted duplicate of its fluorescence spectrum and not its mirror image (Figure 3c), as is the case for hypericin in DMSO (Figure 2a).

In DMF hexamethylhypericin both absorbs and emits in the visible (Figure 4b).

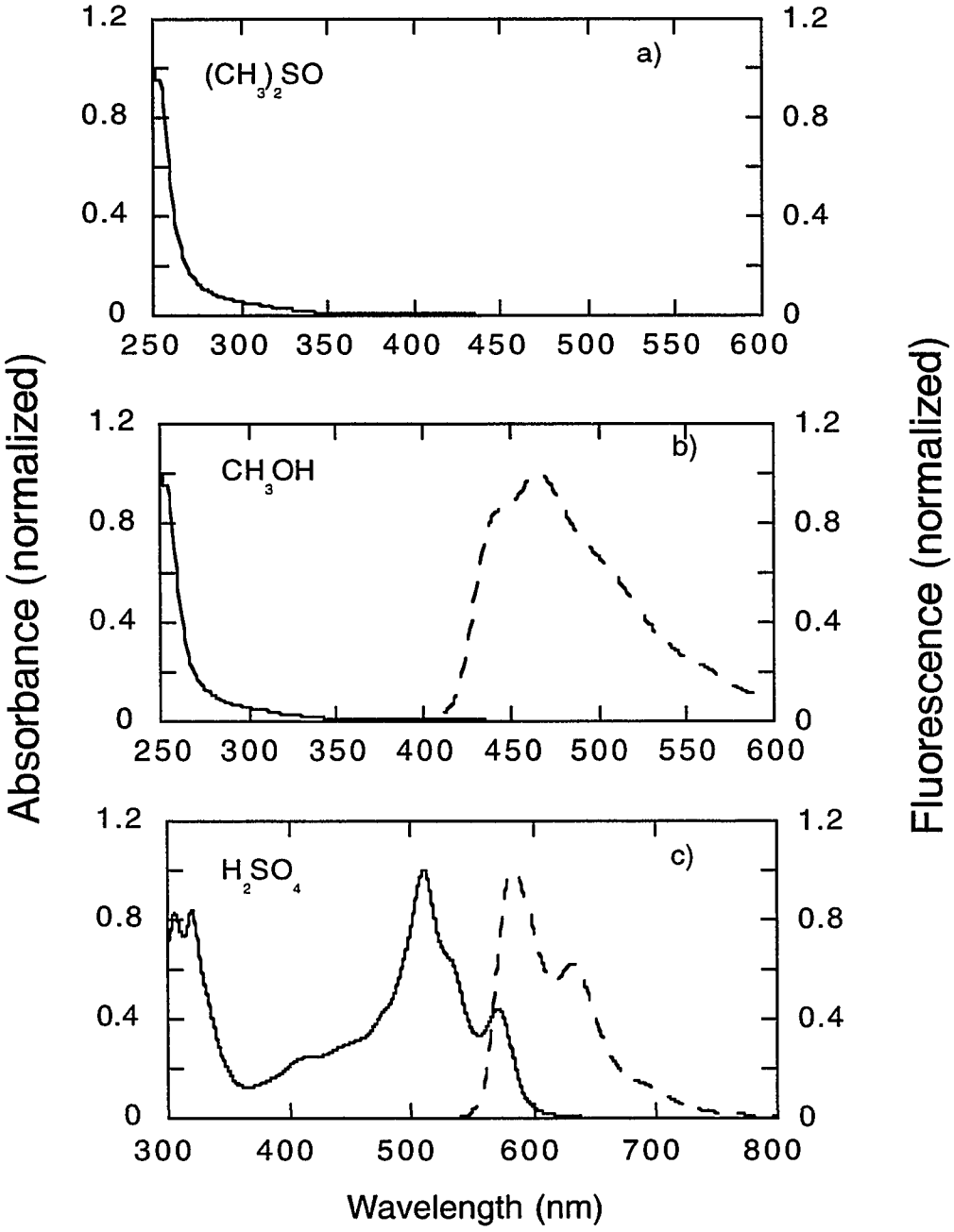

Figure 3. Normalized fluorescence spectra (——) and absorption spectra (____) of the hypericin analog lacking hydroxyl groups, mesonaphthobianthrone [15]. The solvents used are DMSO (top), methanol (middle), and sulfuric acid (bottom).

Its absorption spectrum is distinctly blue-shifted and broader with respect to that of hypericin in DMF (Figure 4a). Its emission spectrum is broad and structureless. In H_2SO_4, however, the absorption spectrum shifts to the red and acquires structure similar to that of hypericin. Similarly, the fluorescence spectrum sharpens, and a distinct shoulder appears to the red of the maximum (Figure 4c). The change in going from DMF to H_2SO_4 as a solvent for hexamethylhypericin is visually quite striking. In DMF the solution is a faint orange color. In H_2SO_4, it takes on the pink color characteristic of all hypericin solutions.

Regardless of the solvent (DMF, H_2SO_4, or methanol) the fluorescence quantum yield of hexamethylhypericin is always at least 100 times less than that of hypericin in the corresponding solvent. We suggest that this result indicates the importance of intersystem crossing as a nonradiative process in untautomerized hypericin.

C. Mesonaphthobianthrone: Probing Solute Heterogeneity Using Mixed Solvents

In order to assess the extent of inhomogeneity in the ground and the excited states, we measured the fluorescence spectrum of mesonaphthobianthrone in varying H_2SO_4/MeOH mixtures (Figure 5). At low H_2SO_4 concentrations (< 45 %), the emission spectra are featureless and broad. At high H_2SO_4 concentrations (> 80 %), the emission spectra are essentially identical to that in pure H_2SO_4 and are characterized by narrower, sharper bands. The width and intensity of these bands, as estimated from a fit to a sum of log-normal functions, are summarized in Table II. The ground-state heterogeneity is also illustrated by the variation of the fluorescence spectra with respect to excitation wavelength.

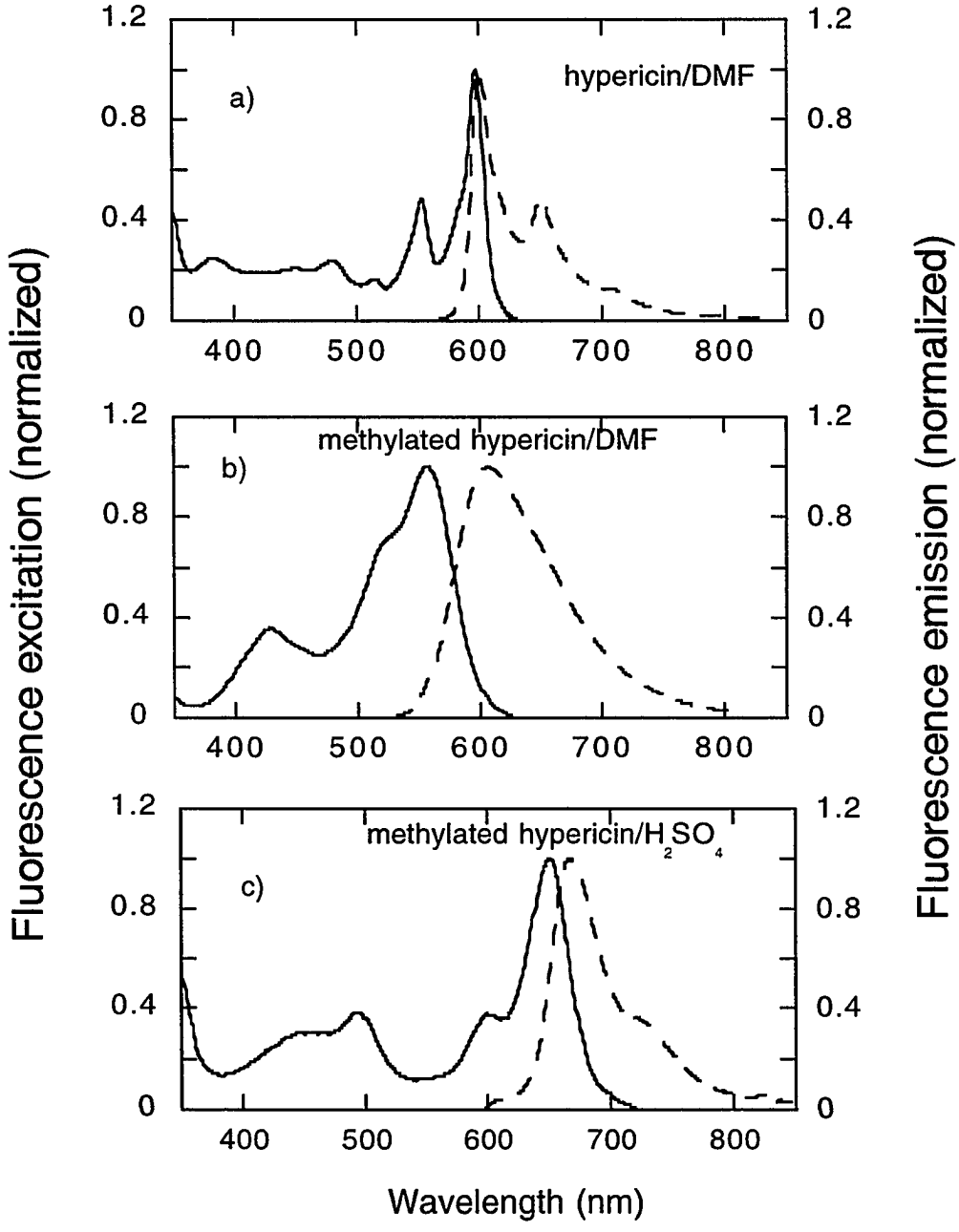

Figure 4. Normalized fluorescence spectra (– – –) and fluorescence excitation spectra (——) of hexamethylhypericin: (a) hypericin in DMF for purposes of comparison; (b) hexamethylhypericin in DMF; (c) hexamethylhypericin in H_2SO_4.

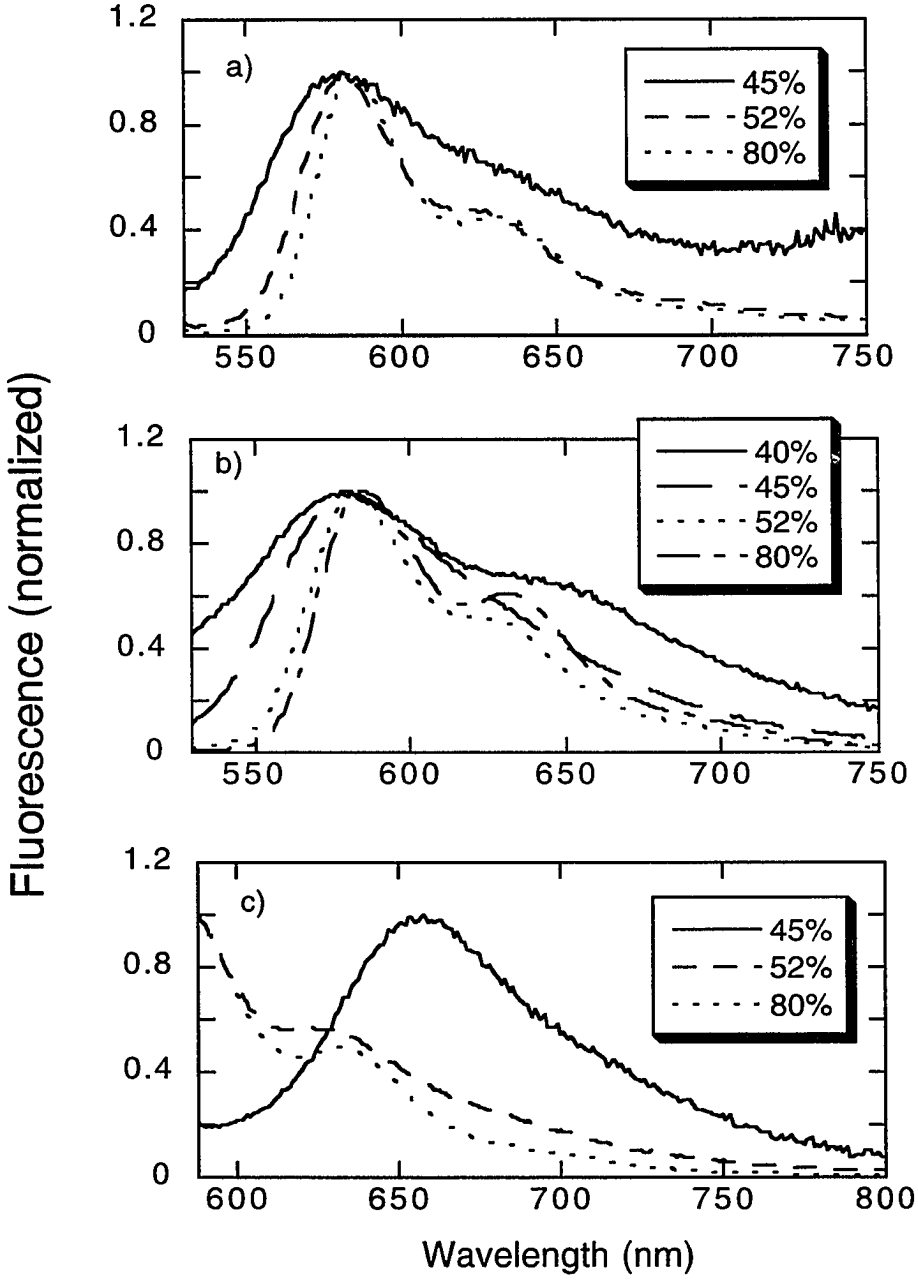

Figure 5. Fluorescence spectra of the hypericin analog, mesonaphthabianthrone, in mixtures (v/v) of H_2SO_4 and methanol. The percentage of H_2SO_4 in the mixture is indicated in the Figure. Spectra are collected at 22°C. The excitation wavelengths used are (a) 256 nm, (b) 511 nm, and (c) 580 nm.

Table II. Summary of Analog Photophysics in H_2SO_4/Methanol (v/v) Mixtures

%H_2SO_4	τ_1 (ns)	τ_2 (ns)[a,b]	λ^{max}_{ems} (nm)	I_1/I_2[c]	I_1(fwhm) (nm)	I_2 (fwhm) (nm)
45	1.8	(0.20) 15.5	582, 646	2.98	65.7	84.8
48	2.0	(0.21) 8.2	582, 625	1.93	37.7	55.5
52	2.0	(0.22) 8.2	583, 630	2.12	42.0	54.2
54	1.2	(0.62) 8.8	581, 630	2.08	51.7	61.8
56	1.5	(0.82) 12.0	581, 626	1.92	43.3	56.2
58	1.1	(0.82) 11.2	582, 629	1.98	43.7	55.4
60	0.9	(0.87) 12.5	583, 632	2.04	48.7	56.9
80	1.3	(0.93) 15.1	586, 636	2.05	45.4	53.5
100	___	(1.00) 15.0	586, 635	2.10	44.4	49.2

[a] Owing to the low solubility of mesonaphthobianthrone in these solutions, the fluorescence signal was in all cases very small. Hence only 3000-4000 counts could be collected in the maximum channel of any decay curve. This in combination with the use of a full-scale time base of 20 ns, which limits the dynamic range of the experiments, contributes to the uncertainty in the measured lifetime values. For purposes of discussion, we consider the short- and long-lived components to remain constant over the range of mixtures studied. Mixtures that are less than 45% H_2SO_4 afford very little or no observable fluorescence red of ~580 nm.

[b] λ_{ex} = 288 nm; λ_{em} 550 nm; 20°C. Under these detection conditions, the band at 467 nm, characteristic of pure methanol solutions is not observed. The species giving rise to this band has a fluorescence lifetime of ~600 ps. The fluorescence lifetimes are thus fit to only a sum of two exponentially decaying components: $F(t) = A_1\exp(-t/\tau_1) + A_2\exp(-t/\tau_2)$, where $A_1 + A_2 = 1$. The value in parentheses is the amplitude of the longer-lived lifetime component.

[c] I_1 and I_2 refer to the intensities of the bands at ~580 and ~630, respectively. The position of these bands is difficult to determine owing to the large width at lower concentrations of H_2SO_4.

D. Hypericin: Probing Solute Heterogeneity Using Mixed Solvents and pH

As indicated in Figure 2b, hypericin in concentrated sulfuric acid is fluorescent. This fluorescence, however, is quenched upon adding water to the solution. A solution that is 33% water exhibits no fluorescence (Figure 6b). Figure 6c presents the absorbance spectra of hypericin at pH values below 3; Figure 6d, at pH values above 11. Although small changes in the absorption spectra are apparent at low pH, the changes are dramatic at high pH.

There are two possible factors for the reduction of hypericin fluorescence upon the addition of water, both of which may contribute. As noted in Table I, hypericin is insoluble in water in the pH range from about 3 to 11. At low pH (< 3), hypericin is soluble but nonfluorescent. It is possible that at pH < 3 hypericin forms nonfluorescent, soluble aggregates. The decrease in fluorescence intensity of H_2SO_4/H_2O mixtures as the amount of H_2O increases (Figure 6b) may be attributed to a corresponding increase of such a nonfluorescent aggregate. Alternatively, the second explanation is that water forms very tight complexes with hypericin that prevent protonation of the carbonyl groups either from the internal hydroxyl groups or from external proton sources in solution. There is precedent for such a role for water: the presence of water has been argued to stop excited-state proton transfer in 7-azaindole [16,20]. Hydrogen bonding impurities are known to retard excited-state proton transfer in 3-hydroxyflavone [21,33].

While both of these arguments are plausible, it remains to be explained why hypericin exhibits weak fluorescence in basic solution (pH > 11, Figure 6d). Perhaps at high pH hypericin is less likely to form aggregates. Also, at high pH deprotonation of the ß hydroxyl group produces an anion whose charge can be delocalized. Such an

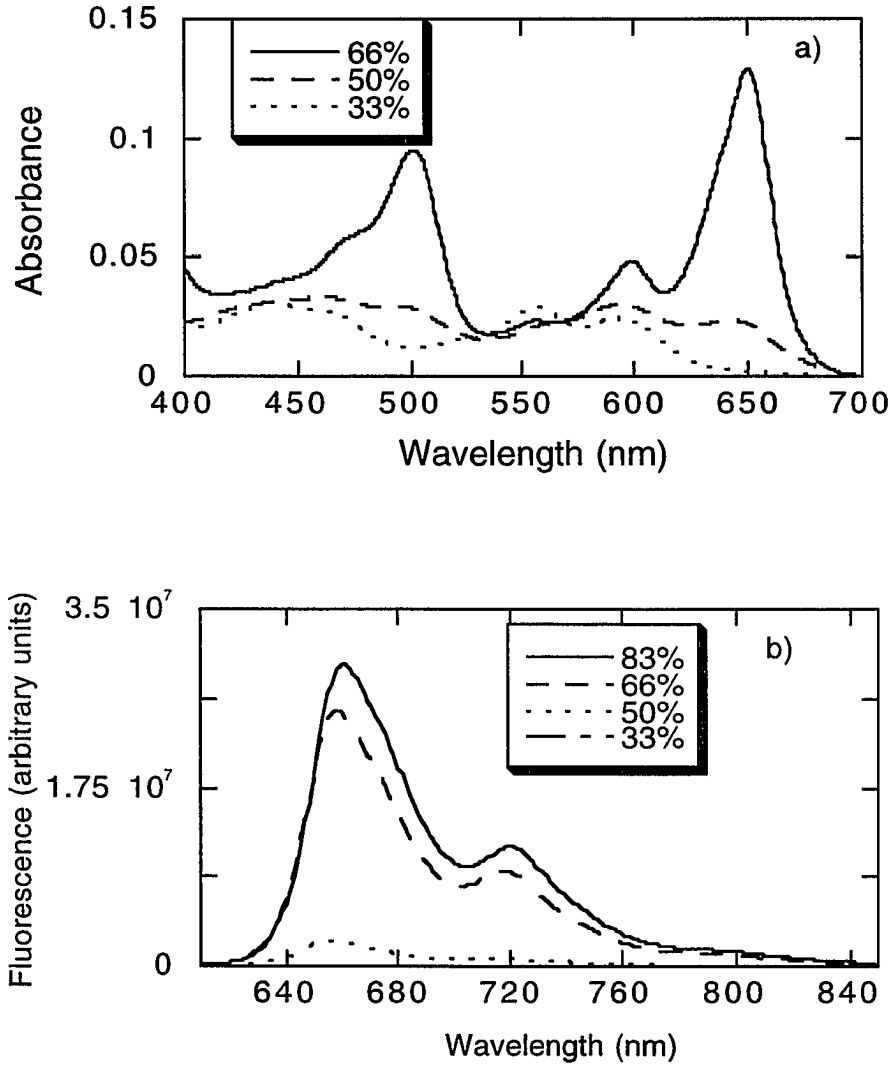

Figure 6. Absorbance and fluorescence spectra of hypericin in mixtures (v/v) of H_2SO_4 and water. (a) Changes in hypericin absorbance as a function of H_2SO_4 concentration. (b) Changes in hypericin fluorescence as a function of H_2SO_4 concentration; λ_{ex} = 400 nm. The solution that is 33% H_2SO_4 is completely nonfluorescent and superimposable on the baseline.

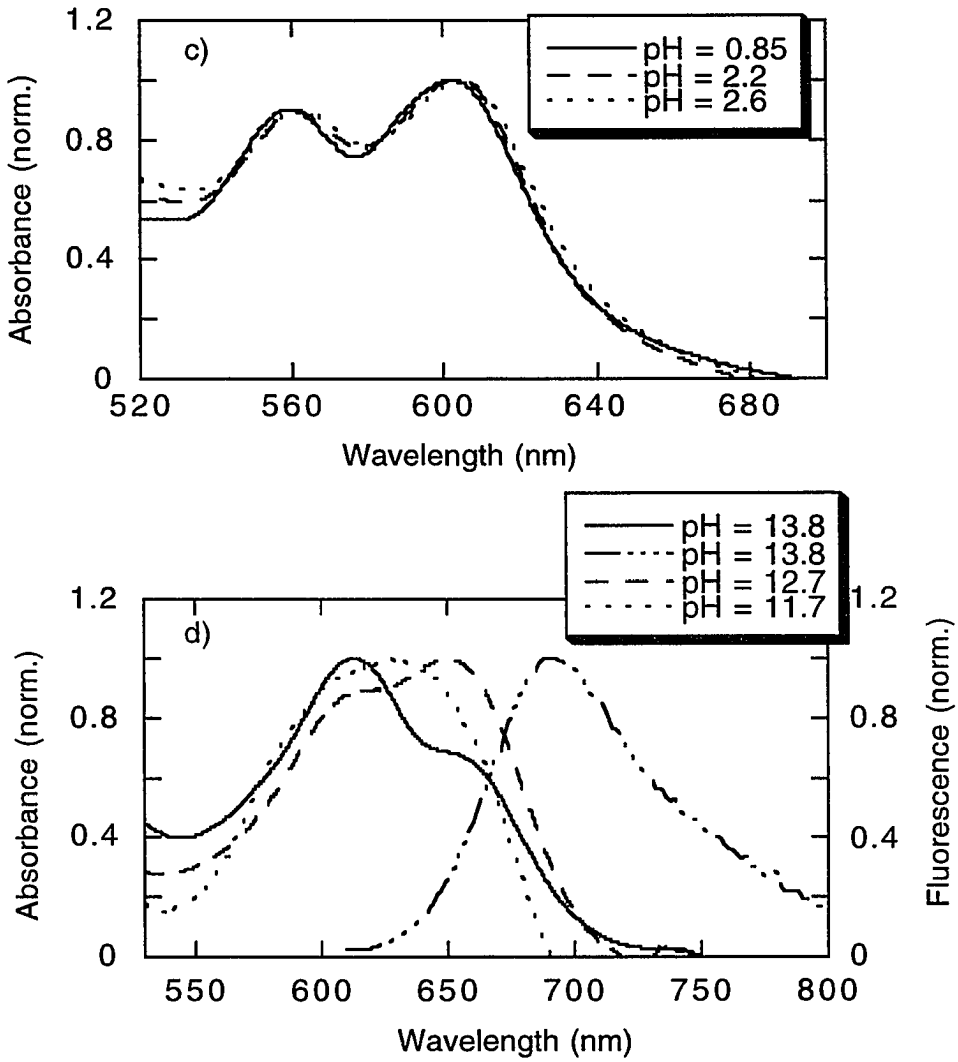

Figure 6 (cont.) (c) Absorbance of hypericin at low pH. (d) Absorbance of hypericin at high pH. The titration in this figure most likely represents more than two species. Note that the dotted line whose maximum lies between the other two maxima is not obtained at an intermediate pH. In parts (c) and (d) the pH was adjusted with H_2SO_4 and KOH. In (d) the arrow indicates the fluorescence spectrum at pH 13.8. In each panel, the concentration of hypericin is held constant in order to ensure proper normalization of the data.

anion would of course also be produced upon intramolecular proton transfer to the carbonyl.

Further investigation of both ground- and excited-state heterogeneity and the possibility of solute aggregation is afforded by both time-resolved fluorescence and absorption measurements, which are described below.

II. Fluorescence Lifetimes and Anisotropy Decay

Table I summarizes the fluorescence lifetimes of hypericin obtained in a variety of protic and aprotic solvents. The fluorescence lifetime is always single exponential and usually between 5 and 6 ns in duration. It is relatively insensitive to temperature. Arrhenius plots obtained from the fluorescence lifetime of hypericin in DMSO yield an activation energy of 0.55 kcal/mol. Mesonaphthobianthrone, in either sulfuric or triflic acid yields a single-exponential lifetime of 15 ns (λ_{ex} = 288 nm) either when collecting emission from both bands simultaneously or each band separately.

Lifetime measurements (λ_{ex} = 288 nm, λ_{em} 550 nm) w ere also performed on the mesonaphthobianthrone in mixtures of H_2SO_4 and MeOH. In the solvent mixtures, two lifetime components were obtained whose weights varied as a function of acid concentration (Table II), with the long component (15 ns) dominating at high H_2SO_4 concentrations.

Similar experiments (data not shown) were carried out with mesonaphthobianthrone in H_2SO_4/CH_3CN solutions. The solutions, however, became extremely exothermic at high concentrations of H_2SO_4; and thus solutions with H_2SO_4 higher than 30% were not investigated. The results were identical to those of the H_2SO_4/MeOH experiments with the exception of the lack of a fluorescence band in the blue region of

the spectrum (~470 nm; see Figure 2).

It has been suggested that in water hypericin forms nonfluorescent, high molecular weight (> 8000) aggregates [22]. Since the molecular weight of hypericin is 538, this corresponds to a complex of > 15 molecules. (Song, Yamazaki, and coworkers [36] have suggested that at moderately high pH hypericin forms dimers that are essentially nonfluorescent.) In order to determine that hypericin in the nonaqueous solutions in which it is fluorescent is not aggregated, we measured its fluorescence anisotropy decay in MeOH and DMSO. Because in all cases, using visible or ultraviolet excitation, within experimental error and using the appropriate time resolution, a limiting anisotropy equal to the theoretical limit (r(0) = 0.40) was observed and because the depolarization was complete within 15 ns (Figure 7), we conclude that high molecular weight aggregates are negligible in our experiments and that we are investigating primarily the monomer. The anisotropy decay of hypericin is described well by a sum of two exponentially decaying components. The more rapid of these is approximately 80 ps in methanol (Figure 7a). In order to resolve this component and the limiting anisotropy accurately and in order to estimate the duration of the longest depolarizing event, the measurements were performed on two different time scales. The data in Figure 7b indicate that the slower event is characterized by a 7.1-ns time constant. Hypericin thus may be considered as an example of an approximately symmetric rotor in which two types of depolarizing motion may be observed. The 80-ps component most likely reflects a spinning motion about an axis perpendicular to the plane of the molecule while the 7.1-ns component can be attributed to overall tumbling of the molecule. A simple calculation indicates that the longer of the two components we observe is consistent with such a motion. The rotational diffusion time [23], τ_r, is given by $1/6D = V\eta/kT$, where V is the molecular volume, η is the solvent viscosity, k is Boltzmann's constant,

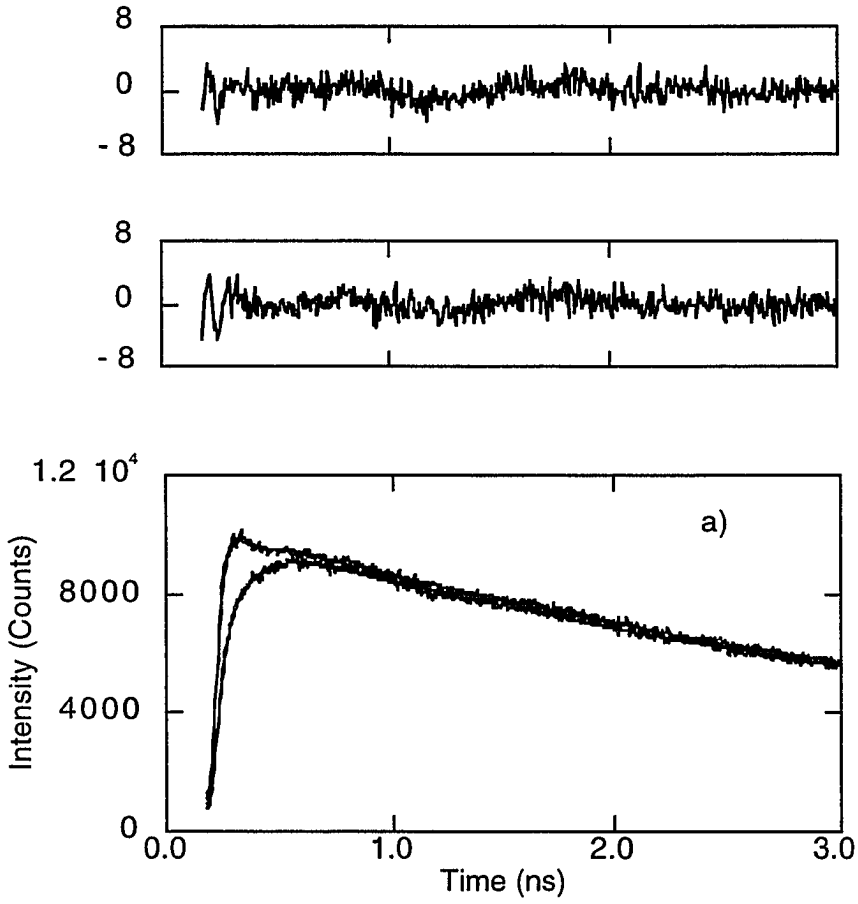

Figure 7. Fluorescence anisotropy decay of hypericin in methanol, λ_{ex} = 288 nm, λ_{em} 345 nm, 20°C. The measurements were performed with the apparatus employing a rotating analyzer polarizer described elsewhere [17] and using a full-scale time base of (a) 3 ns and (b) 15 ns. The results are as follows. (a) r(t) = 0.23 exp(-t/79 ps) + 0.18, χ^2 = 1.4. The bump at ~0.5 ns in the upper curve (parallel intensity) is due to the instrument function.

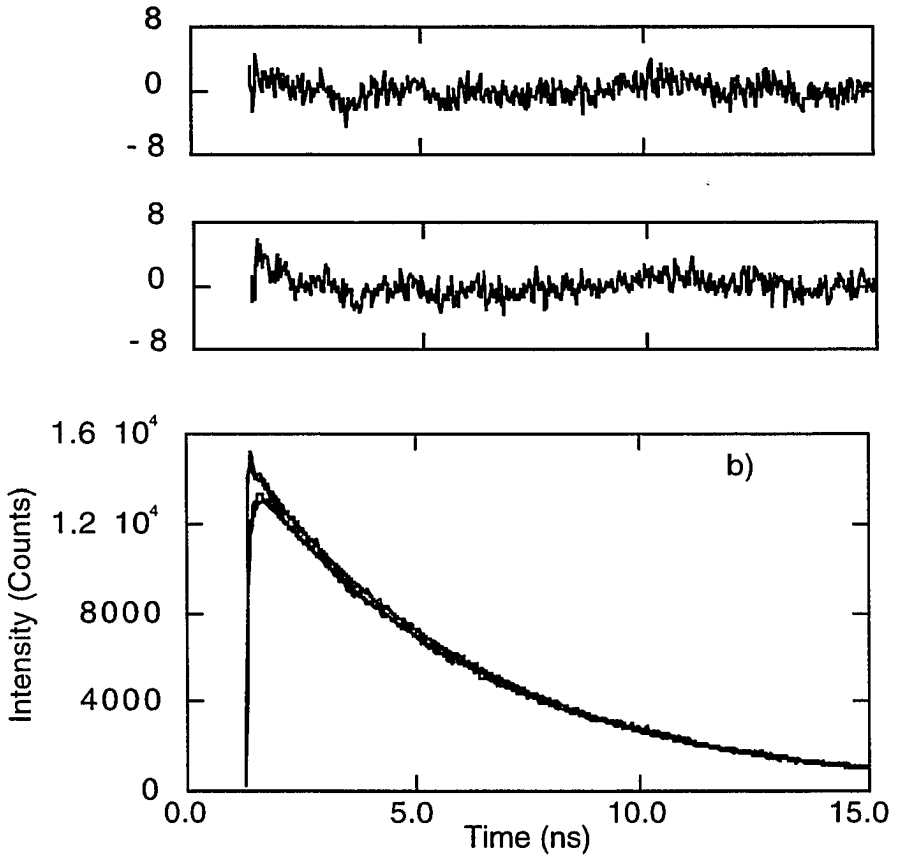

Figure 7 (cont.). (b) $r(t) = 0.141 \exp(-t/98\ ps) + 0.003 \exp(-t/7100\ ps)$, $\chi^2 = 1.7$. Similar results are obtained using visible (576 nm) excitation. Although the 15-ns time base is too coarse to resolve accurately the fast decay component and, more importantly, the limiting anisotropy demonstrates clearly that the curves for the parallel and perpendicular intensities coalesce on this time scale. As discussed in the text, the duration of the slower component of anisotropy decay obtained from the fit, 7.1 ns, is reasonable for a sphere of the dimensions of hypericin undergoing rotational diffusion in methanol.

and T is the absolute temperature. Taking hypericin to be a sphere of radius 6.4 Å, a rotational diffusion time of 1.5 ns is obtained for MeOH at 298 K. This time is certainly a lower limit since the effective molecular volume of hypericin would be expected to be larger owing to hydrogen bonding of the hypericin hydroxyl groups (in the bay region, most likely) to the solvent.

Finally, given the inhomogeneity of the hypericin sample, the observation that in all cases where the appropriate time resolution is employed (Figure 7a) the limiting anisotropy of 0.40 is obtained indicates that the distribution of absorbing and emitting transition dipole momemts are all parallel, within experimental error.

III. Time-Resolved Absorption Measurements

A. Excited-State Absorption and Stimulated Emission

Figures 8a-c present time-resolved spectra of hypericin upon optical excitation. At least three distinct events are apparent in Figure 8a: ground-state bleaching; excited-state absorption arising from a newly generated species; and stimulated emission. As we have demonstrated elsewhere [12], the species producing the new absorption decays in 6-12 ps, depending on the solvent. The spectrum of the stimulated emission requires an identical time in order to be fully evolved. In CH_3CN, this time is about 10 ps (Figure 8b).

At longer wavelengths (Figure 8c) a broad photoinduced absorption is apparent in both hypericin and mesonapthobianthrone in all the solvents investigated. As we suggested elsewhere [12] and as we conclude below (see Figure 11), this broad absorption arises from a solvated electron. The extent to which the spectrum shifts and

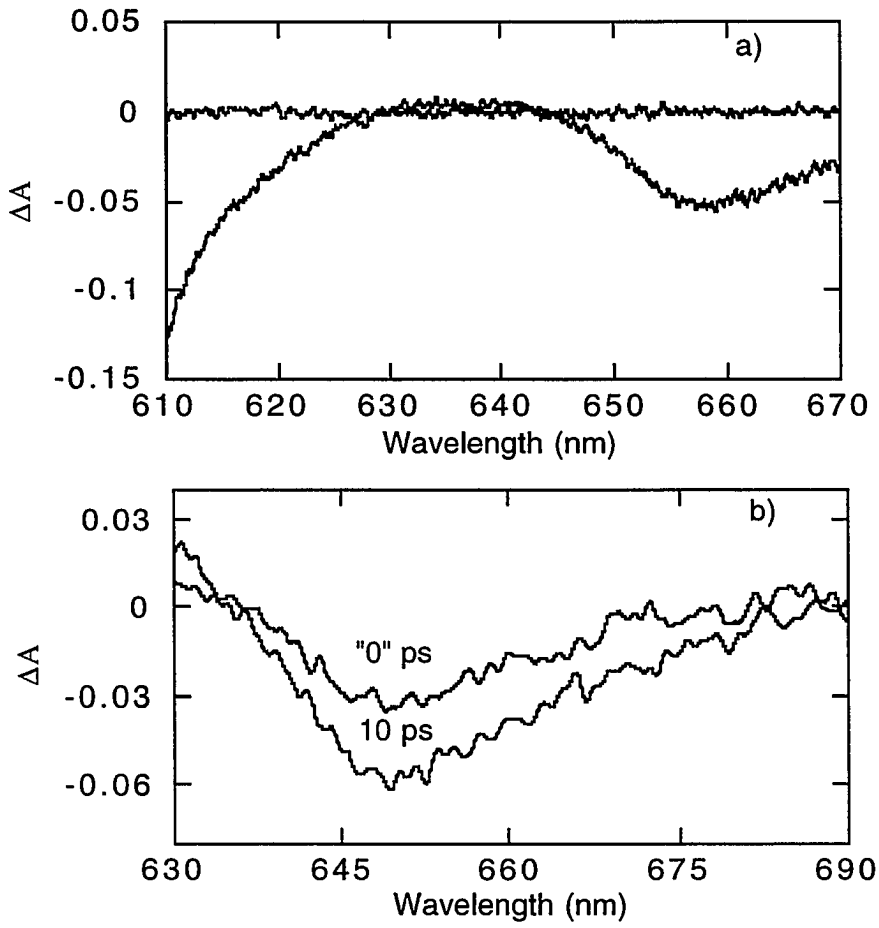

Figure 8. Time-resolved absorption spectra.

(a) Excited-state spectrum of hypericin in DMSO at "time zero." The horizontal line is the control experiment obtained by making the probe precede the pump pulse. At negative delay times no signal is expected, as is observed. This spectrum should be compared to that taken for hypericin in methanol [12] in order to appreciate the spectral shift induced upon changing solvent. At least three events are observed. From shorter to longer wavelength they are: bleaching of the ground-state absorption ($\lambda < 630$nm, compare with the steady-state absorption spectrum, Figure 2a); appearance of a new species giving rise to absorption (630 nm λ 645 nm); and negative absorption (stimulated emission, $\lambda > 645$ nm), which appears in a region where there is no ground-state absorption and hence cannot be attributed to bleaching.

(b) Growth of stimulated emission from hypericin in CH_3CN as a function of time. Spectra are shown for a "zero-time" delay (pump superimposed on probe pulse) and a 10-ps time delay.

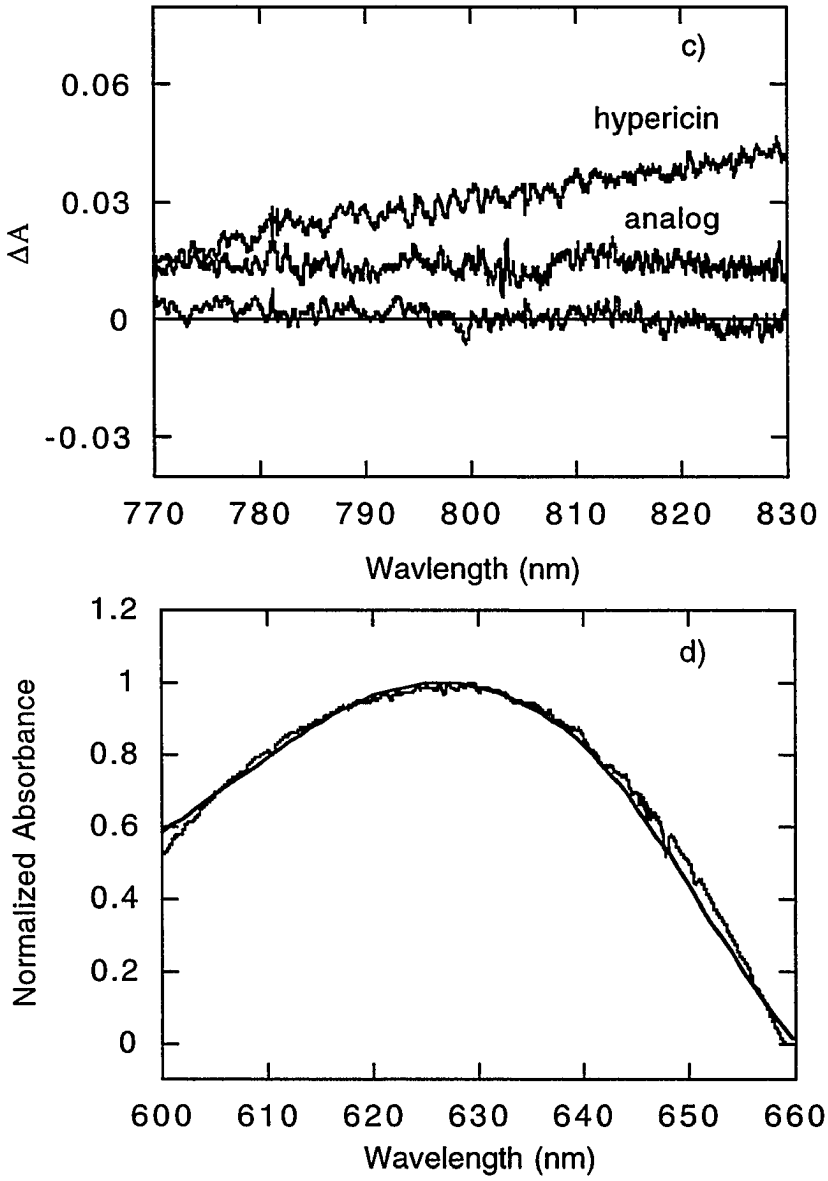

Figure 8 (cont.).

(c) Excited-state spectrum of hypericin and mesonaphthobianthrone in DMSO at long wavelength (770 nm λ 830 nm). As discussed in the text and in the caption to Figure 10, this broad absorbance in the red is attributed to a solvated electron that is produced biophotonically.

(d) Test of the time-resolved absorption spectrometer by superimposing a spectrum of nile blue in ethanol on one obtained with a conventional double-beam steady-state spectrometer (- -).

overlaps that of the stimulated emission can render the determination of whether the electron is produced monophotonically or biphotonically difficult [12].

Figure 8d presents a spectrum of nile blue taken with our transient absorption spectrometer superimposed upon a nile blue spectrum obtained with a conventional steady-state double-beam spectrometer. The agreement between the two is excellent and provides a high level of confidence in the results obtained from the time-resolved absorption apparatus.

Tuning the probe wavelength to the absorption feature appearing in the region from 620-635 nm for hypericin in MeOH (a similar feature is present from 630-645 nm in DMSO) permits the observation of a rapid decay component of about 6 ps [12]. Because this excited-state species absorbs in a region where there is ground-state absorbance, bleaching measurements of the ground state of hypericin yield a finite rise time. Thus, measurement of the time required to bleach fully the ground state provides an alternative and, because of the larger signal, more accurate method of determining the lifetime of the short-lived excited state produced upon light absorption. Figure 9 presents such ground-state bleaching measurements for hypericin in MeOH, MeOD, and DMSO. Within experimental error, deuteration of the solvent does not affect the decay of the excited state. Also, no isotope effect is observed when deuterated hypericin is used. A similar result has been reported for 3-hydroxyflavone [21] and for benzothiazole [24]. The absence of an isotope effect was used [24] to rule out tunneling as the mechanism of proton transfer and to point out that vibrational degrees of freedom other than O-H or O-D are involved in the proton or deuteron transfer.

The stimulated emission, to which we have referred above, arises from a fluorescent excited-state species. Figure 10 demonstrates that the stimulated emission rises with time constants of 6.7 and 9.2 in MeOH and DMSO, respectively. (Figure 11f indi-

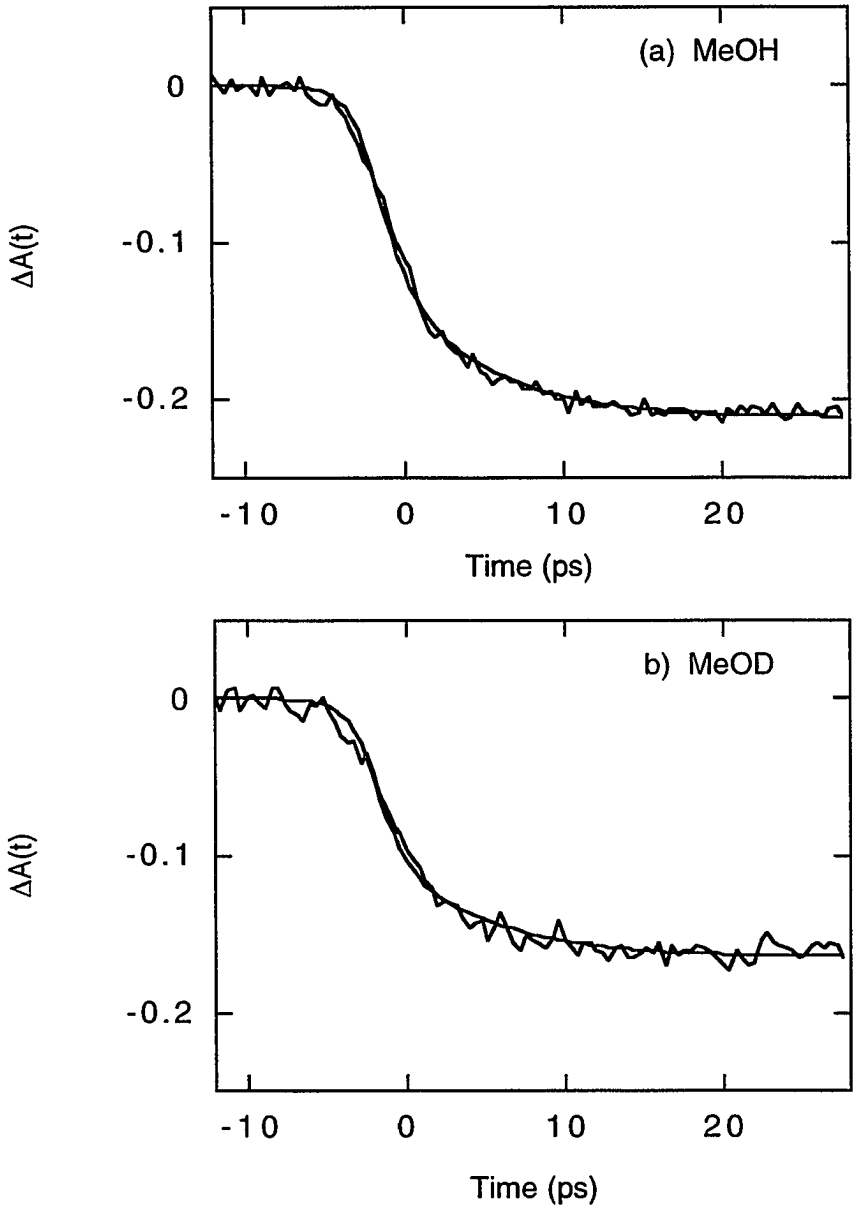

Figure 9. Time delay for the bleaching of hypericin at 22°C.

(a) MeOH, λ_{ex} = 588nm and λ_{probe} =600 nm: A(t) = 0.1 0exp(-t/5.6 ps) - 0.21;
(b) MeOD, λ_{ex} = 588nm and λ_{probe} =600 nm: A(t) = 0.07e xp(t/6.4 ps) - 0.16;

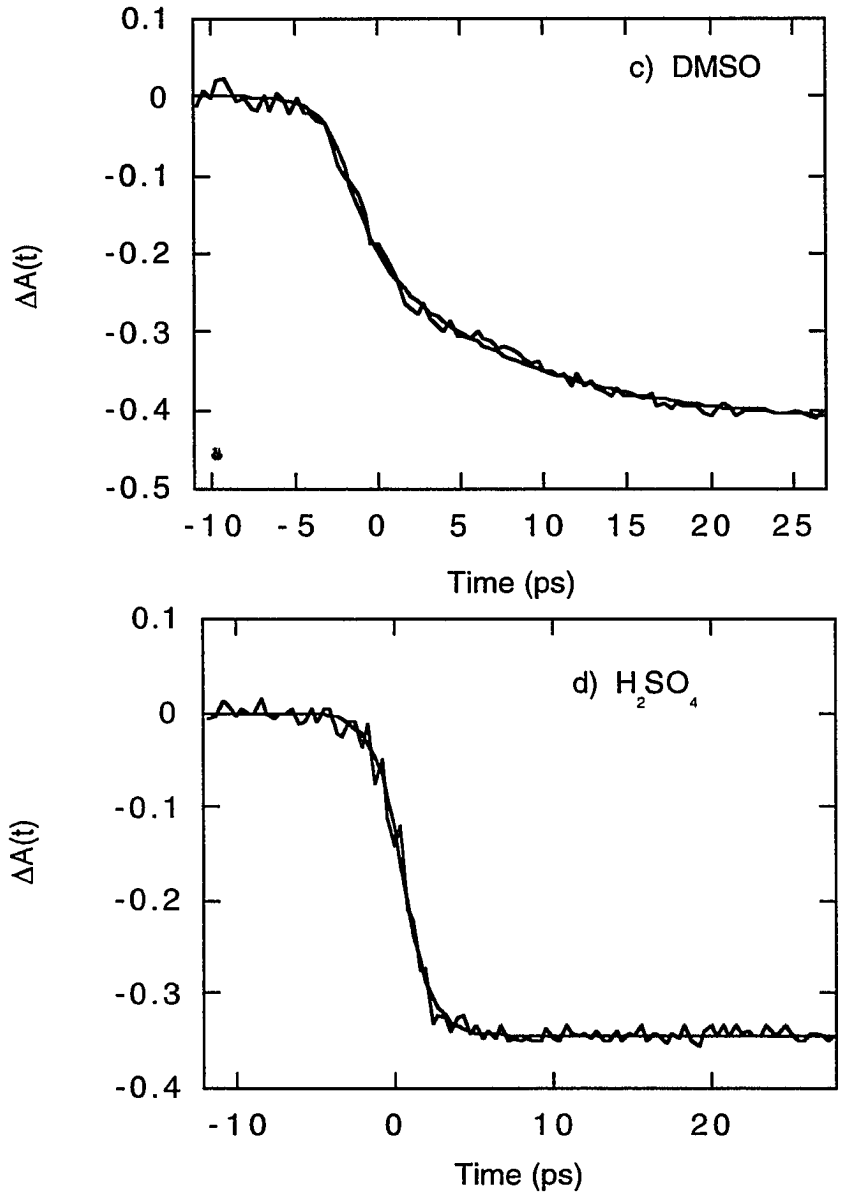

Figure 9 (cont.).

(c) DMSO, λ_{ex} = 588nm and λ_{probe} = 610 nm: A(t) = 0.23e xp(-t/9.6 ps) - 0.41;

(d) H_2SO_4, λ_{ex} = 588nm and λ_{probe} = 630 nm. The bleaching is fully developed within the time resolution of the apparatus. This result argues for the protonation of both carbonyl groups of hypericin in the ground state.

Struve and coworkers [29] have also observed a finite rise time for the ground state bleaching of stentorin.

cates a similar result for CH_3CN.) Within experimental error, the time constants for the rise time of stimulated emission are identical to those obtained, from ground-state bleaching measurements, for the decay of the excited-state produced at time zero. We conclude, therefore, that this excited-state species decays into the fluorescent species, which in turn gives rise to the stimulated emission.

Comparison of the kinetics of the stimulated emission (Figures 10 and 11f) indicates that in all cases there is a component that appears instantaneously and decays in less than 2 ps. We argue below that this component results from the ground-state heterogeneity of hypericin: that is, from an equilibrium between the untautomerized (or normal) form and a partially tautomerized form. This component is not observed for hypericin or for the hypericin analog, mesonaphthobianthrone in concentrated H_2SO_4, where in the ground state the two carbonyl sites are expected to be protonated. It is possible that the fast component observed in the stimulated emission signal arises from vibrational relaxation of a "hot" tautomer or other excited state. We tentatively rule out this explanation because the duration of the component is independent of excitation wavelength.

Hypericin in H_2SO_4 (λ_{ex} = 588 nm) exhibits only instantaneous bleaching (Figure 9d) at probe wavelengths of 600, 630, 660, and 690 nm. The absence of a finite bleaching time for hypericin in H_2SO_4 is significant. In the light of the discussion below and Figure 12, this result can be interpreted in terms of complete protonation of the carbonyl groups in the ground state. For hypericin in H_2SO_4 (λ_{probe} = 755 nm), an absorbance is detected that does not decay on a 20-ps t ime scale. We have also investigated the transient spectra of mesonaphthobianthrone in both DMSO and H_2SO_4. In DMSO between 500 and 720 nm, no signal was detected. The inability to resolve absorption transients is consistent with the lack of steady-state fluorescence and dem-

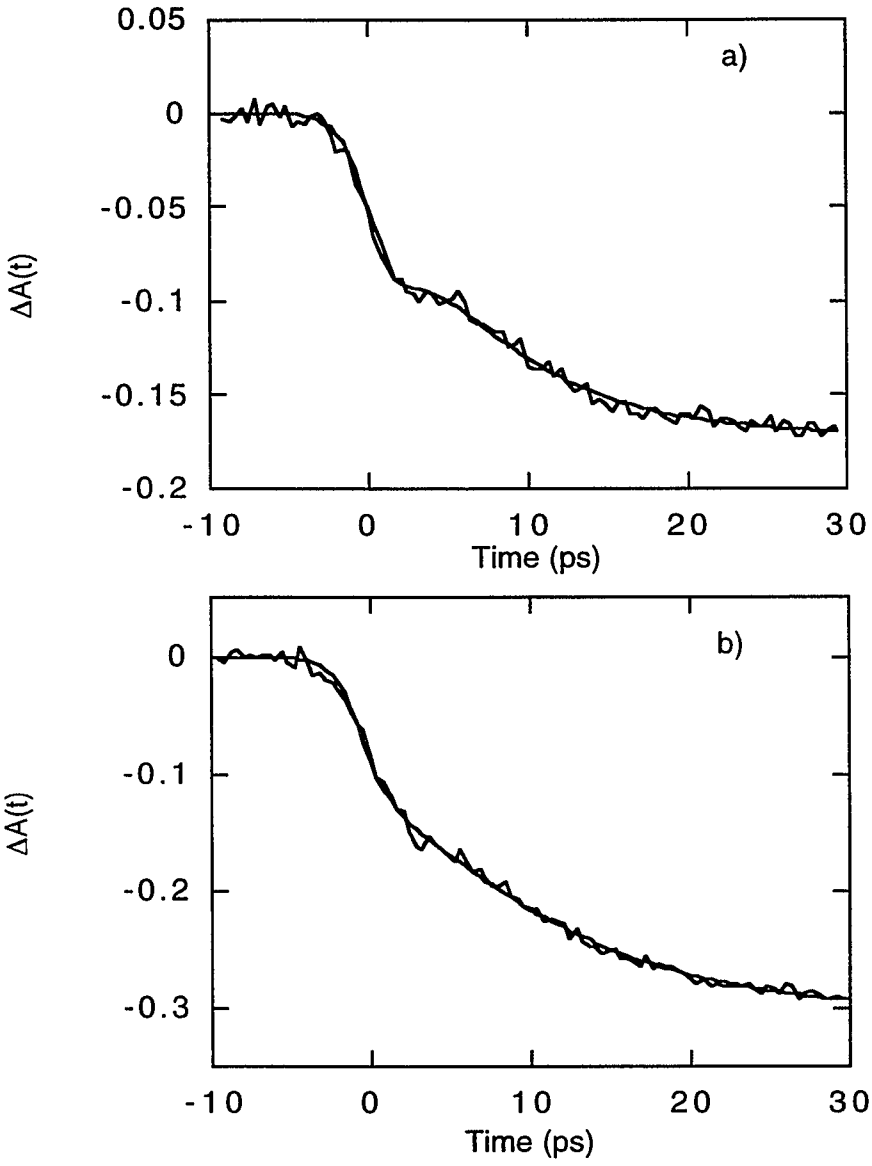

Figure 10. Kinetics of stimulated emission in hypericin. Note in each case the component that appears instantaneously. Compare these results also with the data for CH_3CN (Figure 11f).

(a) MeOH, λ_{ex} = 588nm and λ_{probe} = 645 nm: A(t) = 0.1 7[exp(-t/6.7 ps) - 1] -0.14exp(-t/1.9 ps).

(b) DMSO, λ_{ex} = 588nm and λ_{probe} = 658 nm: A(t) = 0.30[e xp(-t/9.2 ps) - 1] -0.13exp(-t/1.9 ps).

onstrates the very short excited-state lifetime (< 1 ps) of the unprotonated species. Between 770 and 830 nm, a positive absorption feature was observed. In all cases, the long-lived transient absorbing at long-wavelengths is assigned to a solvated electron (Figure 11 and discussion below).

B. Photoionization Is Biphotonic

Previously we proposed that [12] hypericin (in methanol) produced photoelectrons; but we were unable to determine whether photoionization was monophotonic or biphotonic because of the overlapping spectral contributions of stimulated emission and absorbance from the solvated electron. Figure 11 presents a series of results that demonstrates that photoionization occurs in hypericin and that it occurs biphotonically.

Excited-state absorption at 750 nm is demonstrated in hypericin in methanol upon photoexcitation. This absorption can be quenched by addition of acetone (1.0 M solution), an electron scavenger [25] (Figure 11a). The spectrum of this absorbing species in methanol is given in reference 12 and it is consistent with known spectral data for the solvated electron in methanol [26]. Furthermore, as a control experiment we demonstrate the production and quenching of solvated electrons from indole, which is known to photoionize [18,27] (Figure 11b). Whether photoionization occurs monophotonically is usually determined [18,27,28] by plotting the logarithm of the electron yield (or something proportional to it, such as its optical density) against the logarithm of the pump intensity. The slope of the resulting line gives the number of photons involved in the ionization process. Although at low pump intensity the slope is 0.9 ± 0.3 for hypericin in methanol, this result is not unambiguous evidence of monophotonic ionization because of the overlapping contribution of stimulated emission, which pro-

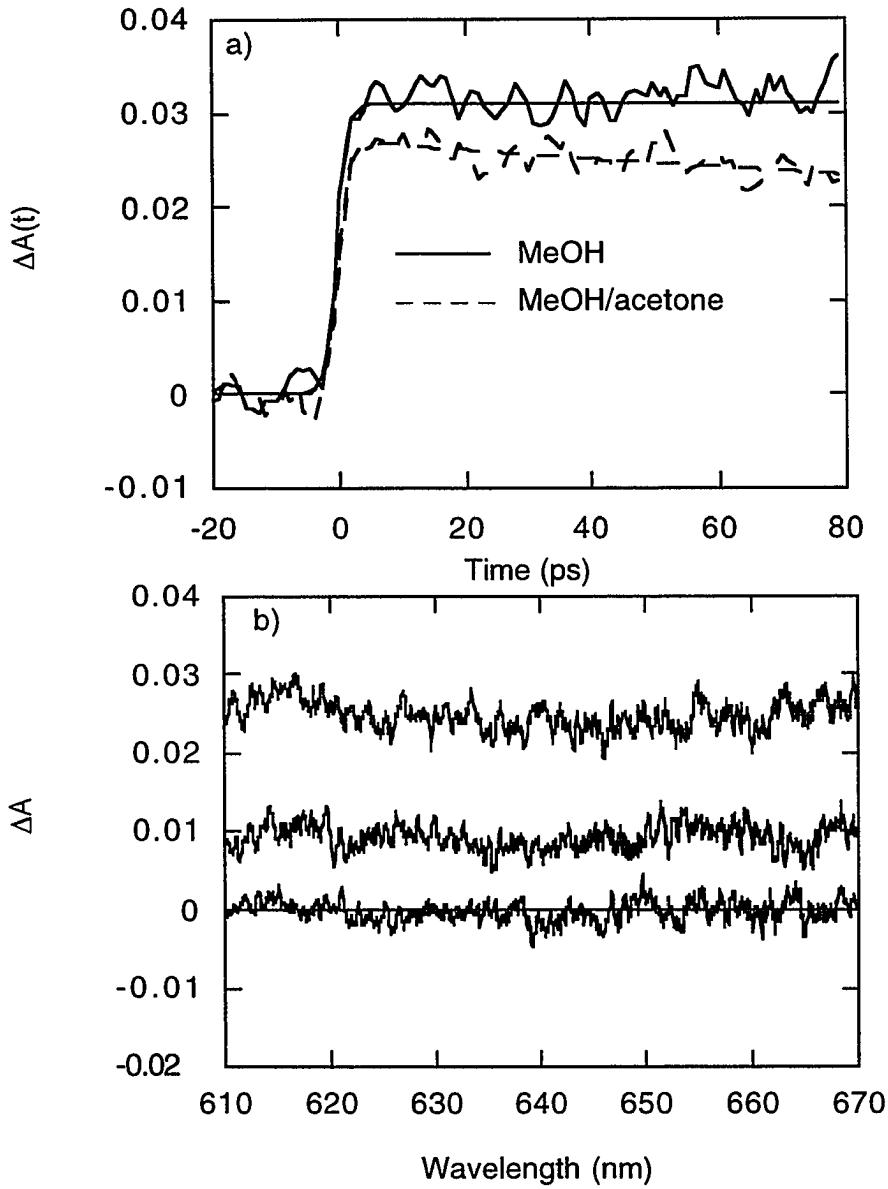

Figure 11. Demonstration that the species absorbing at long-wavelengths is a solvated electron that is produced biphotonically.

(a) Hypericin in (————) methanol and in (- - -) methanol that is 1.0 M in acetone. Acetone is known to be an electron scavenger [25]. λ_{ex} = 588 nm, λ_{probe} = 750 nm.

(b) Indole, which is known to produce electrons monophotonically [18,27]. Top: indole in methanol. Middle: indole in methanol that is 1.0 M in the electron scavenger, acetone. Bottom: probe pulse at negative delay to provide a baseline or control experiment. λ_{ex} = 294 nm.

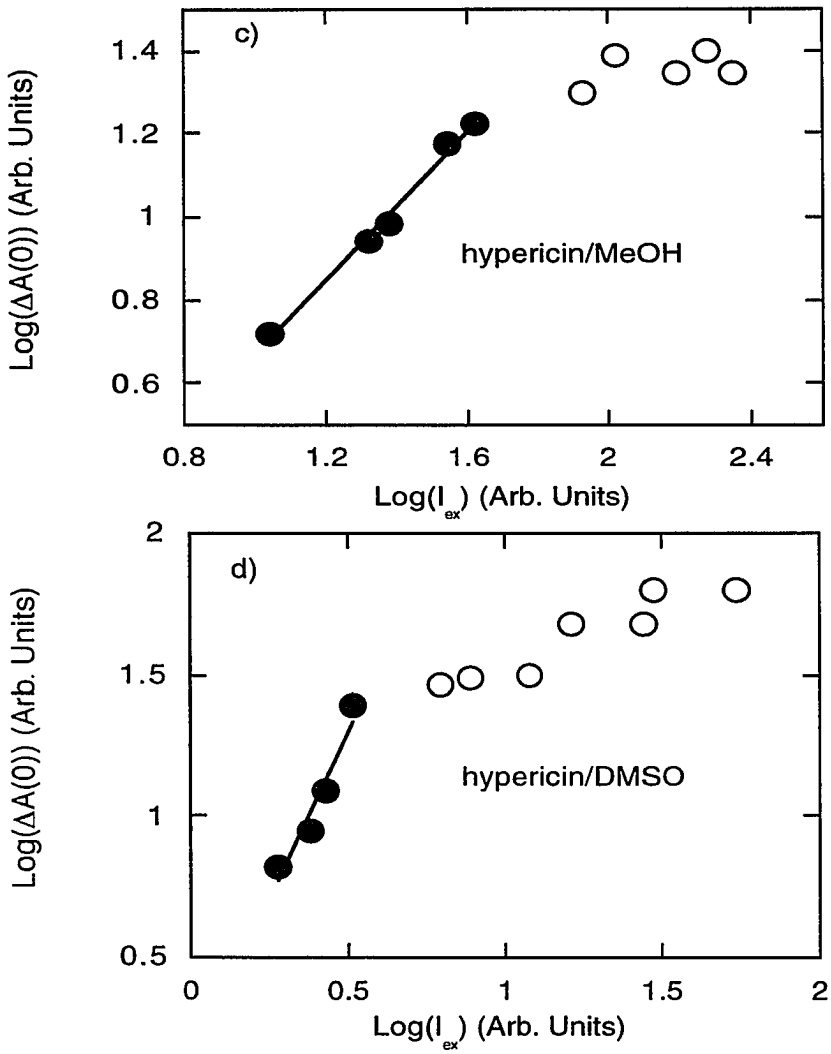

Figure 11 (cont.)

(c) Plot of log $A(t=0)_{790\ nm}$ vs $\log I_{ex}$ for hypericin in methanol. $\lambda_{ex} = 588$ nm. Although the blackened circles can be fit to a slope of 0.9 ± 0.3, the presence of stimulated emission in this spectral region renders interpretation of the slope ambiguous [12]. Note that at higher excitation or pump pulse energies, the points deviate from the line of approximately unit slope. The open circles represent a regime where the pump is so intense that the photoelectron signal begins to saturate.

(d) Plot of log $A(t=0)_{790\ nm}$ vs $\log I_{ex}$ for hypericin in DMSO. $\lambda_{ex} = 588$ nm. In this case, the blackened circles can be fit to a slope of 2.3 ± 0.3. The difference in slope between this example and that of methanol is most likely due to the spectral shifts induced by the solvents. Compare for example Figures 2a and 8a of this article with the corresponding Figures of reference 12.

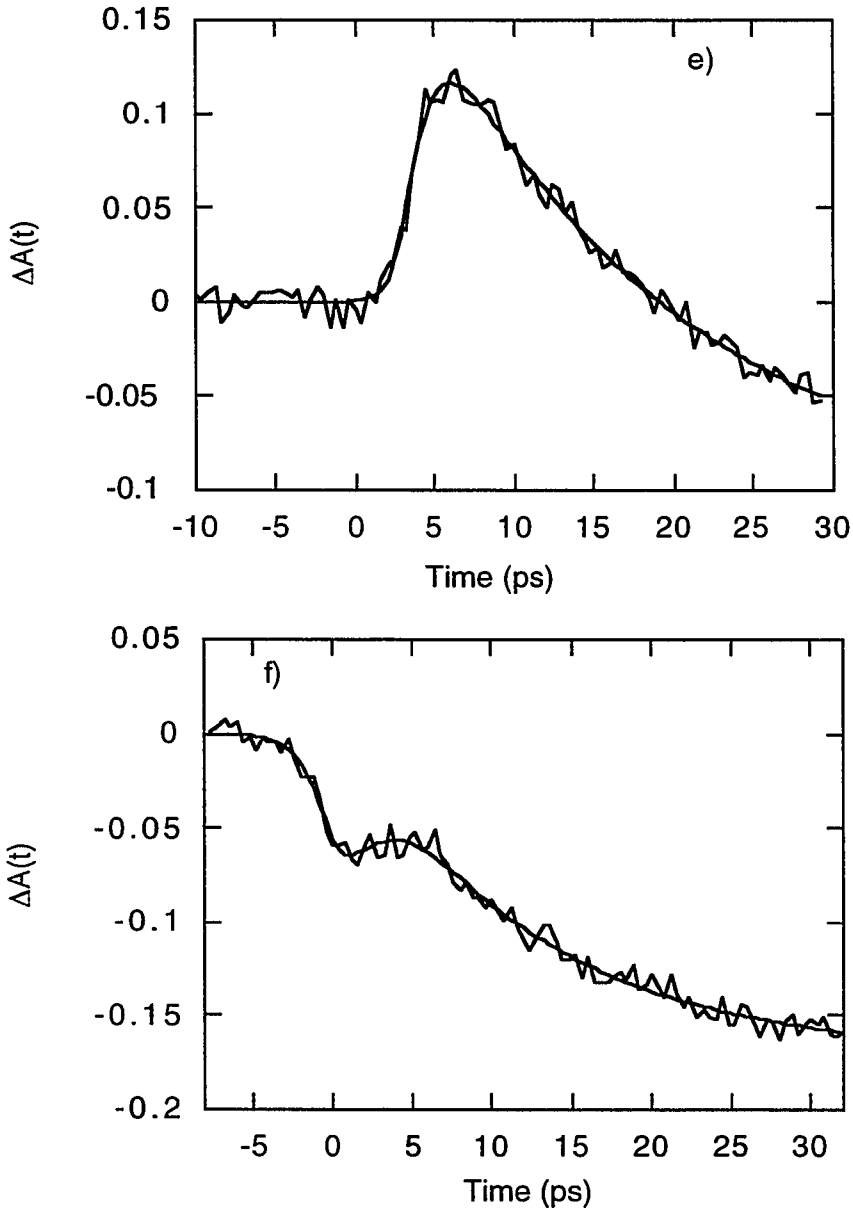

Figure 11. (cont.)

(e) Hypericin in CH_3CN, λ_{ex} = 588 nm, λ_{probe} = 645 nm.

(f) Hypericin in CH_3CN, λ_{ex} = 588 nm, λ_{probe} = 645 nm. Here, however, the pump intensity in reduced by a factor of 10 with respect to that for the experiment in panel (e). A(t) = 0.1 9[exp(-t/11.2 ps) - exp(-t/)] - 0.1 9exp(-t/1.4 ps) + 0.025.

vides an apparent diminution of the electron absorption (Figure 11c). In DMSO, on the other hand, the ground- and excited-state spectra of hypericin are sufficiently different that the log-log plot yields a slope of 2.3 ± 0.3 (Figure 11d).

Finally, another convincing piece of evidence for the biphotonic ionization of hypericin is the measurement of the kinetics of transient absorption in a region where both stimulated emission and electron absorption may be present (Figures 11e,f). At high pump intensities an initial strong transient absorbance is observed for hypericin in CH_3CN. When the pump intensity is decreased by a factor of ten, all that is observed is the stimulated emission described above.

Discussion

A. Assignment of Excited-State Processes

Figure 12 presents ground- and excited-state kinetic schemes for mesonaphthobianthrone that are consistent with the data. Time-resolved fluorescence measurements in H_2SO_4/MeOH mixtures indicate the presence of two lifetime components, ~2 and ~15 ns, whose amplitudes change with acid concentration. The amplitude of the 15-ns component increases with acid concentration. Furthermore, no rise time for fluorescence is observed for the mesonaphthobianthrone. Similarly, contrary to the case of hypericin, no measureable rise time is observed in the bleaching of the ground-state absorption and no rapid (6-12-ps) decay component is observed in the excited-state absorption of mesonaphthobianthrone.

Bearing in mind these above results and noting that protonation of the carbonyls of mesonaphthobianthrone cannot arise from any intramolecular source and that the

fluorescence lifetime of mesonapthobianthrone is very short-lived, which is demonstrated by the absence of steady-state fluorescence in DMSO and the inability to observe any excited-state aborption even with ~1-ps resolution, the ground-state equilibrium is considered in terms of two parallel protonation equilibria. We propose that in the ground state, the unprotonated, the singly protonated, and the doubly protonated species exist together in equilibrium. Upon optical excitation, at time zero, this same ground-state population is projected into the excited state in proportion to the relative extinction coefficients. We note that identical kinetic data are obtained using either excitation wavelengths of 294 or 588 nm. The short fluorescence lifetime of the unprotonated species prevents an excited-state equilibrium from being established with the singly- or doubly-protonated species. The argument against sequential ground-state protonation equilibria is that if, as we propose, the singly- and doubly-protonated species have lifetimes of 2 and 15 ns, respectively, then the 15-ns component would be expected to appear with an ~2-ns rise time, which is not observed.

The case for hypericin is similar, but not identical to, that of mesonaphthobianthrone. The fundamental difference is that the hydroxyl groups ß to the carbonyls provide an intramolecular source of protons that is lacking in the deshydroxy analog. Also, the observation of a finite ground-state bleaching time that corresponds with the decay time of an excited-state absorption and stimulated emission suggest that the protonation equilibria of hypericin are sequential. A possible explanation for the hypericin photophysics is the following. In the ground state, three species (at least) may coexist in equilibrium: the untautomerized or "normal" form, N; the monotautomerized form, MT; and the ditautomerized form, DT. By analogy with mesonaphthobianthrone, DT corresponds to the species with the long (~6 ns) fluorescence lifetime. Because stimulated emission corresponding to a long-lived component does not appear instantaneously

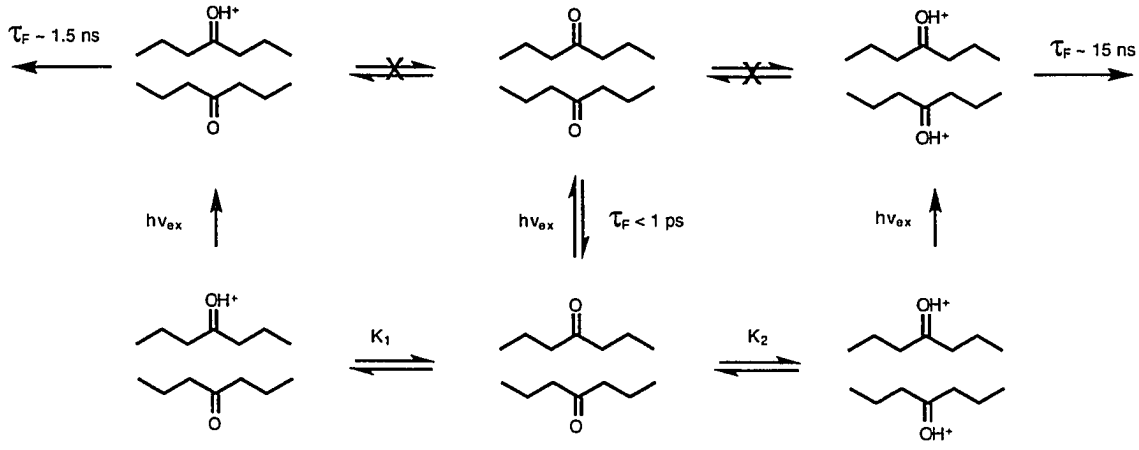

(a) mesonaphthobianthrone

Figure 12. Kinetic schemes for (a) mesonaphthobianthrone and (b) hypericin taking into account both ground- and excited-state species. The structures of mesonaphthobianthrone and hypericin are abbreviated; and only two of the six hydroxyl groups of hypericin are indicated in the Figure. The schemes presented are the simplest that are consistent with the experimental data. Because of the irresolvably short excited-state lifetime of unprotonated mesonaphthobianthrone (a), an excited-state equilibrium is not expected to be established with either of its protonated forms.

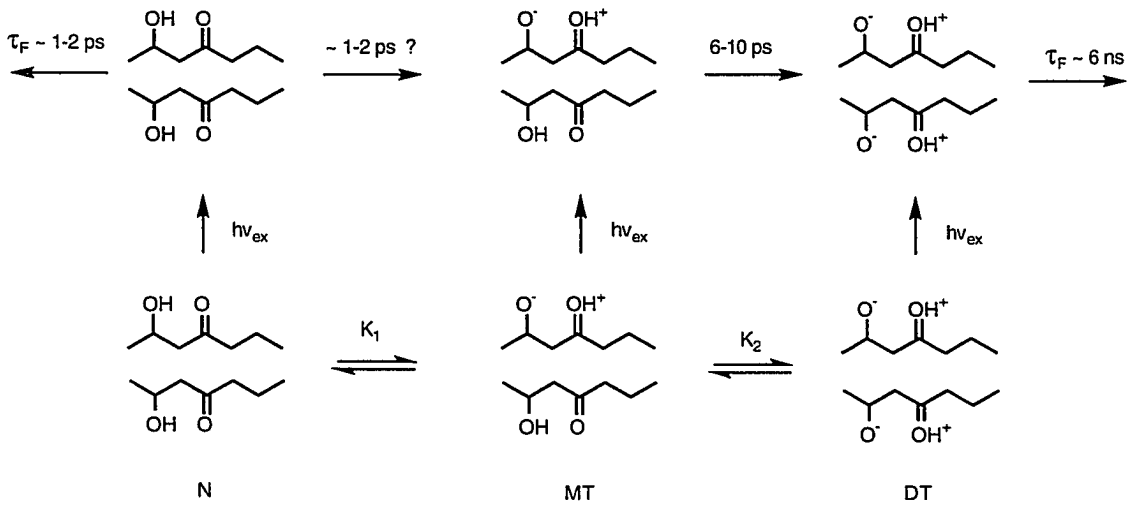

(b) hypericin

Figure 12 (cont.). For the sake of completeness, we note that for the case of hypericin (b) it may be possible that N^* undergoes a two-proton transfer reaction that converts it directly to DT^*. In part (b) of this Figure as well as in Figure 1, the proton is shown to interact strongly with the carbonyl oxygen by means of a hydrogen bond. This interaction is reasonable given the rapidity of the excited-state process as well as the observation that hydrogen-bonding solvents do not interfere with the rate of the process [37] (methanol and DMSO give qualitatively similar results), as is observed for example in 3-hydroxyflavone [21]. It must be borne in mind, however, that the proton transfer reaction is a charge transfer process and that the tautomer is likely to possess some ionic or charge separated character which is oversimplified by the Figures presented here. In support of this ionic character is the observation that the time constant for the excited-state process decreases with increasing solvent polarity [37].

(within our resolution), we suggest that the population of DT in the ground state is negligible. On the other hand, the heterogeneity of the stimulated emission signal from hypericin in DMSO and CH_3CN may be attributed to significant ground-state population of both N and MT. By analogy with mesonaphthobianthrone in DMSO, the normal form of hypericin is expected to have a very short fluorescence lifetime, whose duration can be estimated from the stimulated emission signals as 1-2 ps. An interesting observation by Weiner and Mazur [30] that is consistent with this description (especially those aspects dealing with ground-state heterogeneity and photoinduced deprotonation of the hydroxyl group) is that hypericin in the absence of light yields an EPR signal that is enhanced upon illumination. They suggest that the EPR signal resembles that of a semiquinone radical.

It is likely that N^* undergoes a rapid one-proton transfer to produce MT^* (Figure 12). In order to produce a significant amount of MT^*, the one-proton reaction would need to occur in 1-2 ps. (It is also possible that N^* executes a double-proton transfer to form DT^* directly.) In several systems excited-state proton transfer has been shown to occur on a time scale of hundreds of femtoseconds [21,24,34]. Of particular relevance to the problem of hypericin are the 1-(acylamino)anthraquinones [34] and disubstituted anthraquinones [35]. For example, Barbara and coworkers have shown that excited-state proton transfer occurs in 100 fs in 1-(dichloroacetylamino)anthraquinone.

We tentatively assign the 6-12 ps rise time in the stimulated emission signals to a one-proton transfer reaction converting MT^* to DT^*. We thus attribute the excited-state species of corresponding decay time in the transient absorption measurements (reference 12 and Figure 9) to MT. There are three possible reasons why a 6-12-ps decay component is not observed in the stimulated emission data. The first is that in the ground state [N] > [MT]. The second is that at the probe wavelengths we employ,

the emission intensity of MT^* is negligible compared to that of N^* and DT^*. The third is that if indeed the reaction N MT^* occurs, the stimulated emission from MT^* at the probe wavelength will be compensated for, at least partially, by the excited-state absorption of MT^*.

Song, Yamazaki, and coworkers [36] have recently presented steady-state spectra and fluorescence lifetimes of hypericin under various conditions. They argue that the excited-state pK_a of hypericin is larger than that of the ground state: 12.2 as opposed to 11.7 (Falk and coworkers [39] have made similar arguments). They also propose, based on comparison of the fluorescence spectra of related compounds, that hypericin has no substantial intramolecular hydrogen bonding. Consequently, they suggest that if excited-state proton transfer is an important nonradiative process in hypericin, such a process is intermolecular and not intramolecular. These conclusions clearly differ from ours. First, it is unlikely that the pK_a of the fluorescent species of hypericin can be measured since it is formed from a species that decays in 6-12 ps. Determination of pK assumes that equilibrium can be established between the conjugate acid and base. Second, while comparisons with the spectra of analogs such as anthraquinones are instructive, they must take into account the nonaggregated species of hypericin existing in both the ground and the excited states. Third, insofar as we are justified in using the fluorescence spectra of mesonaphthobianthrone and hexamethylhypericin in H_2SO_4 to attribute the long-lived fluorescence in hypericin to a species with protonated carbonyl groups, the presence of the 6-12-ps rise time for long-lived fluorescence in both aprotic and protic solvents demonstrates that in hypericin proton transfer occurs in the excited state and intramolecularly. Fourth, and most importantly, our observation of stimulated emission that rises in 6-12 ps into a long-lived species indicates that steady-state fluorescence and conventional photon counting measurements do not measure

the primary photophysical events in hypericin.

B. Potential Difficulties and Unresolved Questions

There are several questions that arise from the results presented upon and from the conclusions drawn from them. We summarize them here and try to respond to them.

1. A possible objection to the assignment of the excited-state process in hypericin to a tautomerization reaction is the observation of a "mirror symmetry" relationship between the fluorescence spectrum and the visible absorption spectrum (Figure 2). We suggest that the observation of a mirror symmetry between the emission and the absorption spectra is consistent with the excited-state proton transfer process if it is kept in mind that tautomerized hypericin, in the form of MT, already exists in the ground state. We argue that MT is similar enough to DT structurally that absorption by MT and fluorescence from DT^* is what produces the mirror symmetry.

2. The assignment of the excited-state process to intramolecular proton transfer may be criticized because we do not observe an isotope effect. There is precedent for proton transfer processes that do not exhibit an isotope effect [21,24]. Whether an isotope effect is observed will also depend on such factors as the degree to which the reaction is nonadiabatic and characterized by tunneling through a potential barrier [38] or if the reaction occurs by means of a barrierless (or small barrier) process in which the role of vibrational motions other than the O-H stretch are important. The solvent dependence of the time constant for the excited-state process is also consistent with its assignment to proton transfer. The time constant for the reaction decreases with increasing solvent polarity, as measured by $E_T(30)$, which is consistent for a process that

involves the transfer of a charged particle, molecular rearrangement, and charge reorganization [38,45].

3. Construction of molecular models of hypericin and a recent x-ray structure [42] indicate that the aromatic polycycle is twisted. One might argue that the excited-state transients observed reflect transitions from one form of conformational isomer to another. Because such a process involves a large amplitude motion, it would be expected to be viscosity dependent. In solvents in which the viscosity changes by a factor of 60 we see, however, no more than a change of a factor of two in the time constant of the longer-lived excited-state transient (~6-12 ps). Furthermore, the rate of the excited-state process is completely uncorrelated to viscosity: the small variation in rate cited can be effected just a easily when the viscosity is increased by less than a factor of two, i.e. from methanol to acetonitrile [37]. This excludes the assignment to a conformational transition.

4. The kinetic scheme indicated is not the only one consistent with the data, but it is, we believe, the simplest. There are quite likely more species involved than the few we have depicted. This is certainly suggested by the complexity of the steady-state spectra presented. In particular, we must note that tautomeric forms of DT can exist with the proton being donated from the "upper right" and the "lower left" hydroxyl groups as well as by the "upper left" and "lower left" hydroxyl groups, as indicated in Figure 12.

5. A problem for which at present we do not have a completely satisfactory response is why we observe no emission from MT^*. It may be that there is not a large enough population of the species to be detected in the midst of all the other transients observed. This question requires further investigation.

6. We have tentatively assigned the rapid decay of N^* to formation of MT^*. Other nonradiative pathways such as internal conversion are also a possibility as is

demonstrated by the anthraquinones [34,35]. We note, however, that both the triplet yield and the fluorescence quantum yield of hypericin have been reported to be very high and that $\phi_F + \phi_{ISC} \sim 1$ [9,10]. It thus seems unlikely that other nonradiative processes, besides proton transfer, play a significant role in the deactivation of N^*.

7. Spectroscopic studies of well-defined synthetically prepared hypericin tautomers will help to clarify the ground- and excited-state chemistry of hypericin. Falk and coworkers [43] have reported the synthesis of a compound, which they identify, based solely upon NMR measurements, as the salt of the hypericin tautomer (DT). This molecule was selected as a target for organic synthesis on the basis of semiempirical calculations (MNDO) [41-44].

The molecule synthesized by Falk and coworkers has an absorption spectrum that is structured and very similar to that of the normal form of hypericin, except that it is slightly blue shifted. Consequently, it bears a mirror image relationship to the fluorescence spectrum of hypericin. This observation is consistent with our argumentin point 1 above that partially tautomerized hypericin exists in the ground state. It is also an indication that in the case of hypericin it is not reasonable to require the absence of mirror symmetry between the aborption spectrum of the normal species and the emission spectrum of its fluorescent tautomer.

Falk and coworkers also indicate that upon prolonged heating their compound reforms the normal species but that irradiation (of an unspecified duration or intensity at an unspecified temperature) is insufficient to convert the normal form to the DT tautomer or vice versa [47]. They argue that the absence of interconvertability in the presence of light precludes an excited-state proton transfer mechanism. Although this conclusion is possible, it is certainly not unique because it assumes that the excited-state potential surface is the same as, or at least very similar to, that of the ground state

and because it ignores the multidimensionality of these potential surfaces—that is, the energy must strictly speaking be considered in terms of at least 157 normal coordinates (assuming the solvent coordinates may be neglected).

Figure 13 is presented in order to respond to the conclusions of Falk and coworkers. It presents crude approximations of the ground- and excited-state surfaces for hypericin based upon our current knowledge of the system that is summarized largely in Figure 12. In the ground state MT lies only slightly in energy above N and is separated from N by a modest barrier. On the other hand, because no long lived fluorescence from hypericin appears instantaneously, DT lies much higher in energy than either MT or N and (based on the work of Falk and coworkers) is also separated from MT by a substantial barrier. The ~1-2-ps lifetime of N^* leads us to consider a barrierless transition converting N^* into MT^*. Preliminary temperature-dependent measurements in ethylene glycol [37] indicate that there is a small barrier (~1.5 kcal/mol) between MT^* and DT^*. Depending on the location of the minimum of the DT^* potential well with respect to the barrier separating MT and DT, initially prepared N^* will mostly return to MT and ultimately to N.

Figure 13 is also capable of explaining the mirror symmetry in the hypericin absorption and emission spectra. The position of the potential well of DT^* affords "cross-well" transitions (both in absorption and emission) between DT^* and MT. A similar cross-well transition has been invoked by Barbara and coworkers to interpret the fluorescence spectra of 1-(acylamino)anthraquinones [34].

Finally, it is an open question whether light absorption by the hypericin tautomer, DT, would access the same region of the excited-state potential surface that is probed by exciting the normal form of hypericin, N, and thus allowing it to evolve on this surface. In other words, the fate of N^* is determined by the curvature of the potential

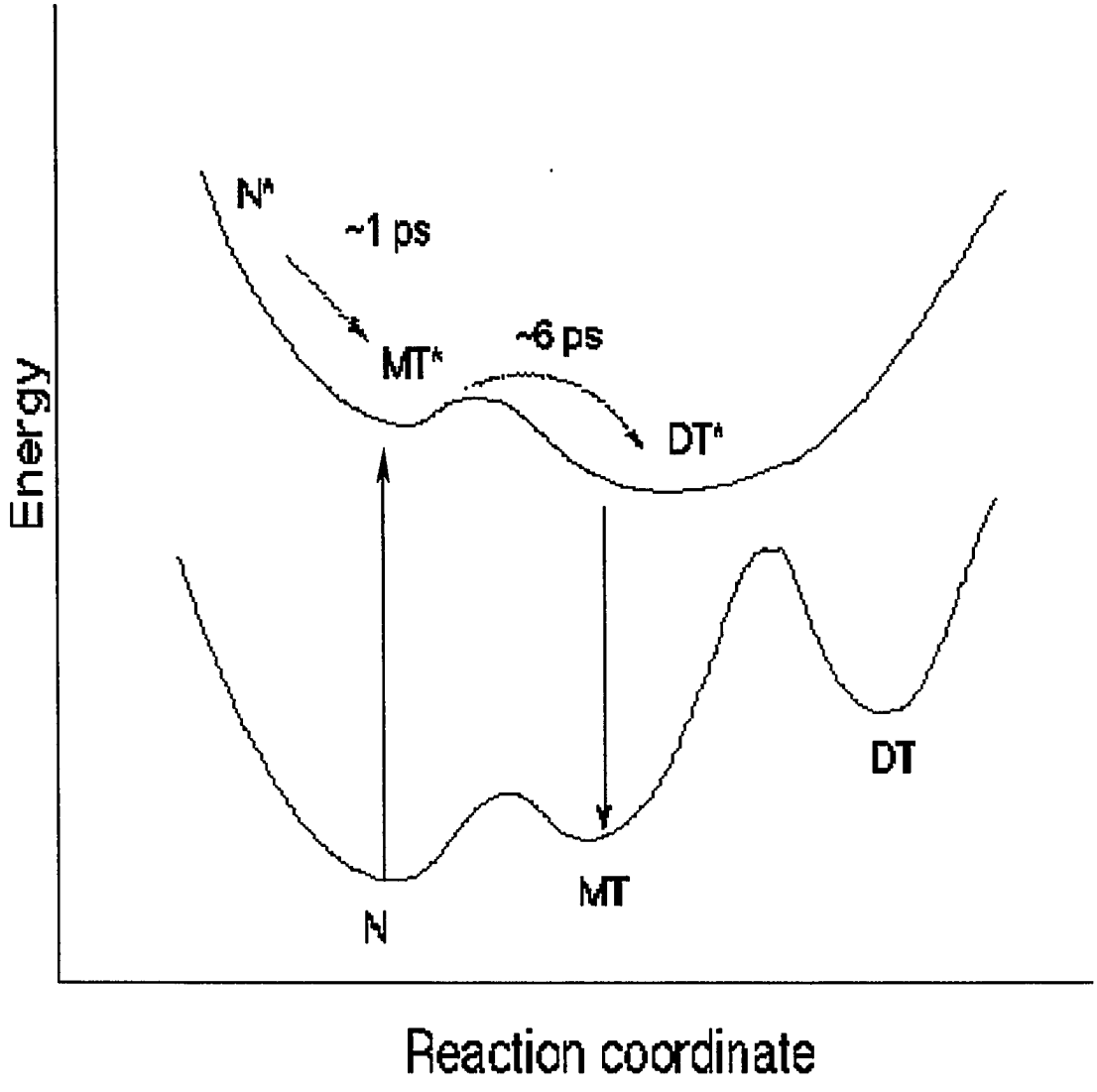

Figure 13. Ground- and excited-state energy surfaces of hypericin. See the Discussion. The values given are for methanol. The likelihood of a "cross-well" transition connecting DT^* to MT depends on the coupling of the vibrational levels in the MT^* and DT^* wells. This kind of cross-well transition has been invoked by Barbara and coworkers in their work with anthraquinones [34]. Cross-well transitions have been investigated in detail by Somorjai and Hornig [46].

energy surface on which it finds itself upon optical excitation, and this in turn is determined by Franck-Condon factors. A priori, there is no reason to assume that the normal form of hypericin, N, will execute a trajectory in which it finishes as DT. The same is true for the hypericin tautomer, DT.

8. All the results obtained in our laboratory—and elsewhere--support the existence of excited-state tautomerism in hypericin or at least are consistent with it. We have exploited every method currently available to us to verify that excited-state tautomerization occurs in hypericin. The strength of our argument rests on the absorption and emission spectra of the methylated and the deshydroxy hypericins in aprotic and protic solvents taken in conjunction with the transient spectroscopy of hypericin itself. It must be noted, however, that the only indisputable and direct proof for an excited-state proton transfer reaction is the demonstration of the bleaching of the carbonyl stretching frequency as a function of time subsequent to laser excitation. Such measurements require a tunable infrared probe pulse coupled to a visible or ultraviolet pump pulse. Only recently has this type of measurement been performed on molecules generally believed to execute excited-state proton transfer [24]. We are currently preparing an experiment with a picosecond, tunable infrared probe pulse.

Conclusions

The deshydroxy hypericin analog, mesonaphthobianthrone, and hexamethylhypericin have proved useful in elucidating the ground- and excited-state kinetics of hypericin. In aprotic solvents such as DMSO, mesonaphthobianthrone is nonfluorescent and exhibits no absorbance in the visible region of the spectrum. In a strong acid such as H_2SO_4, however, the absorbance and fluorescence spectra of

mesonaphthobianthrone closely resemble those of hypericin in aprotic solvents. Similarly, only in sulfuric acid do the absorption and emission spectra of hexamethylhypericin resemble those of hypericin. These results are most easily explained by requiring the fluorescent states of both mesonaphthobianthrone and hypericin to bear protonated carbonyl groups. These results do not indicate what the protonation dynamics are in either the ground or the excited states. Nor do they explain why protonation of the carbonyls so drastically alters the optical spectra.

The presence of two carbonyl groups in the analogs and in hypericin naturally leads to speculation concerning the extent of their protonation in the ground and excited states. Steady-state and time-resolved fluorescence measurements of mesonaphthobianthrone in H_2SO_4/MeOH mixtures proved to be especially useful in investigating solute heterogeneity. The fluorescence spectra in mixed solvents are strongly dependent on the excitation wavelength. Also in the solvent mixtures two lifetime components, ~2 and ~15 ns, are observed. The shorter component is attributed to a singly protonated carbonyl; the longer component, to a doubly protonated carbonyl. In mixed solvents, both states of protonation are proposed to exist in the ground state because no rise times are detected in the time-resolved fluorescence. In pure H_2SO_4 the doubly protonated species is believed to be predominant because the fluorescence lifetime is 15 ns across the emission spectrum.

Evidence for both ground- and excited-state heterogeneity and for excited-state tautomerization in hypericin comes from transient absorption measurements—and, in particular, the kinetics of stimulated emission from the excited states of hypericin. The finite rise time observed for the appearance of the stimulated emission indicates that a fluorescent species is being created in the excited state. From the titrations of mesonaphthobianthrone, we have inferred that the fluorescent species is protonated at the

carbonyl groups. The origin of the slowly rising stimulated emission component (6-12 ps in the solvents considered here) is attributed to the species that produces a new transient absorption immediately upon excitation (Figure 8a) and which is detected either directly through the decay of its absorption or indirectly through the finite bleaching time of the ground state (Figure 9). We have suggested that the species producing this absorbance transient is a monotautomer of hypericin that already exists in the ground state in equilibrium with the untautomerized or normal form of hypericin (Figure 12). We propose that the normal form of hypericin is revealed in the component of stimulated emission that appears instantaneously and decays in 1-2 ps (Figures 10 and 11f). Such a rapid decay time of the hypericin species with unprotonated carbonyls is consistent with the absence of fluorescence in mesonaphthobianthrone in aprotic solvents (Figure 3). Given the demonstrated heterogeneity of hypericin even in pure solvents (Figures 10 and 11f), the observation of single exponential fluorescence decay (Table I) is interpeted in terms of the existence of only one species that is long lived enough to produce measurable excited state emission (as detected either by steady-state or traditional photon-counting methods). This fluorescent species is attributed, as discussed above, to a doubly tautomerized hypericin molecule. These conclusions have important implications for the photoinduced biological activity of hypericin and hypericin-like molecules.

The photophysics of hypericin are complicated, and much study is required before the role of light for its antiviral activity and photoreceptor roles is understood. Our results suggest that the primary photoprocess of hypericin is rapid, excited-state proton transfer. Because of the demonstrated antiviral [2-5] and photophobic and phototactic [6] roles played by hypericin and hypericin-like chromophores, elucidating their nonradiative pathways has enormous practical benefits. In addition, this work indicates

that hypericin provides an interesting model system with which to study the fundamental aspects of excited-state proton transfer reactions. The influence of the solvent on the rate of proton transfer will be discussed in detail elsewhere.

Acknowledgment

J.W.P. is an Office of Naval Research Young Investigator. We thank Professor G. A. Kraus for helpful discussion, samples, and assistance in preparing the analogs. Ms. P. Sheaff provided technical assistance, and Professor A. W. Schwabacher graciously provided us access to his laboratory facilities.

References

1. Durán, N.; Song, P.-S. *Photochem. Photobiol.* 1986, **43**, 677-680. Hypericin and its photodynamic action.
2. Meruelo, D.; Lavie, G.; Lavie, D. *Proc. Natl. Acad. Sci. USA* 1988, **85**, 5230-5234. Therapeutic agents with dramatic antiretroviral activity and little toxicity at effective doses: Aromatic polycyclic diones hypericin and pseudohypericin.
3. Lavie, G.; Valentine, F.; Levin, B.; Mazur, Y.; Gallo, G.; Lavie, D.; Weiner, D.; Meruelo, D. *Proc. Natl. Acad. Sci. USA* 1989, **86**, 5963-5967 Studies of the mechanisms of action of the antiretroviral agents hypericin and pseudohypericin; Degar, S.; Prince, A. M.; Pascual, D.; Lavie, G.; Levin, B.; Mazur, Y.; Lavie, D.; Ehrlich, L. S.; Carter, C.; Meruelo, D. *AIDS Res. Hum. Retroviruses* 1992, **8**, 1929-1936 Inactivation of the Human Immunodeficiency Virus by Hypericin: Evidence for Photochemical Alterations of p24 and a Block in Uncoating.

4. Lenard, J.; Rabson, A.; Vanderoef, R. *Proc. Natl. Acad. Sci. USA* 1993, **90**, 158-162 Photodynamic inactivation of infectivity of human immunodeficiency virus and other enveloped viruses using hypericin and rose bengal: inhibition of fusion and syncytia formation.

5. Carpenter, S.; Kraus, G. A. *Photochem. Photobiol.* 1991, **53**, 169-174 Photosensitization is required for inactivation of equine infectious anemia virus by hypericin.

6. Tao, N.; Orlando, M.; Hyon, J.-S.; Gross, M.; Song, P.-S. *J. Am. Chem. Soc.* 1993, **115**, 2526-2528 A new photoreceptor molecule from *Stentor coerulus.*; Song, P.-S.; Kim, I.-K.; Florell, S.; Tamai, N.; Yamazaki, T.; Yamazaki, I. *Biochim. Biophys. Acta* 1990, **1040**, 58-65 Structure and function of the photoreceptor stentorins in *Stentor coerulus.* II. Primary photoprocess and picosecond time-resolved fluorescence; Song, P.-S. *Biochim. Biophys. Acta* 1981, **639**, 1-29 Photosensory transduction in *Stentor coerulus* and related organism.

7. Cubbedu, R.; Ghetti, F.; Lenci, F.; Ramponi, R.; Taroni, P. *Photochem. Photobiol.* 1990, **52**, 567-573 Time-gated fluorescence of blepharismin, the photoreceptor pigment for photomovement of *blepharisma.*

8. Lenci, F.; Ghetti, F.; Gioffré, D.; Passarelli, V.; Heelin, P. F.; Thomas, B.; Phillips, G. O.; Song, P.-S. *J. Photochem. Photobiol. B: Biol.* 1989, **3**, 449-453 Effects of the molecular environment on some spectroscopic properties of *Blepharisma* photoreceptor pigment.

9. Racinet, H.; Jardon, P.; Gautron, R. *J. Chim. Phys.* 1988, **85**, 971-977 Formation d'oxygene sigulet photosensibilisee par l'hypericine etude cinetique en milieu micillaire non ionique.

10. Bourig, H.; Eloy, D.; Jardon, P. *J. Chim. Phys.* 1992, **89**, 1391-1411 Formation et reactivite de l'oxygene singulet photosensibilise par l'hypericin dans des lipo-

somes de dipalmitoylphosphatidylcholine. Mise en evidence d'une photooxydation retardee.

11. Yang, K.-C.; Prusti, R. K.; Walker, E. B.; Song, P.-S.; Watanabe, M.; Furuya, M. *Photochem. Photobiol.* 1986, **43**, 305-310 Photodynamic action in *Sentor coerulus* sensitized by endogeneous pigment stentorin.

12. Gai, F.; Fehr, M. J.; Petrich, J. W. *J. Am. Chem. Soc.* 1993, **115**, 3384-3385 Ultrafast excited-state processes in the antiviral agent, Hypericin.

13. Song, P.-S.; Walker, E. B.; Auerbach, R. A.; Robinson, G. W. *Biophys. J.* 1981, **35**, 551-555 Proton release from *Stentor* photoreceptors in the excited states.

14. Walker, E. B.; Lee, T. Y.; Song, P.-S. *Biochim. Biophys. Acta* 1979, **587**, 129-144 Spectroscopic characterization of the *Stentor* photoreceptors.

15. Koch, W.; Saito, T.; Yoshida, Z. *Tetrahedron* 1972, **28**, 3191-3201 Photodimerization of halogenated anthrone derivatives.

16. Chen, Y.; Rich, R. L.; Gai, F.; Petrich, J. W. *J. Phys. Chem.* 1993, **97**, 1770-1780 Fluorescent species of 7-azaindole and 7-azatryptophan in water.

17. Rich, R. L.; Chen, Y.; Neven, D.; Négrerie, M.; Gai, F.; Petrich, J. W. *J. Phys. Chem.* 1993, **97**, 1781-1788 Steady-state and time-resolved fluorescence anisotropy of 7-azaindole and its derivatives.

18. Gai, F.; Rich, R. L.; Petrich, J. W. *J. Am. Chem. Soc.* Monophotonic ionization of 7-azaindole, indole, and their derivatives and the role of overlapping excited states. In press.

19. Bender, M. L.; Komiyama, M. Cyclodextrin Chemistry; Springer-Verlag; Berlin; 1978.

20. Chou, P.-T.; Martinez, M. L.; Cooper, W. C.; Collins, S. T.; McMorrow, D. P.; Kasha, M. *J. Phys. Chem.* 1992, **96**, 5203-5208 Monohydrate catalysis of excited-state double-proton transfer in 7-azaindole.

21. Schwartz, B. J.; Peteanu, L. A.; Harris, C. B. *J. Phys. Chem.* 1992, **96**, 3591-3598 Direct observation of fast proton transfer: Femtosecond photophysics of 3-hydroxyflavone.

22. Giese, A. C. in Photochemical and Photobiological Reviews, Volume 5. Smith, K. C., Ed. Plenum; New York; 1980. p. 229.

23. Fleming, G. R. Chemical Applications of Ultrafast Spectroscopy; Oxford University Press; New York; 1986.

24. Frey, W.; Laermer, F.; Elsaesser, T. *J. Phys. Chem.* 1991, **95**, 10391-10395 Femtosecond studies of excited-state proton and deuterium transfer in benzothiazole compounds.

25. Weisenfeld, J. M.; Ippen, E. P. *Chem. Phys. Lett.* 1980, **73**, 47-50 Dynamics of electron solvation in liquid water.

26. Hart, E. J.; Anbar, M. The Hydrated Electron; Wiley-Interscience; New York, 1970.

27. Bent, D. V.; Hayon, E. *J. Am. Chem. Soc.* 1975, **97**, 2612-2619 Excited state chemistry of aromatic amino acids and related peptides. III. Tryptophan.

28. Lin, S. H.; Fujimura, Y.; Neusser, H. J.; Schlag, E. W. Multiphoton Spectroscopy of Molecules; Academic Press; New York; 1984.

29. Tao, N.; Song, P.-S.; Savikhin, S.; Struve, W. S. *J. Phys. Chem.* 1993, **97**, 12379-12386 Ultrafast pump-probe spectroscopy of the photoreceptor stentorins from the ciliate *Stentor coeruleus*.

30. Weiner, L.; Mazur, Y. *J. Chem. Soc. Perkin Trans. 2* 1992, 1439-1442 EPR studies of hypericin. Photogeneration of free radicals and superoxide.

31. Dick, D. L.; Rao, T. V. S.; Sukumaran, D.; Lawrence, D. S. *J. Am. Chem. Soc.* 1992, **114**, 2664-2669 Molecular encapsulation: Cyclodextrin-based analogues of heme-containing proteins.

32. Xu, W.; Demas, J. N.; DeGraff, B. A.; Whaley, M. *J. Phys. Chem.* 1993, **97**, 6546-6554 Interactions of Pyrene with cyclodextrins and polymeric cyclodextrins.

33. Barbara, P. F.; Walsh, P. K.; Brus, L. E. *J. Phys. Chem.* 1989, **93**, 29-34 Picosecond kinetic and vibrationally resolved spectroscopic studies of intramolecular excited-state hydrogen atom transfer.

34. Smith, T. P.; Zaklika, K. A.; Thakur, K.; Walker, G. C.; Tominaga, K.; Barbara, P. F. *J. Phys. Chem.* 1991, **95**, 10465-10475 Spectroscopic studies of excited-state intramolecular proton transfer in 1-(acylamino)anthroquinones.

35. Flom, S. R.; Barbara, P. F. *J. Phys. Chem.* 1985, **89**, 4489-4494 Proton transfer and hydrogen bonding in the internal conversion of S_1 anthraquinones.

36. Yamazaki, T.; Ohta, N.; Yamazaki, I.; Song, P.-S. *J. Phys. Chem.* 1993, **97**, 7870-7875 Excited-state properties of hypericin: Electronic spectra and fluorescence decay kinetics.

37. Gai, F.; Fehr, M. J.; Petrich, J. W. Unpublished data.

38. Borgis, D.; Hynes, J. T. *J. Chem. Phys.* 1991, **94**, 3619-3628 Molecular-dynamics simulation for a model nonadiabatic proton transfer reaction in solution; Borgis, D.; Hynes, J. T. in The Enzyme Catalysis Process, Eds.,

Cooper, J.; Houben, J. L.; Chien, L. C.; Plenum Press: New York, 1989. p. 293.; Azzouz, H.; Borgis, D. *J. Chem. Phys.* 1993, **98**, 7361-7374 A quantum molecular-dynamics study of proton-transfer reactions along asymmetrical H bonds in solution.

39. Falk, H.; Meyer, J.; Oberreiter, M. *Monatsh. Chem.* 1992, **123**, 277-284 Deprotonation and protonation of hydroxyphenanthroperylenes.

40. Falk, H.; Schoppel, G. *Monatsh. Chem.* 1992, **123**, 931-938 On the synthesis of hypericin by oxidative trimethylemodin anthrone and emodin anthrone dimerization: Isohypericin.

41. Etzlstorfer, C.; Falk, H.; Müller, N. *Monatsh. Chem.* 1993, **124**, 431-439 Tautomerism and stereochemistry of dihydroxyperylenequinones: Force field investigations.

42. Etzlstorfer, C.; Falk, H.; Müller, N.; Schmitzberger, W.; Wagner, U. G. *Monatsh. Chem.* 1993, **124**, 751-761 Tautomerism and stereochemistry of hypericin: Force field, NMR, and x-ray crystallographic investigations.

43. Etzlstorfer, C.; Falk, H.; Oberreiter, M. *Monatsh. Chem.* 1993, **124**, 923-929 On the tautomerism of hypericin: The 1,6-dioxo tautomer.

44. Semiempirical methods are known not to handle intramolecular hydrogen bonding well. See, for example: Jensen, J. H.; Gordon, M. S. *J. Am. Chem. Soc.* 1991, **113**, 7917-7924 The conformational potential energy surface of glycine. A theoretical study. (and references therein). Other doubly tautomerized forms exist, and it is possible that a higher-level calculation with incorporation of solvent will show they are lower in energy than suggested [41-43].

45. Keirstead, W. P.; Wilson, K. R.; Hynes, J. T. *J. Chem. Phys.* 1991, **95**, 5256-5267 Molecular dynamics of a model S_N1 reaction in water.

46. Somorjai, R. L.; Hornig, D. F. *J. Chem. Phys.* 1962, **36**, 1980-1987 Double minimum potentials in hydrogen-bonded solids.

47. Falk and coworkers state that the compound they identify as the hypericin tautomer requires heating at 80°C for two days in DMSO in order to convert it in its ground state into the normal hypericin species [43]. If there is a substantial barrier between DT^* and MT^* in the excited-state, it is not clear that in the absence of heating optical excitation will effect the back reaction.

CHAPTER 4. THE ROLE OF SOLVENT IN EXCITED-STATE PROTON TRANSFER IN HYPERICIN

A paper published in the *Journal of Physical Chemistry*[1]

F. Gai[2], M. J. Fehr[2], and J. W. Petrich[2,3]

Abstract

The excited-state proton transfer of hypericin is monitored by the rise time (~6-12 ps in the solvents investigated) of the component of stimulated emission corresponding to the formation of the long-lived (~5 ns) fluorescent tautomer. The assignment of this excited-state process to proton transfer has been verified by noting that a hypericin analog (mesonaphthobianthrone) lacking nonlabile protons is not fluorescent unless its carbonyl groups are protonated. Recent experimental studies on other systems have suggested that three solvent properties play important roles in excited-state proton transfer: viscosity, hydrogen-bonding character, and dynamic solvation. We find that for hypericin in a range of protic, aprotic, hydrogen-bonding, and nonhydrogen-bonding solvents in which the viscosity changes by a factor of 60 and the average solvation time

---

[2] Graduate students and Associate Professor, Department of Chemistry, Iowa State University. Synthesis, steady-state measurements, and CCD measurements performed by M. J. Fehr.

[3] To whom correspondence should be addressed.

changes by a factor of 100, the excited-state proton transfer rate of hypericin is uncorrelated with these properties and varies not more than a factor of two (~6-12 ps) at room temperature. The relative contribution of the bulk solvent polarity is considered and the role of intramolecular vibrations of hypericin on the proton transfer rate is discussed.

Introduction

Hypericin (Figure 1) is a naturally occurring polycyclic quinone that has received recent notoriety for its antiviral capacity—in particular its ability to deactivate the human immunodeficiency virus (HIV) [1]. The antiviral activity of hypericin requires light [2]. Hypericin is also very closely related, both structurally and spectrally, to the chro

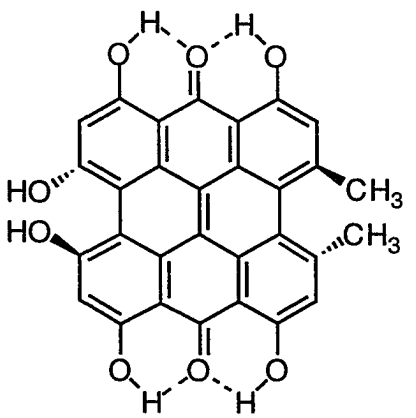

a) hypericin

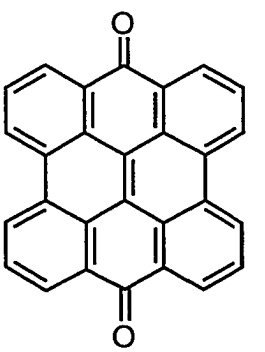

b) mesonaphthobianthrone

Figure 1. Structures of a) hypericin and b) mesonaphthobianthrone.

mophore of the photoreceptor complexes of the protozoan ciliates, Stentor coerulus [3] and Blepharisma japonicum [4]. The hypericin-like chromophore is responsible for the photophobic and phototactic responses of the microorganism [3,4]. Optical excitation of hypericin produces both singlet oxygen [5] and a pH decrease [6].

Figure 2 gives the steady-state absorption and fluorescence spectra of hypericin in octanol. The spectra of hypericin are very similar in all solvents in which it is soluble with the exception of shifts in absorbance and emission maxima. In previous work we have shown that in hypericin the ground state, and consequently the excited state, is inhomogeneous. Figure 3 presents a kinetic scheme based upon our current knowledge of the hypericin photophysics, which is discussed in detail elsewhere [7,8]. The salient observations consistent with this scheme are the following:

1. Immediately upon optical excitation a transient species is produced whose absorption lies between 620 and 650 nm, depending upon the solvent. In methanol measurement of the decay of this absorbance or of the rise time for the bleaching of the ground-state absorption, which overlaps the spectrum of the newly formed excited state, yields a lifetime of ~5-6 ps.

2. The hypericin analog with no hydroxyl groups and hence no intramolecular proton source, mesonaphthobianthrone, provides no absorption or emission in the visible region of the spectrum in aprotic solvents such as DMSO, unlike hypericin. In concentrated sulfuric acid, however, the absorption and emission spectra of the analog are very similar to those of hypericin. We thus interpreted these data in terms of the necessity of protonated carbonyl groups for the production of fluorescence at wavelengths longer than 580 nm. This result indicates that in the ground state, at least one of the carbonyls of hypericin is protonated. This result also suggests the likelihood of excited-state tautomerization in hypericin.

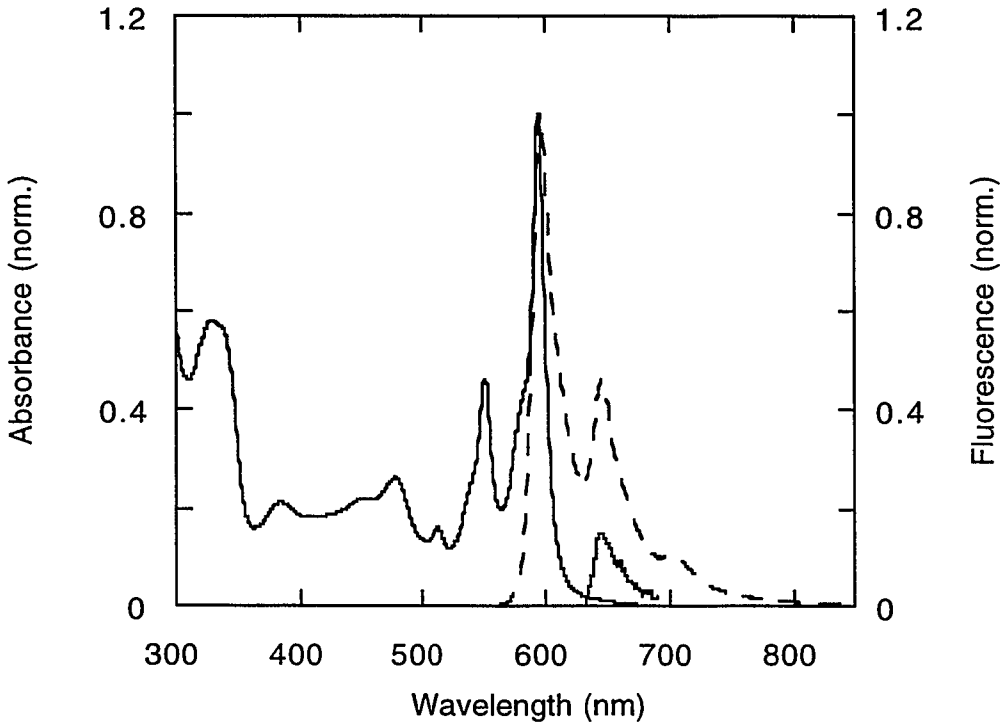

Figure 2. Normalized fluorescence spectrum (——) and absorption spectrum (___) of hypericin in octanol. The steady-state emission spectrum bears a "mirror symmetry" relationship to the visible portion of the absorption spectrum. We attribute this part of the absorption spectrum to the presence of ground-state MT (see Figure 3). The solid curve centered at ~650 nm is the spectrum of the stimulated emission that appears instantaneously and decays in ~12 ps (Figures 5 and 7). It is the "zero time" curve from Figure 4 scaled according to the relative amplitudes of the components of stimulated emission appearing instantaneously and with a finite rise time in the region from 640-645 nm (Figure 7 and Table I). We propose that this emission arises from untautomerized hypericin that exists in equilibrium with a monotautomer in the ground state.

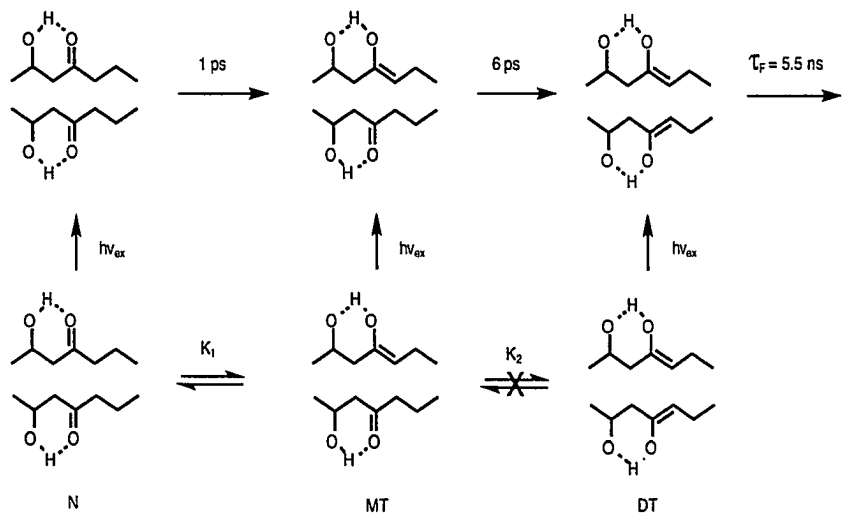

hypericin

Figure 3. Proposed kinetic scheme for hypericin in the ground and the excited states. The values quoted are for methanol. Hypericin is represented schematically: only two of its six hydroxyl groups are pictured. We note that the tautomeric forms of DT can exist with the proton being donated from the "upper right" and the "lower left" hydroxyl groups as well as by the "upper left" and "lower left" hydroxyl groups, as indicated in the Figure. The delocalization of the double bonds upon tautomerization may contribute significantly to the intramolecular component of the reorganization energy. We have tentatively assigned the rapid decay of N^* to formation of MT^*. Other nonradiative pathways such as internal conversion are also a possibility as is demonstrated by the anthraquinones [35]. We note, however, that both the triplet yield and the fluorescence quantum yield of hypericin have been reported to be very high and that $\Phi_F + \Phi_{ISC} \sim 1$ [5]. It thus seems unlikely that other nonradiative processes, besides proton transfer, play a significant role in the deactivation of N^*. A problem for which at present we do not have a completely satisfactory response is why we observe no emission from MT^*. It may be that there is not a large enough population of the species to be detected in the midst of all the other transients observed. This question requires further investigation.

3. The occurrence of excited-state tautomerization in hypericin is verified by the rise time of the stimulated emission signal, which measures the excited-state population. In methanol, the rise time of the stimulated emission is within experimental error identical to the decay of the absorption transient produced upon optical excitation. Another confirmation of the excited-state proton transfer process is that in H_2SO_4 there is no transient with time constant > 1 ps [8]. This indicates that in the ground state the entire population of hypericin is already protonated and does not require an excited-state reaction to produce the long-lived fluorescent species (Figure 4).

We have suggested that upon light absorption hypericin undergoes excited-state proton transfer in ~5 ps in MeOH and ~9 ps in DMSO [7,8]. This small variation in rate has led us to inquire in more detail about the role of the solvent on the excited-state proton transfer.

The scheme presented in Figure 3 is the simplest that is consistent with the experimental data [7,8]. Two species are believed to be in equilibrium in the ground state, N and MT: normal, or untautomerized, and monotautomerized forms of hypericin. Evidence for this is the appearance in the stimulated emission of an instantaneous component (N^*) decaying with one lifetime and the appearance in transient absorption and bleaching measurements of another component decaying with a different lifetime (MT^*). We propose that negligible amounts of the ditautomerized form exist in the ground state because in the absence of strong acid no long-lived (nanosecond duration) fluorescence appears instantaneously. Measurements of the hypericin analog lacking hydroxyl groups, mesonaphthobianthrone, suggest that protonation of both carbonyl groups of hypericin is a prerequisite for long-lived fluorescence. The decay of MT^* matches the rise of DT^* demonstrating their kinetic relatedness. It is likely that N^* tautomerizes to form MT^* and that this proton transfer step represents the component

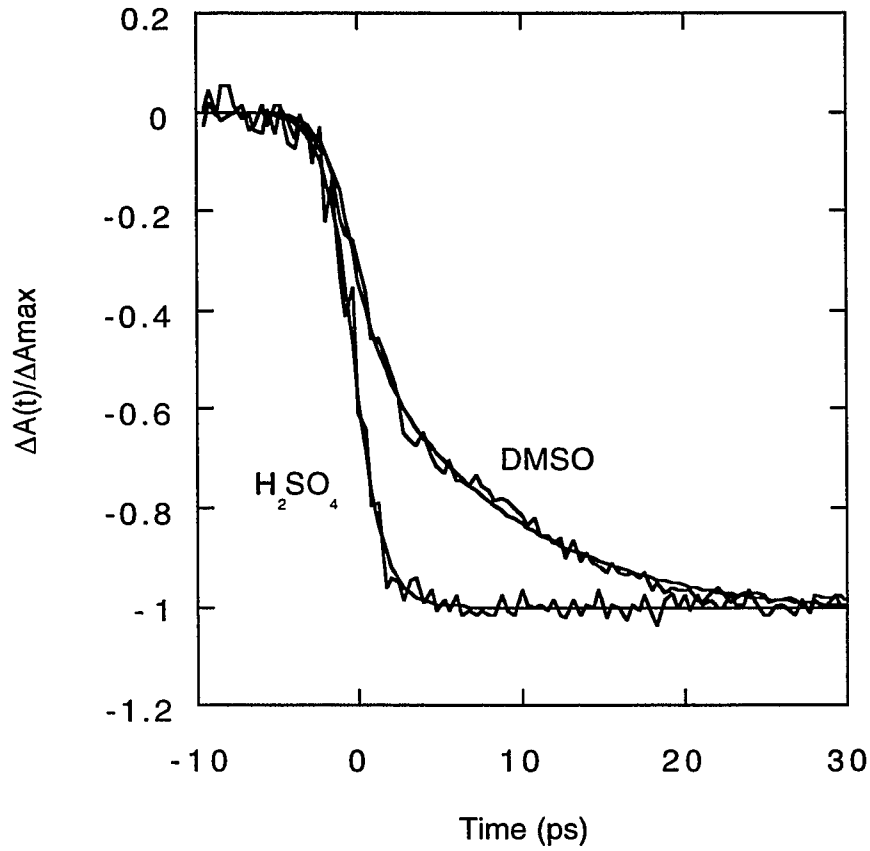

Figure 4. Comparison of the rise time for the formation of excited-state transients as measured by the delay time required to bleach maximally the ground-state absorption [7,8] (Table I). This rise time is finite for hypericin in an aprotic solvent where a portion of the ground-state population is not tautomerized (DMSO). But in a solvent where the entire ground-state population is protonated (H_2SO_4), the rise time is instantaneous. The fits to the data are as follows:

DMSO, λ_{probe} = 610 nm: $A(t) = 0.23\exp(-t/9.6) - 0.41$;

H_2SO_4, λ_{probe} = 630 nm: the bleaching of the ground-state absorption is complete within the time resolution afforded by the system and the excited state formed is long-lived on the time scale of the measurement.

of stimulated emission appearing instantaneously and decaying rapidly. For completeness, we note that it may be possible that N^* undergoes a two-proton transfer reaction that converts it directly to DT^*. Song, Yamazaki, and coworkers [9] have presented results on hypericin from which they conclude that excited-state intramolecular proton transfer does not occur. All of their conclusions, however, are based on observations of the long-lived fluorescence that is produced from the excited state whose duration is only several picoseconds. While their conclusions are thus not appropriate for the primary photoprocesses of hypericin, they may be relevant to the tautomer, which we refer to as DT^*. The light-induced pH drop produced by hypericin may result from the intermolecular deprotonation of the tautomer by the solvent.

In this article the excited-state tautomerization of hypericin is studied in a range of solvents that vary greatly in their viscosity, their average solvation time, their ability to form hydrogen bonds with the solute, and polarity. The choice of solvents and solvent properties studied was determined by reports in the literature suggesting they play an important role in other proton transfer systems. Of all the solvent properties investigated, only polarity was well correlated with the proton transfer time. We compare results obtained in these model systems for excited-state proton transfer with those of the more complex system, hypericin, whose fascinating biochemical action and enormous medicinal potential have clearly been demonstrated to depend on light.

Materials and Methods

Hypericin was obtained from Carl Roth GmbH & Co. and used without further purification. The hypericin analog, mesonaphthobianthrone (Figure 1), was prepared as described by Koch et al. [10]. Solvents were obtained from Aldrich. Fluorescence

spectra were measured with a Spex Fluoromax. The time-resolved absorption (stimulated emission) experiments were performed with 1 -ps resolution with the apparatus described elsewhere [11-13]. Transient absorption spectra were obtained with a liquid nitrogen cooled charge-coupled device (CCD) (Princeton Instruments LN/CCD-1152UV) mounted on an HR320 (Instruments SA, Inc.) monochromator with a grating (1200g/mm) blazed at 5000 Å. The CCD pixels were binned such as to allow simultaneous collection of both the probe and the reference beams, I and I_0 respectively, of the transient absorption spectrometer. For the absorption and stimulated emission experiments, identical kinetics were observed whether the pump beam was rotated parallel, perpendicular, or at the magic angle (54.7°) to the probe beam. Unless otherwise indicated, experiments were performed at room temperature, 22°C. Measuring excited-state kinetics by the increase in probe transmission owing to stimulated emission is a well known technique. See references 23 for an example of its application to a system executing excited-state proton transfer, 3-hydroxyflavone. Temperature dependent measurements were performed with an Air Products system. A helium expander module (DE-202) is connected to a water-cooled compressor (HC-2) for helium exchange. The cryostat is evacuated by a Welch Duo Seal mechanical pump.

In all cases the pump-probe data include a contribution from stimulated emission that grows in with a finite risetime and a contribution from stimulated emission that appears instantaneously. The component with the finite risetime is represented by a rising exponential with a positive prefactor a_1 $[\exp(-t/\tau_1) - 1]$. For large values of t, the amplitude of this term is determined by the stimulated emission corresponding to the long-lived—several nanoseconds—fluorescent state that does not decay on the time scale of the experiment. The instantaneous component of stimulated emission is represented in the data fitting analysis by an exponential with a negative prefactor, $-a_2$. In

addition, long-lived absorption owing to the prescence of the solvated electron [8] may in some cases need to be taken into account by a constant, c. There are thus four possible factors to be considered in the pump-probe data: (1) stimulated emission with a finite rise time that arises from (2) a long-lived fluorescent state; (3) instantaneous components of stimulated emission; and (4) long-lived transient absorption owing to the presence of the solvated electron. The pump probe data are thus fit to the following form, which takes into account the above contributions in the order in which they have been discussed:

$$A(t) = a_1 [\exp(-t/\tau_1) - 1] - a_2 \exp(-t/\tau_2) + c. \quad (1)$$

The construction of the spectrum (Figure 2) of the species, N^*, giving rise to the instantaneous component of stimulated emission that decays rapidly is performed as follows. First, the spectrum of the stimulated emission at "time zero" is obtained (Figure 5). Because this spectrum is obtained at zero time, it does not include contributions from the state that grows in with a finite time constant. Second, the amplitude of this spectrum at a given wavelength, with respect to that of the steady-state spectrum, is determined from the ratio of the amplitude of the component of stimulated emission appearing instanteously, $[N^*]$, to that of the component appearing with a finite time constant from $[MT^*]$ (Figures 3 and 7 and Table I). It might be objected that the shape of this spectrum does not accurately represent that of the transient in question because of the presence of other species absorbing at the probe wavelength. The only other transient species with significant oscillator strength in this spectral region is the solvated electron [8]. We note that the absorption spectra of the solvated electrons in methanol, ethanol, and isopropanol are all very broad and that the maximum of the

spectrum shifts to longer wavelength with increasing size of the alkyl chain [14]. For isopropanol, for example, the maximum is at ~800 nm and the absorbance tails off slowly towards shorter wavelengths. The spectrum of the solvated electron in octanol would be expected to be shifted even farther to the red. We thus conclude that the distortion of the emission spectrum that we attribute to N^* from the solvated electron is negligible and that if any distortion were to be expected, it would appear on the red, not the blue, edge of the spectrum.

Results

Figure 5 presents the negative-going transient absorbance signal of hypericin in octanol. This signal is attributed to stimulated emission from excited-state hypericin because it is observed in a region where there is no ground-state absorbance. The signal thus cannot be assigned to ground-state bleaching. The salient feature of the Figure is that a finite time is required for the stimulated emission to be fully developed. We have thus used the rise time of stimulated emission as a measure of the time required to produce the long-lived excited-state species. We have argued [8] that measurable fluorescence (by steady-state or conventional photon counting techniques) in hypericin is obtained only from the species with both carbonyl groups protonated.

In all the solvents in which we have investigated hypericin, except strong acids such as sulfuric and triflic acid where it is expected to have both carbonyl groups protonated, we observe a finite "rise time" for the ground-state bleaching. Such a phenomenon is most easily rationalized by the presence of an excited-state species, produced within the excitation pulse, that has oscillator strength in the same region as the ground-state molecules. We have directly observed such an excited-state species in transient

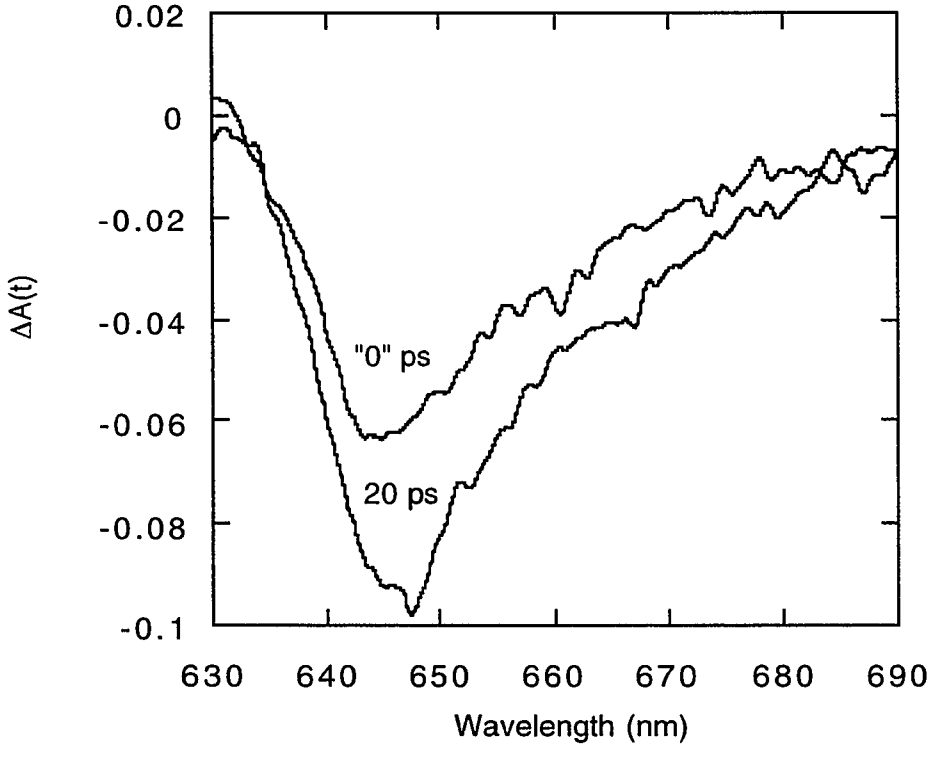

Figure 5. Time evolution of stimulated emission of hypericin in octanol.

absorption measurements [7,8]. As indicated by the summary presented in Table I, the agreement between the lifetime of this excited state and the rise time of the "slow" component of the stimulated emission is excellent. We have discovered that measurement of the rise time for ground-state bleaching provides a more accurate determination of the lifetime of the short-lived excited state that is a precursor, MT^*, to the long-lived fluorescent species of hypericin, DT^*. Measurement of the decay of the transient absorbance of MT^* can be obfuscated by the presence of absorption from the biphotonically produced solvated electron [8] as well as from stimulated emission—or transient absorption from the species producing the stimulated emission.

Figures 6 and 7 also indicate that upon optical excitation a species is created that produces stimulated emission immediately and that subsequently decays. This prompt stimulated emission is consistent with the suggestion made above (and in the caption to Figure 3) that at least two ground-state species are optically excited. Figure 6 and Table I suggest that the solvent seems to affect the ground-state equilibrium between N and MT, which is subsequently manifested in the ratio of the components of stimulated emission appearing with an instantaneous or a finite rise time, I_F/I_S. The component of the stimulated emission that appears instantaneously is not attributable to vibrational relaxation because its decay is the same whether the excitation is at 294 or 588 nm. Furthermore, it does not arise from dynamic solvation of the excited state [15] because it decays equally rapidly in acetonitrile and ethylene glycol, whose average solvation times differ by a factor of 100 (Table I, Figure 6). We suggest that the rapid decay of N^* represents a tautomerization step to MT^*. This is discussed in more detail elsewhere [8].

Figure 7 demonstrates the variation in the stimulated emission kinetics of hypericin in octanol as a function of probe wavelength. Tuning the probe from 640 to 675 nm

Table I. Dependence of Proton Transfer Times in Hypericin in Selected Solvents[a]

Solvent	η(cP)[b]	$\langle\tau_S\rangle$[c] (ps)	$E_T(30)$ [33]	decay time[d,f] (ps)	rise time[e,f] (ps)	I_F/I_S[f,g]
MeCN	0.37	0.9	45.6	10.8 (600 nm)	11.6 (645 nm)	1.0 (645 nm)
BuCN	0.57	3.6	43.1	11.7 (600 nm)	10.4 (645 nm)	1.2 (645 nm)
CCl_4/ BuCN[h]					12.8 (645 nm)	
MeOH	0.57	3.3, 6.2	55.4	6.4 (600 nm)	6.7 (645 nm)	0.84 (645 nm)
DMSO	1.99[i]	3.1, 1.2	45.1	9.6 (610 nm)	9.2 (658 nm)	0.43 (658 nm)
BuOH	2.75	61	50.2	7.5 (600 nm)	11.0 (645 nm)	0.75 (645 nm)
OcOH	7.36[i]		48.3	10.3 (610 nm)	12.6 (645 nm)	0.49 (640 nm) 0.51 (645 nm)
EgOH	18.25	100	56.3	5.8 (600 nm)	6.4 (645 nm)	1.2 (645 nm) 0.99 (650 nm)

[a] All experiments were performed at room temperature, 22°C.

[b] Except where otherwise noted, the solvent viscosity at 22°C [32].

[c] Average solvation time as determined from measurements of time-resolved Stokes shifts. The cited solvation times are obtained from the tablulation in reference 15.

[d] Decay of the excited-state absorption as measured by the rise time for the ground-state bleaching of hypericin. The absence of a value indicates that the measurement was not performed.

[e] "Long" component of the rise time of stimulated emission, which is attributed to the intramolecular proton transfer in hypericin.

[f] The value in parentheses is the probe wavelength.

[g] Ratio of the component of stimulated emission appearing instantaneously, I_F, to that appearing with a finite rise time, I_S. The dependence of this ratio on solvent can be interpreted in terms of a ground-state equilibrium between N and MT (Figure 3) insofar as the emission spectra of N^* and MT^* do not change greatly with respect to solvent at the probe wavelength.

[i] Viscosity at 25°C [34].

[h] The ratio of solvents in the mixture is 1/4 and is based on volume. This corresponds to a solution of 0.18 mole fraction in CCl_4. The viscosity of the mixture was not determined.

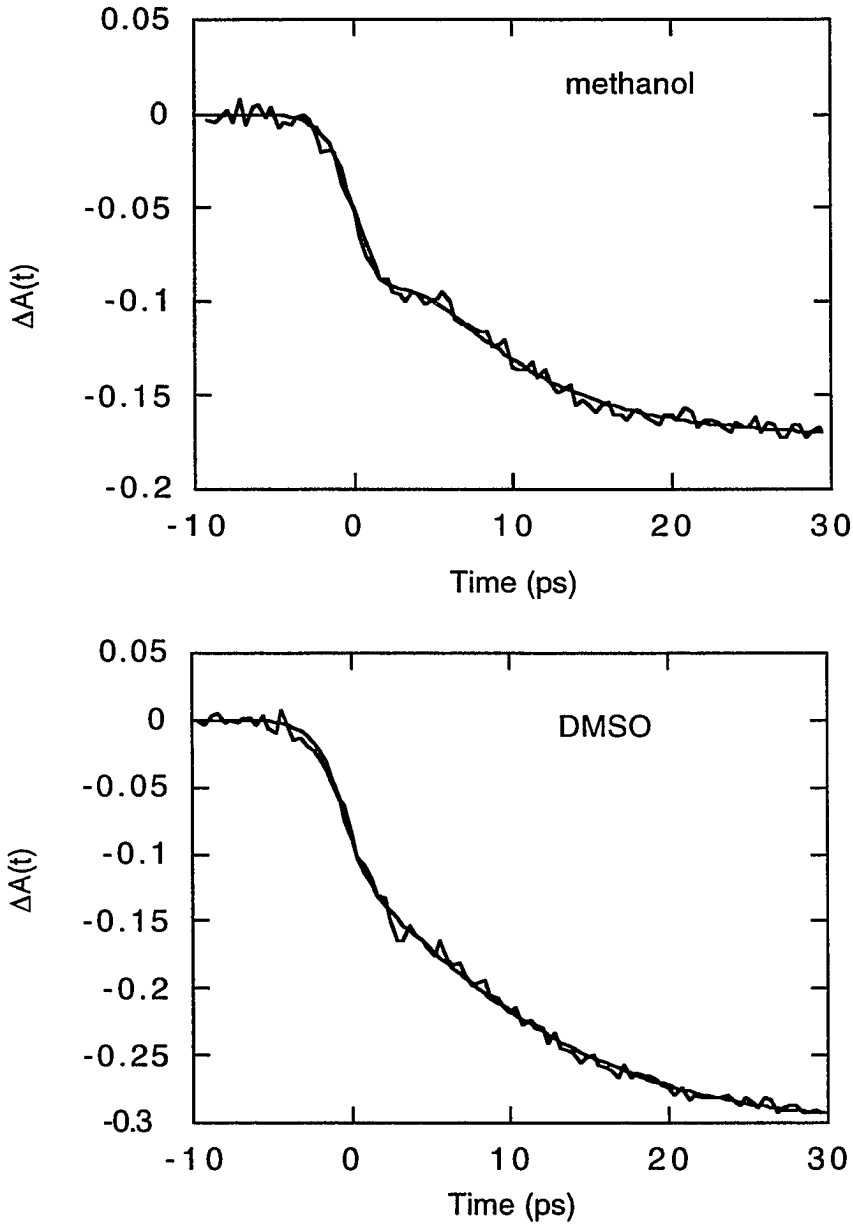

Figure 6. Time-resolved stimulated emission profiles of hypericin in (from top to bottom) methanol, DMSO, and ethylene glycol, and acetonitrile. λ_{ex} = 588 nm. See Table I for further details.

methanol: A(t) = 0.1 7[exp(-t/6.7 ps) - 1] - 0.14exp(-t/1.9 ps);
DMSO: A(t) = 0.30[e xp(-t/9.2 ps) - 1] - 0.13exp(-t/1.9 ps);

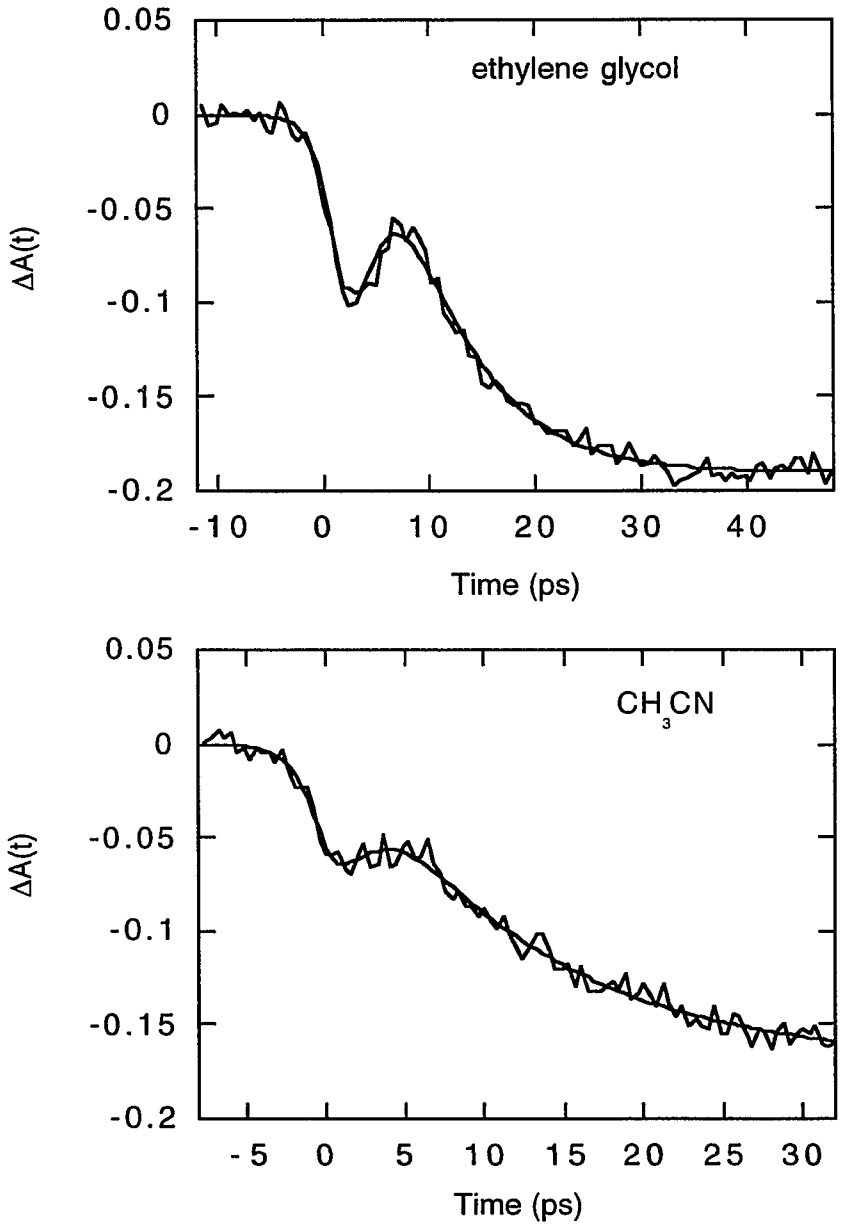

Figure 6 (cont.)

ethylene glycol: A(t) = 0.45[e xp(-t/6.4 ps) - 1] - 0.53exp(-t/2.4 ps) + 0.26;
acetonitrile: A(t) = 0.1 9[exp(-t/11.2 ps) - 1] - 0.19exp(-t/1.4 ps) + 0.025.

reveals smoothly varying contributions of the components of stimulated emission that appear instantaneously and that appear with a finite rise time. The instantaneous component is most easily identified at 640 and 675 nm. The simplest interpretation of these data is that the normal form of hypericin, N^*, which we suggest gives rise to the instantaneous component has a fluorescence spectrum that in some regions is more intense than that of the fully tautomerized form, DT^*. The solid curve centered at ~650 nm in Figure 2 represents the fluorescence spectrum of N^* obtained from the ratio of the instantaneous to the rising components (Table I).

Measurements of the slower component of the stimulated emission in ethylene glycol over a rather limited temperature range were used to construct an Arrhenius plot (Figure 8). The barrier for this proton transfer reaction is thus estimated to be 1.5 kcal/mol in ethylene glycol. Lastly, Figure 9 presents a plot of the time constant for the slower component against solvent polarity as measured by $E_T(30)$.

Discussion

In a range of solvents, both hydrogen bonding and nonhydrogen bonding and protic and aprotic, over which the viscosity and the average solvation time change by factors of 60 and 100, respectively, the proton transfer time as measured by the rise time of the longer-lived component of the stimulated emission is found to be uncorrelated with these properties and to change by at most a factor of two. This result is very surprising when it is considered in the context of other examples of excited-state proton transfer.

Hochstrasser and coworkers [16] have observed proton transfer rates for a 2-phenyl-benzotriazole bearing an octyl group on the 5-position that agree very well with

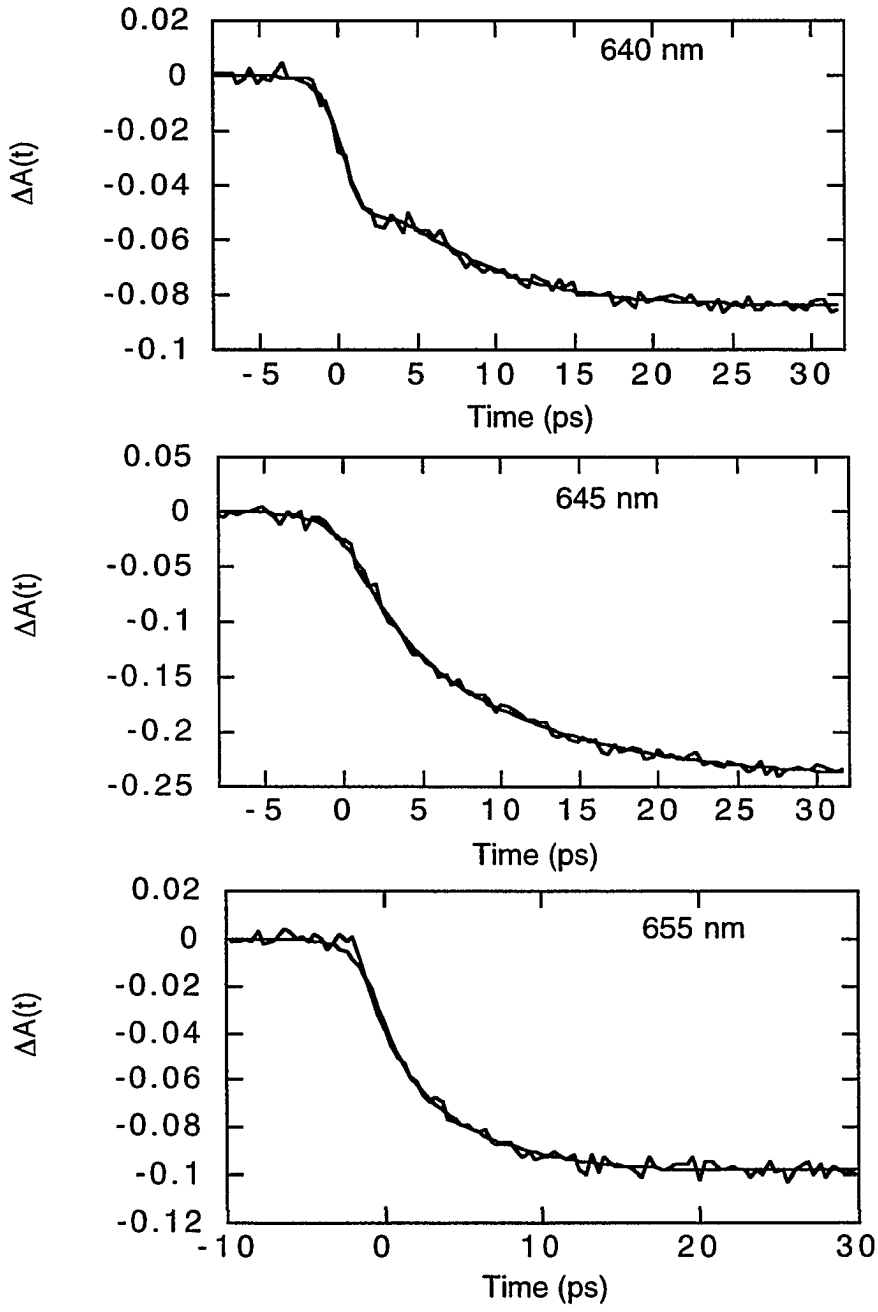

Figure 7. Stimulated emission profiles of hypericin in octanol at different probe wavelengths, λ_{ex} = 588 nm. Probe wavelengths are indicated in the panels.

λ_{probe} = 640 nm: A(t) = 0.086[e xp(-t/11.0 ps) - 1] -0.042exp(-t/13.4 ps);
λ_{probe} = 645 nm: A(t) = 0.47[e xp(-t/12.6 ps) - 1] - 0.24exp(-t/18.8 ps);
λ_{probe} = 655 nm: A(t) = 0.097[e xp(-t/7.6 ps) - 1] - 0.054exp(-t/11.0 ps);

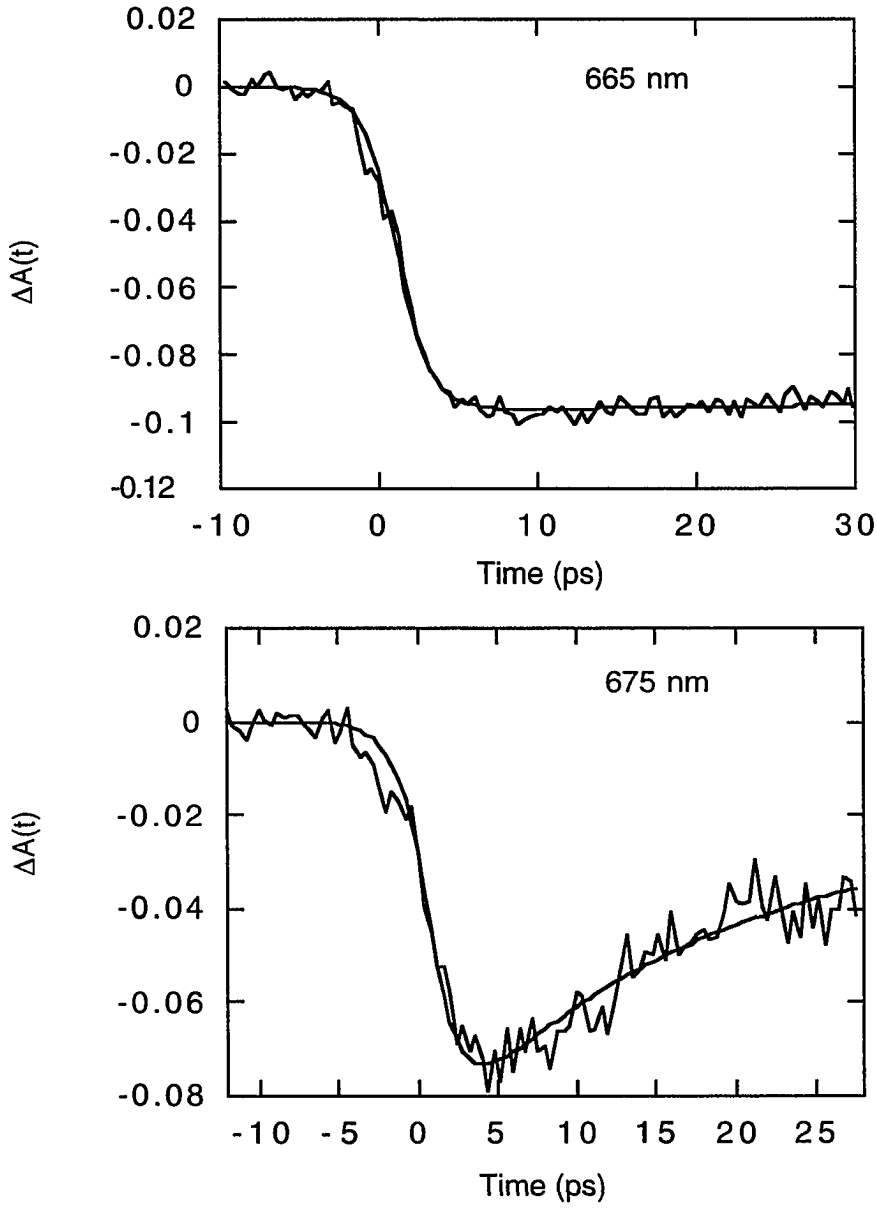

Figure 7 (cont.)

λ_{probe} = 665 nm: A(t) = -0.1 2;

λ_{probe} = 675 nm: A(t) = -0.067e xp(-t/16.0 ps) - 0.022.

the longitudinal relaxation time of the solvent, τ_L. These data are particularly intriguing because despite this dependence on τ_L no time-dependent Stokes shift is observed in this system.

The time-dependent Stokes shift is related to τ_L and is characterized by an average solvation time $<\tau_S>$ [15,17]. When a solute is promoted to its excited state, its charge distribution is altered. The solvent is no longer in equilibrium and must relax to its new equilibrium structure, thus affording the temporally evolving Stokes shift. Charge transfer reactions similarly alter the charge distribution of the solute, and in many cases the rates of such reactions have been shown to depend on the dynamic response of the solvent, characterized by τ_L or $<\tau_S>$, to the charge-transferred species [16,17].

In hydrogen-bonding solvents such as alcohols, on the other hand, the ability of the solvent to weaken or to break the intramolecular hydrogen bond in 3-hydroxyflavone is the rate determining factor in the excited-state proton transfer reaction [18-23]. If both the carbonyl and the alcohol groups of 3-hydroxyflavone are strongly coordinated to different solvent molecules, proton transfer occurs relatively slowly, on a time scale of 10 ps [23]. If, however, the intramolecular hydrogen bond of the solute is not perturbed (as occurs in hydrocarbon solvents such as methylcyclohexane) excited-state proton transfer is very rapid. Harris and coworkers have measured this time to be ~240 fs [23]. These workers have also proposed that if a single alcoholic solvent molecule can form a cyclic hydrogen-bonding interaction with the carbonyl and the alcohol groups of the solute, an even more rapid transfer time of ~80 fs results. Similarly rapid proton transfer times have been observed in benzothiazole derivatives [24,25]. These results have been interpreted in terms of the wavepacket prepared upon optical excitation. The evolution of this wavepacket towards the tautomeric form on the excited-state potential surface will initially depend very strongly on the vibrations displaced upon light

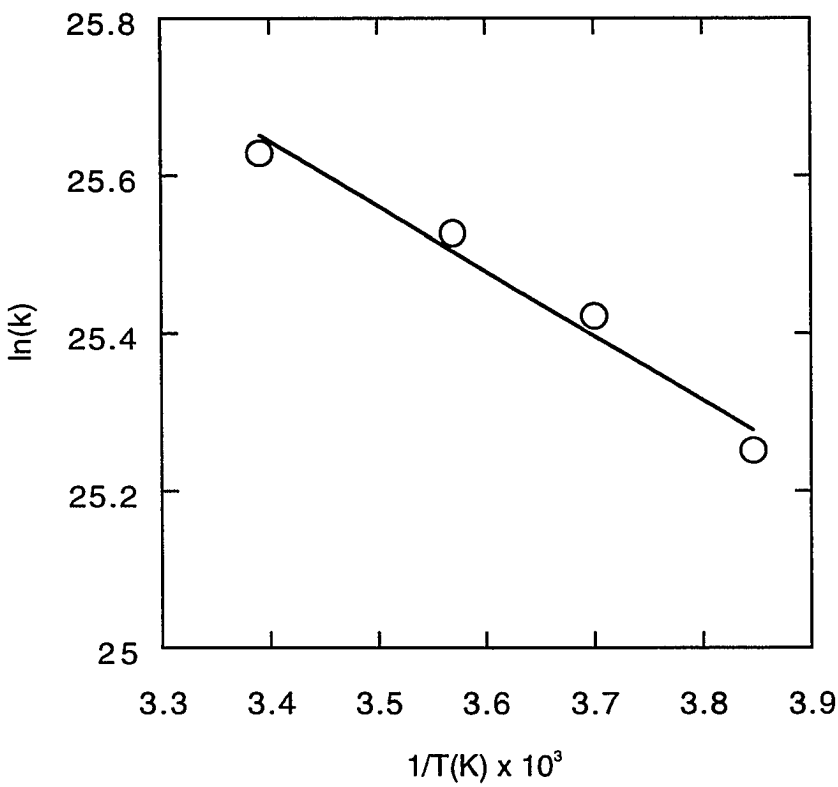

Figure 8. Arrhenius plot of the time constant of the longer-lived component of stimulated emission in hypericin in ethylene glycol.

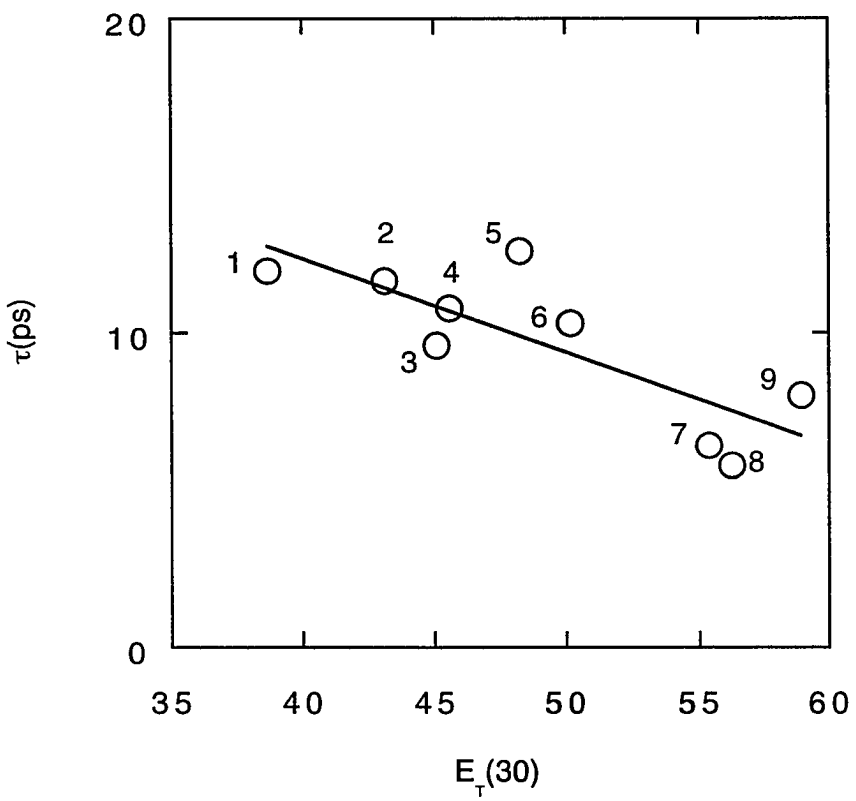

Figure 9. The time constant of the longer-lived component of stimulated emission in hypericin plotted as a function of polarity as measured by $E_T(30)$ [33]: 1, diethylene glycol dimethyl ether; 2, butyronitrile; 3, DMSO; 4, acetonitrile; 5, 1-octanol; 6, 1-butanol; 7, methanol; 8, ethylene glycol; 9, 2,2,2-trifluoroethanol.

absorption [23,24].

The proton transfer time in hypericin ranges from about 6 to 12 ps in the solvents we have investigated and hence is similar to the proton transfer time observed in 3-hydroxyflavone and attributed to solute-solvent structures in which two different alcohol molecules are coordinated to the carbonyl and alcohol groups of the solute [23]. Such a state of solvation cannot, however, explain the proton transfer rates in hypericin because the same results are obtained in both hydrogen-bonding and nonhydrogen-bonding solvents. This suggests that the intramolecular interactions between the O—H•••O group formed by the alcohol oxygen, the proton, and the carbonyl oxygen of hypericin are much stronger than any potential hydrogen bonding interactions with the solvent.

The assignment of the excited-state process to intramolecular proton transfer may be criticized because we do not observe an isotope effect [8]. There is precedent for proton transfer processes that do not exhibit an isotope effect [23,25]. Whether an isotope effect is observed will also depend on such factors as the degree to which the reaction is nonadiabatic and characterized by tunneling through a potential barrier [26] or if the reaction occurs by means of a barrierless (or small barrier) process in which the role of vibrational motions other than the O-H stretch are important [27].

Hynes, Borgis, and coworkers [26] have presented a theory of proton transfer in both adiabatic and nonadiabatic limits. Three coordinates play an important role: the coordinate for the proton itself; the intramolecular separation of the two atoms (in this case oxygens) between which the proton is transferred; and a collective solvent coordinate. In this treatment, the electrons are always treated adiabatically; but the proton transfer process is considered to be in a nonadiabatic or an adiabatic limit depending on the separation of the oxygen atoms. For a large (> 2.7 Å) separation, the wavefunction for the proton is localized about one of the oxygens and a sufficiently large barrier exists

that proton transfer must be viewed as a nonadiabatic tunneling process. (The rate of this tunneling process is modulated by the oxygen-oxygen separation and the solvent fluctuations.) If, however, the separation is small (< 2.7 Å), the barrier to proton transfer is greatly decreased and the extent to which tunneling contributes to the rate of proton transfer can be greatly reduced. Finally, in reactions that involve the generation of charged or partially charged species, the solvent polarity is expected to accelerate the rate. For example, in a reaction taking covalent reactants to ionic products, the products will be better solvated by a polar substance such as water than a nonpolar substance such a methylcyclohexane. Stabilization of the potential surface for the ionic species with respect to that for the covalent species will lower the point at which they cross and hence decrease the activation energy for the process [28].

In the case of hypericin, the distances [29,30] between the keto and hydroxy oxygens (as measured starting from the 1 and 14 positions and moving clockwise around the polycycle in Figure 1) between which the proton is transferred are all consistent with an adiabatic process: 2.45, 2.53, 2.49, and 2.53 Å. The solvent dependence of the time constant for the excited-state process is also consistent with its assignment to proton transfer. The time constant decreases with increasing solvent polarity, as measured by $E_T(30)$, and suggests a process that involves the transfer of a charged particle, molecular rearrangement, and charge reorganization [26,28]. Finally, temperature-dependent measurements in ethylene glycol (Figure 8) indicate that there is a small barrier (~1.5 kcal/mol) between MT^* and DT^*. This small barrier is in agreement with the short distances between oxygens in hypericin.

Construction of molecular models of hypericin and a recent x-ray structure [29] indicate that the aromatic polycycle is twisted. One might argue that the excited-state transients observed reflect transitions from one form of conformational isomer to an-

other. Because such a process involves a large amplitude motion, it would be expected to be viscosity dependent. In solvents in which the viscosity changes by a factor of 60 we see, however, no more than a change of a factor of two in the time constant of the longer-lived excited-state transient (~6-12 ps). Furthermore, the rate of the excited-state process is completely uncorrelated to viscosity: the small variation in rate cited can be effected just a easily when the viscosity is increased by less than a factor of two, i.e. from methanol to acetonitrile (Table I). This excludes the assignment to a conformational transition.

An obvious question that remains is whether intramolecular vibrational modes other than those modulating the oxygen-oxygen separation play a role in the reaction. Resonance Raman measurements will be indispensable in providing a response. Peteanu and Mathies [27] have shown that in the case of 2-hydroxyacetophenone, which is believed to execute a barrierless excited-state proton transfer, there is no displacement in the O-H stretching coordinate upon optical excitation. This result suggests that vibrations other than proton motion are responsible for the initial displacement of the wavepacket away from the Franck-Condon region of the excited state. Consistent with these Raman measurements are the observations of Harris and coworkers [23] and of Elsaesser and coworkers [24,25] of proton transfer rates that are independent of isotopic substitution. Cotton and coworkers [31] have measured the resonance Raman spectrum of hypericin under various conditions and observed bands in the region from ~1620 to 620 cm^{-1}, some of which were tentatively identified.

Conclusions

Measurements of the stimulated emission of hypericin with 1-ps resolution have been used to monitor the creation and decay of excited and hence fluorescent states. The excited-state characterized by nanosecond lifetimes and observed in steady-state measurements [8,9] appears in roughly 6 to 12 ps. The rise time for the appearance of this emission is attributed to an excited-state proton transfer reaction. The similarity of the rates in both hydrogen-bonding and nonhydrogen-bonding solvents is the most surprising result given what is known about the behaviour of 3-hydroxyflavone in these solvents. Polarity is the only solvent property that is well correlated with the proton transfer time. In addition to the slower, ~6-12-ps rise time, a component of the stimulated emission is observed that appears instantaneously. This component is attributed to a ground-state untautomerized (normal, N) form of hypericin that decays rapidly, most probably by forming the excited-state tautomer MT^*. The observation of this component demonstrates the inhomogenous distribution of hypericin structures in the ground state and hence in the excited state. A proton transfer reaction with a time constant of 6-12 ps is relatively slow [19-25]. Hypericin thus provides an extremely useful system with which to test current theories of proton transfer [26].

In conclusion, the primary photoprocess occurring in hypericin is intramolecular proton transfer, whose rate depends on solvent polarity. Understanding the light induced activity in hypericin is of significance for appreciating its biochemical role in protozoa and exploiting its medicinal activity against viruses.

Acknowledgments

J.W.P. is an Office of Naval Research Young Investigator. M.J.F. is supported by an AASERT training grant from the ONR. F.G. is the recipient of a fellowship from Phillips Petroleum. Professor J. T. Hynes provided many very helpful comments. We thank Professor W. S. Struve for loaning us his low temperature equipment. We are also grateful to Professor H. Falk for providing us the x-ray coordinates of hypericin.

References

1. Meruelo, D.; Lavie, G.; Lavie, D. *Proc. Natl. Acad. Sci. USA* 1988, **85**, 5230; Lavie, G.; Valentine, F.; Levin, B.; Mazur, Y.; Gallo, G.; Lavie, D.; Weiner, D.; Meruelo, D. *Proc. Natl. Acad. Sci. USA* 1989, **86**, 5963; Degar, S.; Prince, A. M.; Pascual, D.; Lavie, G.; Levin, B.; Mazur, Y.; Lavie, D.; Ehrlich, L. S.; Carter, C.; Meruelo, D. *AIDS Res. Hum. Retroviruses* 1992, **8**, 1929; Lenard, J.; Rabson, A.; Vanderoef, R. *Proc. Natl. Acad. Sci. USA* 1993, **90**, 158.
2. Carpenter, S.; Kraus, G. A. *Photochem. Photobiol.* 1991, **53**, 169.
3. Tao, N.; Orlando, M.; Hyon, J.-S.; Gross, M.; Song, P.-S. *J. Am. Chem. Soc.* 1993, **115**, 2526; Song, P.-S.; Kim, I.-K.; Florell, S.; Tamai, N.; Yamazaki, T.; Yamazaki, I. *Biochim. Biophys. Acta* 1990, **1040**, 58; Song, P.-S. *Biochim. Biophys. Acta* 1981, **639**, 1; Tao, N.; Song, P.-S.; Savikhin, S.; Struve, W. S. *J. Phys. Chem.* 1993, 97, 12379.

4. Cubbedu, R.; Ghetti, F.; Lenci, F.; Ramponi, R.; Taroni, P. *Photochem. Photobiol.* 1990, **52**, 567; Lenci, F.; Ghetti, F.; Gioffré, D.; Passarelli, V.; Heelin, P. F.; Thomas, B.; Phillips, G. O.; Song, P.-S. *J. Photochem. Photobiol. B: Biol.* 1989, **3**, 449.

5. Durán, N.; Song, P.-S. *Photochem. Photobiol.* 1986, **43**, 677; Racinet, H.; Jardon, P.; Gautron, R. *J. Chim. Phys.* 1988, **85**, 971; Bourig, H.; Eloy, D.; Jardon, P. *J. Chim. Phys.* 1992, **89**, 1391.

6. Yang, K.-C.; Prusti, R. K.; Walker, E. B.; Song, P.-S.; Watanabe, M.; Furuya, M. *Photochem. Photobiol.* 1986, **43**, 305; Song, P.-S.; Walker, E. B.; Auerbach, R. A.; Robinson, G. W. *Biophys. J.* 1981, **35**, 551; Walker, E. B.; Lee, T. Y.; Song, P.-S. *Biochim. Biophys. Acta* 1979, **587**, 129-144.

7. Gai, F.; Fehr, M. J.; Petrich, J. W. *J. Am. Chem. Soc.* 1993, **115**, 3384.

8. Gai, F.; Fehr, M. J.; Petrich, J. W. *J. Am. Chem. Soc.* 1993. Submitted for publication.

9. Yamazaki, T.; Ohta, N.; Yamazaki, I.; Song, P.-S. *J. Phys. Chem.* 1993, **97**, 7870.

10. Koch, W.; Saito, T.; Yoshida, Z. *Tetrahedron* 1972, **28**, 3191.

11. Chen, Y.; Rich, R. L.; Gai, F.; Petrich, J. W. *J. Phys. Chem.* 1993, **97**, 1770.

12. Rich, R. L.; Chen, Y.; Neven, D.; Négrerie, M.; Gai, F.; Petrich, J. W. *J. Phys. Chem.* 1993, **97**, 1781.

13. Gai, F.; Rich, R. L.; Petrich, J. W. *J. Am. Chem. Soc.* In press.

14. Hart, E. J.; Anbar, M. The Hydrated Electron; Wiley-Interscience: New York, 1970.

15. Barbara, P. F.; Jarzeba, W. *Adv. Photochem.* 1990, **15**, 1-69.

16. Kim, Y. R.; Yardley, J. T.; Hochstrasser, R. M. *Chem. Phys.* 1989, **136**, 311.

17. Kosower, E. M.; Huppert, D. *Ann. Rev. Phys. Chem.* 1986, **37**, 127; Maroncelli, M.; MacInnis, J.; Fleming, G. R. *Science* 1989, **243**, 1674; Barbara, P. F.; Walker, G. C.; Smith, T. P. *Science* 1992, **256**, 975.

18. Brucker, G. A.; Swinney, T. C.; Kelley, D. F. *J. Phys. Chem.* 1991, **95**, 3190; Swinney, T. C.; Kelley, D. F. *J. Phys. Chem.* 1991, **95**, 10369; Swinney, T. C.; Kelley, D. F. *J. Chem. Phys.* 1993, **99**, 211.

19. Barbara, P. F.; Walsh, P. K.; Brus, L. E. *J. Phys. Chem.* 1989, **93**, 29.

20. Strandjord, A. J. G.; Barbara, P. F. *J. Phys. Chem.* 1985, **89**, 2355.

21. McMorrow, D.; Kasha, M. *J. Phys. Chem.* 1984, **88**, 2235.

22. Brucker, G. A.; Kelley, D. F. *J. Phys. Chem.* 1987, **91**, 2856.

23. Schwartz, B. J.; Peteanu, L. A.; Harris, C. B. *J. Phys. Chem.* 1992, **96**, 3591.

24. Laermer, F.; Elsaesser, T.; Kaiser, W. *Chem. Phys. Lett.* 1988, **148**, 119.

25. Frey, W.; Laermer, F.; Elsaesser, T. *J. Phys. Chem.* 1991, **95**, 10391.

26. Borgis, D.; Lee, S.; Hynes, J. T. *Chem. Phys. Lett.* 1989, **162**, 19; Borgis, D.; Hynes, J. T. in The Enzyme Catalysis Process, eds. Cooper, A.; Houben, J; Chien, L. Plenum; New York, 1989; pp. 293-303; Borgis, D.; Hynes, J. T. *J. Chim. Phys.* 1990, **87**, 819; Borgis, D.; Hynes, J. T. *J. Chem. Phys.* 1991, **94**, 3619; Borgis, D. in Electron and Proton Transfer in Chemistry and Biology, eds Müller, A.; Ratajczak, H.; Junge, W.; Diemann, E. Elsevier; Amsterdam, 1992; p. 345; Azzouz, H.; Borgis, D. *J. Chem. Phys.* 1993, **98**, 7361.

27. Peteanu, L. A.; Mathies, R. A. *J. Phys. Chem.* 1992, **96**, 6910.

28. Keirstead, W. P.; Wilson, K. R.; Hynes, J. T. *J. Chem. Phys.* 1991, **95**, 5256.

29. Etzlstorfer, C.; Falk, H.; Müller, N.; Schmitzberger, W.; Wagner, U. G. *Monatsh. Chem.* 1993, **124**, 731.

30. Falk, H. Personal communication.

31. Raser, L. N.; Kolaczkowski, S. V.; Cotton, T. M. *Photochem. Photobiol.* 1992, **56**, 157.

32. Viswanath, D. S.; Natarajan, G. Data Book on the Viscosity of Liquids; Hemisphere publishing: New York, 1989.

33. Reichardt, C. Solvents and Solvent Effects in Organic Chemistry; VCH: Weinheim, 1988.

34. Riddick, J. A.; Bunger, W. B.; Sakano, T. K. Organic Solvents: Physical Properties and Methods of Purification; Wiley: New York, 1986.

35. Smith, T. P.; Zaklika, K. A.; Thakur, K.; Walker, G. C.; Tominaga, K.; Barbara, P. F. *J. Phys. Chem.* 1991, **95**, 10465; Flom, S. R.; Barbara, P. F. *J. Phys. Chem.* 1985, **89**, 4489; Inoue, H.; Hida, M.; Nakashima, N.; Yoshihara, K. *J. Phys. Chem.* 1982, **86**, 3184.

CHAPTER 5. THE ROLE OF OXYGEN IN THE PHOTOINDUCED ANTIVIRAL ACTIVITY OF HYPERICIN

A paper published in *Bioorganic Medicinal Chemistry Letters*[1]

M. J. Fehr[2], S. L. Carpenter[2,3], and J. W. Petrich[2,3]

Abstract

Hypericin displays photoinduced antiviral activity. We examine the photoinduced antiviral activity of hypericin under both oxygenated and hypoxic conditions and observe that hypericin is equally toxic under both conditions. These results indicate that while singlet oxygen may play a role in the antiviral activity of hypericin, it does not play a major role.

Introduction

The naturally occurring polycyclic quinone, hypericin (Figure 1), possesses important and diverse types of biological activity [1]. It has been shown that hypericin

---

[1] Reprinted with permission from *Bioorganic Medicinal Chemistry Letters* **1994**, *4*, 1339.

[2] Graduate student, Assistant Professor, and Associate Professor, Department of Chemistry and Department of Microbiology, Immunology, and Preventive Medicine, Iowa State University.

[3] To whom correspondence should be addressed.

inactivates the human immunodeficiency virus (HIV)[2-6]. That antiviral activity requires lightwas first demonstrated in a lentivirus closely related to HIV, equine infectious anemia virus (EIAV), by Carpenter and Kraus [6]. Hypericin produces singlet oxygen very efficiently (with a quantum yield of 0.737), and many studies have suggested that its antiviral activity is due to the production of singlet oxygen [2-6].

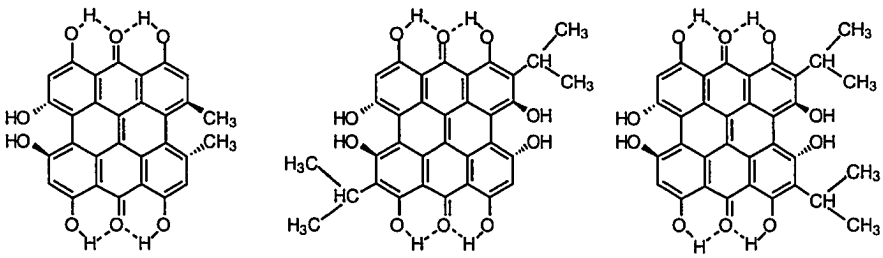

Figure 1. Structures of hypericin (a) and the two possibilities for the chromophore of Stentor coerulus (b and c) [16].

The excited-state reactivity of hypericin, however, extends well beyond the photosensitization of oxygen to form singlet oxygen. Redepenning and Tao have measured the formal potential of hypericin in DMSO by cyclic voltammetry and concluded that in its excited state it is both a good oxidizing and reducing agent [8]. Diwu and Lown observed both singlet oxygen and superoxide radical upon illumination of hypericin with 580- nm light under aerobic conditions [9]. They also indirectly observed the formation of a semiquinone radical species in the absence of oxygen. Mazur and coworkers have obtained similar results [10-11]. The role of singlet oxygen in the inactivation of mammalian cell activity has also recently been examined by Dahl [15]. In

this work, it was concluded that ~10^{12}-10^{13} singlet oxygen collisions were required to inactivate a cell. Elucidating the reactivity of excited-state hypericin and the subsequent reactivity of molecules that it encounters is essential for understanding the light-induced mechanism of antiviral activity. The mechanism of photosensitization by a given molecule in its excited state can be classified into two types of processes [22,24]. In Type I processes, the excited-state photosensitizer interacts first with the substrate, which may go on to react with another reagent, which is usually oxygen. In Type II processes, the excited-state photosensitizer interacts first with oxygen, thus producing singlet oxygen, which subsequently goes on to react with the substrate.

We have questioned the relative importance of singlet oxygen in the toxicity of hypericin towards HIV and related viruses [12-14]. For example, hypericin is closely related, both structurally and spectrally, to the photoreceptor of the protozoan ciliates, Stentor coerulus (Figure 1) and Blepharisma japonicum [16-18]. This photoreceptor confers upon the organism its biologically necessary photophobic and phototactic responses. Under conditions of ambient light the stentorin chromophore and hypericin are nontoxic to the organism. On the other hand, the singlet oxygen produced from these chromophores is toxic to S. coerulus under high light flux (~5000 W/m^2) [19]. It is an open question, therefore, whether the limited exposure to room light in the experiments of Carpenter and Kraus and of other workers is toxic to EIAV, HIV, and other retroviruses because of photosensitized generation of singlet oxygen by hypericin or because of the presence of additional nonradiative decay processes of the excited states of hypericin [2-6]. We have provided the first detailed investigation that uses both ~1-ps time resolution and a white-light continuum to examine and to unravel the excited-state primary photoprocesses of hypericin and have suggested that the excited-state transients we observe, coupled with data from model compounds, can be

interpreted in terms of tautomerization [12-14]. The results and conclusions of these time-resolved studies are of particular interest in the context of earlier observations and suggestions of Song and coworkers that the excited states of hypericin-like chromophores produce protons upon photoexcitation [18-21]. We thus proposed that deprotonation of the tautomer results in the reported pH decrease. Whether such processes are in fact responsible for the antiviral activity of hypericin is as yet uncertain, but it is clear that a detailed investigation of the excited-state chemistry of hypericin is required in order to unravel the mechanism of antiviral activity. In order to determine the relative importance of oxygen for the antiviral activity of hypericin, we have performed experiments where EIAV was challenged with hypericin and light under hypoxic conditions.

Experimental

Titration of infectious virus: All experimental manipulations were done in subdued light. Cell-free stocks of the MA-1 isolate of EIAV containing approximately 10^5 focus-forming units/ml (FFU/ml) of EIAV, were diluted 1:10 in Hank's buffered saline solution (HBSS) [26-27]. Hypericin (Carl Roth GmbH & Co.) was added to a final concentration of 10 µg/ml.

Illumination and deoxygenation: Deoxygenation of samples by bubbling either N_2 or Ar was done in light-tight containers. Hypericin/EIAV samples were exposed to light from a 300 W projector bulb fitted with a cut-off filter blocking wavelengths shorter than 575 nm. The irradiance at the sample was estimated to be 170 W/m^2 in the spectral range in which hypericin absorbs, 575-600 nm. Alternatively, deoxygenation was effected by using ß-carotene (Sigma) as a singlet oxygen scavenger (Table 2) [22, 25]. In neither case was oxygen seen to be required for antiviral activity. Solutions of ß-

carotene were made up in a Hank's medium/ethanol mixture (95/5 v/v). Samples of EIAV, hypericin, and varying aliquots of the ß-carotene mixture were irradiated at 598 nm (24-nm bandpass, ~100 W/m^2) for 20 min. with a Photon Technology International 150-W lamp (LPS-220) coupled to a monochromator.

Oxygen assays: Deoxygenation efficiency was evaluated by two separate techniques. A dissolved oxygen test kit (Hach, OX-2P) showed dissolved oxygen levels after one hour of deoxygenating to have fallen from an initial concentration of 5 mg/L (1.56×10^{-4} M) to below the detection limit of 0.2 mg/L (6.25×10^{-6} M). An alternate method of testing for dissolved oxygen is via the bioluminescence of the firefly luciferase/luciferin reaction. Oxygen is necessary in this system for the production of light [23]. Light output was measured with a liquid-nitrogen cooled charge-coupled device (CCD) (Princeton Instruments LN/CCD-1152UV) mounted on an HR320 (Instruments SA, Inc.) monochromator with a grating (1200g/mm) blazed at 5000 Å. A solution of 1.0×10^{-5} M luciferin and 1.6×10^{-8} M luciferase and a solution of 1.0×10^{-4} M ATP were simultaneously deoxygenated in the same apparatus as the EIAV/hypericin experiments. The reaction was initiated by injecting 0.5 ml of the deoxygenated ATP solution into the luciferin/luciferase solution. Three successive 30-second integrations yielded spectra that were superimposable on the background spectra of the CCD. Light could be generated from the reaction system by opening it to the atmosphere. Lack of light generation was taken to indicate that oxygen levels were negligible.

A focal immunoassay similar to that previously described was used for quantitation of infectious virus [6]. Results are expressed in terms of FFU/ml supernatant.

Results and Discussion

Tables 1 and 2 compare the antiviral activity of hypericin under aerobic and hypoxic conditions. Hypericin is toxic in the presence and the absence of oxygen (although the data suggest that hypericin in a hypoxic environment does not inactivate EIAV as effectively as in an oxygenated environment.) While these results do not unambiguously rule out the Type II mechanism, they do demonstrate the importance of the Type I mechanism, particularly that direct interaction of hypericin itself with the virus is important for the remarkable antiviral properties of hypericin. It is of interest that Meruelo and coworkers report that sodium azide (NaN_3), which is believed to scavenge singlet oxygen--as well as to quench other oxidants and sensitizer excited-states, inhibits the light-induced activity of hypericin to inhibit reverse transcriptase activity of murine Radiation leukemia virus (RadLV) [5,22,25]. This argument, however, is based upon the observation that this effect occurs only if NaN_3 is allowed to incubate 10 min. with the sample before the introduction of hypericin. They argue that since addition of NaN_3 subsequent to a 30-min. incubation with hypericin and exposure to light has little effect on the toxicity that singlet oxygen is responsible for the antiviral activity. An alternative interpretation of the former result is that preincubation of NaN_3 facilitates quenching of the excited state of hypericin and consequently inactivates antiviral activity, which is not necessarily based upon singlet oxygen.

The antiviral mechanism and the target of hypericin activity are as yet unclear. Meruelo and coworkers have observed that in the presence of light hypericin induces significant changes in the HIV capsid protein, p24, and the p24-containing gag precursor, p55, as indicated by Western blot analysis [3,4]. They have also observed that recombinant p24 in the presence of light forms an anti-p24 immunoreactive material of

a molecular weight of 48 kilodaltons. They have consequently suggested that cross-linking and other alterations of p24 occur and that such alterations may inhibit the release of reverse transcriptase activity. It is significant that these workers found that under ambient lighting conditions, hypericin did not inhibit the binding of gp120 to CD4 cells and that it did not inhibit the formation of syncytia (large, abnormal multinucleated cells formed by the fusion of infected cells with uninfected CD4 cells) [3,4]. On the other hand, inhibition of gp120 binding was observed under conditions of more intense illumination: i.e., when samples were placed ~10 cm away from a fluorescent light source for 30 minutes [3]. The highest concentration of hypericin used by Meruelo and coworkers is 2 μg/ml (~4 μM). Lenard et al., on the other hand, observed that syncytia formation was inhibited by illumination for 1 hour in the presence of 1 μM hypericin [4]. Because of the similarity in behavior between hypericin and the photosensitizer, rose

Table 1. Effect of Oxygen on the Antiviral Activity of Hypericin

Illumination time (min)[a]	Infectious virus (FFU/ml)	
	oxygenated[b]	hypoxic[c]
0	10,200	14,500 (N_2)
10	0	25 (N_2)
0	2,475	5,975 (Ar)
10	0	225 (Ar)

[a] Illumination was effected with a 300 W projector bulb fitted with a cut-off filter blocking wavelengths shorter than 575 nm.

[b] The oxygen content of the sample was determined by letting it equilibrate with the atmosphere.

[c] Hypoxic conditions were obtained by passing argon or nitrogen gas over the samples for 1 hour before and during illumination.

bengal, Lenard et al. concluded that singlet oxygen was the essential factor in toxicity, even though hypericin proved itself to be much more toxic. These workers quoted an irradiance of 800-900 footcandles, which is 12-14 W/m^2 at 555 nm. This latter figure is an underestimate of the energy that is actually available to be absorbed by hypericin since footcandles are a measure of visible light, whose detectability by eye is a maximum at ~555 nm. In other words, the figure that is quoted gives no information on the

Table 2. Effect of a Singlet Oxygen Scavenger on the Antiviral Activity of Hypericin

[ß-carotene] (μM)	Infectious virus with hypericin (FFU/ml)	Infectious virus without hypericin (FFU/ml) [a]
80	0	3,000
64	0	4,800
48	0	6,400
32	0	8,400
16	0	> 10,000
0	0	10,000

[a] Control experiments.

irradiance over the spectral range utilizable by hypericin (and transparent to glass) from about 300 to 600 nm [4]. If we assume that the radiant energy provided by the source in this example is constant over this spectral range, then the sample is actually exposed to an irradiance of 3700-4200 W/m^2.

It is useful to consider our experiments in the context of the others referred to above. The toxicity to S. coerulus and to syncytia under high, but not ambient or low, light flux and the ability of hypericin to kill HIV and EIAV under conditions of low or ambient light flux suggest that several mechanisms of toxicity may be involved [3-5,19]. The relative importance of Type I and II mechanisms in virus inactivation may depend on the intensity of light. Under high irradiance, the formation of singlet oxygen by a Type II mechanism would be predominant, whereas under low irradiance the antiviral activity would be primarily due to a Type I reaction. Such reasoning may explain the differences among investigators in characterizing the antiviral mechanism of hypericin cited above. At high irradiance, there is both inhibition of gp120 binding and inhibition of cell fusion, events that depend on interactions between virus and cell membranes [3,4]. Interestingly, the effects are not reported to occur at low irradiance, where inhibition is associated with alterations in the viral capsid protein [3]. This may indicate that Type II reactions target the viral membrane, whereas Type I reactions may attack other stages in the life cycle of the virus. This may also explain the absolute dependence on oxygen for the anti-tumor effect of hypericin [24]. Thomas and Pardini found that hypericin uptake in EMT6 mouse mammary carcinoma cells was associated with membrane components, both at the cell surface and in intracellular organelles [24]. Although they did not discuss the mechanisms of hypericin-induced cell killing, their observation of an absolute dependence on oxygen for the anti-tumor effect of hypericin in the presence of light (20-30 W/m^2) suggests that toxicity is due to membrane-associated damage produced by singlet oxygen. Much evidence exists that singlet oxygen is the primary mechanism of hypericin-mediated damage to cell membranes [1]. Our results indicate that under conditions of ambient light (low intensity), oxygen is not required for hypericin to exhibit antiviral activity. While it is certainly likely that singlet oxygen may play a role,

especially under conditions of high hypericin (and oxygen) concentrations or intense light fluxes, it is not essential. Much work remains in order to determine whether it is the singlet or triplet state of hypericin that is responsible for its antiviral activity and to determine the mechanism of this activity.

Acknowledgments

M.J.F is the recipient of an AASERT fellowship from the Office of Naval Research. J.W.P is an Office of Naval Research Young Investigator. Support for parts of this work was provided by a Carver grant. We thank Yvonne Wannemuehler for excellent technical assistance and Professor W.S. Jenks for the use of his 150-W lamp/ monochromator system.

References

1. Duran, N., and Song, P.-S. Photochem. Photobiol. 1986, 48, 677.
2. Meruelo, D., Lavie, G., and Lavie, D. Proc. Natl. Acad. Sci. USA 1988, 85, 5230.
3. Degar, S., Prince, A.M., Pascual, D., Lavie, G., Levin, B., Mazur, Y., Lavie, D., Ehrlich, L.S., Carter, C., and Meruelo, D. AIDS Res. Hum. Retroviruses 1992, 8, 1929.
4. Lenard, J., Rabson, A., and Vanderoef, R. Proc. Natl. Acad. Sci. USA 1993 90, 158.
5. Meruelo, D., Degar, S., Nuria, A., Mazur, Y., Lavie, D., Levin B., and Lavie, G. Natural Products as Antiviral Agents; C.K. Chu and H.G. Cutler, Eds.; Plenum Press: New York. 1992; pp 91-119 (and references therein).

6. Carpenter, S., and Kraus, G.A. Photochem. Photobiol. 1991, 53, 169.

7. Racinet, H., Jardon, P., and Gautron, R. J. Chim. Phys. 1988, 85, 971.

8. Redepenning, J., and Tao, N. Photochem. Photobiol. 1993, 58, 532.

9. Diwu, Z., and Lowen, J.W. Free Radical Biology and Medicine 1993, 14, 209.

10. Weiner, L., and Mazur, Y. J. Chem. Soc. Perkins Trans. 2 1992, 1432.

11. Malkin, J., and Mazur, Y. Photochem. Photobiol. 1993, 57, 929.

12. Gai, F., Fehr, M.J., and Petrich, J.W. J. Am. Chem. Soc. 1993, 115, 3384.

13. Gai, F., Fehr, M.J., and Petrich, J.W. J. Phys. Chem. Submitted.

14. Gai, F., Fehr, M.J., and Petrich, J.W. J. Phys. Chem. Submitted.

15. Dahl, T. Photochem. Photobiol. 1993, 57, 248.

16. Tao, N., Orlando, M., Hyon, J.-S., Gross, M., and Song, P.-S. J. Am. Chem. Soc. 1993, 115, 2526.

17. Cubbedu, R., Ghetti, F., Lenci, F., Ramponi, R., and Taroni, P. Photochem. Photobiol. 1990, 52, 567.

18. Lenci, F., Ghetti, F., Gioffre, D., Passarelli, V., Heelin, P.F., Thomas, B., Phillips, G.O., and Song, P.-S., J. Photochem. Photobiol. B: Biol. 1989, 3, 449.

19. Yang, K.-C., Prusti, R.K., Walker, E.B., Song, P.-S., Watanabe, M., Furuya, M. Photochem. Photobiol. 1986, 43, 305.

20. Song, P.-S., Walker, E.B., Auerbach, R.A., Robinson, G.W. Biophys. J. 1981, 35, 551.

21. Walker, E.B., Lee, T.-Y., Song, P.-S. Biochim. Biophys. Acta 1979, 587, 129.

22. Foote, C.S. Light-Activated Pesticides; J.R. Heitz and K.R. Downum, Eds.; American Chemical Society: Washington, DC. 1987; p 22.

23. McElroy, W., and Deluca, M. Chemi and Bioluminescence J.G. Burr, Ed.; Marcel Dekker, Inc.: New York, 1985; pp 387-399.

24. Thomas, C., and Pardini, R. Photochem. Photobiol. 1992, 55, 831.

25. Valenzeno, D.P. Photochem. Photobiol. 1987, 46, 147.

26. Carpenter, S.L., Evans, L.H., Sevoian, M., and Chesebro, B. J. Virol. 1987, 61, 3783.

27. Kraus, G.A., Pratt, D., Tossberg, J., and Carpenter, S.L. Biochem. Biophys. Res. Commun. 1990, 172, 149.

CHAPTER 6. CHEMILUMINESCENT ACTIVATION OF THE ANTIVIRAL ACTIVITY OF HYPERICIN: A MOLECULAR FLASHLIGHT

A paper published in the *Proceedings of the National Academy of Science*[1]

S. Carpenter[2,3], M. J. Fehr[2], G. A. Kraus[2], and J. W Petrich[2,3]

Abstract

Hypericin is a naturally occurring photosensitizer that displays potent antiviral activity in the presence of light. The absence of light in many regions of the body may preclude the use of hypericin and other photosensitizers as therapeutic compounds for the treatment of viral infections *in vivo*. The chemiluminescent oxidation of luciferin by the luciferase from the North American firefly, *Photinus pyralis*, was found to generate sufficiently intense and long-lived emission to induce antiviral activity of hypericin. Light-induced virucidal activity of hypericin was demonstrated against equine infectious anemia virus (EIAV), a lentivirus structurally, genetically, and antigenically related to the human immunodeficiency virus (HIV). The implications for exploiting chemiluminescence as a "molecular flashlight" for effecting photodynamic therapy against virus-infected cells and tumor cells are discussed.

---

[2] Assistant Professor, Graduate student, Professor, and Associate Professor, Departments of Microbiology, Immunology, and Preventive Medicine and Chemistry, Iowa State University. Steady-state measurements, selected assays, and calculations performed by M. J. Fehr.

[3] To whom correspondence should be addressed.

Introduction

The need for effective antiviral therapies for treatment of human immunodeficiency virus (HIV) infections has acquired increasing urgency with the realization that there may be years before an effective vaccine is in widespread use [1]. Three compounds currently are approved for use in treatment of HIV-1 infections, and all target the viral enzyme reverse transcriptase [2]. The eventual emergence of drug-resistant viral variants likely contributes to the fact that the present therapies may delay, but do not completely block, the progression to clinical disease in HIV-1 (human immunodeficiency virus Type 1) infected persons. Consequently, attention currently is focused on the development of combination therapies that employ a variety of compounds targeting different stages in the virus life cycle. A promising candidate is hypericin (Figure 1), a naturally occurring polycyclic quinone that displays potent light-induced antiviral activity against a number of enveloped viruses, including HIV-1 [3-7].

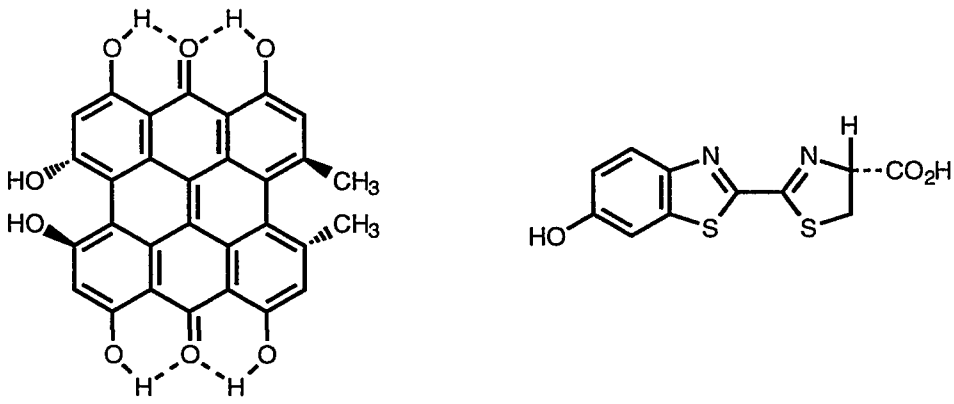

Figure 1. Hypericin (a) and luciferin (b).

Hypericin is a photosensitizing compound [8]. The antiviral activity of hypericin is enhanced more than 100-fold in the presence of light [3-7]. Upon illumination, hypericin produces singlet oxygen very efficiently, with a quantum yield of 0.73 [9]; and some studies have suggested that its antiviral activity is due to the production of singlet oxygen [4-6]. The excited-state reactivity of hypericin, however, extends well beyond the photosensitization of oxygen to form singlet oxygen. Recent work suggests that antiviral activity may be due to complex mechanisms involving the superoxide anion and hypericinium ion, implicating a Type I radical mechanism [10-12]. Moreover, we have observed that oxygen is not required for the antiviral activity of hypericin [13].

The mechanism by which hypericin inactivates HIV infectivity is not clear. Meruelo and coworkers [4,5] have reported that in the presence of light, hypericin induces significant changes in the HIV capsid protein, p24; and they suggest that cross-linking and other alterations of p24 may inhibit the release of reverse transcriptase activity. It is significant that these workers found that under ambient lighting conditions, 4 μM hypericin did not inhibit the binding of gp120 to CD4 cells, nor the formation of syncytia. However, inhibition of gp120 binding was observed under conditions of more intense illumination [4]. Other studies also have reported inhibition of syncytia formation under relatively high levels of illumination [6]. Together, these results suggest that observed differences in the biological effects of photoactivated hypericin depend on the irradiance and the concentration of photosensitizer. Thus, under relatively low light conditions, there is minimal damage to viral and/or cell membranes and the antiviral activity is associated with changes in viral capsid proteins. With increasing light intensity, the biological effects expand to include interactions between virus and cell membranes.

The usefulness of photosensitizers such as hypericin for treatment of viral infections *in vivo* is hampered by the dependence on light for optimal virucidal activity. In

this article we discuss a strategy to place in the proximity of hypericin a chemiluminescent light source so that photodynamic therapy can be extended to all regions of the body. What is required is a light source that emits a broad band of wavelengths in the region where the photoactive molecule adsorbs. An excellent choice for the light source is luciferin (Figure 1). The reaction of luciferin with the enzyme luciferase and molecular oxygen produces light in the 520-680 nm region with a quantum efficiency of about unity; [14-18] (Figure 2). Hypericin adsorbs light strongly in this range (Figure 3), suggesting that energy transfer between the product of the chemiluminescent reaction (Figure 2) and hypericin may be sufficient to effect significant antiviral activity.

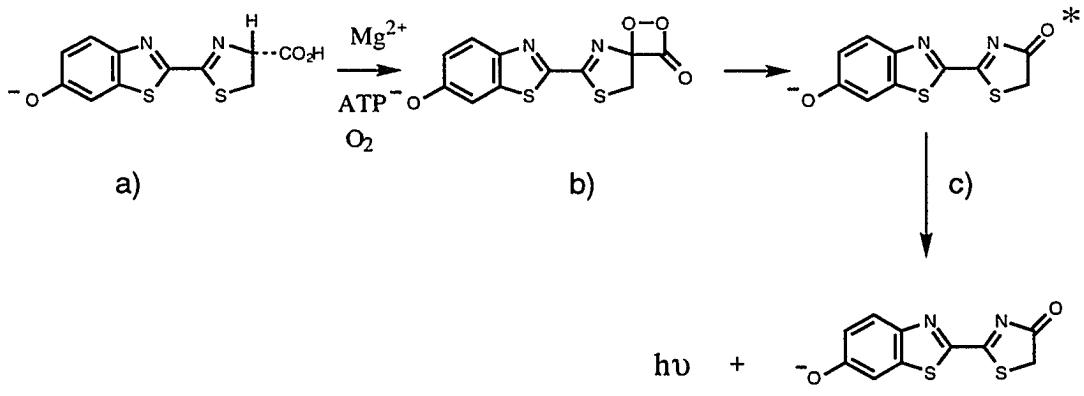

Figure 2. Crucial intermediates in the production of firefly chemiluminescence. [14,18,24].Luciferin (a) is catalyzed by the enzyme luciferase in the presence of ATP, Mg^{2+}, and O_2 to form the high energy four-member peroxide or dioxetanone intermediate (b). This intermediate subsequently decarboxylates to form the chemiluminescent species oxyluciferin (c).

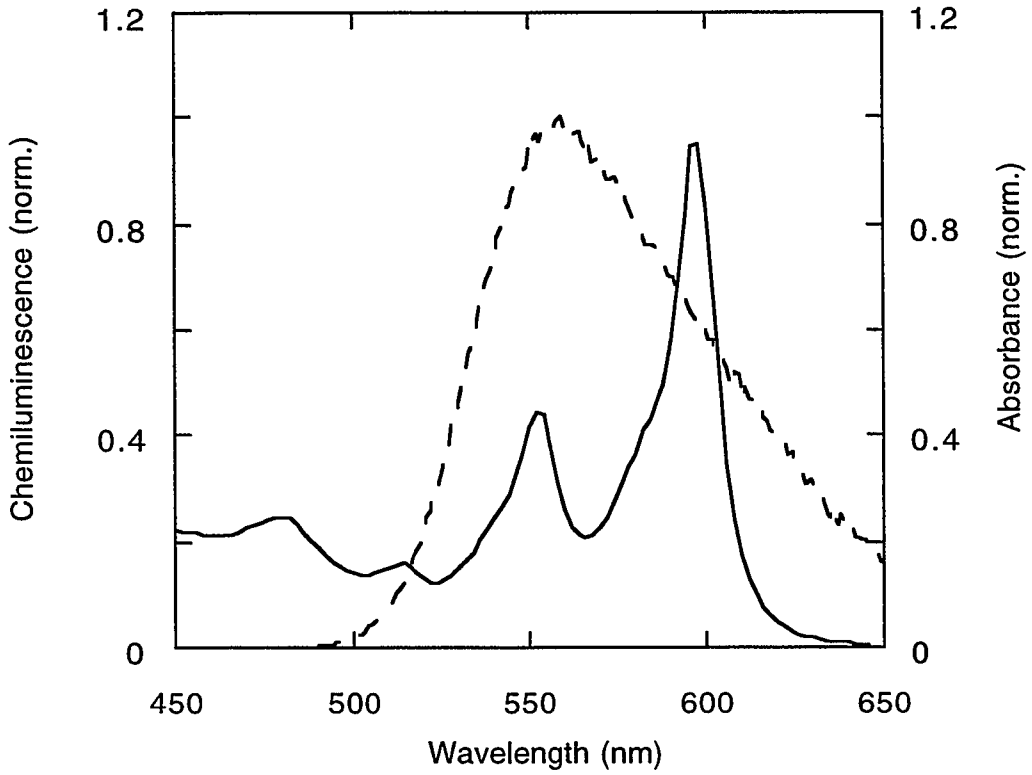

Figure 3. Spectral overlap between the visible portion of the absorption spectrum of hypericin and the chemiluminescence from the luciferase catalyzed oxidation of luciferin. The reaction is carried out at 25°C in glycylglycine buffer containing 2.67 x 10^{-7} M luciferase; 1.18 x 10^{-6} M luciferin, and 5 x 10^{-5} M ATP. The efficiency of the nonradiative energy transfer in a Förster energy transfer mechanism is given by R_0, the critical distance. R_0 is the distance at which the rate of energy transfer is equal to the inverse of the fluorescent lifetime of the donor: for randomly oriented donors and acceptors. R_0 can be calculated from the fluorescence spectrum of the donor and the absorption spectrum of the acceptor [21-23]

$$k_{ET} = \frac{1}{\tau_F}\left(\frac{R_o}{R}\right)^6, \qquad R_o^6 = \frac{9000(\ln 10)\phi_D}{128\,\pi^5 n^4 N}\,\frac{2}{3}\int_o^\infty F_D(\nu)\varepsilon_A(\nu)\nu^4 d\nu.$$

where n is the index of refraction of the medium, N is Avogadro's number, ϕ_D is the fluorescence quantum yield of the donor, $F_D(\nu)$ is the spectrum of the donor emission normalized to one on a wavenumber scale, and $\varepsilon_A(\nu)$ is the decadic molar extinction coefficient (in liter mol^{-1} cm^{-1}) on a wavenumber scale.

Materials and Methods

Reagents. Hypericin was obtained from Carl Roth GmbH & Co. and solubilized in DMSO to 1 mg/ml. Stock solutions were stored at 4°C. Luciferase from the North American firefly (*Photinus pyralis*) and luciferin were obtained from Sigma, resuspend in glycylglycine buffer (25 mM glycylglycine, 15 mM $MgSO_4$, 4 mM EGTA, pH 7.8) and aliquots were stored at -60°C.

Optical measurements. For optical assays, luciferase and luciferin were resuspended in glycylglycine buffer and reactions were initiated by the addition of a freshly prepared solution of ATP. Light output was measured with a liquid-nitrogen cooled charge-coupled device (CCD) (Princeton Instruments LN/CCD-1152UV) mounted on an HR320 (Instruments SA, Inc.) monochromator with a grating (1200 g/mm) blazed at 5000 Å. Handling of reagents before initiation of the luciferase/luciferin reaction was done under extremely low lighting levels.

Cells and virus. Equine dermal cells (ATCC CCL57) were grown in Dulbecco's modified Eagle's medium supplemented with 20% fetal bovine serum and antibiotics (DMEM). The MA-1 isolate [19] of equine infectious anemia virus (EIAV) was used in all assays.

Titration of infectious virus. Cell-free stocks of EIAV containing approximately 10^5 focus-forming units/ml (FFU/ml) of EIAV, were diluted 1:10 in Hank's buffered saline solution (HBSS) in 24-well tissue culture plates and hypericin, luciferin, and luciferase were added to the final concentrations indicated in the Figure legends. Chemiluminescence was initiated by the addition of ATP. Plates were wrapped with aluminum foil and incubated 30 min at room temperature. Controls included samples in which hypericin or luciferase were omitted and samples incubated in ambient room light. Vi-

rus infectivity was quantitated using a focal immunoassay similar to that previously described [3,19,20]. Results are expressed in terms of focus forming units (FFU) per ml supernatant. All experimental manipulations were done in subdued light.

Results

First it is necessary to compare the chemiluminescent emission of the luciferase catalyzed oxidation of luciferin and the absorption spectrum of hypericin in the red region of the visible spectrum (Figure 3). The high degree of overlap between these spectra supports the hypothesis that the chemiluminescent emission generated from the luciferin/luciferase reaction is capable of photoactivating hypericin. Further support for this hypothesis is demonstrated by the finding that, in the presence of hypericin, the chemiluminescent emission of the luciferase/luciferin reaction is attenuated in the region corresponding to the absorption spectrum of hypericin (Figure 4). Calculations based on Förster theory suggest that the so-called "critical distance" for energy transfer between these two species is about 100 Å (see the caption to Figure 3). The critical distance, R_0, is the distance at which the rate of energy transfer is equal to the rate at which the excited state of the donor decays. In other words, R_0 is the distance at which the rate of energy transfer is equal to the rate of fluorescence decay: and Φ_F is the fluorescence lifetime, and R is the separation between randomly oriented donors and acceptors [21-23]. The large value of 100 Å obtained for R_0 is partly a result of the high degree of spectral overlap between the chemiluminescent emission, but it is also a result of the extremely efficient yield of chemiluminescence. Approximately one photon is produced for every molecule of luciferin [14-18]: that is, the quantum yield of the donor, Φ_D, is unity. Comparable values of R_0 are observed for the pigments that con-

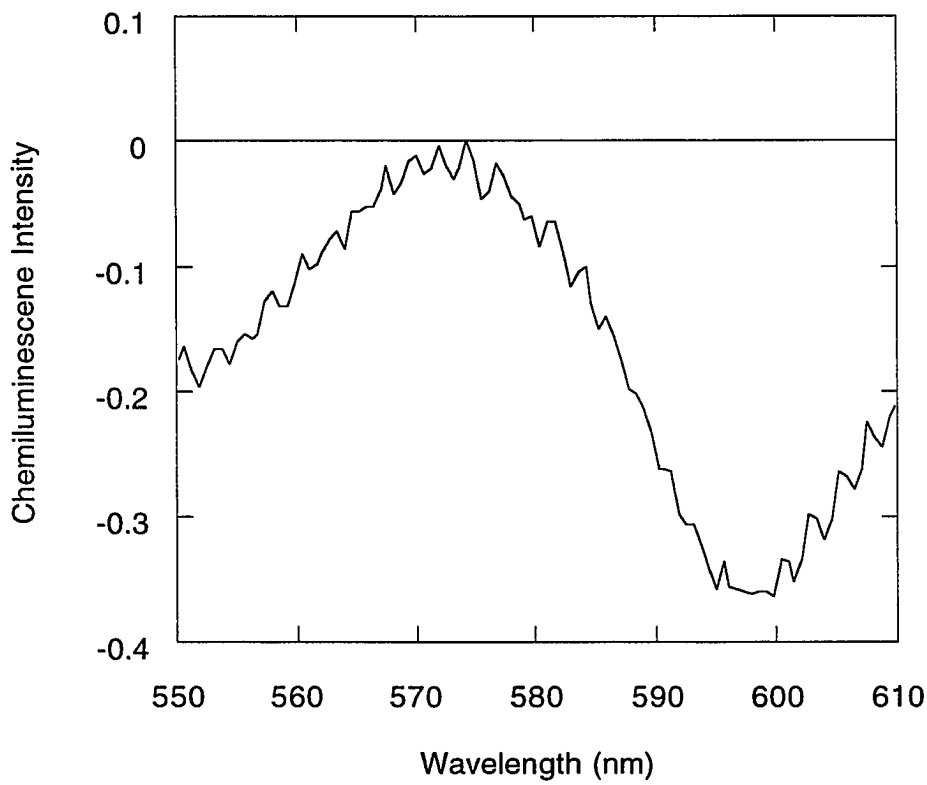

Figure 4. Attenuation of luciferin chemiluminescence by hypericin

stitute donor-acceptor pairs for energy transfer in photosynthesis [23]. Therefore, energy transfer between luciferin/luciferase and hypericin is possible even when the donor and the acceptor are not constrained to be at a fixed distance or orientation with respect to each other. These results immediately suggest the possibility of exciting hypericin by means of a chemiluminescent reaction to exploit its photoinduced virucidal activity without an external light source.

$$k_{ET} = k_F \left(\frac{R_o}{R}\right)^6 ; \text{ where } k_F = \frac{1}{\tau_F} \qquad 1.$$

To test the idea that the chemiluminescent reaction can induce virucidal activity in hypericin, cell-free EIAV was treated with varying concentrations of hypericin in a 1 ml solution containing luciferin and luciferase (Figure 5). Reactions were incubated 30 min at room temperature in the dark, and inoculated onto ED cells in the presence of 8 µg/ml polybrene. At high concentrations of hypericin, there is approximately a ten-fold reduction of viral infectivity under conditions where the sole source of excitation was the chemiluminescent luciferin/luciferase system. The chemiluminescent light-generating system was not, however, as effective in activating hypericin as illumination from a continuous source. A major difference in the light output from the chemiluminescent reaction and, for example, ambient fluorescent light is that the light intensity from the chemiluminescent reaction decreases with time. Figure 6 depicts the rapid decay in chemiluminescence following luciferase-catalyzed oxidation of luciferin. Further experiments were done to determine if increased antiviral activity could be achieved by an increase in the amount of light initially available for hypericin activation. A linear decrease in viral infectivity was observed when the concentration of luciferase was varied in the presence of a constant concentration of hypericin (Figure 7). This suggests that optimal activation of hypericin depends on the local concentration of energy donors.

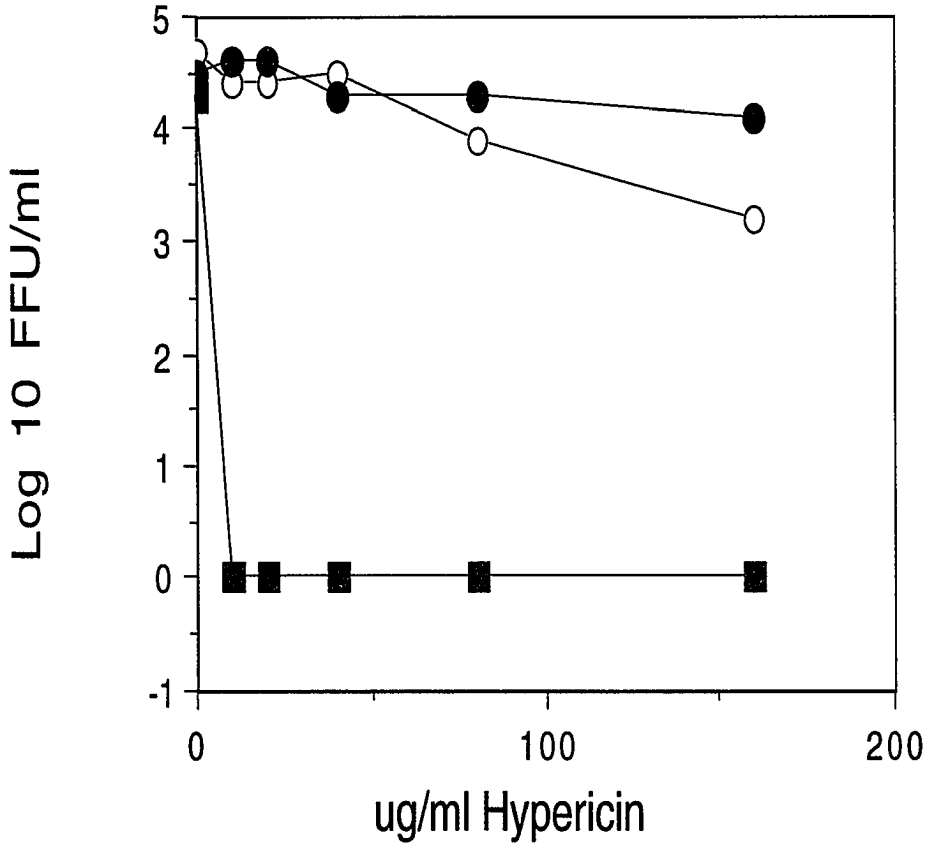

Figure 5. Effect of chemiluminescence on the antiviral activity of hypericin. EIAV was incubated in the dark at room temperature in the presence of 0.8 μM luciferase, 10 μM luciferin, 2 mM ATP, and increasing amounts of hypericin (O). Control samples include those containing virus and hypericin only (●), and parallel samples exposed to ambient room light (■). Infectious virus was titrated using a focal immunoassay, and the results are reported as focus-forming units/ml (FFU/ml) reaction.

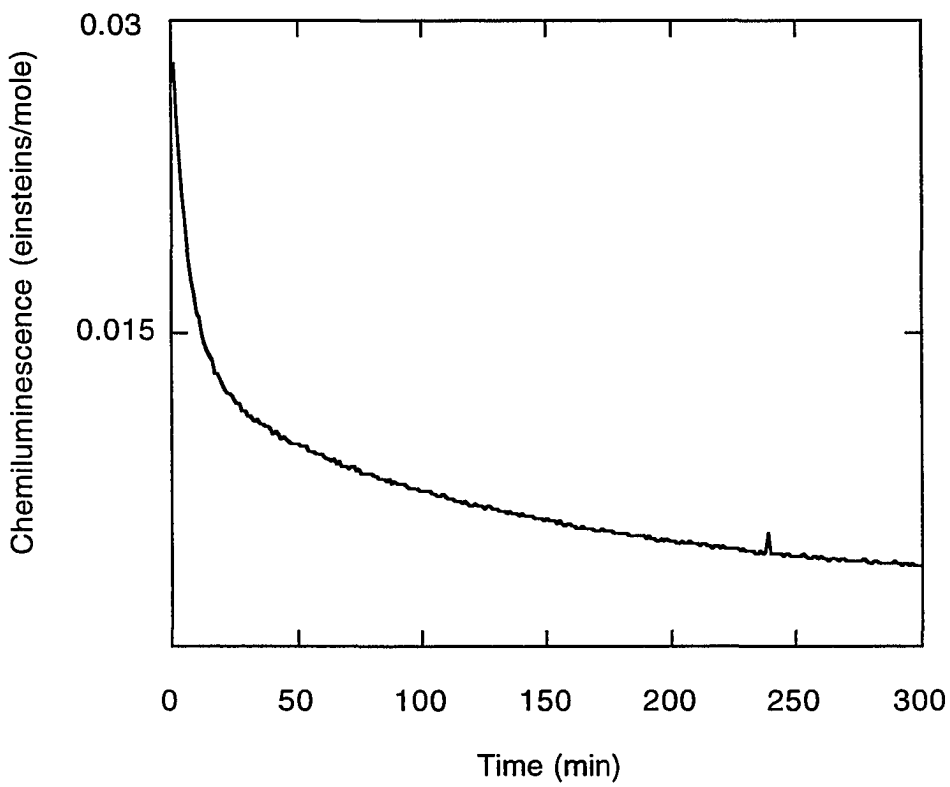

Figure 6. TIme course of the chemiluminescent reaction of luciferin and luciferase.

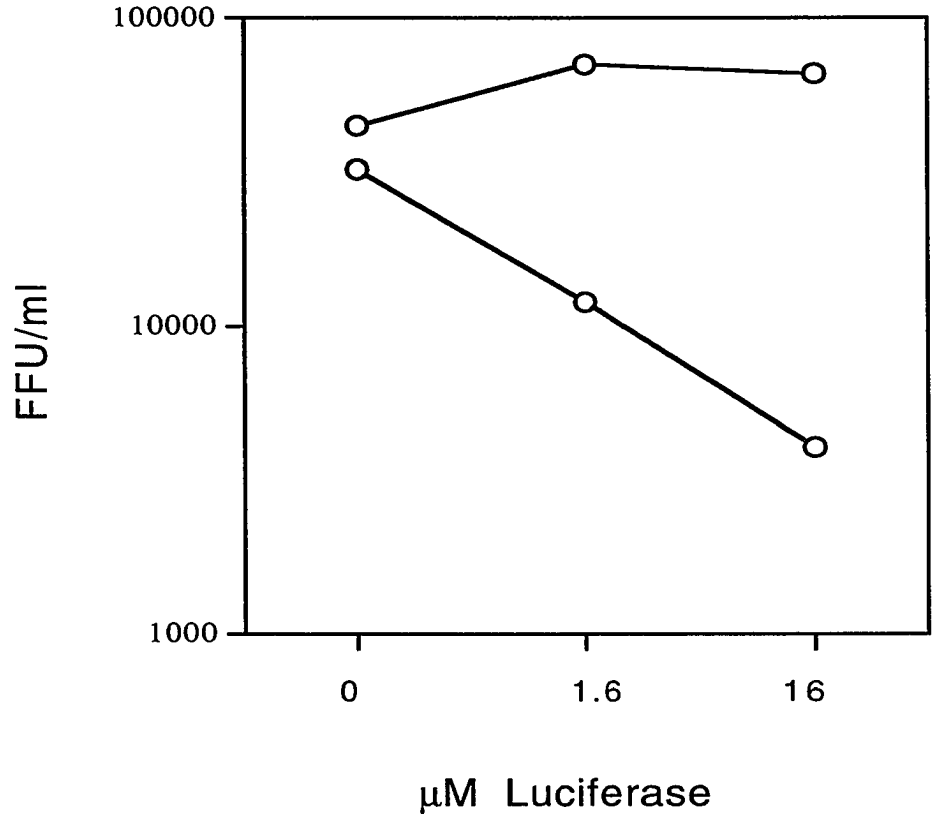

Figure 7. Effect of luciferase concentration on antiviral activity of hypericin after chemiluminescence. EIAV was incubated with 0(●) or 10 (O) μg of hypericin per ml in the presence of 5 mM luciferin, 2 mM ATP, and increasing amounts of luciferase. Reaction mixtures were incubated in the dark for 30 minutes at room temperature, and results are reported as FFU per ml of reaction mixture.

Discussion

Hypericin is a naturally occurring photosensitizer that displays potent antiviral activity against a variety of clinically important enveloped viruses, including HIV-1. One drawback to the use of hypericin and other photosensitizers as effective chemotherapeutic agents for treatment of viral infections *in vivo* is the requirement for light for optimal virucidal activity. A possible approach to circumvent this problem is the development of methods for chemiluminescent activation of hypericin *in vivo*. In the present report, we have demonstrated that the chemiluminescent reaction of luciferin and luciferase produces a sufficient amount of light to bleach the absorption spectrum of the virucidal agent, hypericin, even when there is no covalent attachment between these two reactants. Most importantly, the amount of light transferred to hypericin under these conditions is sufficient to produce significant antiviral activity. It is important here to stress that the mechanism of activation of hypericin is not the same in the two cases. Activation of hypericin by a light source, such as a projector bulb, involves the *emission* of a photon from the source and its subsequent *absorption* by hypericin. In the chemiluminescent reaction between luciferin and luciferase, an excited-state singlet, oxyluciferin, is produced [24]. Oxyluciferin is subsequently capable of being deactivated *nonradiatively* by Förster energy transfer to hypericin (Figure 3).

The chemiluminescent system is not as effective (Figure 5) in activating the antiviral activity of hypericin as is a continuous source of illumination. This is most likely a result of suboptimal distance and orientation between the donor and acceptor. Thus, the antiviral activity of hypericin increases proportionally with increasing concentrations of luciferase, providing further evidence that the limitation of the chemiluminescent reaction is the availability of localized concentrations of acceptable energy donors, which specifically interact with hypericin. Therefore, the proximity of the reactants may

be more crucial for the virucidal activity than the concentration of any one reactant. Any *in vivo* application of chemiluminescent activation of hypericin would require a delivery system that ensures a high local concentration of hypericin and luciferin/luciferase.

It is possible that in some cases the reduced antiviral activity of hypericin when using chemiluminescence as compared to an external light source may result from the consumption of oxygen by the luciferase/luciferin reaction (see the caption to Figure 2). In the presence of oxygen, hypericin produces singlet oxygen very efficiently (with a quantum yield of 0.73 [9]), and some studies have suggested that its antiviral activity is due to the production of singlet oxygen [4-6]. If so, localized depletion of oxygen by lucifern/luciferase may be expected to reduce the antiviral activity of hypericin. We [13,25,26] have, however, questioned the relative importance of singlet oxygen in the toxicity of hypericin towards HIV and related viruses. For example, hypericin is closely related [27], both structurally and spectrally, to the photoreceptor of the protozoan ciliates, *Stentor coerulus* and *Blepharisma japonicum* [27,28]. This photoreceptor confers upon the organism its biologically necessary photophobic and phototactic responses. Under conditions of ambient light the stentorin chromophore and hypericin are nontoxic to the organism. On the other hand, the singlet oxygen produced from these chromophores is toxic to *S. coerulus* under high light flux (~5000 W/m^2) [29]. It is an open question, therefore, whether the virucidal activity of hypericin following limited exposure to room light [3-6] is due to photosensitized generation of singlet oxygen by hypericin, or because of the presence of additional nonradiative decay processes of the excited states of hypericin. Recent studies in our laboratory indicate that oxygen is not required for antiviral activity of hypericin, although in some cases it may play a role [13]. An alternative origin for the photoinduced antiviral activity of hypericin may lie in its ability to produce a photogenerated pH drop, as is observed with the stentorin chro-

mophore [30-31]. We have identified rapid intramolecular proton transfer in hypericin [25,26], which is likely to precede the solvent acidification. Furthermore, several investigations have documented the importance of pH in the replication cycle of certain enveloped viruses by regulating uncoating [32-34].

The finding that the antiviral activity of hypericin can be activated by chemiluminescent reactions may have important implications for the development of novel methods for treatment of viral infections such as HIV-1. *In vivo* generation of luciferase could be accomplished using gene therapy approaches that employ luciferase as a susceptibility gene. Moreover, expression of the luciferase gene could be regulated if placed under the control of a promoter containing HIV-1 TAR sequences, limiting photoactivation of hypericin to virus-infected cells. This would result in a "molecular flashlight" in which light is turned on or off, depending on the presence of a transacting viral protein. Recent studies demonstrating the tumoricidal effects [35] of hypericin suggest that similar technology could be applied to gene therapy approaches for the treatment of cancer. This work is concerned with a theoretical approach to antiviral therapies; and more practical issues must await further experimentation. Further efforts to optimize the energy transfer between luciferin and hypericin are needed to improve the feasibility of the "molecular flashlight" as a viable anti-viral and anti-cancer therapy.

Acknowledgment

J.W.P. is an Office of Naval Research Young Investigator. M.J.F. is supported by an AASERT training grant from the Office of Naval Research. Portions of this work were funded by Carver grants awarded to both G.A.K. and S.L.C. and to J.W.P. We thank

Yvonne Wannemuehler for technical assistance.

References

1. Haynes, B. F. (1993) *Science* **260**, 1279-1286.
2. Johnston, M. I. & Hoth, D. F. (1993) *Science* **260**, 1286-1293.
3. Carpenter, S. & Kraus, G. A. (1991) *Photochem. Photobiol.* **53**, 169-174.
4. Meruelo, D., Lavie, G., & Lavie, D. (1988) *Proc. Natl. Acad. Sci. Usa* **85**, 5230-5234.
5. Degar, S., Prince, A. M., Pascual, D., Lavie, G., Levin, B., Mazur, Y., Lavie, D., Ehrlich, L. S., Carter, C., & Meruelo, D. (1992) *AIDS Res. Hum. Retroviruses* **8**, 1929-1936.
6. Lenard, J.; Rabson, A. & Vanderoef, R. (1993) *Proc. Natl. Acad. Sci. U.S.A.* **90**, 158-162.
7. Hudson, J. B.; Lopez-Bazzocchi, I. & Towers, G. H. N. (1991) *Antiviral Res.* **15**, 101-112.
8. Duran, N. & Song, P.-S. (1986) *Photochem. Photobiol.* **48**, 677.
9. Racinet, H., Jardon, P., & Gautron, R. (1988) *J. Chim. Phys.* **85**, 971-977.
10. Redepenning, J. & Tao, N. (1993) *Photochem. Photobiol.* **58**, 532-535.
11. Diwu, Z. & Lowen, J. W. (1993) *Free Radical Biology and Medicine* **14**, 209-215.
12. Weiner, L. & Mazur, Y. (1992) *J. Chem. Soc. Perkins Trans.* 1439-1442.
13. Fehr, M. J., Carpenter, S. L., & Petrich, J. W. (1994) *Bioorg. Med. Chem. Lett.* **4**, 1339-1344.
14. Hopkins, T. A., Seliger, H. H., White, E. H., & Cass, M. W. (1967) *J. Am. Chem. Soc.* **89**, 7148-7149.

15. McElroy, W. D. & DeLuca, M. (1981) in *Bioluminescence and Chemiluminescence*, eds. DeLuca, M. & McElroy, W. D. (Academic Press, New York), pp. 179-186.

16. McCapra, F. M. & Perring, K. D. (1985) in *Chemi- and Bioluminescence*, ed. Burr, J. G. (Marcell Dekker, New York), pp. 359-386.

17. White, E. H. Wörther, H., Seliger, H. H., & McElroy, W. D. (1966) *J. Am. Chem. Soc.* **88**, 2015-2019.

18. Seliger, H. H. & McElroy, W. D. (1960) *Arch. Biochem. Biophys.* **88**, 136-141.

19. Carpenter, S. L., Evans, L. H., Sevoian, M., & Chesebro, B. (1987) *J. Virol.* **61**, 3783-3789.

20. Kraus, G. A., Pratt, D., Tossberg, J., & Carpenter, S. L. (1990) *Biochem. Biophys. Res. Commun.* **172**, 149-153.

21. Förster, Th. (1965) in *Modern Quantum Chemistry Part III: Action of Light and Organic Crystals*, ed. Sinanoglu, O. (Academic Press, NY), p. 93.

22. Michel, J. & Bonacic-Kouteck, V. (1990) *Electronic Aspects of Organic Photochemistry* (Wiley, New York), pp. 81-86.

23. van Grondelle, R. & Amesz, J. (1986) in *Light Emission by Plants and Bacteria*, eds. Govindjee, Amesz, J., & Fork, D. C. (Academic Press, Orlando), pp. 191-223.

24. Koo, J.-A., Schmidt, S. P., & Schuster, G. B. (1978) *Proc. Natl. Acad. Sci. USA* **75**, 30-33.

25. Gai, F., Fehr, M. J., & Petrich, J. W. (1993) *J. Am. Chem. Soc.* **115**, 3384-3385.

26. Gai, F., Fehr, M. J., & Petrich, J. W. (1994) *J. Phys. Chem.* **98**, 5784-5795; Gai, F., Fehr, M. J., & Petrich, J. W. (1994) *J. Phys. Chem.* **98**, in press.

27. Tao, N., Orlando, M., Hyon, J.-S., Gross, M. & Song, P.-S. (1993) *J. Am. Chem. Soc.* **115**, 2526-2528.

28. Cubbedu, R., Ghetti, F., Lenci, F., Ramponi, R., & Taroni, P. (1990) *Photochem. Photobiol.* **52**, 567-573.

29. Yang, K.-C., Prusti, R. K., Walker, E. B., Song, P.-S., Watanabe, M., & Furuya, M. (1986) *Photochem. Photobiol.* **43**, 305-310.

30. Song, P.-S., Walker, E. B., Auerbach, R. A., & Robinson, G. W. (1981) *Biophys. J.* **35**, 551-555.

31. Walker, E. B., Lee, T. Y., & Song, P.-S. (1979) *Biochim. Biophys. Acta* **587**, 129-144.

32. Pinto, L. H., Holsinger, L. J., & Lamb, R. A. (1992) *Cell* **69**, 517-528.

33. Marsh, M. & Helenius, A. (1989) *Adv. Virus Res.* **36**, 107-151.

34. Zhirnov, O. P. (1990) *Virology* **176**, 274-279.

35. Thomas, C. & Pardini, R. S. (1992) *Photochem. Photobiol.* **55**, 831-837.

CHAPTER 7. LIGHT-INDUCED ACIDIFICATION BY THE ANTIVIRAL AGENT HYPERICIN

A paper published in the *Journal of the American Chemical Society*[1]

M. J. Fehr[2], M. A. McCloskey[2,3], and J. W. Petrich[2,3]

Abstract

The naturally occurring polycylcic quinone, hypericin, possesses light-induced antiviral activity against the human immunodeficiency virus (HIV) and other closely related enveloped lentiviruses such as equine infectious anemia virus (EIAV). We have previously argued that hypericin undergoes a fast proton transfer reaction in its singlet state (*J. Phys. Chem.* **1994**, *98*, 5784). We have also presented evidence that the light-induced antiviral activity of hypericin does not depend upon the formation of singlet oxygen (*Biorg. Med. Chem. Lett.* **1994**, *4*, 1339). It is demonstrated here that steady-state illumination of a solution containing hypericin effects a pH drop. When hypericin and an indicator dye, 3-hexadecanoyl-7-hydroxycoumarin, are both imbedded in vesicles, hypericin transfers a proton to the indicator within a time commensurate to its triplet lifetime. Proton transfer to the indicator is not observed when the indicator is proto-

---

[1] Reprinted with permission from the *Journal of the American Chemical Society* **1995**, *117*, 1833.

[2] Graduate student and Associate Professors, Department of Chemistry and Department of Zoology and Genetics, Iowa State University.

[3] To whom correspondence should be addressed.

nated or when the system is oxygenated. Since hypericin is known to form triplets and to generate singlet oxygen with high efficiency, this latter result is taken to confirm triplet hypericin as a source, but not necessarily the only source, of protons.

Introduction

Hypericin (Figure 1) possesses light-induced antiviral activity against the human immunodeficiency virus (HIV) [1] and other closely related enveloped lentiviruses such as equine infectious anemia virus (EIAV) [2]. Hypericin has a large triplet yield (0.70 in ethanol [3]) and is capable of generating significant quantities of singlet oxygen [3-6]. It has up till now been assumed that the virucidal activity of hypericin is a result of its production of singlet oxygen. We, however, have recently reported that oxygen *is not required* for antiviral activity [7]. On the other hand, solutions of the chromophore of the photoreceptor of the protozoan ciliate *S. coerulus*, which is very similar both structurally and spectrally to hypericin, produce a pH decrease upon optical excitation [8]. We have argued that hypericin undergoes excited-state proton transfer in its singlet state [9-11] and that, consequently, it possesses labile protons. We have suggested that the virucidal activity of hypericin may be related to its ability to acidify its environment upon optical excitation [7,9-12]; and we have proposed chemical methods of illuminating hypericin for antiviral therapies [12]. Given the potentially great importance of photogenerated protons from hypericin as an antiviral or antitumor therapy, the present work was performed in order to determine the nature (singlet or triplet) of source of the photogenerated proton. These studies were undertaken largely in phospholipid vesicles suspended in aqueous medium in order both to circumvent the insolubility of hypericin in water as well as to provide a simplified model of the viral mem-

brane, within which hypericin is thought to partition.

Experimental

In order to observe and measure the deprotonation of hypericin, with for example a pH indicator dye, it is necessary that the proton donor and the acceptor are in close enough proximity so that the proton transfer event can be efficiently observed. Since hypericin is insoluble in water from pH 2 to 11, a system that takes all of these factors into account is provided by optically clear phosphatidylcholine vesicles, such as dipalmitoylphosphatidlycholine (DPPC), suspended in aqueous buffer. Hypericin is soluble in the vesicle bilayer; and although hypericin is hydrophobic, a portion of the hypericin population may be reasonably assumed to orient so that the ejected protons are available to the bulk solvent. The vesicles have been prepared by the method described by Huang [13] and are expected to have an outer diameter of ~250-300 Å and an inner diameter of ~120 Å. Huang [13] reports a maximum bilayer dimension of 73 Å, of which ~30 Å corresponds to the hydrocarbon region where hypericin is assumed to be located. The x-ray structure of hypericin indicates that it has a long axis of 10.5 Å and a short axis of 9.6 Å [14]. Consequently, single hypericin molecules are not capable of spanning the bilayer.

The pH indicator dyes used here are either incorporated in the aqueous interior of the vesicle or in the hydrocarbon portion of the lipid bilayer. Two indicators were used to probe the deprotonation of hypericin. BCECF (2'-7'-bis(2-carboxyethyl)-5-(and 6)-carboxyfluoroscein), was obtained from Molecular Probes and used exclusively in the steady-state experiments. The second indicator, used for the time-resolved absorption experiments, was the lipophilic pH indicator 3-hexadecanoyl-7-hydroxycoumarin (Mo-

lecular Probes). All procedures discussed below were carried out under subdued lighting. All solutions were stored in the dark and were usually purged with argon.

Vesicles were prepared according to the procedure of Huang [13]. The specific indicator used in the preparation depended on whether the vesicles were destined for steady-state fluorescence or transient aborption measurements. DPPC (Sigma) was dissolved in 95% ethanol to a final concentration of 2 mM.

For steady-state fluorescence measurements, 5 mL of the DPPC solution and a hypericin/ethanol solution (1 mg/mL) were mixed and then evaporated to dryness on a rotovap. 1 mL of a 0.12 M NaCl/0.03M NaN_3 solution in which 1 mg of BCECF was dissolved were added to the dry product, and the solution was heated to 10 degrees above the DPPC transition temperature (54-56 °C) until all of the DPPC/hypericin/indicator mixture was suspended. NaN_3 was introduced to scavenge oxygen and thus to obviate singlet oxygen production. Vesicles were formed by sonicating the resulting suspension until optically clear using either a Cole Palmer Model 8890 bath sonicator for approximately 1.5 hours or a Fisher Sonic Dismembrator Model 300 fitted with a microtip for 40 minutes. BCECF that was not entrapped inside the vesicle was removed by passing the vesicle system over a size exclusion column (Sepharose 4B).

For time-resolved measurements, 5 mL of the DPPC solution, a hypericin/ethanol solution (1 mg/mL), and a 3-hexadecanoyl-7-hydroxycoumarin/ethanol solution (1 mg/mL) were mixed and then evaporated to dryness on a rotovap. 2 ml of a 0.12 M NaCl/0.03M NaN_3 solution were added to the dry product and the solution was heated to 10 degrees above the DPPC transition temperature until all the DPPC/hypericin/indicator mixture was suspended. Vesicles were prepared as described above. Since, however, all of the indicator is assumed to be partitioned into the bilayer, the system was not passed over a size exclusion column.

Steady-state fluorescence excitation spectra were obtained on a SPEX Fluoromax. For steady-state pH experiments, hypericin was excited by a 300-W tungsten bulb fitted with 575-nm cut-off filters. Background light with the bulb on was less than 0.3 % of the signal. Light available at the cuvette was 8-9 mW. Time-resolved absorption data were obtained with the microsecond flash photolysis system [15] generously made available to us by Professor J. H. Espenson. Kinetic traces were the average of 4 shots. The excitation pulse had a duration of ~600 ns and an energy of ~70 mJ at 490 nm. Steady-state absorption spectra were recorded on a Shimadzu UV-2101PC.

Results and Discussion

A. Hypericin Produces a Light-Induced pH Drop. Steady-State Measurements

Figure 1 presents the steady-state absorption and fluorescence spectra of hypericin in DPPC vesicles in water at pH 8.4. Hypericin is insoluble in pure water from pH 2 to 11, where it forms aggregates [16]. The steady-state spectra resemble those of hypericin in DMSO, which indicates that aggregation is not occurring. In DPPC vesicles, the absorption maximum of hypericin is 598 nm and the fluorescence emission maximum is 599 nm. The spectra at pH 5.9 and pH 8.4 are essentially identical.

Figure 2 demonstrates the ability of hypericin to acidify a solution of the indicator dye BCECF and hence its capacity to produce a light-induced pH drop much like the structurally and spectrally analogous stentorin chromophore [8,17]. BCECF possesses 4 to 5 negative charges at pH values between 6.5 and 7.5, which are responsible for its retention in the aqueous interior of the vesicle. BCECF possesses pH-dependent emis-

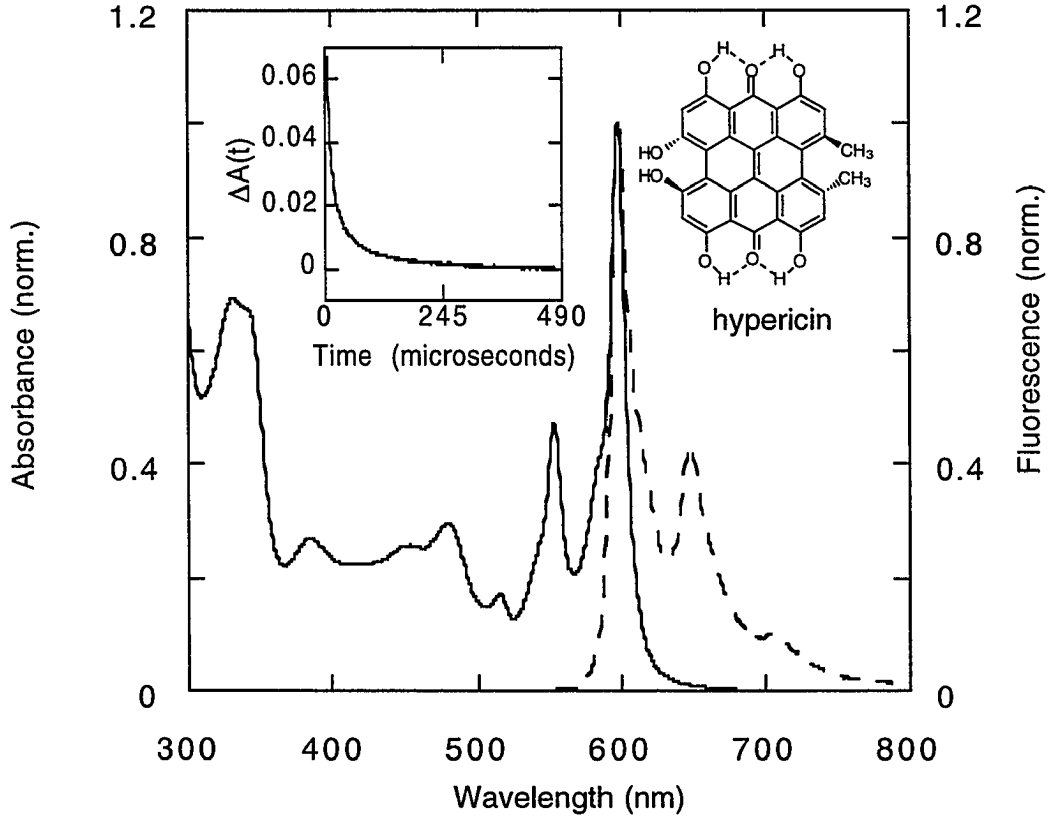

Figure 1.

Steady state absorption (————) and fluorescence (- - - -) spectra of hypericin dissolved in the lipid bilayer of DPPC vesicles suspended in water at pH 8.4. For the absorption spectrum, the hypericin concentration is 23 μM. Based upon the similarity of the absorption spectrum with that in DMSO, the extinction coeffients used are those using DMSO as the solvent. Inset: transient absorption due to triplet hypericin dissolved in the lipid bilayer of DPPC vesicles, $\lambda_{ex} = 490$ nm, $\lambda_{probe} = 505$ nm. $\Delta A(t) = 0.041 \exp(-t/10\ \mu s) + 0.018 \exp(-t/75\ \mu s)$. The hypericin concentration is 24 μM. DPPC vesicles were suspended in water at pH = 8.2. Malkin and Mazur [18] measured the triplet lifetime of hypericin in pure ethanol to be single exponential with a duration of 43 μs.

sion and absorption spectra. Light-induced pH changes were monitored by collecting fluorescence excitation spectra of BCECF at an emission wavelength of 535 nm. The presence of the isosbestic point at 439 nm (which corresponds to an isoemissive point, assuming the exact equivalence of the absorption and fluorescence excitation spectra) facilitates accounting for dye degradation and for dye leakage from the vesicles.

Of the three separate sample preparations, at different initial pH values, a maximum pH change of 0.5 units is observed. It is important to note that this pH change neither reflects the total number of protons ejected by hypericin nor the macroscopic pH of the solution. Rather, it is a measure of the number of protons detected by the indicator. Here, it is useful to consider the following. In a single small unilamellar vesicle (SUV) there is a 50 fold excess of hypericin to BCECF. Not all of the hypericin, however, is necessarily located in a region where dissociated protons can enter the vesicle interior. Because the ratio of phosphatidylcholine between the inner and the outer vesicle bilayer is roughly 1:1.5, hypericin may partition into the outer portion of the vesicle bilayer, away from the interior. It is also likely that one or both of the following occurs: either the majority of the dissociated protons recombine with the parent hypericin anion within the bilayer and never protonate the indicator; or the dissociated protons escape from the parent anion but remain undetected because they are released to the bulk solvent where no indicator is present.

B. A Source of the Photogenerated Proton. Time-Resolved Measurements

In order to determine from which excited electronic state the proton originates, time-resolved measurements were required. The lipophilic indicator, 3-hexadecanoyl-7-hydroxycoumarin, was most suitable for time-resolved absorption measurements (given

the available experimental apparatus) because the extinction coefficient of its unprotonated form in the region from 400-430 nm is larger than that of hypericin and because its extinction coefficient at the laser excitation wavelength (490 nm) is very small (Figure 3).

The decay of the absorbance due to the hypericin triplet in vesicles at 505 nm is presented in the inset to Figure 1. This decay is biphasic with time constants of 10 and 75 μs. It is reasonable to attribute the biphasic decay to various orientations of hypericin in the vesicle bilayer. (The variation in the lifetimes is to be expected given the distribution of vesicles in a given preparation.)

Figure 4a presents the transient at 400 nm of the 3-hexadecanoyl-7-hydroxycoumarin indicator subsequent to excitation of hypericin at 490 nm. The transient is a bleach whose recovery is represented by two time constants: 32 and 170 μs. This signal is interpreted as *proton transfer from hypericin to the indicator on a time scale commensurate to that of the lifetime of triplet hypericin.* It is reasonable for the proton transfer event to be so rapid. (Diffusion of the proton is not expected to be rate limiting (assuming the diffusion constant of the proton to be that in water (9.3×10^{-5} cm^2/s [19])). Protonation of the anionic form of the indicator decreases its population and consequently reduces its absorbance at 400 nm. *The persistant bleach of the indicator at long times can be attributed to the slow reestablishment of equilibrium between the acidic and basic forms of the indicator,* as is observed in other systems [19].

Although hypericin has a ground-state aborption at 400 nm (Figure 1), this signal cannot be attributed to the ground-state of hypericin for the following reasons:

1. At 400 nm the extinction coefficients of the indicator and hypericin are 35,900 and 10,100 $M^{-1}cm^{-1}$, respectively; and the molar ratio of indicator to hypericin is approximately one to one.

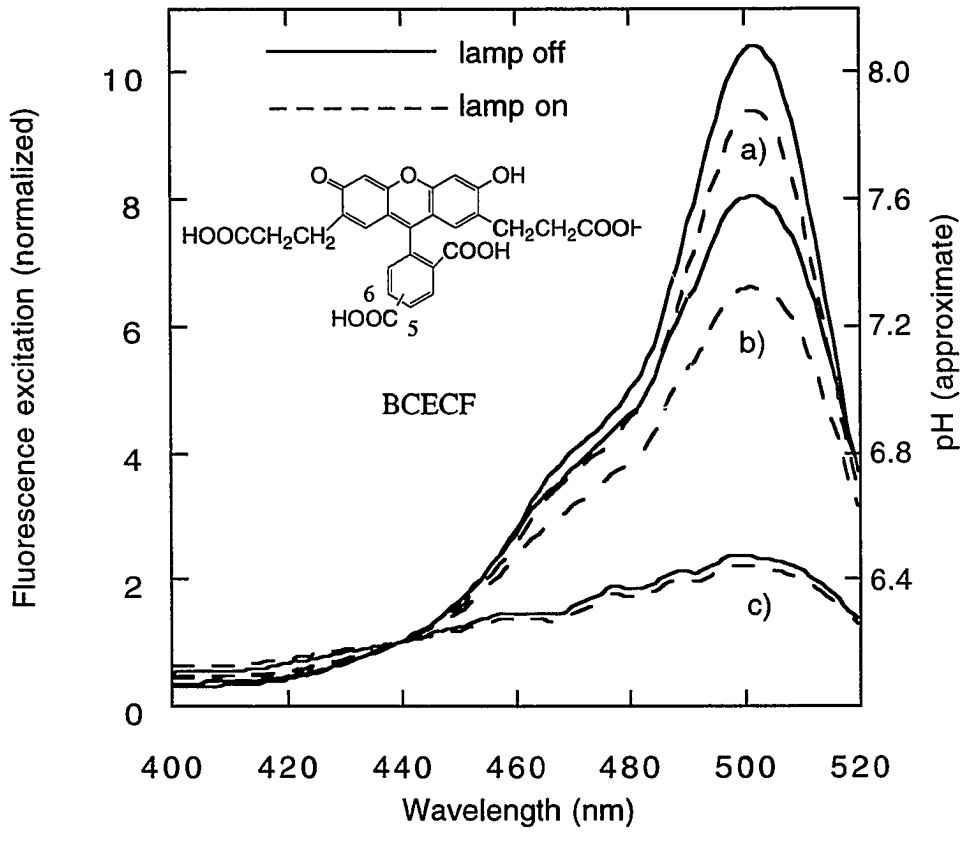

Figure 2.

Fluorescence excitation spectra of BCECF (0.52 μM) entrapped in DPPC vesicles. Hypericin is dissolved in the lipid bilayer at a concentration of 23 μM. Solid lines (————) denote the indicator spectrum in the absence of hypericin illumination; dashed lines (- - -), in the presence of hypericin illumination. See experimental section. Three sets of experiments are depicted in the Figure: (a) initial pH = 8.1; (b) initial pH = 7.6; (c) inital pH = 6.45.

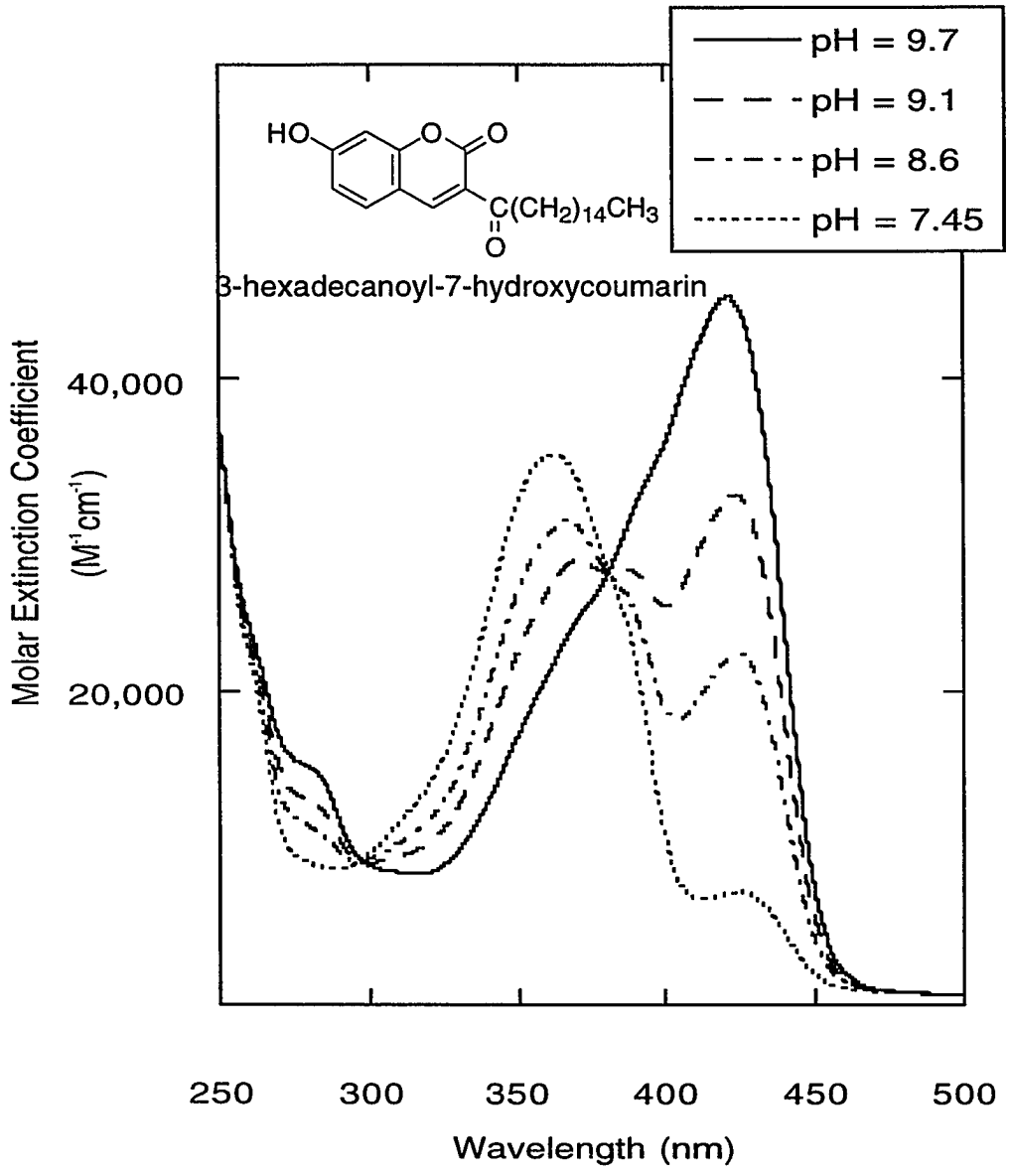

Figure 3.

Absorption spectra, as a function of pH, of 3-hexadecanoyl-7-hydroxycoumarin at the lipid/water interface of DPPC vesicles. Isosbestic points are at 381 nm and 291 nm. The broad triplet absorption spectrum of hypericin and the wavelength of the laser pulse (λ_{ex} = 490 nm) dictated the choice of this dye, which absorbs principally to the blue of 450 nm. The protonated form of the indicator has an absorption maximum at 365 nm; the anionic or deprotonated form, at 425 nm.

2. The time constants for the bleaching recovery in the presence of the indicator are longer than for those observed for hypericin alone in vesicles.

3. Most importantly, at long times *the transient at 400 nm for hypericin alone in vesicles yields a net absorption whereas in the presence of indicator on the same time scale the bleaching has not yet recovered.*

Furthermore, the signal cannot arise from the indicator itself since *3-hexadecanoyl-7-hydroxycoumarin exhibits no transient absorption at 400 nm* (Figure 4a).

Another confirmation of the trace in Figure 4a to a transfer of a proton from hypericin to the indicator is based on the reasoning that if the long component of the kinetic trace representing a persistent bleach is due to the the protonation of the indicator by hypericin, performing the experiment at a pH where the indicator is already completely protonated ought to replace this perisistent bleach with a net absorption at long times that is characteristic of the control experiment using hypericin alone. This result is in fact observed (Figure 4b).

Finally, a goal of this work is to determine if the proton is ejected from the triplet or singlet state. The triplet yield of hypericin in ethanol and in BRIJ 35 micelles is ~0.70 [3-5]. Molecular oxygen efficiently quenches triplet hypericin to form singlet oxygen [3-6]. Consequently, at sufficiently high oxygen levels, the concentration of triplet hypericin should be negligible. Figure 4c demonstrates that when the system of hypericin and the indicator is oxygenated, no bleaching of the indicator is observed. This result, therefore, suggests the absence of proton transfer to the indicator.

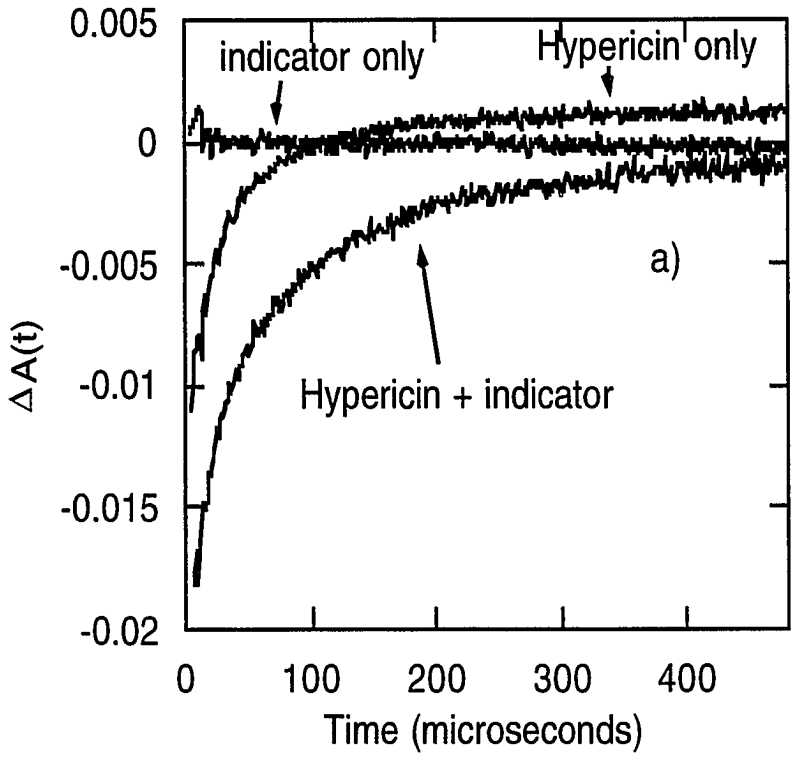

Figure 4.

(a) Transient absorption at 400 nm of 3-hexadecanoyl-7-hydroxycoumarin *subsequent to excitation of hypericin at* λ_{ex} = *490 nm.* Both the indicator (23.3 μM) and hypericin (21.0 μM) are contained in the bilayer of DPPC vesicles at pH 8.4.

The decrease in the anionic form of the indicator owing to excited-state protonation by hypericin monitored by a transient reduction of the induced bleach of the anionic form of the indicator at 400 nm. $\Delta A(t) = -0.012 \exp(-t/32\ \mu s) - 0.0050 \exp(-t/170\ \mu s)$.

The control experiment for hypericin alone in vesicles at pH 8.3 yields a trace that is fit to the form: $\Delta A(t) = -0.0062 \exp(-t/15\ \mu s) - 0.0067 \exp(-t/55\ \mu s) + 0.0080$.

A second control experiment using only the *indicator alone* in vesicles at pH 8.3 yields the trace about zero. This trace demonstrates that in the absence of hypericin no transient absorption is induced in the indicator at 400 nm subsequent to excitation at 490 nm.

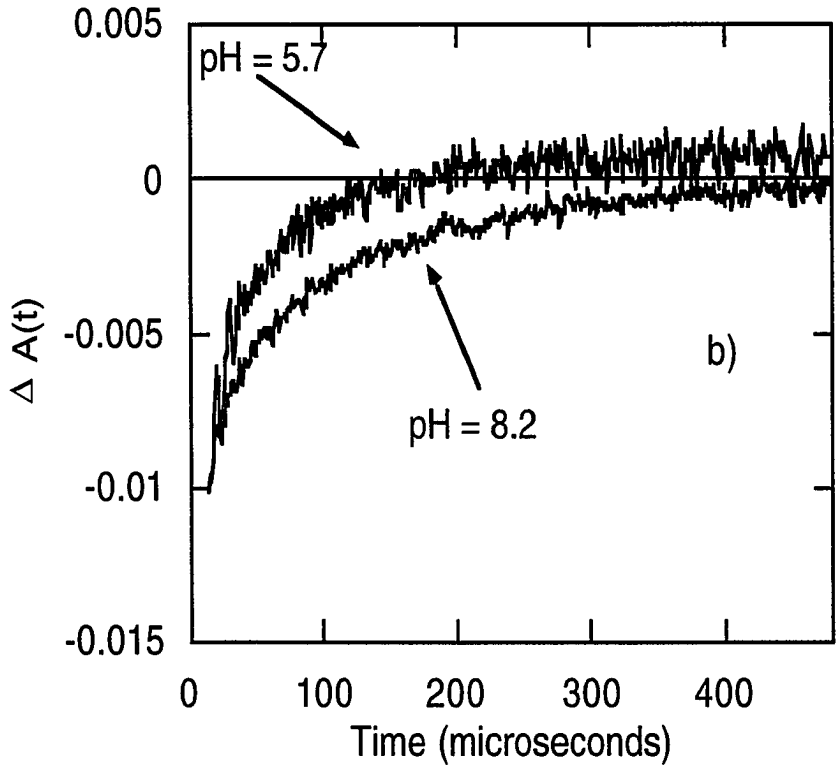

Figure 4 (cont.)

(b) Induced bleaching and its recovery at 400 nm for 3-hexadecanoyl-7-hydroxycoumarin and hypericin in DPPC vesicles at acidic and basic pH; λ_{ex} = 490 nm.

At pH 5.7, $\Delta A(t) = -0.0030 \exp(-t/9.4\ \mu s) - 0.0099 \exp(-t/56\ \mu s) + 0.00080$.

At pH 8.2, $\Delta A(t) = -0.0045 \exp(-t/26\ \mu s) - 0.0065 \exp(-t/130\ \mu s)$.

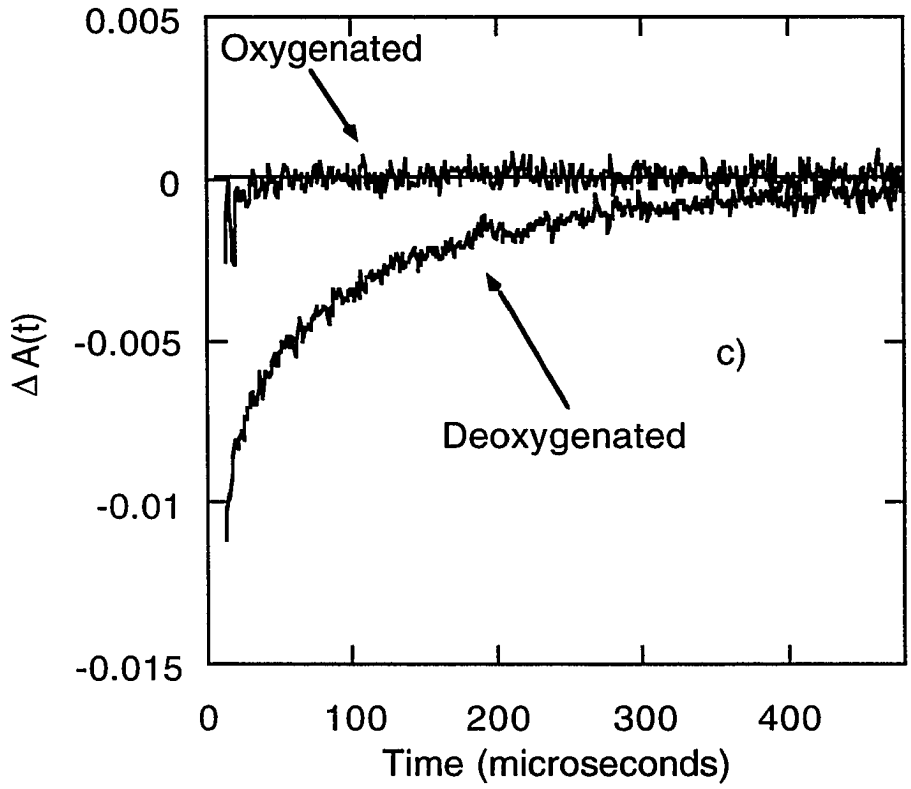

Figure 4 (cont.)

(c) Induced bleaching and its recovery at 400 nm for 3-hexadecanoyl-7-hydroxycoumarin and hypericin in DPPC vesicles in oxygenated and deoxygenated solution; λ_{ex} = 490 nm. The absence of a signal in the oxygenated sample is taken as proof that the triplet state of hypericin is responsible for the protonation event. (Under oxygen levels at which the signal is quenched, hypericin is still fluorescent and the indicator absorption spectrum remains unchanged. Consequently the absence of the signal cannot be a result of quenching the singlet state or of destruction of the indicator.) The transient signal for the deoxygenated sample is described well by $\Delta A(t) = -.0045 \exp(-t/26\ \mu s) - 0.0065 \exp(-t/130\ \mu s)$.

Conclusions

Our previous picosecond experiments provide strong evidence for intramolecular proton transfer in the excited singlet state of hypericin and suggest that hypericin is a source of light-induced protons [9-11]. That hypericin does indeed produce a light induced pH drop is demonstrated by steady-state experiments (Figure 2). Flash photolysis experiments on the microsecond time scale using molecular oxygen as a triplet quencher indicate that the triplet state of hypericin is a proton donor (Figure 4). No conclusions concerning the role of the first excited singlet state of hypericin as a proton donor can be drawn since the time-resolved measurements discussed above cannot detect rapid protonation and deprotonation equilibria between the donor and the acceptor. It is likely that much will be learned by studying the detailed interactions of hypericin with the viral membrane, which have been crudely mimicked here by vesicles.

Acknowledgement

We thank Professor J. H. Espenson and Dr. A. Bakac for the use of their microsecond flash photolysis system and Professor W. Jenks for access to his absorption spectrometer. M. J. F. is the recipient of a GAANN fellowship. J. W. P. is an Office of Naval Research Young Investigator.

References

1. Meruelo, D.; Lavie, G.; Lavie, D. *Proc. Natl. Acad. Sci. USA* 1988, **85**, 5230.
Lavie, G.; Valentine, F.; Levin, B.; Mazur, Y.; Gallo, G.; Lavie, D.; Weiner, D.;

Meruelo, D. *Proc. Natl. Acad. Sci. USA* 1989, **86**, 5963; Degar, S.; Prince, A. M.; Pascual, D.; Lavie, G.; Levin, B.; Mazur, Y.; Lavie, D.; Ehrlich, L. S.; Carter, C.; Meruelo, D. *AIDS Res. Hum. Retroviruses* 1992, **8**, 1929. Lenard, J.; Rabson, A.; Vanderoef, R. *Proc. Natl. Acad. Sci. USA* 1993, **90**, 158.

2. Carpenter, S.; Kraus, G. A. *Photochem. Photobiol.* 1991, **53**, 169.
3. Jardon, P.; Lazorchak, N.; Gautron, R. *J. Chim. Phys.* 1986, **83**, 311.
4. Racinet, H.; Jardon, P.; Gautron, R. *J. Chim. Phys.* 1988, **85**, 971.
5. Bourig, H.; Eloy, D.; Jardon, P. *J. Chim. Phys.* 1992, **89**, 1391.
6. Durán, N.; Song, P.-S. *Photochem. Photobiol.* 1986, **43**, 677.
7. Fehr, M. J.; Carpenter, S. L.; Petrich, J. W. *Bioorg. Med. Chem. Lett.* 1994, **4**, 1339.
8. Song, P.-S.; Walker, E. B.; Auerbach, R. A.; Robinson, G. W. *Biophys. J.* 1981, **35**, 551. Walker, E. B.; Lee, T. Y.; Song, P.-S. *Biochim. Biophys. Acta* 1979, **587**, 129-144.
9. Gai, F.; Fehr, M. J.; Petrich, J. W. *J. Am. Chem. Soc.* 1993, **115**, 3384.
10. Gai, F.; Fehr, M. J.; Petrich, J. W. *J. Phys. Chem.* 1994, **98**, 5784.
11. Gai, F.; Fehr, M. J.; Petrich, J. W. *J. Phys. Chem.* 1994, **98**, 8352.
12. Carpenter, S. L.; Fehr, M. J.; Kraus, G. A.; Petrich, J. W. *Proc. Natl. Acad. Sci. (USA).* In press.
13. Huang, C. *Biochemistry* 1969, **8**, 344.
14. Etzlstorfer, C.; Falk, H.; Müller, N.; Schmitzberger, W.; Wagner, U. G. *Montash. Chem.* **1993**, *124*, 731. Falk, H. Personal communication. Freeman, D.; Frolow, F.; Kapinus, E.; Lavie, D.; Lavie, G.; Meruelo, D.; Mazur, Y. *J. Chem. Soc. Chem. Commun.* **1994**, 891.
15. Connolly, P.; Espenson, J. H.; Bakac, A. *Inorg. Chem.* 1986, **25**, 2169.

16. Yamazaki, T.; Ohta, N.; Yamazaki, I.; Song, P.-S. *J. Phys. Chem.* 1993, **97**, 7870. Sevenants, M. R. *J. Protozool.* **1965**, *12*, 240.

17. Tao, N.; Orlando, M.; Hyon, J.-S.; Gross, M.; Song, P.-S. *J. Am. Chem. Soc.* 1993, **115**, 2526; Song, P.-S.; Kim, I.-K.; Florell, S.; Tamai, N.; Yamazaki, T.; Yamazaki, I. *Biochim. Biophys. Acta* 1990, **1040**, 58; Song, P.-S. *Biochim. Biophys. Acta* 1981, **639**, 1.

18. Malkin, J.; Mazur, Y. *Photochem. Photobiol.* **1993**, *57*, 929.

19. Gutman, M. in *Methods of Biochemical Analysis, Vol. 30*, ed. Glick, D. (Wiley, New York, 1984), p. 1.

CHAPTER 8. THE ROLES OF OXYGEN AND PHOTOINDUCED ACIDIFICATION IN THE LIGHT-DEPENDENT ANTIVIRAL ACTIVITY OF HYPOCRELLIN A

A paper submitted for publication in *Biochemistry*[1]

M. J. Fehr[2], S. L. Carpenter[2,3], and J. W. Petrich[2,3]

Abstract

Hypocrellin A displays photoinduced antiviral activity, in particular against the human immunodeficiency virus (HIV), as does its counterpart, hypericin. Unlike hypericin, however, hypocrellin A absolutely requires oxygen for its antiviral activity. Also, whereas we have previously demonstrated that hypericin functions as a light-induced proton source, we do not observe that hypocrellin A acidifies its surrounding medium in the presence of light. These results are discussed in the context of the ground- and excited-state photophysics of hypericin and its mechanisms of photoactivated virucidal activity.

---

[2] Graduate student and Associate Professors, Department of Chemistry and Department of Microbiology, Immunology, and Preventive Medicine, Iowa State University.

[3] To whom correspondence should be addressed.

Introduction

Hypocrellin A (Figure 1) is a naturally occurring perylene quinone found in a parasitic fungus that is common in parts of the People's Republic of China and Sri Lanka (Diwu & Lown, 1990; Diwu et al., 1989). Hypocrellin has been used as a phototherapeutic agent for various skin diseases and tumors and has been taken orally as a folk medicine for several centuries in China (Diwu & Lown, 1990; Diwu et al., 1989). Like the related polycyclic quinone, hypericin (Meruelo et. al.,1988; Degar et al., 1992; Lenard et al., 1993; Meruelo et. al., 1992; Carpenter & Kraus, 1991), hypocrellin A posseses light-induced toxicity against the human immunodeficiency virus, HIV, and related viruses (Hudson et al., 1994). This common property of hypocrellin A and hypericin has led us to examine in more detail the similarities and differences between these chromophores.

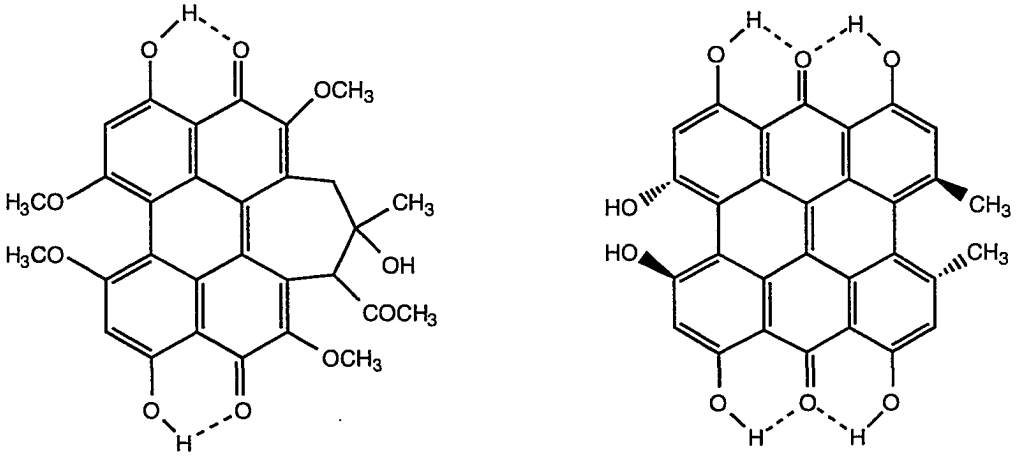

Figure 1. Structures of (a) hypocrellin A and (b) hypericin.

Hypericin has a large triplet yield (0.70 in ethanol (Jardon et al., 1986)) and is capable of generating significant quantities of singlet oxygen (Meruelo et. al.,1988; Degar et al., 1992; Lenard et al., 1993; Meruelo et. al., 1992). The virucidal activity of hypericin results, in part, from production of singlet oxygen. We, however, have recently reported that oxygen *is not required* for antiviral activity (Fehr et al., 1994). We have argued that hypericin undergoes excited-state proton transfer in its singlet state (Gai et al., 1993, 1994a, 1994b) and that, consequently, it possesses labile protons. We have hypothesized that the virucidal activity of hypericin may be related to its ability to acidify its environment upon optical excitation (Fehr et al., 1994; Gai et al., 1993, 1994a, 1994b); and we have proposed chemical methods of illuminating hypericin for antiviral therapies (Carpenter et al.,1994). We have, furthermore, demonstrated that illumination of a solution containing hypericin effects a pH drop. When hypericin and an indicator dye are kept in relatively close proximity by the use of vesicles, hypericin transfers a proton to the indicator within its triplet lifetime (Fehr et al., 1995). Proton transfer to the indicator is not observed when the indicator is protonated or when the system is oxygenated. Since hypericin is known to form triplets and to generate singlet oxygen with high efficiency, this latter result is taken to confirm triplet hypericin as a source, but not necessarily the only source, of protons.

Hypocrellin A has a quantum yield for singlet oxygen of 0.83 in benzene (Diwu & Lown, 1992). It also possesses structural features that are very similar to those of hypericin: in particular, the hydroxyl groups β to the carbonyl groups. Given this latter feature coupled with our understanding of the photophysical properties of hypericin, as summarized above, we would expect hypocrellin A to exhibit other similarities in its light-induced antiviral activity. In particular, we would expect that, like hypericin, hypocrellin does not require oxygen for its virucidal activity and that it is also capable of

intermolecular proton transfer. That we observe neither of these phenomena in hypocrellin suggests an important role for the aromatic skeleton of hypericin and will have implication for the design of other light-induced antiviral agents.

Materials and Methods

Titration of infectious virus: As in our previous work, antiviral assays employ EIAV (equine infectious anemia virus). EIAV is exceptionally well-suited to assay for activity against HIV since it is an enveloped lentivirus structurally, genetically, and antigenically related to HIV (Chiu et al., 1985; Casey et al., 1985; Gonda et al., 1986). All experimental manipulations were performed in subdued light. Cell-free stocks of the MA-1 isolate of equine infectious anemia virus (EIAV) (Carpenter & Kraus, 1991) were diluted 1:10 in phosphate buffered saline (PBS) containing no or 10% fetal bovine serum. Hypericin (Carl Roth GmbH & Co.) or hypocrellin A (Molecular Probes) were added to a final concentration of 10 μg/ml. Deoxygenation and illumination of samples is described below. A focal immunoassay similar to that previously described was used for quantifying infectious virus. Results are given for three independant experiments, and are expressed as focus forming units (FFU) per ml sample.

Oxygen assays: Samples were deoxygenated by bubbling Ar in light-tight containers and exposed to light for 15 minutes from a 300-W projector bulb fitted with a cut-off filter blocking wavelengths shorter than 575 nm. The irradiance at the sample was estimated to be 170 W/m^2 in the spectral range in which hypericin absorbs, 575-600 nm. Hypocrellin/EIAV samples were exposed to identical conditions. Deoxygenation efficiency was evaluated as described previously (Fehr et al., 1994). A dissolved oxygen test kit (Hach, OX-2P) showed dissolved oxygen levels after one hour of deoxygen-

ating to have fallen from an initial concentration of 5 mg/L (1.56×10^{-4} M) to below the detection limit of 0.2 mg/L (6.25×10^{-6} M). An alternate method of testing for dissolved oxygen is via the bioluminescence of the firefly luciferase/luciferin reaction. Oxygen is necessary in this system for the production of light (McElroy & Deluca, 1985). Light output was measured with a liquid-nitrogen cooled charge-coupled device (CCD) (Princeton Instruments LN/CCD-1152UV) mounted on an HR320 (Instruments SA, Inc.) monochromator with a grating (1200g/mm) blazed at 5000 Å. A solution of 1.0×10^{-5} M luciferin and 1.6×10^{-8} M luciferase and a solution of 1.0×10^{-4} M ATP were simultaneously deoxygenated in the same apparatus as the EIAV/hypericin and EIAV/hypocrellin experiments. The reaction was initiated by injecting 0.5 ml of the deoxygenated ATP solution into the luciferin/luciferase solution. Three successive 30-second integrations yielded spectra that were superimposable on the background spectra of the CCD. Light could be generated from the reaction system by opening it to the atmosphere. Lack of light generation was taken to indicate that oxygen levels were negligible.

Light-induced acidification: Attempts to observe a light-induced acidification in both steady-state and time-resolved measurements were performed as described previously (Fehr et al., 1995). Vesicles were prepared according to the procedure of Huang (Huang, 1969). The specific indicator used in the preparation depended on whether the vesicles were destined for steady-state fluorescence or transient aborption measurements. DPPC (Sigma) was dissolved in 95% ethanol to a final concentration of 2 mM.

For steady-state fluorescence measurements, 5 mL of the DPPC solution and a hypocrellin/ethanol solution (1 mg/mL) were mixed and then evaporated to dryness on a rotovap. 1 mL of a 0.12 M NaCl/0.03M NaN_3 solution in which 1 mg of 2',7'-bis(2-carboxyethyl)-5-(and 6)-carboxyfluoroscein (BCECF) (Molecular Probes) was dissolved

were added to the dry product, and the solution was heated to 10 degrees above the DPPC transition temperature (54-56 °C) until all of the DPPC/hypocrellin/indicator mixture was suspended. NaN_3 was introduced to scavenge oxygen and thus to obviate singlet oxygen production. Vesicles were formed by sonicating the resulting suspension until optically clear using either a Cole Palmer Model 8890 bath sonicator for approximately 1.5 hours or a Fisher Sonic Dismembrator Model 300 fitted with a microtip for 40 minutes. BCECF that was not entrapped inside the vesicle was removed by passing the vesicle system over a size exclusion column (Sepharose 4B).

For time-resolved measurements, 5 mL of the DPPC solution, a hypocrellin A/ethanol solution (1 mg/mL), and a 3-hexadecanoyl-7-hydroxycoumarin (Molecular Probes)/ethanol solution (1 mg/mL) were mixed and then evaporated to dryness on a rotovap. 2 ml of a 0.12 M NaCl/0.03M NaN_3 solution were added to the dry product and the solution was heated to 10 degrees above the DPPC transition temperature until all the DPPC/hypocrellin A/indicator mixture was suspended. Vesicles were prepared as described above. Since, however, all of the indicator is assumed to be partitioned into the bilayer, the system was not passed over a size exclusion column.

Steady-state fluorescence excitation spectra were obtained on a SPEX Fluoromax. For steady-state pH experiments, hypocrellin A was excited by a 300-W tungsten bulb fitted with 575-nm cut-off filters. Background light with the bulb on was less than 0.3 % of the signal. The visible power available at the cuvette was 8-9 mW. Steady-state fluorescence excitation spectra were also corrected for scattering from vesicles and nonlinearities in collection of spectra by subtracting a blank of the difference in spectra collected with lamp on and lamp off of BCECF alone in vesicles. Time-resolved absorption data were obtained with the microsecond flash photolysis system (Fehr et al., 1995) generously made available to us by Professor J. H. Espenson. Ki-

netic traces were the average of 4 shots. The excitation pulse had a duration of ~600 ns and an energy of ~70 mJ at 490 nm.

Results and Discussion

Table 1 compares the antiviral activity of hypericin and hypocrellin A under hypoxic and aerobic conditions, as well as under different serum concentrations. The results indicate that, as we observed previously, hypericin posesses significant antiviral acitivity both in the presence and in the absence of oxygen. Hypocrellin A however posesses no antiviral acitivity without the presence of oxygen. The absence of virucidal activity in hypocrellin under hypoxic conditions also provides a further verification of the extent of deoxygenation provided by our experimental protocol.

Table 1 also shows that the serum concentration has neglible effect under either hypoxic or aerobic conditions. The serum concentration was varied to evaluate wether the increased solubiltiy afforded by the increase in serum concentration would positively effect the hypoxic experiment. Since hypericin and hypocrellin A are very hydrophobic, the concentration in the virus membrane is determined by the initial mixing of the phosphate buffered saline (PBS), the virus, and the chromphore/DMSO solution. We hypothesized that by varying the amount of serum, we might more efficiently incorporate the chromophore into the viral membrane and consequently obtain more efficient virucidal activity. The results in Table 1 indicate, however, that 0 or 10% additional serum provide comparable results.

We have previously reported that hypericin affords photoinduced acidification and that this may play a role in its antiviral acitivity. Much to our surprise, hypocrellin A does not display similar behavior under comparable conditions (Figure 2). The steady-

Table 1. Effect of oxygen and serum concentration on the light-dependent antiviral activity of hypericin and hypocrellin.

			Hypericin			Hypocrellin		
			A	B	C	A	B	C
0% Serum[a]	Aerobic[d]	Dark	43,000	140,000	2,400	41,000	84,000	51,000
		Light[c]	0	0	30	0	0	0
	Hypoxic[e]	Dark	29,000	110,000	2,400	34,000	88,000	54,000
		Light[c]	190	0	0	28,000	31,000	4,500
10% Serum[b]	Aerobic[d]	Dark	27,000	130,000	14,000	52,000	36,000	7,500
		Light[c]	0	0	140	0	440	0
	Hypoxic[e]	Dark	34,000	120,000	9,300	54,000	84,000	6,000
		Light[c]	0	0	880	33,000	100,000	16,000

[a] No additional serum besides that which was used to store virus was added (total serum · 1%).

[b] Additional serum (fetal calf serum) was added to PBS to give 10% total volume of fetal calf serum.

[c] Illumination was effected with a 300-W projector bulb fitted with a cut-off filter blocking wavelengths shorter than 575 nm.

[d] The oxygen content of the sample was determined by letting it equilibrate with the atmosphere.

[e] Hypoxic conditions wereobtained by passing argon gas over the samples for 45 minutes before and during illumination.

state results displayed compare the behavior of hypericin and hypocrellin A. Similarly, we do not observe any evidence of transient acidification in microsecond experiments (not shown). We are careful in interpreting these results not to conclude that hypocrellin A is incapable of acidifying its surroundings. It is possible that under these experimental conditions, one cannot observe such a protonation event. For example, hypocrellin A has slightly different solubility properties from those of hypericin. Hypericin is soluble in some polar protic and aprotic solvents and it is insoluble in nonpolar solvents. On the other hand, hypocrellin A is soluble in a wider range of polar protic and aprotic solvents as well as in some nonpolar solvents such as cyclohexane and benzene. Consequently, the absence of observed acidification may be a result of the orientation of hypocrellin A in the vesicle that impedes excited-state intramolecular proton transfer to the indicators, as we have placed them. Absolute verification of the inability of hypocrellin A to execute intramolecular proton transfer will require the investigation of indicator molecules covalently tagged to it.

Conclusions

Given the gross similarities between the structures of hypocrellin A and hypericin, it is surprising that hypocrellin A absolutely requires oxygen for antiviral activity and does not produce observable intramolecular excited-state proton transfer under our experimental conditions. The contrast with hypericin is instructive. Hypericin clearly has multiple modes of light-induced antiviral activity. It also produces singlet oxygen. But it is known that optimum pH values are important in the life cycles of the influenza virus (Bullough et al., 1994) and of paramyxoviruses (Zhirnov, 1990). That hypericin is also a proton source may be quite significant in this context. Finally, we cannot exclude

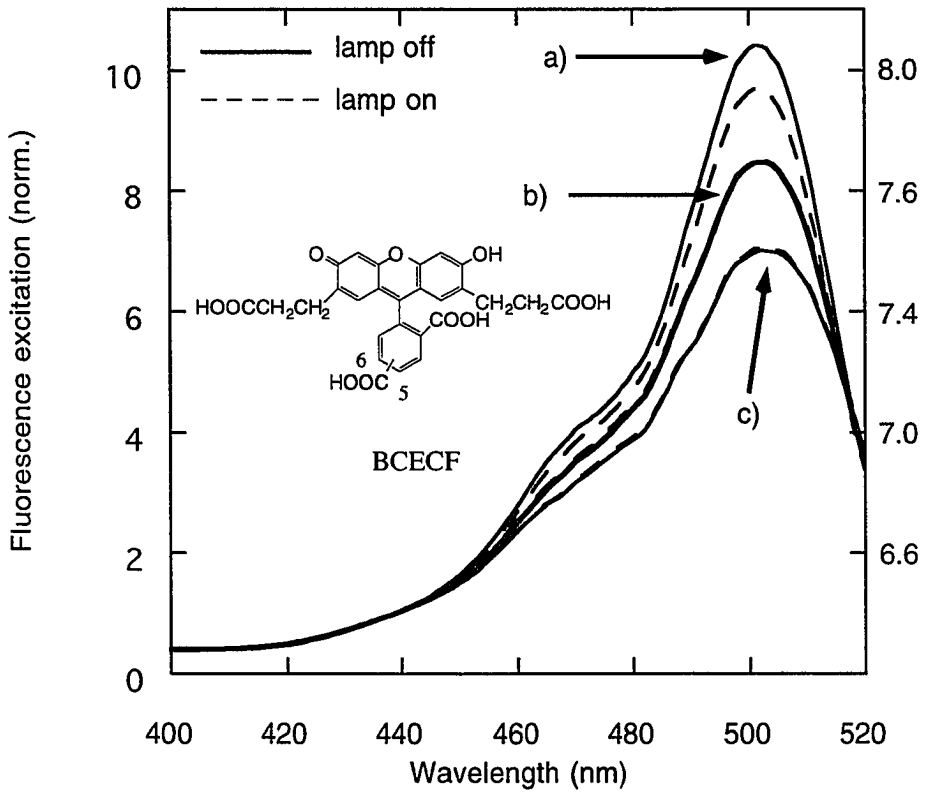

Figure 2: Steady-state acidification by hypericin or hypocrellin A of DPPC vesicle interior as probed by the pH indicator BCECF. A decrease in fluorescence of BCECF indicates an increase in the proton concentration. Chromophores were excited with a 300-W Tungsten lamp fitted with cuttoff filters ($\lambda \geq 575$ nm) to insure that only the chromophore was excited. Fluorescence (as fluorescence excitation) was collected at 535 nm and normalized at the isobestic point of 439 nm to account for dye degradation and leakage. Data is presented as pairs of fluorescence curves with solid lines representing the system without an excitation source (lamp off) and curves with dotted lines representing the system with and excitation source (lamp on).

a. Photoinduced acidification by hypericin.

b and c. Lack of photoinduced acidification by hypocrellin A.

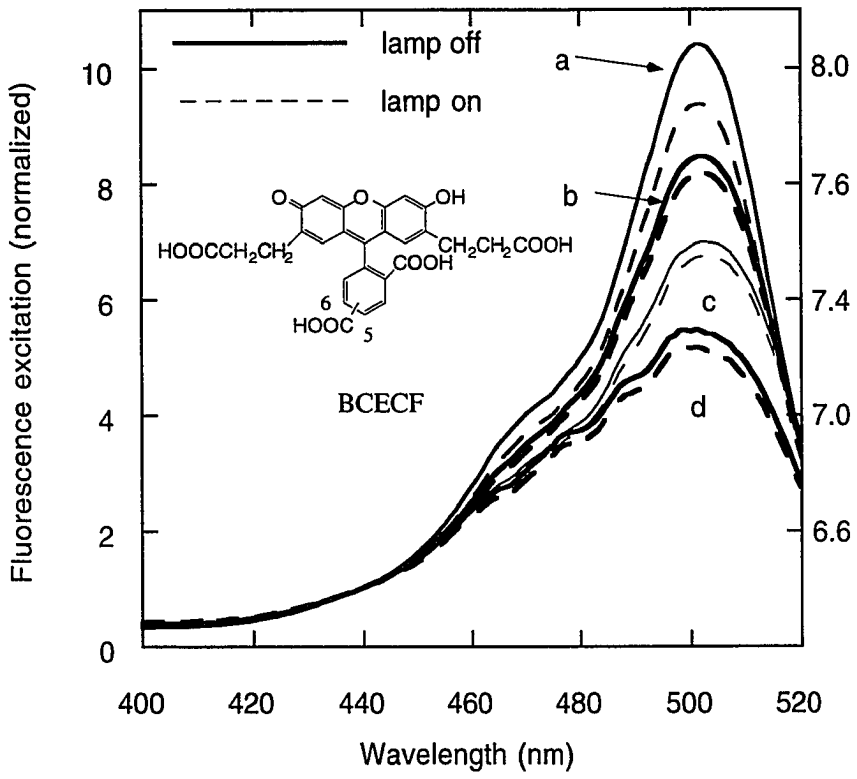

Figure 2 (cont.): Steady-state acidification by hypericin or hypocrellin A of DPPC vesicle interior as probed by the pH indicator BCECF. A decrease in fluorescence of BCECF indicates an increase in the proton concentration. Chromophores were excited with a 300-W Tungsten lamp fitted with cuttoff filters ($\lambda \geq 575$ nm) to insure that only the chromophore was excited. Fluorescence (as fluorescence excitation) was collected at 535 nm and normalized at the isobestic point of 439 nm to account for dye degradation and leakage. Data is presented as pairs of fluorescence curves with solid lines representing the system without an excitation source (lamp off) and curves with dotted lines representing the system with and excitation source (lamp on).

a. Photoinduced acidification by hypericin.

b and c. Apparent photoinduced acidification by hypocrellin A.

d. Change in fluorescence excitation intensity of BCECF alone in vesicles.

The previous figure is corrected by subtracting the difference in the lamp on and lamp off of d from a, b and c.

as an antiviral mechanism the ability of hypericin to perform oxidation-reduction chemistry (Redepenning & Tao, 1993).

It appears that the more complicated and extended structure of hypericin has a much more important role in its antiviral activity than merely to serve as a substrate for hydroxyl and carbonyl groups. The data suggest that the hypericin structure greatly influences its preferential solubility for the viral membrane and that it may play an important role in its ability to shuttle a proton away from itself. With regard to this latter point, previous steady-state work (Diwu et al., 1989) and preliminary time-resolved work from our laboratory suggest that a large percentage of hypocrellin A is already tautomerized in the ground state. If this is so, it is likely that exposure to light merely produces the original, untautomerized, form (Figure 1a). Furthermore, the absence of a second hydroxyl group β to the carbonyl group may hinder charge separation that would be required in order to deliver the proton to the solvent, an external pH indicator, or, for example, a capsid protein of the virus (Meruelo et. al., 1992; Fehr et al., 1994). The results presented here indicate the utility of studying hypericin analogs in unravelling the origins and the mechanisms of the light-induced antiviral activity of hypericin.

Acknowledgements

M.J.F is the recipient of a GAANN fellowship. Support for parts of this work was provided by a Carver grant. We thank Yvonne Wannemuehler for excellent technical assistance. We also thank Professor M. A. McCloskey for advice and assistance and Professor J. H. Espenson for the use of his microsecond flash apparatus.

References

Bullough, P. A., Hughson, F. M., Skehel, J. J., & Wiley, D. C., (1994) *Nature 371*, 37.

Carpenter, S., & Kraus, G.A. (1991) *Photochem. Photobiol. 53*, 169.

Carpenter, S.L., Fehr, M.J., Kraus, G.A., & Petrich, J.W. (1994) *Proc. Natl. Acad. Sci. USA 91*, 12273.

Casey, J. M., Kim, Y., Andersen, P. R., Watson, K. F., Fox, J. L., & Devare, S. G., (1985) *J. Virol. 55*, 417.

Chiu, I.-M., Yaniv, A., Dahlberg, J. E., Gazit, A., Skuntz, S. F., Tronick, S. R., & Aaronson, S. A., (1985) *Nature 317*, 366.

Connolly, P. Espenson, J.H., & Bakac, A. (1986) *Inorg. Chem. 25*, 2169.

Degar, S., Prince, A.M., Pascual, D., Lavie, G., Levin, B., Mazur, Y., Lavie, D., Ehrlich, L.S., Carter, & C., Meruelo, D. (1992) *AIDS Res. Hum. Retroviruses 8*, 1929.

Diwu, Z.J., Jiang, L.J., & Zhang, M.H. (1989) *Sci. Sin. (**B**) 33*, 113.

Diwu, Z., & Lown, J.W. (1990)*Photochem. Photobiol. 52*, 609.

Diwu, Z., & Lown, J.W. (1992) *J. Photochem.. Photobiol. A: Chem. 64*, 273.

Fehr, M.J., Carpenter, S.L., & Petrich, J.W. (1994) *Bioorg. Med. Chem. Lett. 4*, 1339.

Fehr, M.J., McCloskey, M.A., & Petrich, J.W. (1995) *J. Am. Chem. Soc. 117*, 1833.

Gai, F., Fehr, M.J., & Petrich, J.W. (1993) *J. Am. Chem. Soc. 115*, 3384.

Gai, F., Fehr, M.J., & Petrich, J.W. (1994a) *J. Phys. Chem. 98*, 5784.

Gai, F., Fehr, M.J., & Petrich, J.W. (1994b) *J. Phys. Chem. 98*, 8352.

Gonda, M. A., Braun, M. J., Clements, J. E., Pyper, J. M., Wong-Staal, F., Gallo, R. C., & Gilden, R. V., (1986) *Proc. Natl. Acad. Sci. USA 83*, 4007.

Huang, C. (1969) *Biochemistry 8*, 344.

Hudson, J.B., Zhou, J., Chen, J., Harris, L, Yip, L., & Towers, G.H.N. (1994) *Photochem. Photobiol. 60* , 253.

Jardon, P., Lazorchak, N., & Gautron, R. (1986) *J. Chim. Phys. 83*, 311.

Lenard, J., Rabson, A., & Vanderoef, R. (1993) *Proc. Natl. Acad. Sci. USA 90*, 158.

McElroy, W., & Deluca, M. (1985) in *Chemi and Bioluminescence* (J.G. Burr, Ed.) pp 387-399, Marcel Dekker, Inc, New York.

Meruelo, D., Lavie, G., & Lavie, D. (1988) *Proc. Natl. Acad. Sci. USA 85*, 5230.

Meruelo, D., Degar, S., Nuria, A., Mazur, Y., Lavie, D., Levin B., & Lavie, G.(1992) in *Natural Products as Antiviral Agents*; (C.K. Chu & H.G. Cutler, Eds.) pp 91-119 (and references therein), Plenum Press: New York.

Redepenning, J., & Tao, N., (1993) *Photochem. Photobiol. 58*, 532.

Zhirnov, O. P., (1990) *Virology 176*, 274.

CHAPTER 9. GENERAL CONCLUSIONS AND FUTURE WORK

General Conclusions

The preceeding chapters have shown that hypericin's antiviral activity is complex and does not depend only on the generation of singlet oxygen but instead is related to hypericin's primary photophysical processes. We have provided detailed studies of the primary events of hypericin and shown that upon optical excitation hypericin undergoes an intramolecular proton transfer, to its fluorescent state, and hence posesses labile protons. Hypericin is also capable of acidifying its environment and thus is also capable of intermolecular proton transfer. Because of experimental limitations in the flash photolysis system we are currently limited to only detecting protons ejected from the triplet state and are unable to determine if protons are also ejected from the singlet state. Experimental methods to overcome this are discussed in the future work section of this chapter.

In addition to exploring the photophysics and mechanism of antiviral action of hypericin, a method of selectively targeting virally infected cells has been presented. This method involves incorporating the north american firefly gene into mamilian cells under the control of a reporter gene which would be controlled by the entry of the virus. This would result in production of the firelfly enzyme luciferase in the cell. Hypericin, tethered to the oxidizable substrate luciferin, can then be used to selectively kill infected cells without damaging healthy cells.

We have also compared hypericin's antiviral activity to a related compound, hypocrellin A. Hypocrellin A has been reported to posess similar excited-state properties and also has been shown to inactivate HIV. We find that the mechanism of action

of hypocrellin A is different from that of hypericin in that it absolutely requires oxygen to inactivate EIAV. In addition we find that hypocrellin A does not acidify its environment under the same conditions as hypericin.

Future Work

Although we have completed a large amount of work in attempting to deduce the photophysics and mechanism of hypericin's and hypocrellin's antiviral action there still remains a considerable number of projects to be completed.

Hypericin

In order to fully resolve wether a proton is also ejected from the singlet state it is necessary that an indicator molecule be covalently attached to hypericin. This allows the local concentration of hypericin/indicator to remain high while the total concentration remains low enough that experiments can be performed. Pump-probe experiments with 1 ps resolution can then be done to look for a bleach in the indicator population as it is being protonated by hypericin or to look for quenching of the stimulated emission of hypericin.

It will also be important to identify the vibrational modes which are activated upon excitation. Hypericin's large fluorescence quantum yield precludes using normal Raman spectroscopy and it is still an open question as to wether hypericin adsorbed to metal surfaces (necessary in SERRS) properly mimicks hypericin in solution. It is possible, however, to observe the vibrational modes indirectly if the excitation pulse is shorter than the vibrational period. The excitation pulse sets up "oscillations" which

can be fourier transformed into the frequency domain to yield information about the vibrational modes. Such a system is provided by the Ti-Sapphire system which is capable of producing pulses as short as 11 fs. This system is currently being built in our laboratory.

In addition to providing information about vibrational modes, this ultrashort pulsewidth will allow us to resolve faster components. If these faster components exist they will yield further information about the proton transfer.

Hypocrellin A

Much work also remains to be done on the photophysics of hypocrellin. As of yet we have only begun to explore the primary processes which are present and only in ethanol. The question still remains as to why hypocrellin absolutely requires oxygen to inactivate EIAV. Structural analogs such as 3,9 perylenequinone and 4,10 dihydroxy 3,9 perylene quinone will be invaluable in deducing wether proton transfer plays an important role in both the photophysics and antiviral mechanism of hypocrellin.

ACKNOWLEDGEMENTS

First and foremost I would like to thank my major professor, Jacob Petrich, for his encouragement, patience, and most of all for letting me explore my intellectual and experimental bounds. He taught me about science, strengthened my problem solving skills and allowed me the freedom to succeed and fail on my own. Without his support little of this dissertation would exist.

I was also fortunate enough to work closely with Professor Susan Carpenter and her group, particularly Yvonne Wannemuehler. Without their help chapters 5, 6 and 8 would never have been completed.

Professor George Kraus and members of his group were always more than helpfull with my questions on synthesis and provided us with many luciferin and hypericin analogs.

Chapter 7 would not have been possible without the help of Professor Mike McCloskey who taught me about membranes, vesicles and pH indicators. He also allowed me access to his lab and participated in many fruitful scientific discussions.

It was an honor to work with the members of my group. I am particularly indebted to Rebecca Rich, Feng Gai and Doug English and will miss the scientific discussion, disagreements and fun that we shared.

I would like to thank my friends Pam Sheaff, Rick Hale, John Zenner and Lisa Hasvold for making my stay in Ames memorable.

Lastly I would like to thank my parents, Ron and Charlotte Fehr, my brothers and sister in-law, Doug, Debby and David Fehr, my grandmother, Iona Campbell, my aunt, Marilyn Campbell and my uncle, Jon Campbell for standing by me as I have made my wandering journey through life.

APPENDIX 1

USE OF EXPGEN.EXE

The program EXPGEN.EXE generates a double-sided exponential pulse. The user is able to adjust the full width at half maximum as an approximate guess of the pulse used in the pump-probe experiment. The program is used as follows:

1. Begin the program by typing EXPGEN.
2. A prompt will ask for the desired FWHM in picoseconds.
3. A prompt will ask for where the maximum of the double-sided exponential pulse should be placed. It is immaterial where it is placed but it should be place somewhere so that it is not cut off.
4. A prompt will ask for the window size. Since the pump probe data usually has 100 points per window this is the default value.
5. A prompt will ask for a name for the file created.

The program will then create an ASCII file which can be read by the program SPECTRA.

EXPGEN.EXE (Written in PASCAL)

```
program ExpGenerator;
uses Dos,crt;
VAR
 I,numpts: word;
 tau,xmax,fwhm,wsize,pspp,a,b: real;
 x,y : real;
 fname: string;
 datap: text;

 PROCEDURE ReadStr(var st:string); FORWARD;
  {********************* FUNCTION DECLARATION **********************}
```

```
FUNCTION yes: BOOLEAN;
 LABEL rep, esc;
 VAR ch: CHAR;
   ans: ARRAY[1..3] of CHAR;
 BEGIN
 ch:=Readkey;
 if ch=#13 then begin yes:=true; goto esc end;
 repeat
rep:
  if (ch='y') or (ch='Y') or (ch='§') or (ch='Ñ')
      then yes:=true
     else
       if (ch='n') or (ch='N') or  (ch=' ') o r (ch='ç') then yes:=false
         else
          begin write('    ',#8#8#8#8); ch:=Readkey; goto rep end;
  case ch of
   'y': ans:='yes';
   'Y': ans:='Yes';
   'n': ans:=' no';
   'N': ans:=' No';
   '§': ans:=' § ';
   'Ñ': ans:=' Ñ ';
   ' ': ans:=' •,';
   'ç': ans:='ç•,';
  end; {case}
  write(' ',ans,#8#8#8#8);
  ch:=Readkey;
 until (ch=#13);
esc:
 writeln;
END; { yes }

FUNCTION BadFileName( var name: string; key: char) : BOOLEAN;
 label again,again1;
 VAR
    ffile:file;
  filer  :SearchRec;
 BEGIN
again1:
  assign(ffile,name);
 {$I-}
  reset(ffile,1);
```

```
{$I+}
if key='r' then begin
     if ioresult<>0 then
      begin writeln; writeln;
       write('î ©´',name,' • ·„È•·,¢„•,.   àß¨• ®,Ï ®¨Ô ? [§/ ]');
         if not yes then begin BadFileName:=true; exit end
               else begin
                   writeln;write('Ç¢•§®,•  Æ¢Æ• ®¨Ô (· ‡ ·Ë®‡• ®•¨): ');
                   ReadStr(name);
                   goto again1;
               end;
      end
     else close(ffile);
end;
if key='w' then begin
 if ioresult=0 then
         begin writeln;
          writeln('File ',name,' already exist. Overwrite ? [Y/N/Change name]');
    again: case  readkey  of
               'n':; 'N': begin BadFileName:=true; exit end;
               'C':; 'c': begin
                   writeln;write('Input new name (with extension): ');
                   readstr(name);
                   goto again1;
                       end;
              #13:;'y':;'Y': ;
                 else goto again;
          end;
         end;
 rewrite(ffile); close(ffile);
  end;
BadFileName:=false
END; { BadFileName }

  {********************* PROCEDURE DECLARATION **********************}
procedure ReadStr(var st:string);
 var ch:char;
  xpos:byte;
  startx:byte;
  begin
    st:='';
    xpos:=1;
```

```
 startx:=wherex;
 ch:=#0;
 while(ch<>#13) do begin
 gotoxy(startx,wherey);
 write(st);clreol;
 gotoxy(startx+xpos-1,wherey);
 ch:=readkey;
  if ch=#0 then
   ch:=readkey
    else begin
    if not (ch in [#13,#8])
     then begin
       st:=st+ch;
       inc(xpos);
       end;
    if (ch=#8) and (xpos>1)
     then begin
       dec(byte(st[0]));
       dec(xpos);
      end;
    end;
  end;
 writeln;
end; { proc ReadStr }

PROCEDURE askr(var  x: real);
 VAR
  st : string;
  cod: integer;
  i: real;
 label more;
 Begin
more:
  write('<',x:8:4,'> ');
  ReadStr(st);
  if st='' then exit;
  Val(st, I, Cod);
{ Error during conversion to integer? }
  if cod <> 0 then
                  begin writeln; writeln('Input error ! Try again...');
                   goto more;
                  end
```

```
                else x:=i;
 End; { proc askr }

 PROCEDURE aski(var  x: word);
  VAR
   st : string;
   cod: integer;
   i: integer;
  label more;
  Begin
more:
   write('<',x,'> ');
   ReadStr(st);
   if st='' then exit;
   Val(st, I, Cod);
{ Error during conversion to integer? }
   if cod <> 0 then
                begin writeln; writeln('Input error ! Try again...');
                goto more;
                end
           else x:=i;
  End; { proc aski }

 PROCEDURE asks(var  x: string);
  VAR
   st : string;
  label more;
  Begin
more:
   write('<',x,'> ');
   ReadStr(st);
   if st='' then exit;
    x:=st;
  End; { proc asks }

 BEGIN
  numpts:=100; fwhm:=1.0; wsize:=6.0;
  xmax:=2; fname:='dexp.dat';
  writeln(' ***** Double-Sided Exponent Function Generator ****');
  writeln;
  repeat
   write(' F.W.H.M.(in ps)= '); ASKR(fwhm);
```

```
 write(' Maximum location (in ps)= '); ASKR(xmax);
 write(' Window size (in ps)='); askr(wsize);
 write(' Number of points= '); ASKi(numpts);
 writeln; write(' Output file name: '); ASKs(fname);
 if BadFileName(fname,'w') then exit;
 write('  Is everything correct ? [y/n]');
until yes;
 assign(datap,fname);
 rewrite(datap);

 tau:=fwhm/2/ln(2);
 a:=xmax; b:=xmax;
 for i:=0 to numpts do
  begin
   x:=i*wsize/numpts;
   if x<xmax then y:=exp((x-a)/tau)
            else y:=exp(-(x-b)/tau);
   writeln(datap,x,'   ',y);
  end;

 close(datap);
 writeln(' File "',fname,'" has successfully created.');
 repeat until keypressed;
END.
```

APPENDIX 2
USE OF ASYST PROGRAM

The program ASYST handles data collection and basic data manipulation for the pump probe experiment. At the writing of this disertation the ASYST program was intiated from within the Windows portion of the personal computer by double clicking on the ASYST prompt. A menu bar will appear. Hit the escape key and at the next prompt type pp. This initiates the program and a menu window should appear. Two major portions of the ASYST program are regularly used. The data collection window and the translation stage control (motor control).

The data collection window contains numerous prompts to control the number of shots collected for each point, the discrimination for each shot (which should be 80-90%), how long to wait at each point and how many scans should be acquired. The data is collected in an ASCII format and for long number of collections is saved automatically after 20 scans and stored in a file. The data is not overwritten so data can be extracted if the experiment becomes noisy after many scans.

To stop the program hit any key. A prompt will ask if you wish to exit the program or if you wish to change either the y axis or the collection window. Changing the collection window is occasionally usefull if there is a drop in power without an increase in noise.

The translation stage control allows for movement of the stage when the experiment is not running it is usefull for finding zero time and for checking stage flatness. The most important thing to note is that when moving the stage backward it is necessary to enter a negative number into the step size. It is also important to note that 57 steps correspond to 1 ps when moving the stage.